UNIVERSITÉ DE STRASBOURG

ÉCOLE DOCTORALE Sciences de la Vie et de la Santé – ED 414

Institut de biologie moléculaire des plantes (IBMP) - UPR 2357

THÈSE présentée par :

Jing FENG

soutenue le : **13 mars 2015**

pour obtenir le grade de : **Docteur de l'université de Strasbourg**

Discipline/ Spécialité : Aspects moléculaires et cellulaires de la biologie

Caractérisation fonctionnelle des régulateurs chromatiniens ZRF1-like chez *Arabidopsis thaliana*

THÈSE dirigée par :
M. Wen-hui SHEN Directeur de Recherche, Université de Strasbourg

RAPPORTEURS :
M. Julio SAEZ-VASQUEZ Directeur de Recherche, Université de Perpignan
Mme. Mieke VAN LIJSEBETTENS Professeur, Université de Gent (Belgique)

AUTRES MEMBRES DU JURY :
M. André STEINMETZ Directeur de Recherche, CNRS, CRP-Santé Luxembourg
M. MARIO KELLER Professeur, Université de Strasbourg

Acknowledgements

I would like to express my sincerest gratitude to my supervisor, Prof. Wen-hui SHEN for his rigorous training, heartful support for my research in his lab, for his guidance, suggestions, and encouragement, as well as for his help throughout my studies and composition of this thesis. I will benefit for the rest of my life as an independent and creative scientist from the logical reasoning, critical reading and interest-driven attitude I learned from him. I also would like to express my appreciation to Dr. Alexandre BERR for his care and help in my daily life here at Strasbourg.

I am especially grateful to Dr. Donghong CHEN for teaching me experiments containing the methods and how to think and control the direction of my research. At the same time, he gave me advice and suggestions for my life when I first came here. Moreover, I would like to show my sincere appreciation to Prof. Léon OTTEN for kindly helping me.

Needless to say, it was difficult for me to survive in France due to my poor knowledge of French. Many more persons helped me in various ways during my study here. Thanks to all of them.

I am deeply grateful to my parents, for their greatest love, abiding support, encouragement, and understanding.

I am also grateful to the China Scholarship Council (CSC) for funding my PhD program.

Table of Contents

I. GENERAL INTRODUCTION

I.1. Plant development

Plant development is a multiphasic process, with new organ initiation and elaboration occurring throughout the life cycle. According to the traditional view point in plant developmental biology, development is inextricably coupled with growth. Growth is the irreversible change in the size of cells and plant organs due to both cell division and cell expansion. Plant development is punctuated by physiological transitions, such as seed maturation, dormancy and germination separating embryogenesis from vegetative development. Moreover, flowering distinguishes vegetative growth from reproductive growth.

I.1.1 Seed development

Seed development is a pivotal stage in the higher plant life cycle with respect to its significance in maintaining the stability of species. Seed development comprises two major phases: embryo development and seed maturation. Embryogenesis starts with a morphogenesis phase and ends at the heart stage, when all embryo structures have come into form (Mayer *et al*., 1991). During the morphogenesis phase, the basic body plan of the plant is established with the specification of the shoot-root axis and the formation of the embryonic organ and tissue systems. A seed containing a full-size embryo undergoes maturation. Major characteristics of the maturation phase include the arrest of embryo morphogenesis, synthesis and accumulation of storage macromolecules, acquisition of desiccation tolerance, inhibition of precocious germination, and metabolic quiescence resulting from desiccation of the seed (Gutierrez *et al*., 2007; Harada, 1997; Vicente-Carbajosa and Carbonaro, 2005).

Plant seed development is regulated by a network of transcription factors that include the *LEAFY COTYLEDON 1* (*LEC1*) and *LEC1-LIKE* (*L1L*) genes as well as the plant specific B3-domain transcription factor genes *ABSCISIC ACID INSENSITIVE3* (*ABI3*), *FUSCA3* (*FUS3*) and *LEC2*. LEC2 acts as a central master regulator, its DNA binding region serving critical roles both during embryo development and seed maturation in *Arabidopsis* (Stone *et al*., 2001). Moreover, LEC2 controls other master regulators. *LEC1* and *L1L* play roles in early embryogenesis. Ectopic expression of *LEC1* activates *LEC2*, *FUS3* and *ABI3* genes (Kagaya *et al*., 2005) and is sufficient to induce embryo formation in vegetative organs (Kwong *et al*., 2003). B3-domain transcription factors act in seed maturation

and activate downstream genes involved in the accumulation of storage proteins and lipids (Ikeda *et al*., 2006). Plants ectopically expressing *LEC2* accumulate seed proteins and lipids in vegetative and reproductive tissues, and trigger somatic embryo formation (Lotan *et al*., 1998; Stone *et al*., 2001). All four *abi3*, *lec1*, *lec2* and *fus3* mutants are severely affected in seed maturation and share some common phenotypes, such as decreased dormancy at maturation and reduced expression of seed storage proteins (Gutierrez *et al*., 2007).

I.1.2 Seed dormancy and germination

A dormant seed does not have the capacity to germinate in a specified period of time under any combination of normal physical environmental factors that are otherwise favourable to its germination. Thus, the transition of the seed from dormancy to germination is a critical step in the life cycle of plants. Dormancy is a complex trait that is controlled by a large number of genes which are affected by both developmental and environmental factors. It is known that the relative levels of plant hormones control seed dormancy and germination. Several studies have shown that ethylene, gibberellic acid and brassinosteroids promote the germination of dormant seeds, but there is now a general agreement that abscisic acid (ABA) is the primary mediator of seed dormancy (Koornneef *et al*., 2002). Moreover, other mechanisms, which might be independent of hormones or specific to the seed dormancy pathway, are also emerging from genetic analysis of "seed dormancy mutants".

Seed dormancy is induced during the seed maturation phase simultaneously with the accumulation of storage compounds, the acquisition of desiccation tolerance and, finally, the quiescence of metabolic activity. Thus, seed dormancy is controlled by four major seed maturation regulators: *ABI3*, *LEC1*, *LEC2* and *FUS3*. In addition, *DELAY OF GERMINATION 1* (*DOG1*) is a key player specific for the induction of seed dormancy in *Arabidopsis* (Bentsink *et al*., 2006). Loss-of-function mutant alleles of *DOG1* are completely nondormant and do not show any other phenotypes (Bentsink *et al*., 2006).

I.1.3 Meristem development

A meristem is a tissue containing undifferentiated cells (meristematic cells) which give rise to various organs of the plant and keep the plant growing. Plants

possess different types of meristems that control both primary and secondary organ growth. Both roots and shoots have meristematic tissues at their tips. These tissues are called apical meristems and are responsible for the lengthening of roots and shoots. The shoot apical meristem (SAM) comprises a small, dome-shaped population of undifferentiated cells, which is formed during embryonic development and after seed germination gives rise to the stem, leaves, and flowers. The root apical meristem (RAM) is also formed during embryo development, but after seed germination it gives rise to the root system. In order to fulfill these functions, the meristem must maintain a balance between the self-renewal of a reservoir of central stem cells and organ initiation from peripheral cells. Throughout the life of the plant, the rate of cell division and cell elongation in the meristems is regulated by complex, overlapping signaling networks that include the feedback regulation of meristem maintenance genes and the signaling of plant hormones.

I.1.3.1 Shoot meristem maintenance by WUS-CLV feedback loop

The shoot meristem is composed of three zones exhibiting different functions. The central zone (CZ) at the tip of SAM contains the slowly dividing stem cells, which are necessary for the indeterminate growth and development of the plant. The peripheral zone (PZ) surrounds CZ and ultimately gives rise to lateral organs. The rib meristem (RM) is located beneath CZ; division and elongation of rib meristem cells give rise to the stem of the plant. The organizing center (OC) residing in RM acts as the stem cell niche; it specifically expresses the homeodomain transcription factor *WUSCHEL (WUS)* (Mayer *et al*., 1998). *WUS* is both necessary and sufficient for stem cell specification (Laux *et al*., 1996). Mutations in *WUS* result in the mis-specification of stem cells and premature termination of the shoot. Thus, restriction of *WUS* transcription to cells of the OC is critical for maintaining a constant number of stem cells, and this is mediated by the *CLAVATA* (*CLV*) signaling pathway (Brand *et al*., 2000; Fletcher *et al*., 1999; Mayer *et al*., 1998).

In the *WUS-CLV* pathway, the expression of *WUS* is controlled by the three *CLV* genes (*CLV1, CLV2,* and *CLV3*) that act together in a signal transduction pathway and restrict stem cell fate (Brand *et al*., 2000). *CLV3* encodes a putative signalling peptide and is expressed in the CZ cells. CLV1 represents a putative receptor kinase (Clark *et al*., 1997), and CLV2 is a presumed accessory protein of the signalling complex which lacks the kinase domain and contributes to the stability of

CLV1 (Jeong *et al*., 1999). The emerging mechanism comprises three steps: firstly, CLV3 protein is secreted from the CZ cells into the extracellular space; secondly, it acts as a signaling molecule that binds to and activates a heterodimeric receptor complex containing CLV1 and CLV2; lastly, the activated complex restricts the expression of *WUS* to a small domain in the deeper regions of the meristem, the OC (Brand *et al*., 2000). As a consequence, *wus* mutants lack the meristem, and loss of *CLV1*, *CLV2*, or *CLV3* activity leads to an accumulation of meristem cells and to a gradual increase in size of the shoot meristem dome (Fletcher *et al*., 1999). Moreover, in this pathway, *WUS* not only specifies stem cell fate in overlaying cells of the CZ, it also activates its own negative regulator CLV3 by binding to the genomic regions of *CLV3* to activate its transcription (Yadav *et al*., 2011). Thus, the WUS-CLV feedback system forms a self-correcting mechanism for maintaining a constant number of stem cells and the SAM size.

I.1.3.2 Shoot meristem maintenance by *KNOX* transcription factors

In parallel to the WUS–CLV signaling pathway, equally essential for SAM maintenance is the Class-I *KNOTTED1*-like homeobox (*KNOX*) genes, which encode homeodomain transcriptional regulators, including *BREVIPEDICELLUS (BP)/KNAT1*, *KNAT2*, *KNTA6* and *SHOOT MERISTEMLESS (STM)*. They have been identified to play an essential role in the development and to be complementary to *WUS* in the maintenance of the stem cell niche in the SAM (Endrizzi *et al*., 1996; Hake *et al*., 2004; Long *et al.*, 1996; Tsuda *et al*., 2011). Among these genes, *STM* is required for both the establishment and maintenance of SAM and is expressed throughout the SAM, but not in lateral organ primordia. *BP*/*KNAT1*, *KNAT2*, and *KNAT6* are also specifically expressed in SAM and have partially redundant roles with *STM* in SAM maintenance (reviewed in Scofield and Murray, 2006). Loss-of-function *stm* weak mutants show meristem defects in maintaining SAM organisation, and the *stm* strong mutants totally fail to establish the SAM during embryogenesis. Moreover, overexpression of *STM* can lead to the formation of ectopic meristems (Long *et al.*, 1996; Scofield *et al*., 2014). In contrast, mutations in *KNAT1/BP*, *KNAT2* or *KNAT6* alone do not obviously affect shoot meristem development or function (Byrne *et al*., 2002; Douglas *et al*., 2002, Venglat *et al*., 2002; Dean *et al*., 2004). *KNAT1/BP* and *KNAT2* expression levels are increased by *STM* induction while in STM-RNAi lines,

KNAT1/BP and *KNAT2* are down-regulated. But overexpression of neither *KNAT1/BP* nor *KNAT2* causes an increase in *STM* mRNA (Gallois *et al*., 2002; Lenhard *et al*., 2002; Scofield *et al*., 2013). This indicates that *STM* can regulate *BP* and *KNAT2*, but *BP* and *KNAT2* have no action in the regulation of *STM*. Moreover, *STM* plays a major role in maintaining shoot meristems. *BP* regulates internode development (Douglas *et al*., 2002; Venglat *et al*., 2002) and contributes, together with *STM*, to SAM maintenance (Byrne et al., 2002). In addition, *KNAT6* function is integrated in a network comprising *STM* and the *CUC* genes to regulate organ separation and to maintain the SAM. *KNAT2*, the member closest to *KNAT6*, did not display such a role (Belles-Boix *et al.*, 2006).

I.1.3.3 Phytohormones in shoot meristem development

Many studies showed that phytohormones and transcription factors cooperate to balance meristem maintenance and organ formation (Figure I.1). KNOX transcription factors promote meristem function partly through repression of biosynthesis of gibberellin (GA) (Chen *et al*., 2004; Hay *et al*., 2002; Sakamoto *et al*., 2001). They target and repress the transcription of genes encoding GA20 oxidase enzymes, which are required for GA biosynthesis (Chen *et al*., 2004; Sakamoto *et al*., 2001). Moreover, GA reduction enhances phenotypes associated with *KNOX* overexpression. However, *KNOX*-mediated repression of GA biosynthesis would not be sufficient to maintain reduced GA levels. Thus, there is a synergistic action with another pathway by which KNOX proteins activate transcription of *GA2* oxidase genes, which encode GA catabolic enzymes, at the leaf–meristem boundary (Hay *et al*., 2002; Sakamoto *et al*., 2001). Altering GA levels is not sufficient to rescue *KNOX* mutant phenotypes (Hay *et al*., 2002), indicating that KNOX proteins control additional processes in the SAM.

Indeed, STM induces cytokinin (CK) synthesis to inhibit cellular differentiation; in addition it functions to organize undifferentiated cells into a self-sustaining meristem (Jasinski *et al*., 2005; Yanai *et al*., 2005) (Figure I.1). In CK biosynthesis pathway, adenosine phosphate-isopentenyltransferases (IPTs) catalyze the transfer of an isopentenyl group from dimethylallyl diphosphate to an adenine nucleotide (ATP, ADP, or AMP) (Kakimoto, 2001; Takei *et al*., 2001). STM promotes induction of *IPT* gene expression (Jasinski *et al*., 2005; Yanai *et al*., 2005). Conversely, expression of *IPT* under control of the *STM* promoter can partially rescue

some traits of the *stm* mutant phenotypes (Yanai *et al*., 2005). Furthermore, CK triggers a rapid increase in mRNA levels of the *KNOX* genes (Rupp *et al*., 1999). It appears that a positive feedback loop exists between *STM* and CK signalling to coordinately control SAM activity. CK also stimulates the expression of genes involved in GA catabolism to reinforce the low GA levels established by the KNOX proteins within the SAM (Jasinski *et al*., 2005; Wolters and Jürgens, 2009).

In addition, CK signaling has also been associated with the WUS-CLV pathway (Figure 1). CK acts as a downstream signaling network of the WUS-CLV feedback loop. In *Arabidopsis*, CK is perceived by a multi-step phosphorelay pathway. Three transmembrane histidine kinases have been identified as CK receptors: they are the ARABIDOPSIS HIS KINASE 2 (AHK2), AHK3, and CYTOKININ RESPONSE1 (CRE1)/AHK4 (Inoue *et al*., 2001; Riefler *et al.*, 2006; Su *et al*., 2011). Upon CK perception, AHKs could activate the ARABIDOPSIS RESPONSE REGULATOR (ARR) proteins, for example *ARR7/15*, through the phosphorelay system (Hwang *et al.*, 2012). The WUS-CLV feedback loop interacts with CK through perceiving CK signalling to positively regulate the shoot meristem. Type-A ARR7 and ARR15 have been validated as negative regulators of CK signalling (To *et al*., 2004; To and Kieber, 2008), and are required for *CLV3* expression (Zhao *et al*., 2010). Ectopic expression of *WUS* represses the negative A-type ARRs (Leibfried *et al.*, 2005). Moreover, overexpression of an A-type ARR inhibits *WUS* expression and can mimic the *wus* mutant phenotype. It thus appears that CK not only maintains shoot meristem function, but is also involved in regulating the size of the stem cells.

Auxin also plays a critical role in the maintenance of the shoot meristem. There is much evidence for an extensive cross-talk between auxin and cytokinin during shoot meristem development (Cheng *et al*., 2013; Su *et al*., 2011). *YUCCA* genes encode key enzymes which catalyse a rate-limiting step of auxin biosynthesis (Cheng *et al*., 2006). In *yucca* mutants with reduced auxin levels, the expression levels of *ARR7* and *ARR15* are dramatically increased in SAM. Similar results were observed in *pin1* mutants (Zhao *et al*., 2010). These observations suggest that *ARR7* and *ARR15* activation can be directly induced by the loss of local auxin accumulation. It is likely that auxin and CK signalling converge on shoot meristem function regulation by controlling A-type *ARR* activity.

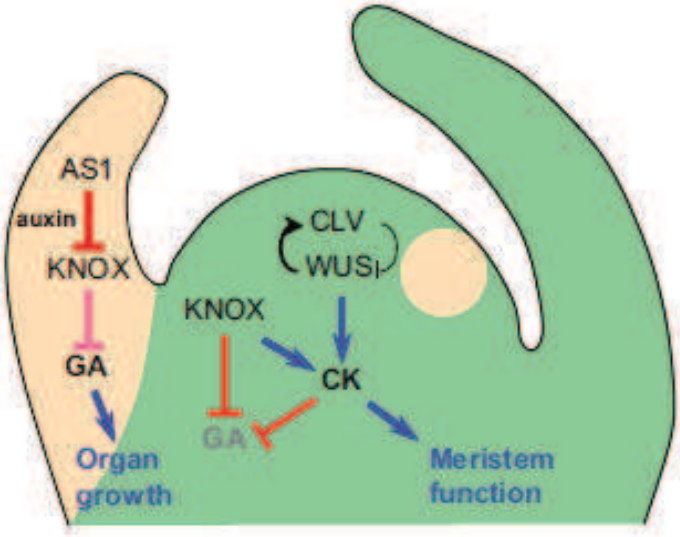

Figure I.1. Participation of hormones in meristem identity

This promotion is reinforced by at least one member of the *KNOX* family. Gibberellin (GA) function is repressed at the meristem by CK and *KNOX* by inhibition of GA biosynthesis. On the other hand, emerging primordia experience an increase in GA activity because the product of the *AS1* gene and auxin repress the expression of the *KNOX* gene that inhibits GA biosynthesis. Beige colour represents nascent primordia. (From Alabadi *et al.*, 2009).

I.1.3.4 SHR/SCR pathway in maintenance of the root stem cell niche

The root is composed of three main regions: the meristematic zone (MZ), the elongation zone (EZ), and the differentiation zone (DZ). The quiescent center (QC) cells (four in *Arabidopsis thaliana*), whose function resembles those of the OC in the shoot meristem, are located in the region at the tip of MZ. QC is essential for the maintenance of the stem cell fate of the surrounding cells (van den Berg *et al*., 1997). QC, together with the surrounding stem cells, constitute the root stem cell niche (SCN) which provides the source of cells for the formation of all root tissues (Dinneny and Benfey, 2008; van den Berg *et al*., 1995).

SHORT ROOT (*SHR*) and *SCARECROW* (*SCR*), encode members of the GRAS family of transcription factors, and they play essential roles in QC establishment and stem cell maintenance (Helariutta *et al*., 2000; Sabatini *et al*., 2003). The SHR protein is expressed in the stele, but moves out of the stele into the endodermis and QC, where it upregulates SCR (Nakajima *et al*., 2001). The expression of *SCR* in the QC was shown to be both necessary and sufficient for the specification of the QC and the maintenance of the stem cells (Sabatini *et al*., 2003).

However, the expression of SCR in the QC region could not rescue the root meristem defects of SHR mutant seedlings. Moreover, SCR has a role for restricting SHR movement. Disruption of either SHR or SCR expression results in the formation of a short root that fails to maintain the QC and meristem (Helariutta *et al*., 2000; Lucas *et al*., 2011; Sabatini *et al*., 2003).

I.1.3.5 WOX5-IAA17 feedback circuit in root development

The homeobox gene *WUSCHEL-RELATED HOMEOBOX 5* (*WOX5*), a homologue of *WUS*, is a major regulator of the root stem cell activity. *WOX5* is expressed exclusively in the QC cells and is required for maintenance of distal stem cell (DSC) fate (Sarkar *et al*., 2007). In the *wox5* mutant, root tips show more DSC differentiation, and overexpression of *WOX5* inhibited DSC differentiation (Ding and Friml, 2010). Auxin and *WOX5* have opposite effects on DSC activity. Both exogenous auxin application and stimulation of auxin biosynthesis enhance DSC differentiation. This indicates that auxin acts as a positive signal for the differentiation of DSC. Genetic experiments suggest that auxin enhances DSC differentiation through downstream transcriptional repression of the *WOX5* homeobox regulator of stem cell activity (Ding and Friml, 2010).

Auxin signaling requires IAA17/AUXIN RESISTANT3 (AXR3) as well as auxin response factors (ARF10 and ARF16). Both ARF10 and ARF16 negatively regulate *WOX5* transcription and restrict *WOX5* transcripts to the QC center (Ding and Friml, 2010). Moreover, WOX5 modulates free auxin production and restricts its own expression via IAA17-dependent feedback regulation (Tian *et al*., 2014). The WOX5-IAA17 feedback circuit assures the maintenance of auxin response maximum in the root tip and thereby contributes to the maintenance of DSC populations.

I.1.3.6 Auxin and PLT in maintenance of root meristem

PLETHORA1 (*PLT1*) and *PLT2* genes, which encode members of the AP2 class of transcription factors, are essential for QC and stem cell activity. Accordingly, *PLT* expression is detected in the stem cell niche (Aida *et al*., 2004; Galinha *et al*., 2007). PLT proteins have been shown to act in a dosage-dependent manner, high levels of PLT being required to maintain stem cell fates, whereas low PLT activity promotes their differentiation (Galinha *et al*., 2007). *PLT* expression is regulated by

auxin and is dependent on auxin response factors (Aida *et al*., 2004). An interaction network of *PINs* and *PLTs* functions in controlling auxin-mediated root patterning: PIN proteins restrict *PLT* expression in the basal embryo region to initiate the root primordium; in turn, *PLT* genes maintain *PIN* transcription, which stabilizes the position of the stem cell niche (Blilou et al., 2005; Dinneny and Benfey, 2008; Grieneisen *et al*., 2007).

I.1.3.7 Auxin and cytokinin cross-talk in maintenance of root meristem

A genetic framework has shown that cytokinin and auxin interact antagonistically to control the balance of cell division and differentiation in the root meristem. On the one hand, CK stimulates cell differentiation by suppressing auxin signalling and transport. On the other hand, auxin promotes cell division by inactivating CK signalling (Dello Ioio *et al.*, 2008; Moubayidin *et al*., 2009). During this interaction, CK and auxin regulate the size of root meristem tissue by means of the effect on the expression of *SHORT HYPOCOTYL 2 (SHY2/IAA3)*, a member of the Aux/IAA gene family (Tian *et al*., 2003; Dello Ioio *et al.*, 2008), which suppresses the expression of *PINFORMED* (*PIN*) auxin transport facilitator genes inducible by auxin. The mechanism is described as follows: in the transition zone (TZ), CK activates SHY2 transcription factor by means of ARR1, a member of cytokinin signaling regulators, which directly binds to the promoter of *SHY2* (Dello Ioio *et al*., 2008). Then, activation of *SHY2* inhibits *PIN* genes expressed in the TZ, causing the redistribution of auxin for cell differentiation (Dello Ioio *et al.*, 2008; Moubayidin *et al*., 2009). On the other hand, auxin mediates degradation of SHY2 protein and thereby stabilizes PIN expression levels (Tian *et al*., 2003; Dello Ioio *et al.*, 2008). Auxin influences the CK level because SHY2 down-regulates *IPT*, which is the rate-limiting enzyme in CK biosynthesis (Dello Ioio *et al*., 2008).

I.1.4 Flowering time regulation

Flowering is a central event in the life cycle of plants, representing the transition from vegetative growth to reproductive development. The process is accompanied by the transformation from SAM into an inflorescence meristem (IM). This transition is a result of responses to various endogenous and exogenous signals that later integrate to result in flowering. In *Arabidopsis*, flowering time

regulation occurs through two main pathways mediating environmental responses (photoperiod pathway and vernalization pathways) and two pathways that function independently of environmental cues: the autonomous pathway, which promotes flowering under all conditions, and the gibberellin (GA) pathway, which is needed for flowering under non-inductive short-day conditions. Additionally, light quality, ambient temperature, and biotic as well as abiotic stresses can also contribute to floral induction in plants (Srikanth and Schmid, 2011).

A number of signals controlling flowering converge in the regulation of the *FLOWERING LOCUS C* (*FLC)* gene, which encodes a MADS-box transcription factor and represses flowering through the repression of flowering time integrators *FLOWERING LOCUS T* (*FT*) and *SUPPRESSOR OF OVEREXPRESSION OF CO 1* (*SOC1*) (Michaels and Amasino, 1999, 2001; Searle *et al*., 2006). There are five close homologues of *FLC* in the *Arabidopsis* genome, and these are called *MADS AFFECTING FLOWERING1* (*MAF1*) to *MAF5* (Ratcliffe *et al*., 2003; Ratcliffe *et al*., 2001). In the vernalization (long exposure to low temperature) pathway, *FLC* and *MAF1* to *MAF4* act as floral repressors and might contribute to the maintenance of a vernalization requirement, while *MAF5* may play an opposite role to *FLC* (Ratcliffe *et al*., 2003). The autonomous pathway promotes flowering, independently of environmental conditions, by endogenous regulators such as FLD, FVE, FCA and FPA which act to repress the expression of *FLC* to accelerate flowering (Michaels and Amasino, 1999, 2001; Veley and Michaels, 2008). However, in the photoperiod pathway, long-day (LD) conditions accelerate flowering through the function of FT protein, and gibberellic acid signals play a major role in promoting flowering under short days (SDs) by regulating both *LFY* and *SOC1* expression (Lee *et al*., 2000; Moon *et al*., 2003) (Figure I.2).

FT protein is a major component of florigen, which is synthesized in the leaf vasculature and moves through the phloem to SAM (Corbesier *et al*., 2007). Mutations in *FT* cause a considerable delay in flowering, and overexpression of *FT* causes precocious flowering. This indicates that *FT* is necessary and sufficient to accelerate the floral transition (Kobayashi *et al*., 1999). The activation of *FT* requires the expression of *CONSTANS* (*CO*) and *GI*, *CO* encoding the zinc finger transcriptional regulator of the *FT* promoter (Tiwari *et al*., 2010). The activity of *CO* is responsive to light and the circadian clock. CO protein is stable in the light and rapidly degraded in the dark. And GI is a large plant-specific protein involved in circadian

clock function (Fowler *et al*., 1999). However, how *CO* regulates *FT* expression remains largely unknown. Recent research indicates that *Arabidopsis* Morf Related Gene (MRG) group proteins MRG1 and MRG2 interact with CO to activate *FT* expression in leaves (Bu *et al*., 2014). In the SAM, FT, by binding to the transcription factor FD, activates the expression of *LFY* and *AP1*, and thereby induces flowering (Corbesier *et al*., 2007; Kobayashi and Weigel, 2007; Wigge, 2011).

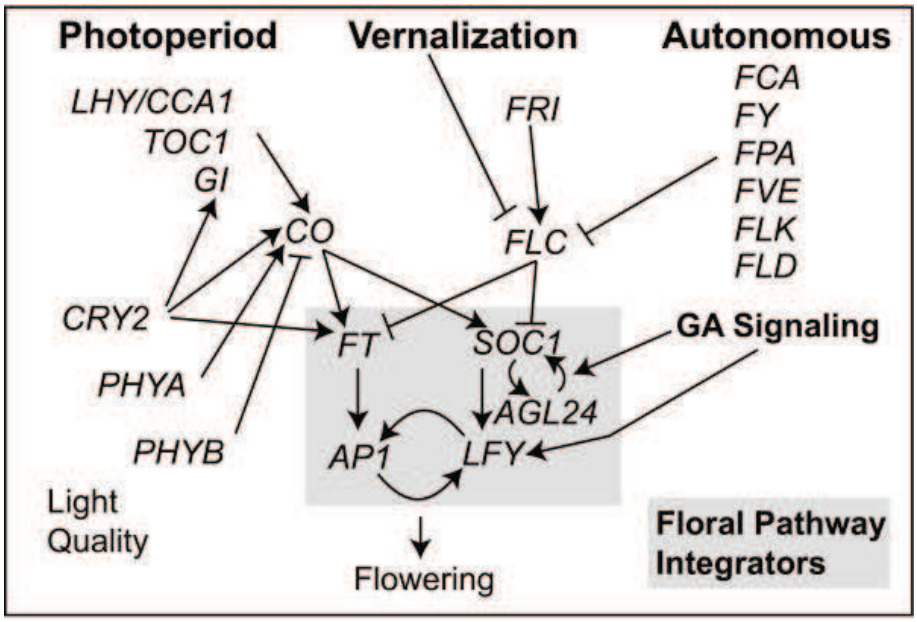

Figure I.2. A simplified schematic shows flowering time gene interactions in *Arabidopsis thaliana* (Ballerini and Kramer, 2011)

I.1.5 Flower development

Flowers are the reproductive structures of angiosperms. They are composed of four distinct types of organs: sepals, petals, stamens, and carpels. Floral organs are generated by a flower meristem (FM) (Jenik and Irish, 2000; Kwiatkowska, 2006), which is produced by IM. FMs arise from the main SAM and they are able to transform from one to another meristem (Nardmann and Werr, 2007; Prunet *et al*., 2009). KNOX homeodomain transcription factors keep meristematic cells in an undifferentiated state, while the WUS-CLV negative feedback loop maintains a constant population of stem cells in the SAM. These genes are expressed in a similar way in the FM compared to the SAM. Thus, during its first developmental stages, FM homeostasis seems to be achieved by roughly the same molecular mechanisms as it is in the SAM (Prunet *et al*., 2009).

However, the FM also differs from the SAM. The FM growth pattern is determinate; stem cells are only transiently maintained within the FM. At stage 6 of flower development (Smyth *et al*., 1990), *WUS* expression is shut off, which results in the disruption of floral stem cell maintenance. That is to say, the activity of the FM stops and floral meristems only form a fixed complement of organs. The differences between the SAM and FMs are determined by meristem identity genes, for example, *APETALA1* (*AP1*) or *LEAFY* (*LFY*) (Irish and Sussex, 1990; Schultz and Haughn, 1991; Weigel *et al*., 1992).

The MADS-box protein AG, which serves as a key factor in specifying the identities of stamens and carpels (Bowman et al., 1989), plays an essential role in terminating the floral meristem (Lenhard *et al*., 2001; Lohmann *et al*., 2001). In *ag* mutant flowers, the expression of *WUS* and *CLV3* is not down-regulated, but is rather continually expressed during the formation of many whorls of floral organs (Lenhard *et al*., 2001). Moreover, WUS can induce AG expression. Thus, AG and WUS form a negative feedback loop to terminate stem cell activity in flower buds. There are two parallel mechanisms: early in floral development, AG directly represses *WUS* expression by recruiting Polycomb group (PcG) complexes (Liu *et al*., 2011); later, AG activates the C2H2 zinc-finger-encoding *KNUCKLES* (*KNU*) gene, which in turn directly or indirectly represses *WUS* expression (Sun *et al*., 2009).

In addition to AG-WUS pathway, a number of other genes are also known for their functions in floral meristem regulation. These include *ULTRAPETALA1 (ULT1)*, *SUPERMAN (SUP)*, *CRABS CLAW* (*CRC*).

The *ULT1* gene encodes a SAND domain-containing protein, which is a negative regulator of stem cell accumulation in the floral meristem and maintains floral meristem determinacy (Carles *et al*., 2005). Loss-of-function of *ULT1* results in larger floral meristems with more floral organs than wild-type flowers and a decrease in floral meristem determinacy. Genetic and molecular studies revealed that *ULT1* negatively regulates the size of the *WUS*-expressing domain in the floral meristem. This repression may act upstream of *AG* and establish the proper floral meristem determinacy, acting through the WUS-AG temporal feedback loop (Carles *et al*., 2005).

I.2. Histone modifications consisting of small chemical moieties in chromatin-remodeling

Chromatin is a highly ordered structure found in cells, consisting of DNA, protein and RNA. The primary protein components of chromatin are histones. Histones are highly basic proteins, found in the nuclei of eukaryotic cells, which package and order the DNA into structural units named nucleosomes. A nucleosome is the most fundamental unit of chromatin and is composed of roughly 146 bp of DNA wrapped around the histone octamer comprising two molecules each of the four core histones H2A, H2B, H3 and H4 (Luger *et al*., 1997) (Figure I.3a).

I.2.1 Post translational modifications of histones

These core histones are predominantly globular except for the flexible, protruding, highly basic amino-terminal tails (histone H2A and H2B also have a carboxy-terminal tail). These histone tails are essential for the higher-order folding of chromatin fibres, and they also provide binding sites for non-histone regulatory proteins. They are subject to a vast array of post-translational modifications, such as: methylation, phosphorylation, acetylation and ubiquitination (Figure I.3b). In addition, modifications also occur in their globular domains (Marks *et al*., 2001). These modifications can occur at many sites and have different biochemical functions, but not all will be on the same histone at the same time. The timing of the appearance of a modification will depend on the signaling conditions within the cell. Modifications on histones are dynamic and rapidly changing. They can appear and disappear on chromatin within minutes following a stimulus arriving at the cell surface. Histone modifications can affect genome function via at least two distinct mechanisms: the first by disrupting contacts between nucleosomes, thereby loosening chromatin structure and promoting transcriptional activity; the second by serving as docking sites for recruiting nonhistone proteins to relevant genomic loci (Kouzarides, 2007; Laugesen and Helin, 2014).

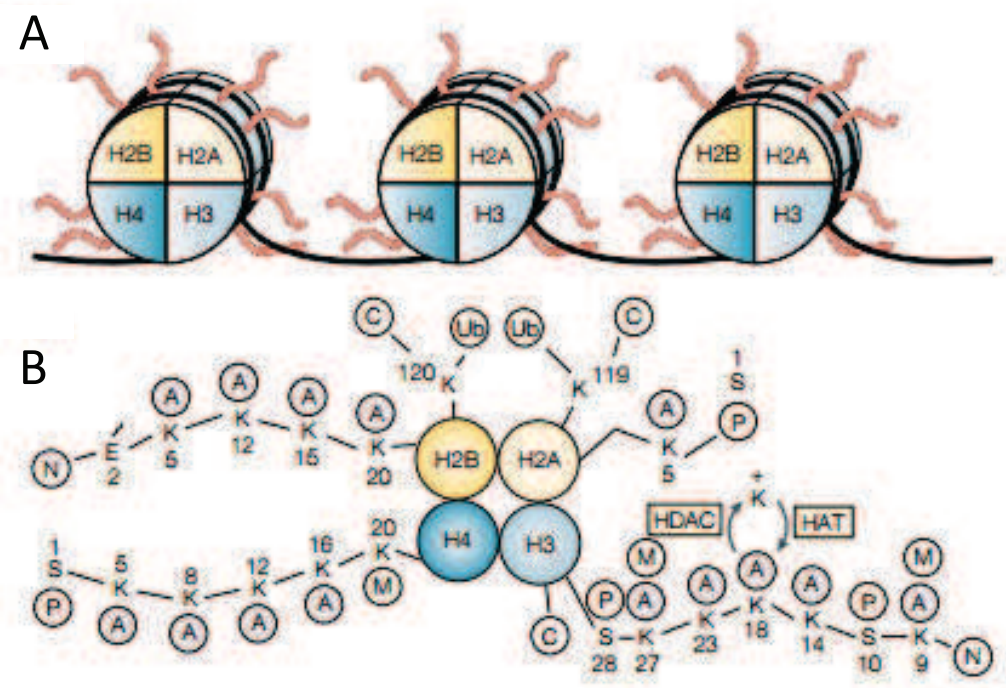

Figure I.3. Schematic of histone structure in nucleosomes

A. The core proteins of nucleosomes are designated H2A (histone 2A), H2B (histone 2B), H3 (histone 3) and H4 (histone 4). Each histone is present in two copies, so the DNA (black) wraps around an octamer of histones - the core nucleosome.

B. The amino-terminal tails of core histones. Lysines (K) in the amino-terminal tails of histones H2A, H2B, H3 and H4 are potential acetylation/deacetylation sites for histone acetyltransferases (HATs) and histone deacetylases (HDACs). Acetylation neutralizes the charge on lysines. A, acetyl; C, carboxyl terminus; E, glutamic acid; M, methyl; N, amino terminus; P, phosphate; S, serine; Ub, ubiquitin. (Adapted from Marks *et al*., 2001)

I.2.1.1 Histone methylation/demethylation

Histone methylation is a process by which methyl groups are transferred to amino acids of histone proteins of chromosomes . This reaction is catalyzed by histone methyltransferases (HMTs) which can be classified into three types: the lysine-specific SET domain containing HMTs, the non-SET domain-containing lysine HMTs, and the arginine HMTs. Histones can be methylated on lysine (K) and arginine (R) residues, but methylation is most commonly observed on lysine residues of the tails of histones H3 and H4. In particular, lysine methylation at H3K4, H3K9, H3K27, H3K36, and H4K20 is mediated by lysine methyltransferases (KMTs) that contain a SET domain. The SET domain was first identified as a shared sequence motif in three *Drosophila* proteins, suppressor of variegation [Su (var) 3–9], enhancer of zeste

[E(z)], and homeobox gene regulator trithorax [Trx] (Martin and Zhang, 2005). These lysines can be either mono-(K^{me1}), or di-(K^{me2}), or tri-methylated (K^{me3}). These incremental methylation states can lead to diverse outcomes. According to recent findings, H3K9, H3K27, and H4K20 methylation is associated mainly with repressed transcription, whereas methylation of H3K4 and H3K36 is associated with activated transcription (Guenther *et al*., 2007). Histone methylation is a process that can be reversed by histone lysine demethylases (KDMs) to eliminate methylation. So far, there are more than 50 human KMTs and 30 KDMs that have been identified (Arrowsmith *et al.*, 2012; Spannhoff *et al*., 2009). KDMs contain two major families: the KDM1 family including KDM1A/LSD1 and KDM1B/LSD2, and the Jumonji C (JmjC) domain-containing protein family including 14 members of KDMs. KDMs and KMTs work coordinately to maintain normal global histone lysine methylation levels and to regulate gene expression patterns.

I.2.1.2 Histone acetylation/deacetylation

Acetylation was the first histone modification to beidentified. Acetylation and deacetylation of lysine residues on histone 3 and histone 4 at the N-terminal tail have been shown to play a regulatory role in gene activation and repression, respectively. This reversible modification is the result of the fine-tuned balance of the activities of histone acetyltransferases (HATs) and histone deacetylases (HDACs). Histone acetylation is usually carried out by protein complexes involving HATs utilizing acetyl Coenzyme-A (acetyl-CoA) as a cofactor. In histone acetylation, HAT molecules facilitate the transfer of an acetyl group from a molecule of acetyl-CoA to the $NH3^{+}$ group on Lysine. In histone deacetylation the acetyl group can be transferred back to CoA or to ADP-ribose by NAD-dependent deacetylases (Denu, 2003).

The effect of acetylation is to change the overall charge of the histone tail from positive to neutral, thus decreasing its affinity for DNA. This leads to a change in nucleosomal conformation thereby increasing the accessibility of transcriptional regulatory proteins to the chromatin template. Thus, acetylation of histones is known to increase the expression of genes through transcription activation (Fukuda *et al*., 2006). Following deacetylation of the histone tails, the DNA becomes more tightly wrapped around the histone cores, making it more difficult for transcription factors to bind to the DNA. This leads to decreased levels of gene expression and is known as gene silencing.

HATs are classified into two categories based on their subcellular distribution (Roth *et al*., 2001). The type A HATs, including the Gcn5-related N-acetyltransferases (GNAT), MYST (MOZ, Ybf2/Sas3, Sas2, Tip60), p300/CBP and basal transcription factors (including TFIID), are responsible for acetylation of nuclear histones and thus are directly involved in regulating chromatin assembly and gene transcription (Carrozza *et al.*, 2003). Type B HATs contains nuclear receptor cofactors. They act on newly synthesized histones before incorporation. The HDAC family consists of 18 members in humans which are grouped into four classes (Gregoretti *et al*., 2004): the class I includes HDACs 1, 2, 3, and 8. These enzymes are closely related to the yeast transcriptional regulator Rpd3. The class II is divided into two subgroups, class IIA and class IIB. Class IIA includes HDACs 4, 5, 7, and 9, while Class IIB includes HDACs 6 and 10. All these enzymes are closely related to the yeast Hda1. The class III HDACs are sirtuin family enzymes with 7 members. They are related to the yeast transcriptional repressor Sir2 (Silent information regulator 2) and are NAD^+-dependent. Class IV contains only HDAC11. Although it is related to HDACs 3 and 8, its overall sequence is quite different from the other HDACs.

I.2.1.3 Histone phosphorylation/dephosphorylation

Phosphorylation of histones is also highly dynamic. All four core histones have been shown to be phosphorylated, at their N-terminal tails, on specific serine, threonine and tyrosine residues by a number of protein kinases and dephosphorylated by phosphatases (Oki *et al*., 2007). Phosphorylation on serine is the most common. The phosphorylation reaction transfers a phosphate group from ATP to the hydroxyl group of the target amino-acid side chain by histone kinases. This adds a significant negative charge to the histone and influences the chromatin structure.

Histone phosphorylation is correlated with various cell activities, such as mitosis, meiosis, cell death, DNA repair, recombination, replication and transcription. In these processes, so far only phosphorylation on serine 10 of histone H3 has been linked with transcriptional activation (Prigent and Dimitrov, 2003). Moreover, research indicates that it has a role opposite to transcriptional activation. During mitosis, phosphorylation of this serine residue condenses chromosomes. All this suggests that its effect is context-dependent and might be influenced by other histone modifications (Johansen and Johansen, 2006).

I.2.2 Crosstalk between histone modifications

Although an individual histone modification may have its own downstream effectors or specific roles, the development of organisms is a complex network, which usually requires that the various epigenetic marks work together. Cross regulation between different modifications can produce different outcomes: either in a compatible or a mutually exclusive manner, at the single histone tail level or in the context of the nucleosome or even the chromatin level.

Flowering time is the best studied process for crosstalks, with interactions between several kinds of histone modifications. For instance, *FLC* is a key player for flowering; its expression level is regulated by histone H2B monoubiquitination (H2Bub1) and H3 methylation at the *FLC* locus. In *Arabidopsis*, the loss of H2Bub1 on *FLC* chromatin results in a decrease in H3K4me3 and H3K36me2/3 (Cao *et al*., 2008; Gu *et al*., 2009; Schmitz *et al.*, 2009). *FLOWERING LOCUS D* (*FLD*) is known to influence histone methylation and acetylation in the autonomous pathway (He *et al*., 2003; Liu *et al*., 2007; Yu *et al*., 2011). Lesions in *FLD* result in hyperacetylation of histones and a decreased level of H3K27me3 on *FLC* chromatin (He *et al*., 2003). In addition, crosstalks between methylated residues also happen in flowering time regulation. Deletion of *FLD* increases H3K4me3 levels and reduces H3K27me3 levels (Liu *et al*., 2007; Yu *et al*., 2011). And reduction of H3K4me3 in *atx1* or *sdg25* mutants results in an increase of H3K27me3 on *FLC* (Pien *et al*., 2008).

I.2.3 Histone modifications in plant developmental regulation

Histone modifications influence almost every process in plant development. In the earliest phase of plant development, histone modifications are required for establishing the correct body plan during embryogenesis (Köhler and Makarewitch, 2006; Tai *et al*., 2005). During later stages of the plant life cycle, histone modifications influence patterning of down-ground or the overground structures (Xu *et al*., 2005; Xu and Shen, 2008), flowering time (Cao *et al*., 2008; Gu *et al*., 2009; Xu *et al*., 2009) and fertilization (Köhler and Makarewitch, 2006)

At the cellular level, there is much evidence that the cell cycle (Fleury *et al*., 2007; Sanchez *et al*., 2008), cell division (Alatzas and Foundouli, 2006), cell expansion and cell differentiation (Shen and Meyer, 2004; Xu and Shen, 2008) are partly regulated by histone modifications. During these regulations, not only different

histone modifications cross-talk, but histone modifications are also correlated with the action of most plant hormones.

For instance, the first identified plant PcG protein, CURLY LEAF (CLF), a methyltransferase with specificity for H3K27, is involved in many aspects of development processes. The *clf* mutant causes pleiotropic effects on leaf and flower morphology as well as on flowering time. *CLF* controls these processes via repressing *AG* and *STM* by H3K27me3 (Goodrich *et al*., 1997; Schubert *et al*., 2006). Moreover, silencing of *AG* and *STM* is reflected in reduced enrichment of H3K4me2 (Gendrel et al., 2002. In addition, *STM* has been shown to be a positive factor of cytokinin biosynthesis (Jasinski *et al*., 2005; Yanai *et al*., 2005); therefore silencing *STM* affects the concentration of cytokinin.

I.3. Histone ubiquitination and roles in plant developmental regulation

Histone ubiquitination has a particular interest. This modification is diverse, as it can involve one single ubiquitin molecule (monoubiquitination) or one ubiquitin at multiple sites of the same substrate (multi-monoubiquitination), or chains of ubiquitin (polyubiquitination). The most famous fate of ubiquitinated proteins is their degradation by the 26S proteasome, an ATP-dependent proteolytic machinery that degrades the target protein with concomitant release of the ubiquitin moieties for reuse. Lysine 48-linked chains on the target proteins serve as a signal which is recognized by specific subunits of the 26S proteasome (Smalle and Viestra, 2004). However, there are other modifications such as polyubiquitination with different linkages (Lysine 63-linked chains) or monoubiquitination. Ubiquitination is highly controlled and can be reversed by the action of deubiquitinating enzymes or deubiquitinases (Nijman *et al.*, 2005).

I.3.1 H2A and H2B monoubiquitination in plant developmental regulation

frontiers in
PLANT SCIENCE

REVIEW ARTICLE
published: 13 March 2014
doi: 10.3389/fpls.2014.00083

Dynamic regulation and function of histone monoubiquitination in plants

Jing Feng and Wen-Hui Shen*

Institut de Biologie Moléculaire des Plantes, UPR2357 CNRS, Université de Strasbourg, Strasbourg, France

Edited by:
Hongyong Fu, Institute of Plant and Microbial Biology – Academia Sinica, Taiwan

Reviewed by:
Keqiang Wu, National Taiwan University, Taiwan
Hongyong Fu, Institute of Plant and Microbial Biology – Academia Sinica, Taiwan

***Correspondence:**
Wen-Hui Shen, Institut de Biologie Moléculaire des Plantes, UPR2357 CNRS, Université de Strasbourg, 12 rue du Général Zimmer, 67084 Strasbourg Cedex, France
e-mail: wen-hui.shen@ibmp-cnrs.unistra.fr

Polyubiquitin chain deposition on a target protein frequently leads to proteasome-mediated degradation whereas monoubiquitination modifies target protein property and function independent of proteolysis. Histone monoubiquitination occurs in chromatin and is in nowadays recognized as one critical type of epigenetic marks in eukaryotes. While H2A monoubiquitination (H2Aub1) is generally associated with transcription repression mediated by the Polycomb pathway, H2Bub1 is involved in transcription activation. H2Aub1 and H2Bub1 levels are dynamically regulated *via* deposition and removal by specific enzymes. We review knows and unknowns of dynamic regulation of H2Aub1 and H2Bub1 deposition and removal in plants and highlight the underlying crucial functions in gene transcription, cell proliferation/differentiation, and plant growth and development. We also discuss crosstalks existing between H2Aub1 or H2Bub1 and different histone methylations for an ample mechanistic understanding.

Keywords: chromatin, epigenetics, ubiquitin, histone monoubiquitination, transcription regulation, plant develop-

INTRODUCTION

Ubiquitin (Ub) and Ub-like (e.g., SUMO) proteins constitute a family of modifiers that are linked covalently to target pro- teins. Although ubiquitination (also called ubiquitylation or ubiquitinylation) first came to light in the context of protein destruction, it is now clear that ubiquitination can also carry out proteolysis-independent functions. Ubiquitination can alter biochemical, molecular and/or subcellular localization activi- ties of a target protein. The first ubiquitinated protein to be described was histone H2A in calf thymus, a finding dated more than 36 years ago (Goldknopf et al., 1975; Hunt and Dayhoff, 1977). Yet, only more recently have the underlying mechanisms and regulatory functions of histone ubiquitination begun to emerge (reviewed in Zhang, 2003; Shilatifard, 2006; Weake and Workman, 2008; Braun and Madhani, 2012; Pin- der et al., 2013). Histones are highly alkaline proteins, found in the nuclei of eukaryotic cell, which package and order the DNA into structural units named nucleosomes. A nucle- osome is composed of roughly 146 bp of DNA wrapping around the histone octamer comprising two molecules each of the four core histones H2A, H2B, H3, and H4 (Luger et al., 1997). Histone monoubiquitination together with other types of posttranslational modifications, e.g., acetylation, methyla- tion, phosphorylation, and SUMOylation, can modulate nucleo- some/chromatin structure and DNA accessibility and thus regulate diverse DNA-dependent processes, such as genome replication, repair, and transcription (Zhang, 2003; Shilatifard, 2006; Weake and Workman, 2008; Braun and Madhani, 2012; Pinder et al., 2013).

substrate/acceptor protein, a reaction involving three coordinated
enzymatic activities (reviewed in Hershko and Ciechanover, 1998). Ub is first activated by an ATP-dependent reaction involving the Ub-activating enzyme E1, then conjugated to the active site cys- teine residue of the Ub-conjugating (UBC) enzyme E2, and finally transferred to the target K residue of the substrate protein by the Ub-protein isopeptide ligase E3. Most organisms have only one E1, but dozens of different E2 and hundreds up to thousands of different E3 enzymes, providing the need in coping with effec- tive substrate specificity (Hua and Vierstra, 2011; Braun and Madhani, 2012). Identification and characterization of E3s and some E2s involved in histone ubiquitination had been a key for understanding biological functions of histone ubiquitination in various organisms. Because of its suitability for genomics, genet- ics, and cellular and molecular biological approaches, *Arabidopsis thaliana* is an ideal model to investigate histone ubiquitination functions. In this review, we focus on this

H2B MONOUBIQUITINATION IN *Arabidopsis*

GENOME-WIDE DISTRIBUTION OF H2Bub1

Monoubiquitinated H2B (H2Bub1) was first discovered in mouse cells and was estimated to represent about 1–2% of total cellular H2B (West and Bonner, 1980). Later, H2Bub1 was detected widely throughout eukaryotes spanning from yeast to humans and plants (Zhang, 2003; Shilatifard, 2006; Srid- har et al., 2007; Zhang et al., 2007a; Weake and Workman, 2008). The ubiquitination site is mapped to a highly con- served K residue, H2BK123 in budding yeast, H2BK119 in fission yeast, H2BK120 in

Genome-wide analysis revealed that in *Arabidopsis* as in animals
H2Bub1 is associated with active genes distributed throughout the genome and marks chromatin regions notably in combina- tion with histone H3 trimethylated on K4 (H3K4me3) and/or with H3K36me3 (Roudier et al., 2011). During early photomor- phogenesis, gene upregulation was found to be associated with H2Bub1 enrichment whereas gene downregulation did not show detectable correlation with any H2Bub1 level changes (Bourbousse et al., 2012). In general, H2Bub1 is considered to represent an active chromatin mark

ENZYMES INVOLVED IN REGULATION OF H2Bub1 LEVELS

The budding yeast Rad6 (radiation sensitivity protein 6) was the first factor identified and shown to work as an E2 enzyme involved in catalyzing H2Bub1 formation both *in vitro* and *in vivo* (Robzyk et al., 2000). It contains a highly conserved catalytic UBC domain of approximately 150 amino acids in length with an active-site cysteine for linking Ub. The E3 enzyme working together with Rad6 in catalyzing H2Bub1 formation in budding yeast is Bre1 (Brefeldin-A sensitivity protein 1), which contains a C3HC4-type RING finger domain typical for all E3s (Hwang et al., 2003; Wood et al., 2003). The depletion of either Rad6 or Bre1 eliminates genome-wide H2Bub1 and causes yeast cell growth defects (Robzyk et al., 2000; Hwang et al., 2003; Wood et al., 2003). Human contains at least two homologs of Rad6, namely hHR6A and hHR6B, and two homologs of Bre1, namely RNF20/hBRE1A and RNF40/hBRE1B (Kim et al., 2005; Zhu et al., 2005). In *Arabidopsis*, three homologs of Rad6, namely UBC1, UBC2, and UBC3, were identified and UBC1 and UBC2 but not UBC3 were shown to be redundantly responsible for H2Bub1 formation *in planta* (Cao et al., 2008; Gu et al., 2009; Xu et al., 2009). The two Bre1 homologs HUB1 (HISTONE MONOUBIQUITINATION 1) and HUB2 work non-redundantly, possibly as a hetero-tetramer composed of two copies of HUB1 and two copies of HUB2, in catalyzing H2Bub1 formation in *Arabidopsis* (Fleury et al., 2007; Liu et al., 2007; Cao et al., 2008). H2Bub1 levels are drastically reduced or undetectable in Western blot analysis in the loss-of-function *hub1* and *hub2* single mutants as well as in the *hub1 hub2* and *ubc1 ubc2* double mutants, but are unaffected in the *ubc1*, *ubc2,* and *ubc3* single mutants or in the *ubc1 ubc3* and *ubc2 ubc3* double mutants (Cao et al., 2008; Gu et al., 2009; Xu et al., 2009).

H2Bub1 levels are also regulated by deubiquitination enzymes. Two Ub-specific proteases, Ubp8 and Ubp10, are involved in deubiquitination of H2Bub1 in budding yeast. Strik- ingly, while Ubp8 acts as a component of the SAGA (Spt-Ada-Gcn5-acetyltransferase) complex specifically in H2Bub1 deubiquitination in transcription activation, Ubp10 functions independently of SAGA and primarily acts in Sir-mediated silenc- ing of telomeric and rDNA regions (reviewed in Weake and Workman, 2008). In human, USP22 acts as Ubp8 ortholog in a SAGA complex in H2Bub1 deubiquitination (Weake and Workman, 2008). In *Arabidopsis*, although a SAGA complex remains uncharacterized so far, the Ub protease UBP26/SUP32 has been shown to deubiquitinate H2Bub1 involved in both activation of the *FLC* (*FLOWERING* LOCUS C) gene (Schmitz et al., 2009). More recently, the otubain-like deubiquitinase OTLD1 was reported as implicated in deubiquitination of H2BUb1 and repression of *At5g39160*, a gene of unknown function (Krichevsky et al., 2011).

ROLE OF H2Bub1 IN FLOWERING TIME REGULATION

The timing of flowering is critical for the reproductive success of plants. As compared to wild type, the *hub1* and *hub2* sin- gle mutants as well as the *hub1 hub2* and *ubc1 ubc2* double mutants exhibit an early flowering phenotype whereas but the *ubc1*, *ubc2,* and *ubc3* single mutants and the *ubc1 ubc3* and *ubc2 ubc3* double mutants have a normal phenotype (Cao et al., 2008; Gu et al., 2009; Xu et al., 2009). This early flowering phenotype is detectable under both long-day and short-day photoperiod plant growth conditions. Molecular analyses of the mutants indicate that H2Bub1 controls flowering time primarily through transcriptional activation of *FLC* (**Figure 1**). *FLC* encodes a key transcrip- tion repressor involved in both the autonomous/developmental and vernalization flowering pathways, and its active transcrip-tion is associated with several histone marks, e.g., H3K4me3, H3K36me2/3 and H2Bub1 (reviewed in Berr et

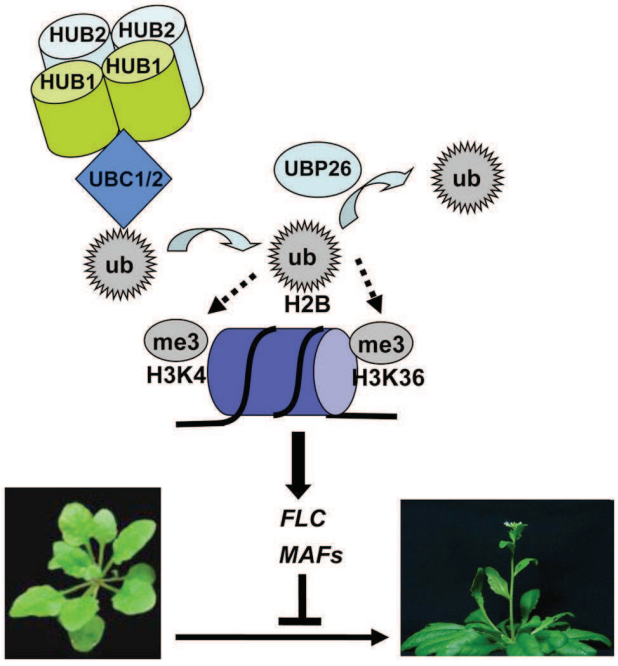

FIGURE 1 | A proposed model for deposition and removal of histone H2B monoubiquitination in transcriptional activation of *FLC* and *MAFs* in flowering time regulation. In this model, HUB1 and HUB2 form a heterotetramer and recruit UBC1 or UBC2 to *FLC*/*MAFs* chromatin, leading to transfer of a ubiquitin (ub) monomer from UBC1 or UBC2 onto H2B. H2Bub1 formation enhances H3K4me3 deposition by methyltransferases, together promoting transcription initiation. UBP26 removes ubiquitin on H2B, favoring H3K36me3 deposition in promoting transcription elongation. Active transcription of *FLC/MAFs* represses *Arabidopsis* flowering, a transition from vegetative to reproductive plant development.

ubc2, *FLC* expression levels are reduced and the *FLC* chromatin shows reduced H2Bub1 levels (Cao et al., 2008; Gu et al., 2009). The loss-of-function mutant *ubp26/sup32* showed also an early flowering phenotype and reduced *FLC* expression but an elevated level of H2Bub1 in the *FLC* chromatin (Schmitz et al., 2009), indicating that not only H2Bub1 formation but also H2Bub1 removal are necessary for *FLC* transcription. Accompanying H2Bub1 reduction compromised levels of H3K4me3 and to a less extent H3K36me2 were detected at *FLC* in *hub1* and *ubc1 ubc2* (Cao et al., 2008), and reduced level of H3K36me3 but elevated level of H3K27me3 was observed at *FLC* in *ubp26/sup32* (Schmitz et al., 2009). On parallels to the knowledge in yeast, it was proposed that the UBC-HUB-mediated H2Bub1 formation is necessary for H3K4me3 deposition at transcription initiation whereas UBP26/SUP32-mediated H2Bub1 removal is required for H3K36me3 deposition during transcription elongation (Cao et al., 2008; Schmitz et al., 2009). Nonetheless, this hierarchy of histone modifications needs to be cautioned because multiple factors are involved in H3K4me3 and H3K36me2/3 depositions and the SDG8 (SET DOMAIN GROUP 8)-mediated H3K36me2/3 deposition remarkably override H3K4me2/3 deposition in *FLC* transcription (Yao and Shen, 2011; Shafiq et al., 2014).

MAF4 and *MAF5*. Some *MAFs* are also downregulated in early flowering mutants *hub1*, *hub2*, *hub1 hub2*, *ubc1 ubc2,* and *ubp26/sup32* (Cao et al., 2008; Gu et al., 2009; Schmitz et al., 2009; Xu et al., 2009). Thus, H2Bub1 may also regulate flowering time through control of *MAF* gene expression under some plant growth conditions.

H2Bub1 FUNCTION IN OTHER PROCESSES

In addition to flowering, many processes also involve other H2Bub1 as evidenced by the *Arabidopsis hub1* studies of and *hub2* mutants. The display reduced seed dormancy associated with reduced expression of several dormancy-related genes, including *DOG1* (*DELAY OF GERMINATION 1*), *ATS2* (*ACYLTRANSFERASE 2*), *NCED9* (*NINE-CIS-EPOXYCAROTENOID DIOXYGENASE 9*), *PER1* (*CYSTEINE PEROXIREDOXIN 1*), and *CYP707A2* (Liu et al., 2007). At vegetative growth stages, the *hub* mutants exhibit pale leaf coloration, modified leaf shape, reduced rosette biomass, and inhibited root growth (Fleury et al., 2007). Cell cycle genes, particularly some key regulators of the G2-to-M transition, are downregulated, which could largely explain the plant growth defects of the *hub* mutants (Fleury et al., 2007). A more recent study shows that several circadian clock genes, including *CCA1* (*CIRCADIAN CLOCK ASSOCIATED 1*), *ELF4* (*EARLY FLOWERING 4*) and *TOC1* (*TIMING OF CAB EXPRESSION 1*), are downregulated and their chromatin regions contain lower levels of H2Bub1 in the *hub* mutants, suggesting that H2Bub1 may contribute to the regulation of plant growth fitness to environment through expression modulation of some circadian clock genes (Himanen et al., 2012). It is worth to note that SDG2-mediated H3K4me3 deposition is also required for expression of several circadian clock genes (e.g., circadian clock genes (Himanen et al., 2012; Malapeira et al., 2012).

During photomorphogenesis, hundreds of genes show upregulation associated with H2Bub1 enrichment in their chromatin in response to light exposure (Bourbousse et al., 2012). Strikingly, over 50% of these genes gain H2Bub1 enrichment upon the 1 h of illumination, illustrating the highly dynamic nature of H2Bub1 deposition during a likely cell division-independent genome regrogramming process. In contrast to the above discussed cases, in this study the H2Bub1 changes is neither accompanied by any detectable changes of H3K36me3 nor required for H3K4me3 enrichment following six hours of light exposure (Bourbousse et al., 2012). In line with the function of H2Bub1 in gene activation in response to light, the *hub1-3* mutant seedlings are overly light sensitive, exhibiting a photobleaching phenotype (Bourbousse et al., 2012).

The *hub1* mutants also show increased susceptibility to the necrotrophic fungal pathogens *Botrytis cinerea* and *Alternaria brassicicola* (Dhawan et al., 2009). Precise role of H2Bub1 in plant defense against pathogens still remains largely unclear. Structure defects, e.g., thinner cell walls and altered surface cutin and wax compositions, together with impaired induction of some defense genes might have partly contributed to the increased susceptibility to pathogen infection in the *hub* mutant plants (Dhawan et al., 2009; Ménard et al., 2014). It is worthy noting that the *sdg8* mutants impaired in H3K36me3 deposition also display reduced resistance to necrotrophic fungal pathogen infection (Berr et al., 2010, 2012; Palma et al., 2010). It will be interesting to study in future research whether

MECHANISMS OF H2Bub1 IN TRANSCRIPTION REGULATION

So far only limited information is available concerning how H2Bub1 enzymes are recruited to the target chromatin. The evolutionarily conserved PAF1 (Polymerase Associated Factor 1) complex interacts with Pol II (RNA polymerase II) and plays a role as a "platform" for association of enzymes involved in H2bub1, H3K4me3, and H3K36me2/3 deposition, linking histone modifications with active transcription (Shilatifard, 2006; Weake and Workman, 2008; Berr et al., 2011; Braun and Madhani, 2012). A direct interaction between PAF1 complex and Rad6-Bre1 has been detected and shown as required for catalyzing H2Bub1 formation (Xiao et al., 2005). As in yeast and animals, deletion or knockdown of PAF1 components markedly reduces H2Bub1 in *Arabidopsis* (Schmitz et al., 2009). Genetic analysis shows that *HUB2* and *ELF8* encoding a PAF1 subunit act in a same floral-repression pathway in *Arabidopsis* flowering time regulation (Gu et al., 2009). Although physical interaction between UBC-HUB and PAF1 needs future investigation, interactions were observed between UBC and HUB (Cao et al., 2008) and between HUB and MED21 (mediator complex subunit 21), a subunit of the evolutionarily conserved Mediator complex (Dhawan et al., 2009). Mediator complex is associated with both general transcription factors and Pol II and is essential for activator-dependent transcription in all

interactors are generally involved in Pol II transcribed genes and thus cannot fully explain why UBC-HUB targets some but not all active genes. It is reasonable to speculate that UBC-HUB recruitment might also involve some gene-specific yet uncharacterized factors.

The next question is how H2Bub1 affects transcription. In yeast and animals, H2Bub1 can promote transcription elongation by enhancing the recruitment of RNA Pol II and by facilitat- ing nucleosome removal through interplay with FACT (facilitates chromatin transcription), an evolutionarily conserved histone chaperone complex (Pavri et al., 2006; Tanny et al., 2007). FACT acts on displacement of H2A/H2B dimer from a nucleosome core, facilitating transcription elongation on chromatin template. In *Arabidopsis*, FACT genetically interacts with HUB1 and plays criti- cal roles in multiple plant developmental processes (Lolas et al., 2010). Yet its precise interplay with H2Bub1 in transcription regulation needs future investigations.

Alternatively or additionally, H2Bub1 may regulate transcription indirectly through crosstalk with H3K4me3 and H3K36me2/3 (Shilatifard, 2006; Weake and Workman, 2008; Berr et al., 2011; Braun and Madhani, 2012). In line with this idea, lack of H2Bub1 in *Arabidopsis* impairs H3K4me3 and H3K36me2 formation in chromatin at *FLC* and clock genes (Cao et al., 2008; Himanen et al., 2012), and elevated H2Bub1 inhibits H3K36me3 formation in the *FLC* chromatin (Schmitz et al., 2009). Nevertheless, in contrast to the requirement of H2Bub1 for genome-wide H3K4me3 formation in yeast, lack of H2Bub1 in *Arabidopsis* barely affects global H3K4me2/3 and H3K36me2/3 levels, as evidenced by Western blot analysis (Cao et al., 2008; Dhawan et al., 2009; Gu et al., 2009) as well as by ChIP (chromatin immunoprecipitation) analysis of light responsive genes during photomorphogenesis (Bourbousse et al., 2012). It is currently unclear to which extent applies the crosstalk of H2Bub1 with H3K4me2/3 and H3K36me2/3 in *Arabidopsis* gene transcription regulation and what are the molecular mechanisms underlying the crosstalk.

Finally, while H2Bub1 is generally associated with active gene transcription, it can also regulate transcription repression in a chromatin context-dependent manner. The *ubp26/sup32* mutant shows release of transgene and transposon silencing (Sridhar et al., 2007) as well as elevated expression of *PHE1* (*PHERES1*) associated with seed developmental defects (Luo et al., 2008). It has been shown that the silencing release is accompanied by reduction of H3K9me2 and of siRNA-mediated DNA methylation and the *PHE1* expression elevation is associated with a reduced level of H3K27me3. Nevertheless, whether these changes of repressive marks are directly linked with H2Bub1 still need to be

H2A MONOUBIQUITINATION IN *Arabidopsis*

PRESENCE OF H2Aub1

In contrast to H2Bub1, H2Aub1 has not been found in yeast and has been generally implicated in transcription repression in ani- mal cells (Weake and Workman, 2008; Braun and Madhani, 2012). Albeit its early discovery and high abundance (about 5–15% of the total H2A) in animal cells (Goldknopf et al., 1975; Hunt and Dayhoff, 1977; Zhang, 2003), H2Aub1 function has only more recently begun to be elucidated, thanking to the first of the human PRC1 (Polycomb repressive complex 1) component Ring1B (also known as Ring2 and RNF2) as a E3 involved in catalyzing H2Aub1 formation (Wang et al., 2004). In *Arabidopsis*, H2Aub1 was undetectable in a large-scale analysis of histone post- translational modifications by mass spectrometry (Sridhar et al., 2007; Zhang et al., 2007a) and had been thought for a long time to be non-existent (Weake and Workman, 2008). However, five PRC1-like RING-finger proteins, namely AtRING1a, AtRING1b, AtBMI1a, AtBMI1b, and AtBMI1c, have been identified in *Ara- bidopsis* (Sanchez-Pulido et al., 2008; Xu and Shen, 2008). More recent immunodetection and *in vitro* enzyme activity assays have revealed that these RING-finger proteins are effectively involved in catalyzing H2Aub1 formation in *Arabidopsis* (Bratzel et al., 2010; Li et al., 2011;

PRC2 AND PRC1 IN H2Aub1 DEPOSITION

Polycomb group (PcG) proteins, first identified in *Drosophila* as repressors of homeotic (*Hox*) genes, are nowadays known to act in multiprotein complexes in transcription repression of a large number of genes in many multicellular organisms including plants (Bemer and Grossniklaus, 2012; Molitor and Shen, 2013; Schwartz and Pirrotta, 2013; Simon and Kingston, 2013). The most intensively studied complexes are PRC1 and PRC2. In *Drosophila*, PRC2 is composed of four core subunits, namely Ez (Enhancer of zeste), Suz12 (Suppressor of zeste 12), Esc (Extra sex combs) and N55 (a 55 kDa WD40 repeat protein), and PRC1 also contains four main subunits, namely Pc (Polycomb), Ph (Polyhomeotic), Psc (Posterior sex combs) and Ring1 (also known as dRing). In mammals, alternate subunit compositions create larger families of related PRC2-type and PRC1-type complexes (Schwartz and Pirrotta, 2013; Simon and Kingston, 2013). Nevertheless, defined biochemical activities of PRC2 and PRC1 are conserved from flies to humans. The clas- sical model proposes a sequential mode of action of the two complexes: PRC2 catalyzes H3K27me3 formation, and PRC1 rec- ognizes the H3K27me3 mark and further mediates downstream H2Aub1 deposition. The PRC1 components, acting as E3 ligases in H2Aub1 formation, are RING-finger proteins: Ring1 in *Drosophila* and Ring1A and Ring1B in human (Braun and Madhani, 2012; Schwartz and Pirrotta, 2013).

In *Arabidopsis*, the four PRC2 core components are highly con- served (**Figure 2**) and encoded by small gene families, and their function in H3K27me3 deposition and transcription repression have been intensively studied (Bemer and Grossniklaus, 2012). In contrast, PRC1 compositions are drastically diverged in plants as compared to animals (Molitor and Shen, 2013). No sequence homologue of Ph could be identified in plants so far. LHP1 (LIKE HETEROCHROMATIN PROTEIN 1), also known as TFL2 (TERMINAL FLOWER 2), binds H3K27me3 and may play a Pc-like function (Turck et al., 2007; Zhang et al., 2007b). This remark- ably differs from the distinct roles of HP1 and Pc in animals, where HP1 binds H3K9me3 involved in hetereochromatin for- mation whereas Pc binds H3K27me3 involved in PRC1-mediated silencing in euchromatin. The best

These RING-finger proteins can be classified into two phylogenic groups: the first group comprises *Drosophila* Ring1, human Ring1A and Ring1B, and *Arabidopsis* AtRING1a and AtRING1b; the second group comprises *Drosophila* Psc, human Bmi1, and *Arabidopsis* AtBMI1a, AtBMI1b, and AtBMI1c. Consistent with their sequence conservation, AtRING1a, AtRING1b, AtBMI1a, and AtBMI1b each can ubiquitinate H2A *in vitro*, and loss of function of *AtBMI1a* and *AtBMI1b* causes H2Aub1 reduction *in planta* (Bratzel et al., and embryonic callus formation in somatic tissues of the *Atring1a Atring1b* and *Atbmi1a Atbmi1b* mutants (**Figure 2B**). The VAL (VP1/ABI3-LIKE) transcription factors can physi- cally interact with AtBMI1 proteins and the *val1 val2* mutant exhibits comparable phenotype to *Atbmi1a Atbmi1b*, suggest- ing that VAL and AtBMI1 proteins may form complexes in repression of embryonic regulatory genes during vegetative development (Yang et al., 2013). Notably, loss of VAL or AtBMI1 causes H2Aub1 reduction in chromatin regions at *ABI3*, *BBM*, *FUS3* and *LEC1* but not *STM* (Yang et al., 2013). Future investigation is necessary to clarify whether AtBMI1 and AtRING1 proteins repress *KNOX* transcription *via* H2Aub1 deposition or other independent chromatin remodeling mecha- nisms.

ROLE OF PRC1-LIKE RING-FINGER PROTEINS IN STEM CELL MAINTENANCE

Plant growth and development largely depend on stem cells located in SAM (shoot apical meristem) and RAM (root apical meristem), whose activities are fine-tuned by multiple families of chromatin factors (Sang et al., 2009; Shen and Xu, 2009). The first uncovered biological role of the *Arabidopsis* PRC1-like RING-finger proteins are on the regulation of SAM activity (Xu and Shen, 2008). While the single loss-of-function mutants *Atring1a* and *Atring1b* have a normal phenotype, the double mutant *Atring1a Atring1b* exhibits enlarged SAM, fasciated stem, and ectopic-meristem formation in cotyledons and leaves. This indicates that *AtRING1a* and *AtRING1b* play a redundant role in stable repression of stem cell activity to allow appropriate lateral organ differentiation. The balances between stem cell maintenance and cell differentiation for organ formation are controlled by specific transcription factors, including KNOX (Class I KNOTTED1-like homeobox) proteins. Strikingly, several *KNOX* genes, e.g., *STM* (*SHOOT-MERISTEMLESS*), *BP* (*BREVIPEDICELLUS*)/*KNAT1*, *KNAT2* and *KNAT6,* are upregulated in *Atring1a Atring1b* (Xu and Shen, 2008). Ectopic expression of *KNOX* genes colocalizes with and precedes ectopic meristem formation. It has been proposed that AtRING1a/b acts as a crucial PRC1 component in conjunction with PRC2 in repression of *KNOX* genes to promote lateral organ formation in the SAM (**Figure 2A**).

ROLE OF PRC1-LIKE RING-FINGER PROTEINS IN EMBRYONIC CELL FATE DETERMINACY

Further characterization of the ectopic meristem structures observed in *Atring1a Atring1b* unravels that these callus structures exhibit embryonic traits (Chen et al., 2010). The *Atbmi1a Atbmi1b* mutant also displays derepression of embryonic traits (Bratzel et al., 2010; Chen et al., 2010). Embryonic callus formation has been observed broadly in somatic tissues of cotyledons, leaves, shoots and roots of the mutant plants. Treatment with an auxin transport inhibitor can inhibit embryonic callus formation in *Atring1a Atring1b*, indicating that a normal auxin gradient is required for somatic embryo formation in the mutant (Chen et al., 2010). Both *Atring1a Atring1b* and *Atbmi1a Atbmi1b* mutants exhibit elevated expression of several key embryonic regulatory genes, including *ABI3* (*ABSCISIC ACID INSENSITIVE 3*), *AGL15* (*AGAMOUS LIKE 15*), *BBM* (*BABYBOOM*), *FUS3* (*FUSCA 3*), *LEC1* (*LEAFY COTYLEDON 1*), and *LEC2* (Bratzel et al., 2010; Chen et al., 2010). It is likely that derepression of these regulatory genes together with *KNOX* has contributed to the ectopic meristem

ROLE OF PRC1-LIKE RING-FINGER PROTEINS IN SEED GERMINATION

Seed germination defines the entry into a new generation of the plant life cycle. It is generally accepted that the process of germination starts with water uptake followed by seed coat rup- ture and is completed following radicle protrusion (Bentsink and Koornneef, 2008). During the very early phase, the embry- onic growth program remains latent and can be reinstated in response to unfavorable environmental cues. With the attain- ment of photosynthetic competence, the irreversible transition to autotrophic growth is accomplished and embryonic program is stably suppressed. A recent study (Molitor et al., 2014) has identified the *Arabidopsis* PHD-domain H3K4me3-binding AL (ALFIN1-like) proteins as interactors of AtBMI1 and AtRING1 proteins and has demonstrated a crucial function of chromatin state switch in establishment of seed developmental gene repres- sion during seed germination (**Figure 2C**). Loss of AL6 and AL7 as well as loss of AtBMI1a and AtBMI1b retards seed ger- mination and causes transcriptional derepression and a delayed chromatin state switch from H3K4me3 to H3K27me3 enrichment of seed developmental genes, including *ABI3* and *DOG1*. The ger- mination delay phenotype of the *al6 al7* and *Atbmi1a Atbmi1b* mutants is more pronounced under osmotic stress (Molitor et al., 2014), suggesting that AL PHD-PRC1 complexes may participate in regulation of seed germination in

ROLE OF PRC1-LIKE RING-FINGER PROTEINS IN OTHER PROCESSES

AtBMI1a and AtBMI1b, also named DRIP1 (DREB2A-INTERACTING PROTEIN 1) and DRIP2, had been reported first as E3 ligases involved in ubiquitination of DREB2A (DEHYDRATION-RESPONSIVE ELEMENT BINDING PROTEIN 2A), a transcription factor controlling water deficit-inducible gene expression (Qin et al., 2008). The *drip1 drip2* mutant shows enhanced expression of water deficit-inducible genes and more tolerance to drought (Qin et al., 2008). Overexpression of *AtBMI1c* accelerates flowering time, which is associated with reduction of *FLC* expression (Li et al., 2011). In addition to SAM maintenance defects and derepression of embryonic traits, the *Atring1a Atring1b* mutant also displays homeotic conversions of floral tissues (Xu and Shen, 2008). Therefore, more precise functions and underlying molecular mechanisms for the PRC1-like RING-finger proteins are still waiting to be uncovered

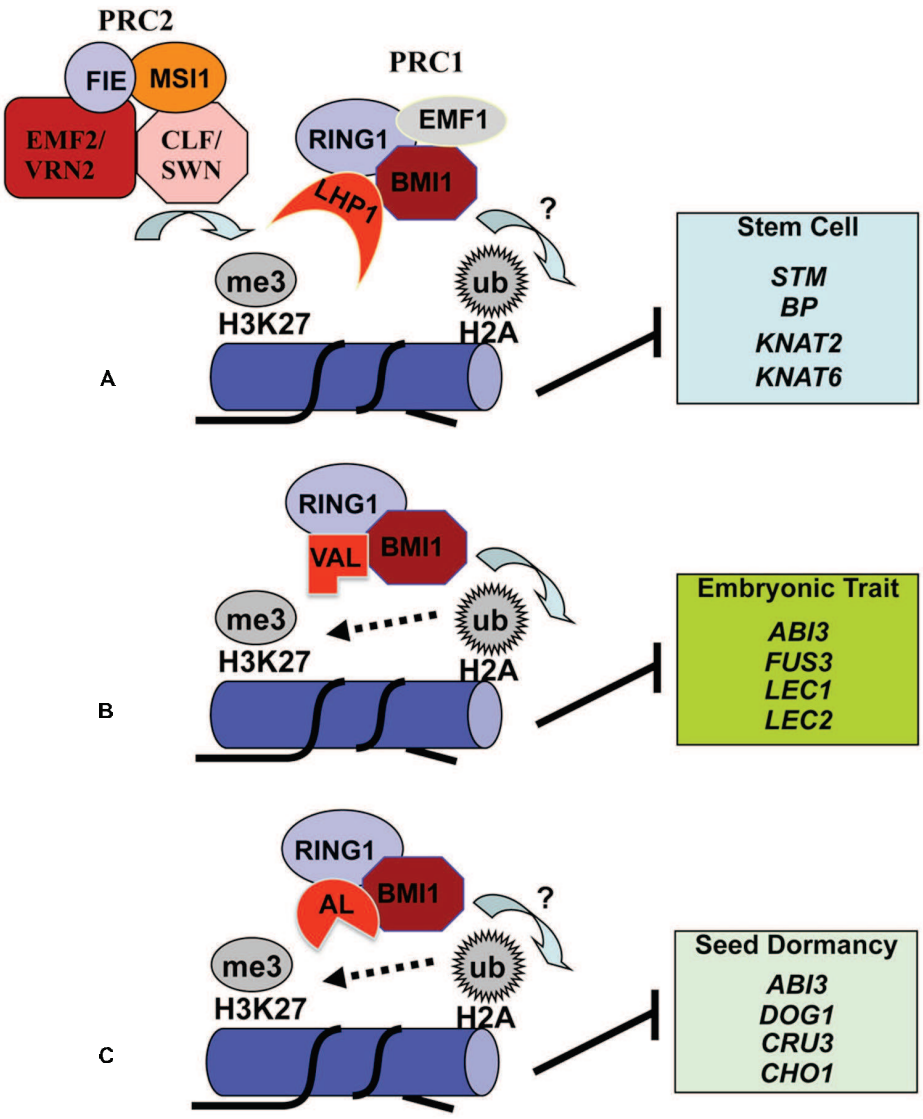

FIGURE 2 | Proposed models for histone H2A monoubiquitination deposition in transcriptional repression of varied target genes. The *Arabidopsis* PRC1-like RING-finger proteins AtRING1a/b (RING1) and AtBMI1a/b/c (BMI1) have the E3 ligase activity in catalyzing H2A monoubiquitination (H2Aub1). Comparable to the classical model of sequential PRC2 then PRC1 action in Polycomb silencing in animal cells, the *Arabidopsis* PRC1-like protein LHP1 binds H3K27me3 pre-deposited by the evolutionarily conserved PRC2 complexes and recruits RING1, BMI1 and possibly also EMF1 through protein–protein interactions **(A)**. This combinatorial action by PRC2 then PRC1 likely plays a broad role in suppression of numerous genes, including the key stem cell regulatory *KNOX* genes that need to be stably repressed during lateral organ development. The transcription factor VAL is involved in recruitment of BMI1 and RING1 in suppression of embryonic trait genes in somatic cells **(B)**. AL proteins bind BMI1 and RING1 and play important roles in suppression of several key seed dormancy regulatory genes to promote germination **(C)**. H3K27me3 deposition at embryonic/seed genes is enhanced by VAL/AL-PRC1 **(B,C)**, unraveling a non-canonical crosstalk between H3K27me3 and H2Aub1. The question marks indicate that H2Aub1 deposition in the specified target gene chromatin still requires future investigation.

during plant development and in plant response to environmental

MECHANISMS OF PRC1-LIKE RING-FINGER PROTEINS IN TRANSCRIPTION REPRESSION

H2Aub1 function in plants is primarily evidenced through investigation of roles of the *Arabidopsis* PRC1-like RING-finger proteins (Xu and Shen, 2008; Bratzel et al., 2010; Chen et al., 2010; Li et al., 2011; Yang et al., 2013). Although these RING-nicely *in vitro* as E3 ligases, their *in vivo* functions in H2Aub1 deposition are still poorly documented. H2Aub1 level in *Ara- bidopsis* seems very low because large-scale analyses of either the histone-enriched or the Ub-affinity-purified protein preparations fail to detect H2Aub1 (Maor et al., 2007; Sridhar et al., 2007; Zhang et al., 2007a; Manzano et al., 2008; Saracco et al., 2009). H2Aub1 has been detected only by using specific antibodies, and in this case *AtBMI1* genes have been shown to act as positive regula- tors for H2Aub1 deposition in

2010; Li et al., 2011; Yang et al., 2013). It is unknown whether any deubiquitinases might cause low levels of H2Aub1 in *Arabidopsis*. In animal cells, several deubiquitinases are characterized as specific for H2Aub1 (Weake and Workman, 2008; Simon and Kingston, 2013). Future characterization of *Arabidopsis* H2Aub1 deubiquitinases may provide useful information regarding regulatory mechanisms of H2Aub1 dynamics.

AtRING1 and AtBMI1 proteins physically interact each other and with the H3K27me3-binding protein LHP1 (Xu and Shen, 2008; Bratzel et al., 2010; Chen et al., 2010), providing a possible recruitment mechanism similar to the classical sequential PRC2 then PRC1 silencing pathway in animal cells. However, the *Atring1a Atring1b*, *Atbmi1a Atbmi1b,* or *Atbmi1a Atbmi1b Atbmi1c* mutant exhibits much more severe phenotypic defects than the *lhp1* mutant does, and *lhp1* enhances the *Atring1a Atring1b* mutant defects. It is thus apparent that AtRING1 and AtBMI1 proteins also act independently from LHP1. Recent identification of the transcriptional regulator VAL as AtBMI1-binding protein and of AL as AtRING1 and AtBMI1 interactor provides some novel insight about recruitment mechanisms (Yang et al., 2013; Molitor et al., 2014). It is particular intriguing that loss of AtBMI1 impairs H3K27me3 enrichment at seed developmental genes during seed germination and vegetative growth (Yang et al., 2013; Molitor et al., 2014). It has also been reported that loss of LHP1 impairs H3K27me3 enrichment at flower gene loci in roots (Derkacheva et al., 2013). These recent findings challenge the classic hierarchical paradigm where PRC2-mediated H3K27me3 deposition precedes PRC1 recruitment (**Figure 2**). It is obvious that future investigations are necessary to better understand the

CONCLUSIONS AND PERSPECTIVES

Studies over the last few years in the model plant *Arabidopsis* have greatly advanced our knowledge about the roles of H2Aub1 and H2Bub1 in transcription regulation in plant growth and development. In view of additional functions described in animal cells for both H2Aub1 and H2Bub1 in DNA damage repair (Bergink et al., 2006; Marteijn et al., 2009; Chernikova et al., 2010; Ginjala et al., 2011; Moyal et al., 2011; Nakamura et al., 2011), it is anticipated that more roles of H2Aub1 and H2Bub1 in plant response to environmental stresses are waiting to be uncovered. Mutagenesis of enzymes involved in H2Aub1 and H2Bub1 deposition or removal is required to address the question whether these enzymes effectively exert their biological functions *via* H2Aub1 and H2Bub1. Identification and characterization of factors associated with these different enzymes will be essential for understanding molecular mechanisms of their recruitment and function at specific targets within the genome. We need to know whether and how their function is spatially and temporally integrated with plant development. Genome-wide tools need to be further explored to provide a global view of links among enzyme or associated factor binding, H2Aub1/H2Bub1 enrichment, H3 methylation, and Pol II occupation. Crosstalks between H2Aub1 or H2Bub1 and

In addition to H2Aub1 and H2Bub1, ubiquitinated H1, H3, and H4 are also found in *Arabidopsis* (Maor et al., 2007; Manzano et al., 2008; Saracco et al., 2009). H3 ubiquitination catalyzed by Rtt101-Mms1 in yeast and by Cul4-DDB1 in human has been recently shown to play an important role in the histone chaperone Asf1-mediated nucleosome assembly (Han et al., 2013). *Arabidopsis* contains a conserved family of CULLINs and CUL4-DDB1 complexes are reported (Shen et al., 2002; Hua and Vierstra, 2011). The Asf1 homologues in *Arabidopsis* are also identified (Zhu et al., 2011). It remains to be investigated whether CUL4-DDB and AtASF1 collaboratively act on nucleosome assembly *via* H3

ACKNOWLEDGMENTS

The work in Wen-Hui Shen laboratory was supported by the French "Centre National de la Recherche Scientifique" (CNRS) and in part by the French "Agence Nationale de la Recherche" (ANR-08-BLAN-0200-CSD7; ANR-12-BSV2-0013-02). Jing Feng
received a fellowship from the China Scholarship Council of

REFERENCES

Bemer, M., and Grossniklaus, U. (2012). Dynamic regulation of Polycomb group activity during plant development. *Curr. Opin. Plant Biol.* 15, 523–529. doi: 10.1016/j.pbi.2012.09.006

Bentsink, L., and Koornneef, M. (2008). Seed dormancy and germination. *Arabidopsis Book* 6:e0119. doi: 10.1199/tab.0119

Bergink, S., Salomons, F. A., Hoogstraten, D., Groothuis, T. A. M., De Waard, H., Wu, J., et al. (2006). DNA damage triggers nucleotide excision repair-dependent monoubiquitylation of histone H2A. *Genes Dev.* 20, 1343–1352. doi: 10.1101/gad.373706

Berr, A., McCallum, E. J., Alioua, A., Heintz, D., Heitz, T., and Shen, W.-H. (2010). *Arabidopsis* histone methyltransferase SET DOMAIN GROUP 8 mediates induction of the jasmonate/ethylene pathway genes in plant defense response to necrotrophic fungi. *Plant Physiol.* 154, 1403–1414. doi: 10.1105/tpc.110.079962

Berr, A., Ménard, R., Heitz, T., and Shen, W.-H. (2012). Chromatin modification and remodelling: a regulatory landscape for the control of *Arabidopsis* defence responses upon pathogen attack. *Cell. Microbiol.* 14, 829–839. doi: 10.1111/j.1462-5822.2012.01785.x

Berr, A., Shafiq, S., and Shen, W.-H. (2011). Histone modifications in transcriptional activation during plant development. *Biochim. Biophys. Acta* 1809, 567–576. doi: 10.1016/j.bbagrm.2011.07.001

Bourbousse, C., Ahmed, I., Roudier, F., Zabulon, G., Blondet, E., Balzergue, S., et al. (2012). Histone H2B monoubiquitination facilitates the rapid modulation of gene expression during *Arabidopsis* photomorphogenesis. *PLoS Genet.* 8:e1002825. doi: 10.1371/journal.pgen.1002825

Bratzel, F., López-Torrejón, G., Koch, M., Del Pozo, J. C., and Calonje, M. (2010). Keeping cell identity in *Arabidopsis* requires PRC1 RING-finger homologs that catalyze H2A monoubiquitination. *Curr. Biol.* 20, 1853–1859. doi: 10.1016/j.cub.2010.09.046

Braun, S., and Madhani, H. D. (2012). Shaping the landscape: mechanistic consequences of ubiquitin modification of chromatin. *EMBO Rep.* 13, 619–630. doi: 10.1038/embor.2012.78

Cao, Y., Dai, Y., Cui, S., and Ma, L. (2008). Histone H2B monoubiquitination in the chromatin of FLOWERING LOCUS C regulates flowering time in *Arabidopsis*. *Plant Cell* 20, 2586–2602. doi: 10.1105/tpc.108.062760

Carlsten, J. O. P., Zhu, X., and Gustafsson, C. M. (2013). The multitalented mediator complex. *Trends Biochem. Sci.* 38, 531–537. doi: 10.1016/j.tibs.2013.08.007

Chen, D., Molitor, A., Liu, C., and Shen, W.-H. (2010). The *Arabidopsis* PRC1-like RING-finger proteins are necessary for repression of embryonic traits during vegetative growth. *Cell Res.* 20, 1332–1344. doi: 10.1038/cr.2010.151

Chernikova, S. B., Dorth, J. A., Razorenova, O. V., Game, J. C., and Brown, J. M. (2010). Deficiency in Bre1 impairs homologous recombination repair and cell

cycle checkpoint response to radiation damage in mammalian cells. *Radiat. Res.* 174, 558–565. doi: 10.1667/RR2184.1

Derkacheva, M., Steinbach, Y., Wildhaber, T., Mozgova, I., Mahrez, W., Nanni, P., et al. (2013). *Arabidopsis* MSI1 connects LHP1 to PRC2 complexes. *EMBO J.* 32, 2073–2085. doi: 10.1038/emboj.2013.145

Dhawan, R., Luo, H., Foerster, A. M., Abuqamar, S., Du, H.-N., Briggs, S. D., et al. (2009). HISTONE MONOUBIQUITINATION1 interacts with a subunit of the Mediator complex and regulates defense against necrotrophic fungal pathogens in *Arabidopsis*. *Plant Cell* 21, 1000–1019. doi: 10.1105/tpc.108.062364

Fleury, D., Himanen, K., Cnops, G., Nelissen, H., Boccardi, T. M., Maere, S., et al. (2007). The *Arabidopsis thaliana* homolog of yeast BRE1 has a function in cell cycle regulation during early leaf and root growth. *Plant Cell* 19, 417–432. doi: 10.1105/tpc.106.041319

Ginjala, V., Nacerddine, K., Kulkarni, A., Oza, J., Hill, S. J., Yao, M., et al. (2011). BMI1 is recruited to DNA breaks and contributes to DNA damage-induced H2A ubiquitination and repair. *Mol. Cell. Biol.* 31, 1972–1982. doi: 10.1128/MCB.00981-10

Goldknopf, I. L., Taylor, C. W., Baum, R. M., Yeoman, L. C., Olson, M. O., Prestayko, A. W., et al. (1975). Isolation and characterization of protein A24, a "histone-like" non-histone chromosomal protein. *J. Biol. Chem.* 250, 7182–7187.

Gu, X., Jiang, D., Wang, Y., Bachmair, A., and He, Y. (2009). Repression of the floral transition via histone H2B monoubiquitination. *Plant J.* 57, 522–533. doi: 10.1111/j.1365-313X.2008.03709.x

Han, J., Zhang, H., Zhang, H., Wang, Z., Zhou, H., and Zhang, Z. (2013). A Cul4 E3 ubiquitin ligase regulates histone hand-off during nucleosome assembly. *Cell* 155, 817–829. doi: 10.1016/j.cell.2013.10.014

Hershko, A., and Ciechanover, A. (1998). The ubiquitin system. *Annu. Rev. Biochem.* 67, 425–479. doi: 10.1146/annurev.biochem.67.1.425

Himanen, K., Woloszynska, M., Boccardi, T. M., De Groeve, S., Nelissen, H., Bruno, L., et al. (2012). Histone H2B monoubiquitination is required to reach maximal transcript levels of circadian clock genes in *Arabidopsis*. *Plant J.* 72, 249–260. doi: 10.1111/j.1365-313X.2012.05071.x

Hua, Z., and Vierstra, R. D. (2011). The Cullin-RING ubiquitin-protein ligases. *Annu. Rev. Plant Biol.* 62, 299–334. doi: 10.1146/annurev-arplant-042809-112256

Hunt, L. T., and Dayhoff, M. O. (1977). Amino-terminal sequence identity of ubiquitin and the nonhistone component of nuclear protein A24. *Biochem. Biophys. Res. Commun.* 74, 650–655. doi: 10.1016/0006-291X(77)90352-7

Hwang, W. W., Venkatasubrahmanyam, S., Ianculescu, A. G., Tong, A., Boone, C., and Madhani, H. D. (2003). A conserved RING finger protein required for histone H2B monoubiquitination and cell size control. *Mol. Cell* 11, 261–266. doi: 10.1016/S1097-2765(02)00826-2

Kim, J., Hake, S. B., and Roeder, R. G. (2005). The human homolog of yeast BRE1 functions as a transcriptional coactivator through direct activator interactions. *Mol. Cell* 20, 759–770. doi: 10.1016/j.molcel.2005.11.012

Krichevsky, A., Zaltsman, A., Lacroix, B., and Citovsky, V. (2011). Involvement of KDM1C histone demethylase–OTLD1 otubain-like histone deubiquitinase complexes in plant gene repression. *Proc. Natl. Acad. Sci. U.S.A.* 108, 11157–11162. doi: 10.1073/pnas.1014030108

Li, W., Wang, Z., Li, J., Yang, H., Cui, S., Wang, X., et al. (2011). Overexpression of AtBMI1C, a Polycomb group protein gene, accelerates flowering in *Arabidopsis*. *PLoS ONE* 6:e21364. doi: 10.1371/journal.pone.0021364

Liu, Y., Koornneef, M., and Soppe, W. J. J. (2007). The absence of histone H2B monoubiquitination in the *Arabidopsis* hub1 (rdo4) mutant reveals a role for chromatin remodeling in seed dormancy. *Plant Cell* 19, 433–444. doi: 10.1105/tpc.106.049221

Lolas, I. B., Himanen, K., Grønlund, J. T., Lynggaard, C., Houben, A., Melzer, M., et al. (2010). The transcript elongation factor FACT affects *Arabidopsis* vegetative and reproductive development and genetically interacts with HUB1/2. *Plant J.* 61, 686–697. doi: 10.1111/j.1365-313X.2009.04096.x

Luger, K., Mader, A. W., Richmond, R. K., Sargent, D. F., and Richmond, T. J. (1997). Crystal structure of the nucleosome core particle at 2.8 A resolution. *Nature* 389, 251–260. doi: 10.1038/38444

Luo, M., Luo, M.-Z., Buzas, D., Finnegan, J., Helliwell, C., Dennis, E. S., et al. (2008). UBIQUITIN-SPECIFIC PROTEASE 26 is required for seed development and the repression of PHERES1 in *Arabidopsis*. *Genetics* 180, 229–236. doi: 10.1534/genetics.108.091736

Malapeira, J., Khaitova, L. C., and Mas, P. (2012). Ordered changes in histone modifications at the core of the *Arabidopsis* circadian clock. *Proc. Natl. Acad. Sci. U.S.A.* 109, 21540–21545. doi: 10.1073/pnas.1217022110

Manzano, C., Abraham, Z., López-Torrejón, G., and Pozo, J. (2008). Identification of ubiquitinated proteins in *Arabidopsis*. *Plant Mol. Biol.* 68, 145–158. doi: 10.1007/s11103-008-9358-9

Maor, R., Jones, A., Nühse, T. S., Studholme, D. J., Peck, S. C., and Shirasu, K. (2007). Multidimensional protein identification technology (MudPIT) analysis of ubiquitinated proteins in plants. *Mol. Cell. Proteomics* 6, 601–610. doi: 10.1074/mcp.M600408-MCP200

Marteijn, J. A., Simon B. J., Mailand N., Lans H., Schwertman P., Gourdin A. M., et al. (2009). Nucleotide excision repair–induced H2A ubiquitination is dependent on MDC1 and RNF8 and reveals a universal DNA damage response. *J. Cell Biol.* 186, 835–847. doi: 10.1083/jcb.200902150

Ménard, R., Verdier G., Ors M., Erhardt M., Beisson F., and Shen W. H. (2014). Histone H2B monoubiquitination is involved in the regulation of cutin and wax composition in *Arabidopsis thaliana*. *Plant Cell Physiol.* 55, 455–466. doi: 10.1093/pcp/pct182

Molitor, A. M., Bu, Z., Yu, Y., and Shen, W. H. (2014). *Arabidopsis* AL PHD-PRC1 complexes promote seed germination through H3K4me3-to-H3K27me3 chromatin state switch in repression of seed developmental genes. *PloS Genet.* 10:e1004091. doi: 10.1371/journal.pgen.1004091

Molitor, A., and Shen, W.-H. (2013). The Polycomb complex PRC1: composition and function in plants. *J. Genet. Genomics* 40, 231–238. doi: 10.1016/j.jgg.2012.12.005

Moyal, L., Lerenthal, Y., Gana-Weisz, M., Mass, G., So, S., Wang, S.-Y., et al. (2011). Requirement of ATM-dependent monoubiquitylation of histone H2B for timely repair of DNA double-strand breaks. *Mol. Cell* 41, 529–542. doi: 10.1016/j.molcel.2011.02.015

Nakamura, K., Kato, A., Kobayashi, J., Yanagihara, H., Sakamoto, S., Oliveira, D. V., et al. (2011). Regulation of homologous recombination by RNF20-dependent H2B ubiquitination. *Mol. Cell* 41, 515–528. doi: 10.1016/j.molcel.2011.02.002

Palma, K., Thorgrimsen, S., Malinovsky, F. G., Fiil, B. K., Nielsen, H. B., Brodersen, P., et al. (2010). Autoimmunity in *Arabidopsis* acd11 is mediated by epigenetic regulation of an immune receptor. *PLoS Pathog.* 6:e1001137. doi: 10.1371/journal.ppat.1001137

Pavri, R., Zhu, B., Li, G., Trojer, P., Mandal, S., Shilatifard, A., et al. (2006). Histone H2B monoubiquitination functions cooperatively with FACT to regulate elongation by RNA polymerase II. *Cell* 125, 703–717. doi: 10.1016/j.cell.2006.04.029

Pinder, J. B., Attwood, K. M., and Dellaire, G. (2013). Reading, writing, and repair: the role of ubiquitin and the ubiquitin-like proteins in DNA damage signaling and repair. *Front. Genet.* 4:45. doi: 10.3389/fgene.2013.00045

Qin, F., Sakuma, Y., Tran, L.-S. P., Maruyama, K., Kidokoro, S., Fujita, Y., et al. (2008). *Arabidopsis* DREB2A-interacting proteins function as RING E3 ligases and negatively regulate plant drought stress–responsive gene expression. *Plant Cell* 20, 1693–1707. doi: 10.1105/tpc.107.057380

Robzyk, K., Recht, J., and Osley, M. A. (2000). Rad6-dependent ubiquitination of histone H2B in yeast. *Science* 287, 501–504. doi: 10.1126/science.287.5452.501

Roudier, F., Ahmed, I., Bérard, C., Sarazin, A., Mary-Huard, T., Cortijo, S., et al. (2011). Integrative epigenomic mapping defines four main chromatin states in *Arabidopsis*. *EMBO J.* 30, 1928–1938. doi: 10.1038/emboj.2011.103

Sanchez-Pulido, L., Devos, D., Sung, Z., and Calonje, M. (2008). RAWUL: a new ubiquitin-like domain in PRC1 RING finger proteins that unveils putative plant and worm PRC1 orthologs. *BMC Genomics* 9:308. doi: 10.1186/1471-2164-9-308

Sang, Y., Wu, M.-F., and Wagner, D. (2009). The stem cell–chromatin connection. *Semin. Cell Dev. Biol.* 20, 1143–1148. doi: 10.1016/j.semcdb.2009.09.006

Saracco, S. A., Hansson, M., Scalf, M., Walker, J. M., Smith, L. M., and Vierstra, R. D. (2009). Tandem affinity purification and mass spectrometric analysis of ubiquitylated proteins in *Arabidopsis*. *Plant J.* 59, 344–358. doi: 10.1111/j.1365-313X.2009.03862.x

Schmitz, R. J., Tamada, Y., Doyle, M. R., Zhang, X., and Amasino, R. M. (2009). Histone H2B deubiquitination is required for transcriptional activation

of FLOWERING LOCUS C and for proper control of flowering in *Arabidopsis*. *Plant Physiol.* 149, 1196–1204. doi: 10.1104/pp.108.131508

Schwartz, Y. B., and Pirrotta, V. (2013). A new world of Polycombs: unexpected partnerships and emerging functions. *Nat. Rev. Genet.* 14, 853–864. doi: 10.1038/nrg3603

Shafiq, S., Berr, A., and Shen, W.-H. (2014). Combinatorial functions of diverse histone methylations in *Arabidopsis thaliana* flowering time regulation. *New Phytol.* 201, 312–322. doi: 10.1111/nph.12493

Shen, W.-H., Parmentier, Y., Hellmann, H., Lechner, E., Dong, A., Masson, J., et al. (2002). Null mutation of AtCUL1 causes arrest in early embryogenesis in *Arabidopsis*. *Mol. Biol. Cell* 13, 1916–1928. doi: 10.1091/mbc.E02-02-0077

Shen, W.-H., and Xu, L. (2009). Chromatin remodeling in stem cell maintenance in *Arabidopsis thaliana*. *Mol. Plant* 2, 600–609. doi: 10.1093/mp/ssp022

Shilatifard, A. (2006). Chromatin modifications by methylation and ubiquitination: implications in the regulation of gene expression. *Annu. Rev. Biochem.* 75, 243–269. doi: 10.1146/annurev.biochem.75.103004.142422

Simon, J. A., and Kingston, R. E. (2013). Occupying chromatin: Polycomb mechanisms for getting to genomic targets, stopping transcriptional traffic, and staying put. *Mol. Cell* 49, 808–824. doi: 10.1016/j.molcel.2013.02.013

Sridhar, V. V., Kapoor, A., Zhang, K., Zhu, J., Zhou, T., Hasegawa, P. M., et al. (2007). Control of DNA methylation and heterochromatic silencing by histone H2B deubiquitination. *Nature* 447, 735–738. doi: 10.1038/nature05864

Tanny, J. C., Erdjument-Bromage, H., Tempst, P., and Allis, C. D. (2007). Ubiquitylation of histone H2B controls RNA polymerase II transcription elongation independently of histone H3 methylation. *Genes Dev.* 21, 835–847. doi: 10.1101/gad.1516207

Turck, F., Roudier, F., Farrona, S., Martin-Magniette, M., Guillaume, E., Buisine, N., et al. (2007). *Arabidopsis* TFL2/LHP1 specifically associates with genes marked by trimethylation of histone H3 lysine 27. *PLoS Genet.* 3:e86. doi: 10.1371/journal.pgen.0030086

Wang, L., Brown, J. L., Cao, R., Zhang, Y., Kassis, J. A., and Jones, R. S. (2004). Hierarchical recruitment of polycomb group silencing complexes. *Mol. Cell* 14, 637–646. doi: 10.1016/j.molcel.2004.05.009

Weake, V. M., and Workman, J. L. (2008). Histone ubiquitination: triggering gene activity. *Mol. Cell* 29, 653–663. doi: 10.1016/j.molcel.2008.02.014

West, M. H. P., and Bonner, W. M. (1980). Histone 2B can be modified by the attachment of ubiquitin. *Nucleic Acids Res.* 8, 4671–4680. doi: 10.1093/nar/8.20.4671

Wood, A., Krogan, N. J., Dover, J., Schneider, J., Heidt, J., Boateng, M. A., et al. (2003). Bre1, an E3 ubiquitin ligase required for recruitment and substrate selection of Rad6 at a promoter. *Mol. Cell* 11, 267–274. doi: 10.1016/S1097-2765(02)00802-X

Xiao, T., Kao, C.-F., Krogan, N. J., Sun, Z.-W., Greenblatt, J. F., Osley, M. A., et al. (2005). Histone H2B ubiquitylation is associated with elongating RNA polymerase II. *Mol. Cell. Biol.* 25, 637–651. doi: 10.1128/MCB.25.2.637-651.2005

Xu, L., Ménard, R., Berr, A., Fuchs, J., Cognat, V., Meyer, D., et al. (2009). The E2 ubiquitin-conjugating enzymes, AtUBC1 and AtUBC2, play redundant roles and are involved in activation of FLC expression and repression of flowering in *Arabidopsis thaliana*. *Plant J.* 57, 279–288. doi: 10.1111/j.1365-313X.2008.03684.x

Xu, L., and Shen, W.-H. (2008). Polycomb silencing of KNOX genes confines shoot stem cell niches in *Arabidopsis*. *Curr. Biol.* 18, 1966–1971. doi: 10.1016/j.cub.2008.11.019

Yang, C., Bratzel, F., Hohmann, N., Koch, M., Turck, F., and Calonje, M. (2013). VAL- and AtBMI1-mediated H2Aub initiate the switch from embryonic to postgerminative growth in *Arabidopsis*. *Curr. Biol.* 23, 1324–1329. doi: 10.1016/j.cub.2013.05.050

Yao, X. Z., and Shen, W.-H. (2011). Crucial function of histone lysine methylation in plant reproduction. *Chin. Sci. Bull.* 56, 3493–3499. doi: 10.1007/s11434-011-4814-3

Zhang, K., Sridhar, V. V., Zhu, J., Kapoor, A., and Zhu, J.-K. (2007a). Distinctive core histone post-translational modification patterns in *Arabidopsis thaliana*. *PLoS ONE* 2:e1210. doi: 10.1371/journal.pone.0001210

Zhang, X., Germann, S., Blus, B. J., Khorasanizadeh, S., Gaudin, V., and Jacobsen, S. E. (2007b). The *Arabidopsis* LHP1 protein colocalizes with histone H3 Lys27 trimethylation. *Nat. Struct. Mol. Biol.* 14, 869–871. doi: 10.1038/nsmb1283

Zhang, Y. (2003). Transcriptional regulation by histone ubiquitination and deubiquitination. *Genes Dev.* 17, 2733–2740. doi: 10.1101/gad.1156403

Zhu, B., Zheng, Y., Pham, A.-D., Mandal, S. S., Erdjument-Bromage, H., Tempst, P., et al. (2005). Monoubiquitination of human histone H2B: the factors involved and their roles in HOX gene regulation. *Mol. Cell* 20, 601–611. doi: 10.1016/j.molcel.2005.09.025

Zhu, Y., Weng, M., Yang, Y., Zhang, C., Li, Z., Shen, W.-H., et al. (2011). *Arabidopsis* homologues of the histone chaperone ASF1 are crucial for chromatin replication and cell proliferation in plant development. *Plant J.* 66, 443–455. doi: 10.1111/j.1365-313X.2011.04504.x

Conflict of Interest Statement: The authors declare that the research was conducted in the absence of any commercial or financial relationships that could be construed as a potential conflict of interest.

Received: 02 January 2014; paper pending published: 24 January 2014; accepted: 22 February 2014; published online: 13 March 2014.

Citation: Feng J and Shen W-H (2014) Dynamic regulation and function of histone monoubiquitination in plants. Front. Plant Sci. ***5****:83. doi: 10.3389/fpls.2014.00083 This article was submitted to Plant Genetics and Genomics, a section of the journal Frontiers in Plant Science.*

I.3.2 Readers of H2B and H2A monoubiquitination

I.3.2.1 Readers of histone H2B monoubiquitination

Readers are proteins with specific domains that recognize and bind to particular modifications (Taverna *et al*., 2007; Plass *et al*., 2013). Chromatin readers are able to identify different modified amino acids and also different modification states of the same amino acid. H2Bub1 has various functions, and it probably exerts molecular and cellular functions by recruiting various H2Bub1-specific readers or preventing the binding of others. There are two types of readers (reviewed in Fuchs and Oren, 2014). One type comprises unmodified H2B readers; H2Bub1 may actually prevent the binding of other factors. Examples are yeast cyclin dependent kinase Ctk1 (Wyce *et al.*, 2007), elongation factor TFIIS (Shema *et al*., 2011) and the splicing factors UIA/U2B (Zhang *et al*., 2013). H2Bub1 disrupts the interaction between Ctk1 and histone H2A to prevent premature phosphorylation of RNA Pol II on Serine 2. H2Bub1 inhibits the loading of TFIIS elongation factor onto chromatin to repress gene expression. And the increased levels of H2Bub1 upon USP49 knockdown prevent the association of U1A and U2B with the chromatin, which results in impaired splicing. Another type comprises H2Bub1-specific readers, such as yeast proteasomal ATPases Rpt4/ Rpt6 (Ezhkova and Tansey, 2004), Dot1 (Oh *et al*., 2010), Cps35 (Lee *et al*., 2007), WDR82, the human orthologue of yeast Cps35 (Shema-Yaacoby *et al.,* 2013; Wu *et al*., 2008), and ASH2L (Wu *et al*., 2013). These readers play a key role in the crosstalk between H2Bub1 and H3 methylation. In addition, the H2Bub1-specific reader SKIP (Bres *et al*., 2009) links H2Bub1 to viral infection. MRG15 (Wu *et al*., 2011), a common subunit of both the MOF and Tip60 complexes, mediates the contribution of H2Bub1 to DNA damage response. BRG1, or BAF155 (Shema-Yaacoby *et al.,* 2013), is a component of the SWI/SNF complex, which, as a novel H2Bub1 reader, helped to shed light on the role of H2Bub1 as a positive transcription regulator.

I.3.2.2 ZRF1, a reader of histone H2A monoubiquitination?

Characteristics of ZRF1

Zuotin related factor 1 (ZRF1) is evolutionary conserved in most species. It is a member of the M-phase phosphoprotein (MPP) family. It localizes to both the nucleus and the cytosol. It contains a tRNA and Z-DNA binding (Zuotin) domain at the

N-terminus, and was isolated as a Z-DNA binding protein in yeast (Zhang *et al*., 1992; Wilhelm *et al*., 1994). Z-DNA is a left-handed DNA double helical structure which is correlated with some important biological processes, such as transcription, replication, and recombination of DNA (Naylor and Clark, 1990; Wahls *et al*., 1990; Witting *et al*., 1991). Zuotin contains a DnaJ motif, which is similar to mammalian HSP-40 (heat shock protein 40) chaperone. DnaJ/Hsp40 proteins all contain the J domain. The DnaJ domain is composed of a 70-amino acid sequence consisting of four helices and a loop region. Between helices II and III it contains a highly conserved tripeptide of histidine, proline, and aspartic acid (the HPD motif) (Qian *et al*., 1996). The DnaJ protein serves to recruit Hsp70 to substrate polypeptides as well as to stimulate Hsp70's adenosine triphosphatase (ATPase) activity, thus stabilizing Hsp70's interaction with the substrate. DnaJ/Hsp40 proteins have been preserved throughout evolution. In addition, they are important for protein translation, folding, unfolding, translocation and degradation (Qiu *et al.*, 2006). Zuotin also binds to ribosomes, in part via interaction with ribosomal RNA (Yan *et al.*, 1998). The Zuotin domain was first identified as containing an ubiquitin-binding domain (UBD) close to the DnaJ domain at the N-terminus in humans.

At the C terminus, ZRF1 contains two tandem repeats of SANT (Swi3, Ada2, NcoR1, and TFIIIB) domains, which are c-Myb-like repeats. The SANT domain consists of three ∝-helices, each of them containing a corresponding, bulky aromatic residue. The region exhibits a sequence-specific DNA binding activity. It was found to exist only in higher eukaryotes (Figure I.4). The SANT domain is commonly associated with a number of chromatin remodeling factors involved in the recruitment of histone acetylases (HAT) or histone deacetylases (HDAC) (Aasland *et al*. 1996; Boyer *et al*., 2004; Chen *et al*., 2014). The two SANT domains can carry out distinct functions; SANT2 may be more conserved than SANT1. But they may have co-evolved as an intact functional unit within ZRF proteins. The ZRF1 SANT domain might function as a molecular sensor, which couples substrate-binding to enzyme catalysis through a compulsory conformational change (Boyer *et al*., 2004). A single SANT domain has been identified in *Micromonas pusilla* MpZRF1 (Chen *et al.*, 2014). Recently, GST pulldown experiments showed that the SANT domains are not required for binding ubiquitin (Richly *et al*., 2010). The SANT domain was found to be essential for asymmetric cell division (Pappas and Miller, 2009). With these domains, ZRF1 is a multifunctional protein involved in transcriptional control through

interaction with multiple factors. The human protein was identified as a leukemia-associated antigen and expression of the gene is upregulated in leukemic blasts.

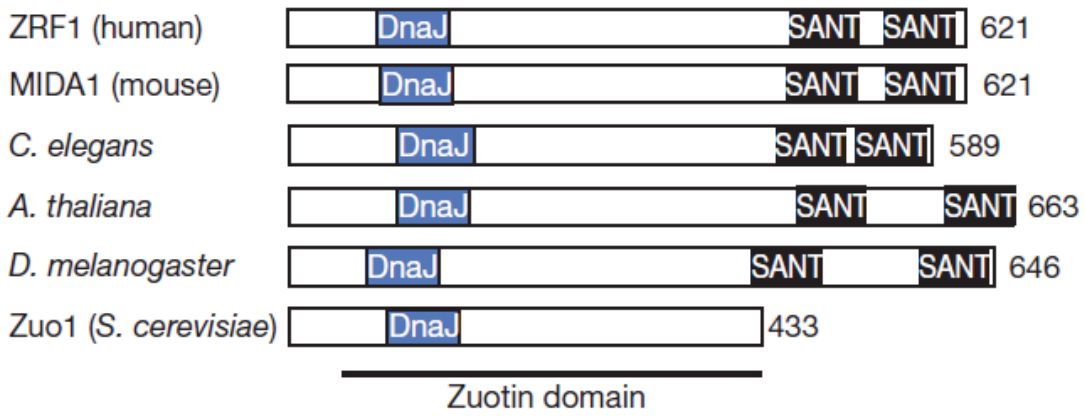

Figure I.4. Schematic diagram of ZRF1 orthologues indicating the DnaJ domain and SANT domains

The numbers along the right-hand side of panels indicate the number of amino acids of the proteins (from Richly *et al*., 2010).

Functions of ZRF1 homologs

In animals, ZUO1-related factor (ZRF) homologs mainly focus on nematodes, mice, and humans.

In *Caenorhabditis elegans*, DNJ11, a ZRF ortholog, exhibits a wide expression pattern and functions in asymmetric cell division and subsequent apoptosis (Chen *et al.*, 2014; Hatzold and Conradt, 2008).

MIDA1 (mouse Id associate 1) is the mouse Zuotin ortholog. Like DNJ11, MIDA1 also shows a ubiquitous expression pattern. GST pull-down experiments showed that MIDA1 associates with the HLH (helix-loop-helix) region of the inhibitor of differentiation (Id) (Shoji *et al*., 1995). Id was also shown to act as a positive growth regulator. MIDA1 has two different domains containing DNA binding activities. One is the Zuotin domain with a Z-DNA binding activity, the other is SANT domain containing a specific DNA binding activity. In growth promotion, Id interacts with MIDA1 to stimulate the sequence-specific DNA binding activity and interrupt Z-DNA binding activity (Inoue *et al.*, 1999, 2000). Antisense oligonucleotides for MIDA1 inhibit the growth of murine leukemia cells and the loss of MIDA1 also strongly interfered with the growth of MEL cells. This growth suppression is consistent with the slow growing phenotype of Zuotin null mutant yeast (Zhang *et al*., 1992). Furthermore,

loss of MIDA1 seemed not to interfere with entry into S phase, but delayed DNA synthesis especially at S phase (Shoji *et al*., 1995). These results demonstrated that MIDA1 regulates cell growth.

Using an antibody recognizing a specific set of phosphopeptides, MPP11/ ZRF1 was identified as a homolog of human Zuotin. This protein is involved in mitotic division (Matsumoto-Taniura *et al*. 1996) and its knockdown leads to pronounced slow growth (Jaiswal *et al*., 2011). Immunofluorescence experiments indicated that MPP11 is localized to the cytosol. Purification of MPP11 revealed that, together with Hsp70L1, it forms a mammalian ribosome-associated complex (mRAC). *In vivo* complementation data demonstrate that the C-terminal domain of MPP11 is not required for complex formation with Hsp70L1. However, complementary experiments demonstrated that mRAC can interact with the yeast ribosome, and can partly complement the yeast RAC mutant in the presence of the C-terminal domain of MPP11 (Otto *et al*., 2005). Recently, ZRF1 was shown to localize to both the cytoplasm and the nuclei in mammalian cells (Richly *et al*., 2010). Current research indicates that MPP11/MIDA1 is a multifunctional protein involved in transcriptional control through interaction with multiple factors.

ZRF1 has been identified as a novel H2A-ubiquitin binding protein (Richly *et al.*, 2010). It is known that PcG proteins catalyze H2A monoubiquitination. To understand the relationship between ZRF1 and PcG proteins Richly *et al*. performed pull-down assays using recombinant fusion protein His-RING1B and H2A-FLAG mononucleosome complexes. These assays showed that RING1B was efficiently released from nucleosomes following incubation with ZRF1. Furthermore, when GST-ubiquitin was incubated with constant amounts of His–RING1B and increasing amounts of His–ZRF1 finally reaching equimolar levels, immunoblot analysis indicated that the level of RING1B decreased. These results show that ZRF1 can compete with RING1B at H2Aubi. Consistent with the previous results, and using the UBD domain of ZRF1, Richly showed that RING1B was replaced by the UBD of ZRF1 (Richly *et al.*, 2010). These results showed that ZRF1 can directly antagonize gene silencing. In addition, ZRF1 can interact with USP21 to promote deubiquitination, which facilitates transcriptional activation. Considering these data they proposed a model (Figure I.5) in which ZRF1 is a chromatin-associated protein that recognizes the H2A mono-ubiquitin mark at lysine 119 (H2AK119ub1) and displaces RING1B (PRC1) from chromatin (Richly and Di Croce, 2011).

MPP11 knockdown results in slow growth and sensitivity to the aminoglycoside G418. Furthermore, MPP11 affects the fidelity of translation (Jaiswal *et al*., 2011). In addition, Demajo I. had obtained consistent results. Knockdown of ZRF1 in five different human AML cell lines led to a strong decrease in cell proliferation and an increase in apoptosis (Demajo *et al*., 2014). However, strikingly, in RA-induced conditions, ZRF1 deletion leads to reduced differentiation. Over-expression of ZRF1 increased the cell differentiation potential following RA treatment. They also found that the ZRF1 effect was dose dependent. Taken together, ZRF1 seems to have a dual role, as a differentiation repressor in basal conditions but then switching to an activator following RA induction. As a repressor, ZRF1 could interact with RARα and control histone acetylation (Demajo *et al*., 2014).

Recent preliminary work suggests that ZRF1 could be involved in embryonic development. ZRF1 was also found to be a key player required for first inducing neural progenitor cell (NPCs) specification from ESCs and then maintaining NPC identity (Aloia *et al.*, 2014). Deletion of ZRF1 did not affect neither mesodermal and endodermal specification from embryonic stem cells (ESCs) nor the stem cell features of several non-neural stem cell lineages, but it led to a significant reduction of neuroectodermal markers. Among these down-regulated genes, several are involved in maintaining NPC identify. Moreover, ZRF1 re-expression restored the expression of the reduced neuroectodermal markers.

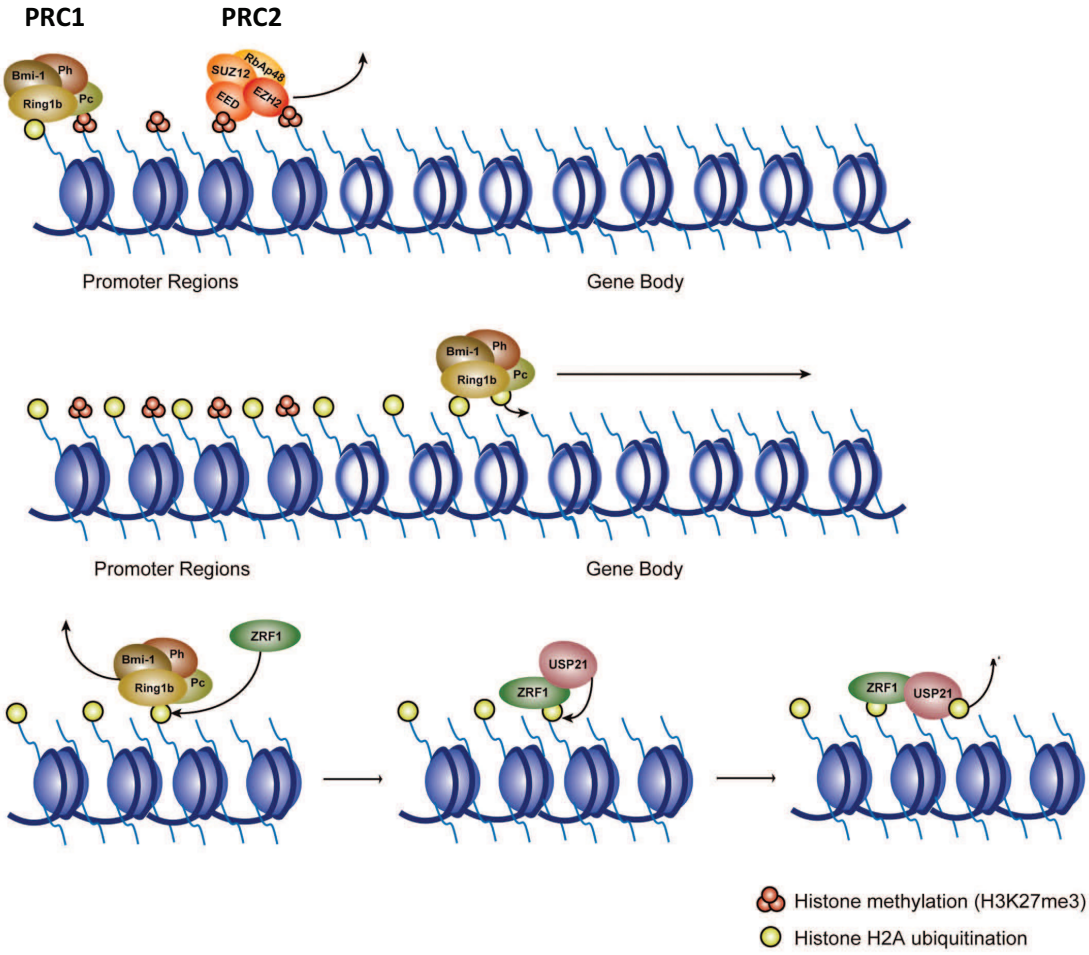

Figure I.5. Hypothetical model for polycomb action at chromatin

In promoter regions (purple nucleosomes), PRC2 carries out specific methylations of H3K27 (red circles). After ubiquitination of histone H2A (yellow circles) at promoter regions, PRC1 propagates into the gene body (light nucleosomes) to carry out ubiquitination. ZRF1 displaces PRC1 complexes by interacting with mono-ubiquitinated chromatin. After PRC1 removal, ZRF1 acts in concert with specific deubiquitinases (USP21) to facilitate deubiquitination. The enzyme might then either propagate to an adjacent nucleosome bound by ZRF1, or propagate together with ZRF1, which could confer multi-substrate binding since it is an oligomer. (Richly and Di Croce, 2011)

II. THESIS OBJECTIVES

The *Arabidopsis* PRC1-like RING-finger homologs (AtRNIG1A/B and AtBMI1A/B/C) have been characterized and shown to catalyze monoubiquitination of H2AK119 (reviewed in Molitor and Shen, 2013; Feng and Shen, 2014). Studies in animals showed that ZRF1 has a H2AK119ub1 reader-like function in the derepression of polycomb-repressed genes (Richly *et al*., 2010). ZRF1 specifically binds to H2AK119ub1 and then displaces PRC1 from chromatin. The depletion of PRC1 subsequently causes the loss of PRC2 from the chromatin, consequently switching polycomb-repressed genes from a repressive to an active state (Richly *et al*., 2010). Two homologs of human ZRF1 have been identified on the *Arabidopsis* genome (Chen *et al*., 2014), and hereinafter are named as AtZRF1a and AtZRF1b. A function for ZRF1 homologues in plants has not been reported so far. Thus my PhD work focuses on the functional characterization of AtZRF1a and AtZRF1b.

Our first objective was to study the gene expression patterns, the subcellular localization, as well as histone-binding activities of AtZRF1a and AtZRF1b. We found that *AtZRF1a* and *AtZRF1b* are broadly expressed in *Arabidopsis* plants and that the AtZRF1b protein binds H2Aub with characteristics similar to those previously reported for the human ZRF1 protein.

While the mammalian ZRF1 function has been studied in cultured cell lines, knowledge of ZRF1 function in the development of the whole organism is still lacking. We used the powerful genetic tool available in *Arabidopsis* to investigate the functions of *AtZRF1a* and *AtZRF1b*. Several independent T-DNA insertion mutant lines were identified. Because of functional redundancy of the two genes, my study subsequently focused on the characterization of two independent double mutants exhibiting simultaneous loss of function of both *AtZRF1a* and *AtZRF1b*; these double mutants are named *Atzrf1a-1 Atzrf1b-1* and *Atzrf1a-2 Atzrf1b-1*. My results showed that *AtZRF1a* and *AtZRF1b* have important roles in cell proliferation and differentiation, flowering time control, and seed germination.

I further investigated the roles of *AtZRF1a* and *AtZRF1b* in transcriptional regulation of genes. I studied the expression levels of selected genes in association with mutant phenotypes of *Atzrf1a-1 Atzrf1b-1* and *Atzrf1a-2 Atzrf1b-1*, as well as genes at the whole genome level by transcriptome analysis of the mutants. This allowed the identification of perturbed genes in the two double mutants, and showed an overlap of perturbed genes between these mutants and PRC1 defective mutants.

Lastly, to get insight into the mechanisms of AtZRF1 in transcriptional regulation, I investigated the H3K4me3, H3K27me3 and H2Aub1 levels in chromatin regions of some expression-perturbed genes in the *Atzrf1a-1 Atzrf1b-1* and *Atzrf1a-2 Atzrf1b-1* mutants. My results showed that loss of AtZRF1 reduces H3K27me3 and H2Aub1 levels to varied degrees depending on the genes examined. Most strikingly, in all examined cases no increase of H2Aub1 could be detected, suggesting that ZRF1-mediated deubiquitination of H2Aub1 is not a major event in transcriptional regulation in *Arabidopsis*.

III. RESULTS

III.1. Conservation, expression pattern and protein subcellular localization of AtZRF1

III.1.1 *Arabidopsis* contains two homologs of ZRF1, AtZRF1a and AtZRF1b

To identify genes with homology to human *ZRF1* in the *Arabidopsis* genome, we performed BLAST searches with full-length human *ZRF1* nucleotide and protein sequences as a query. The sequence analysis revealed that *AtZRF1a* (gene locus At3g11450) and *AtZRF1b* (At5g06110) encode *Arabidopsis* proteins showing high homologies to human ZRF1 (Figure III.1). The *AtZRF1a* mRNA was predicted to encode a protein with 647 amino acid residues and *AtZRF1b* mRNA a protein with 663 amino acid residues. They show 81% identity and 96% similarity to each other at the amino acid sequence level (Figure III.2).

The *AtZRF1a* and *AtZRF1b* genes each contain one intron in their 5′ untranslated region (5'-UTR); no intron was found within the gene body or the 3'-UTR. The AtZRF1a and AtZRF1b proteins share a conserved Zuotin domain at their N-terminus; this domain consists of a DnaJ domain and a potential ubiquitin-binding motif. In addition, they contain a pair of SANT domains at their C-terminus, a feature characteristic for this group of proteins in eukaryotes which is not found in prokaryotes (Chen *et al*., 2014). The SANT domain is proposed to function as a histone modification reader in chromatin remodeling by coupling histone binding with enzyme catalysis (Boyer *et al*. 2004).

III.1.2 AtZRF1b acts as a novel H2Aub binding factor in *Arabidopsis*

To understand the function of AtZRF1b, the *pGEX-4T-1* plasmids and the target fragments (full length ubiquitin and ZRF1bSANT, ZRF1bUBD cDNAs), as well as the *pET30a* plasmids and AtZRF1b truncated cDNAs were digested by restriction enzymes, and then isolated and purified. Each target fragment was ligated into the corresponding vector with DNA ligase. The recombinant plasmids obtained were then introduced into *E. coli* cell line BL21 (DE3) *via* electroporation. Glutathione S-transferase (GST)-tagged ubiquitin proteins and different recombinant AtZRF1b truncated proteins with a His-tag were produced in *E. coli* and used in *in vitro* pull-down assays. In these assays GST and GST-Ubi beads were incubated with total protein extracts of *E. coli* expressing recombinant His-tagged proteins. By western blot

with an anti-His antibody, His-AtZRF1bUBD (a ZRF1 protein only containing the UBD domain) and His-AtZRF1b△SANT (a ZRF1 protein lacking the C-terminal SANT domain) fusion proteins were found to bind GST-Ubi but not GST alone (Figure III.3). To further confirm this interaction, the *Arabidopsis* H2A.1 isoform (At1g51060) cDNA was N-terminally tagged with the FLAG epitope and introduced into a modified pCAMBIA1300 vector under the control of the CaMV35s promoter. The construct was introduced into *Agrobacterium* strain GV3101 and subsequently transformed into WT *Arabidopsis* by the floral-dip method. Then, for pull-down assays, GST, GST-AtZRF1bUBD and GST-AtZRF1bSANT (a ZRF1 protein only containing the C-terminal SANT domains) were incubated with total nuclear protein extracts of *Arabidopsis* plants expressing FLAG-H2A.1. Analysis of these mutants revealed that the conserved UBD-domain is required for Ub binding. The GST-fused UBD-domain fragment of AtZRF1b also can bind H2Aub. Similar binding activities had been previously reported for the human ZRF1 (Richly *et al*., 2010)

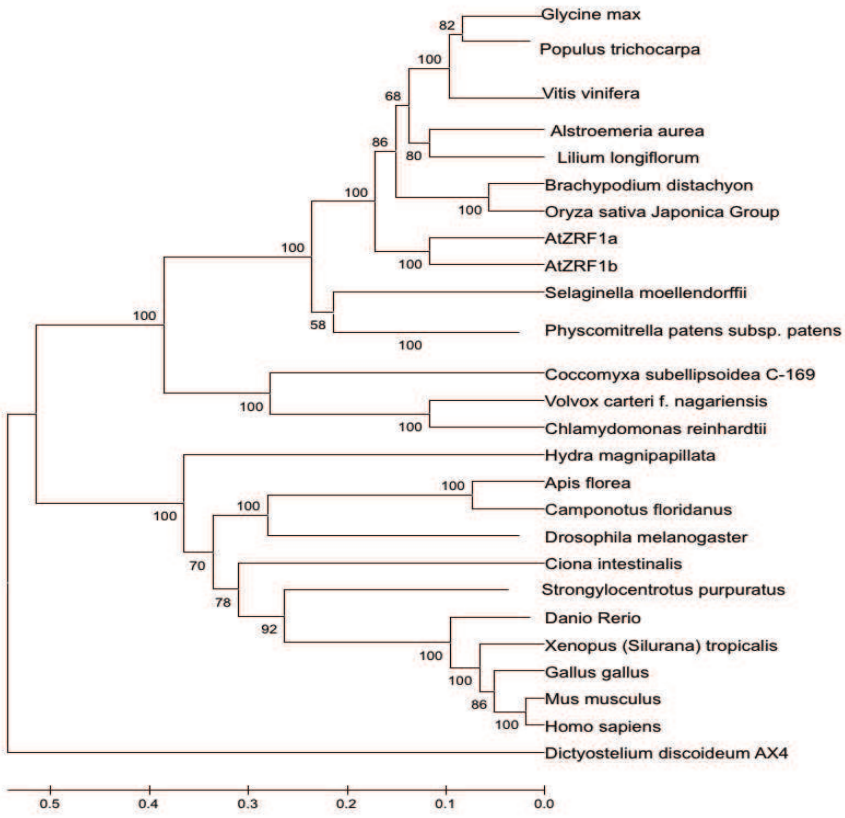

Figure III.1. Phylogram of ZRF1 homologs in several organisms

On the basis of amino acid sequence of the full–length protein, the phylogenetic analysis was performed using MEGA5.0 package with bootstrapping set at 500 replicates.

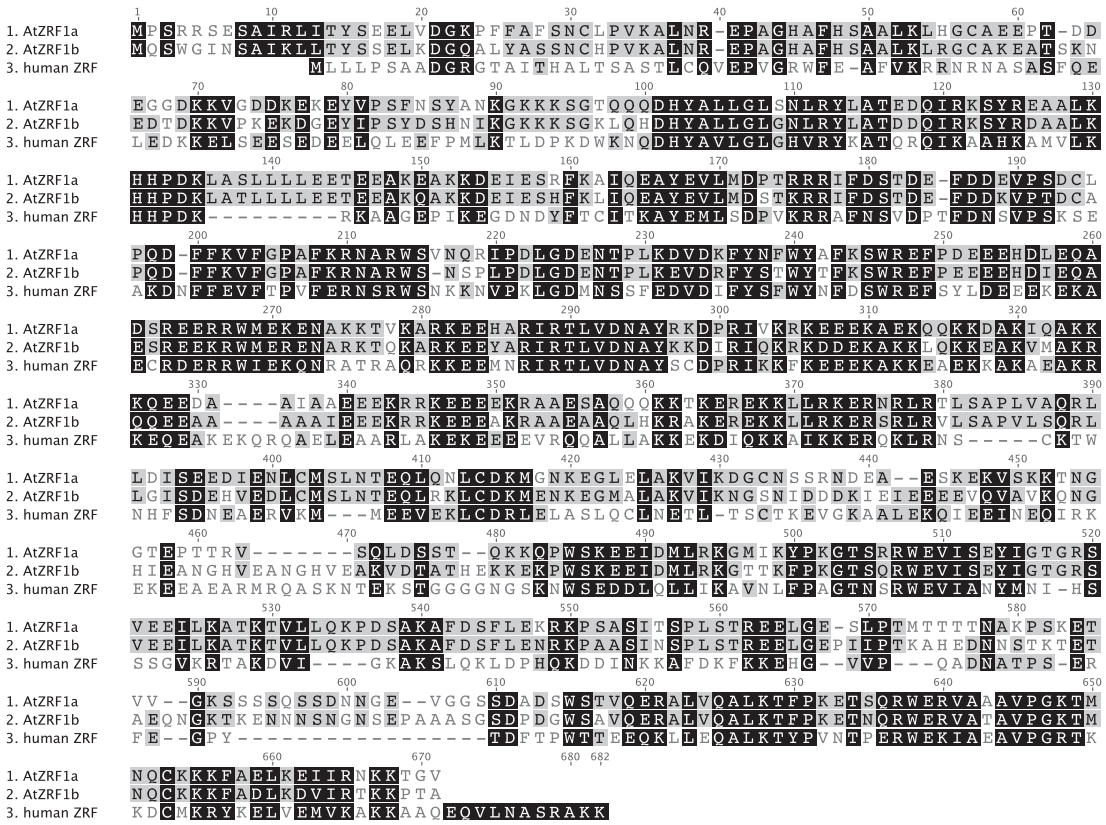

Figure III.2. Alignment of AtZRF1a and AtZRF1b amino acid sequences

White letters in black boxes indicate 100% sequence similarity, white letters in grey boxes indicate 80 to 100% similarity, black letters in grey boxes indicate 60 to 80% similarity, and grey letters on white background indicate <60% similarity. The alignment was generated using CLUSTALW program.

The Zuotin domain starts at position 100 and extends to position 431

The SANT1 domain starts at position 484 and extends to position 524

The SANT2 domain starts at position 615 and extends to position 661

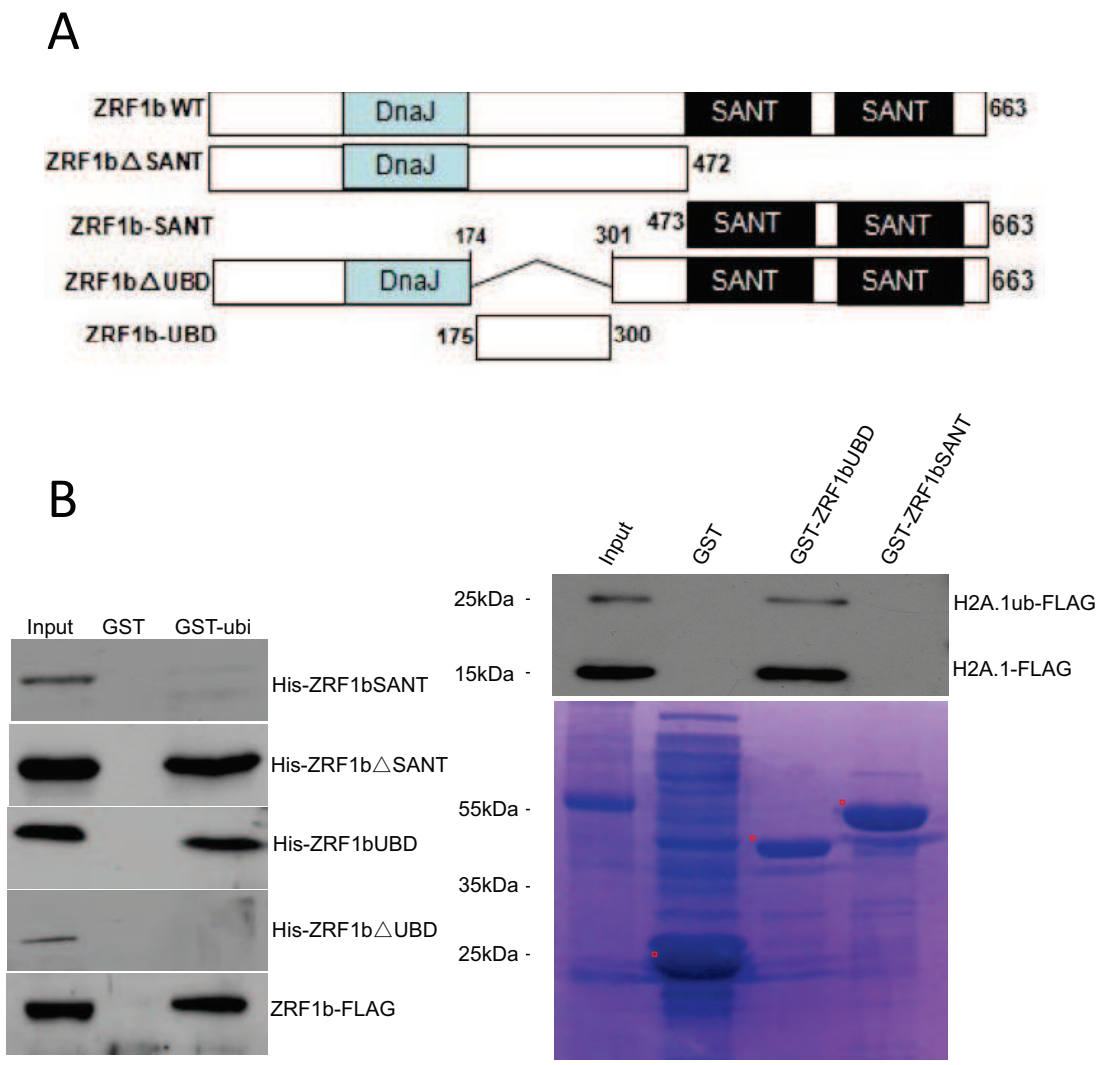

Figure III.3. ZRF1 interacts with H2Aub

A. Schematic representation of full-length and truncated AtZRF1b proteins. The conserved domains DnaJ and SANT are indicated. The numbers along the right-hand side of panels refer to the number of amino acids each of the proteins is composed of.

B. GST pull-downs with GST, GST-ubiquitin (GST-ubi) and GST-ZRF1bUBD or GST-ZRF1bSANT (right panel) and the His-tagged proteins indicated. Bound material was subjected to immunoblot analysis using His and FLAG antibodies. GST, GST-Ubi, GST-ZRF1bUBD and GST-ZRF1bSANT were expressed and purified from *E. coli*. Total protein extracts from either His-tagged fusion proteins expressed in *E. coli* or *35S-3XFLAG-AtZRF1b* expressing *Arabidopsis* line were used as input.

III.1.3 Gene expression pattern and subcellular localization of AtZRF1

To investigate the spatial expression pattern of *AtZRF1a* and *AtZRF1b*, we collected different organs/tissues (whole 5-day-old seedlings and their cotyledons, roots and rosette leaves of 10-day-old seedlings, cauline leaves and stems of 1-month-old plants, floral buds at developmental stage 6 as defined by Smyth and colleagues (Smyth *et al*., 1990), and inflorescences) of wild-type *Arabidopsis* (ecotype Col) plants to extract RNA for RT-PCR. The results show that *AtZRF1a* and *AtZRF1b* are expressed ubiquitously in all organs/tissues tested, with higher levels found in inflorescences (Figure III.4).

To investigate the subcellular localization of AtZRF1, a reporter gene *GFP* (Green Fluorescence Protein) was fused in frame to the amino terminus of *AtZRF1b* using the Gateway cloning system. The construct expressing *GFP-AtZRF1b* driven by the *CAULIFLOWER MOSAIC VIRUS* (*CaMV*) *35S* promoter was introduced into *Agrobacterium tumefaciens* and the resulting strain was used to transform tobacco (*Nicotiana benthamiana*) or *Arabidopsis* (Col) via vacuum infiltration. GFP signals were detected in both the nucleus and cytoplasm of tobacco leaf cells that transiently expressed *GFP-AtZRF1b*. To further confirm the results, we stably expressed GFP-AtZRF1b in transgenic *Arabidopsis* plants. Fluorescence microscopy indicated that GFP-AtZRF1b is found in both the nucleus and the cytoplasm of *Arabidopsis* roots (Figure III.5).

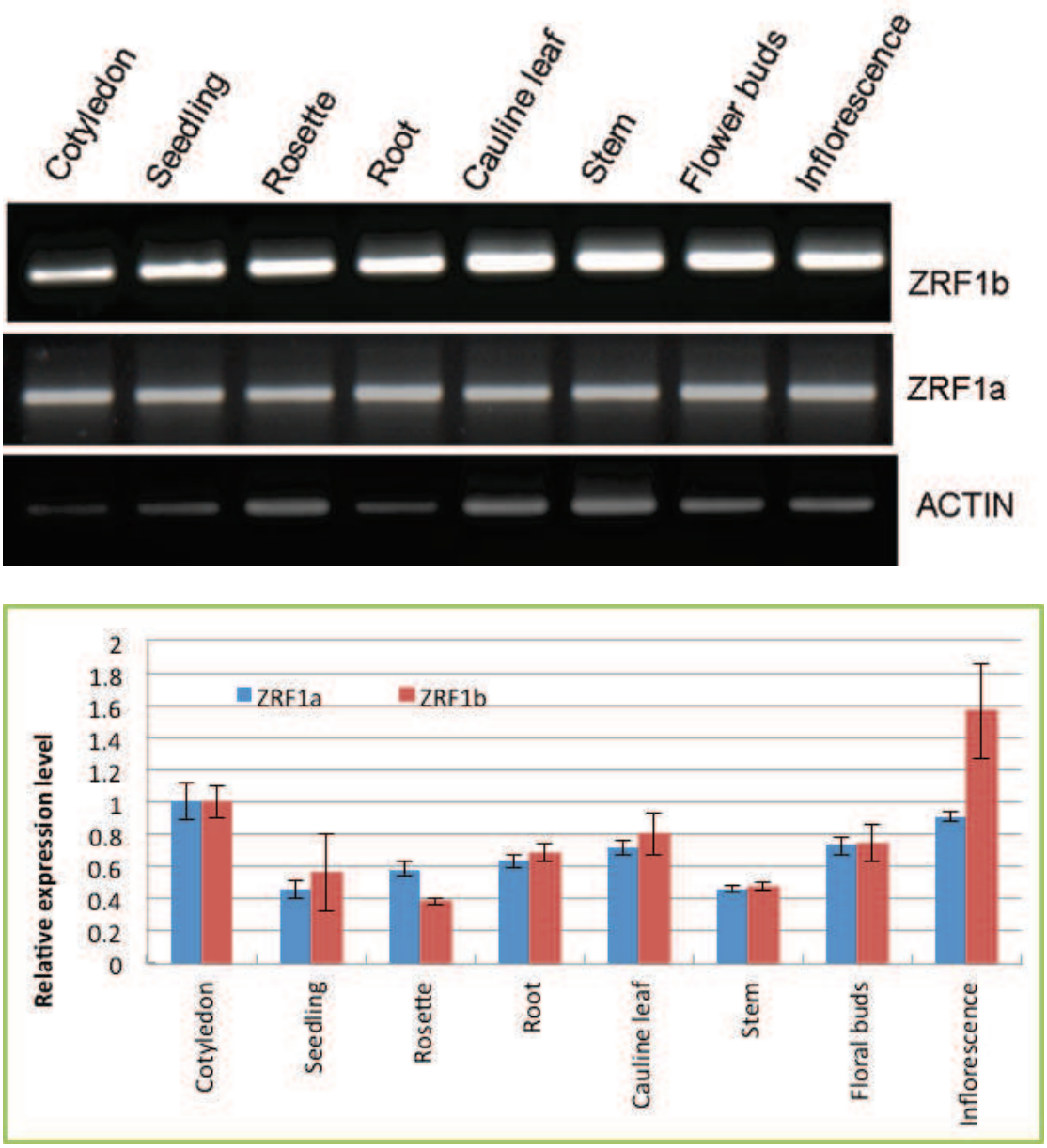

Figure III.4. RT-PCR and Q-PCR analysis of *AtZRF1a* and *AtZRF1b* expression in different organs of the wild-type Col plants

RT-PCR and qRT-PCR-based expression levels of *AtZRF1a* and *AtZRF1b* in different tissues, including cotyledon, seedling, root, rosette leaf, cauline leaf, stem, flower buds and inflorescence of wild-type. Actin acts as an internal reference. The averages of three biological replicates are shown. Each experiment was normalized to *EXP*, *PP2A* and *TIP4.1* expression. Error bar indicates standard error.

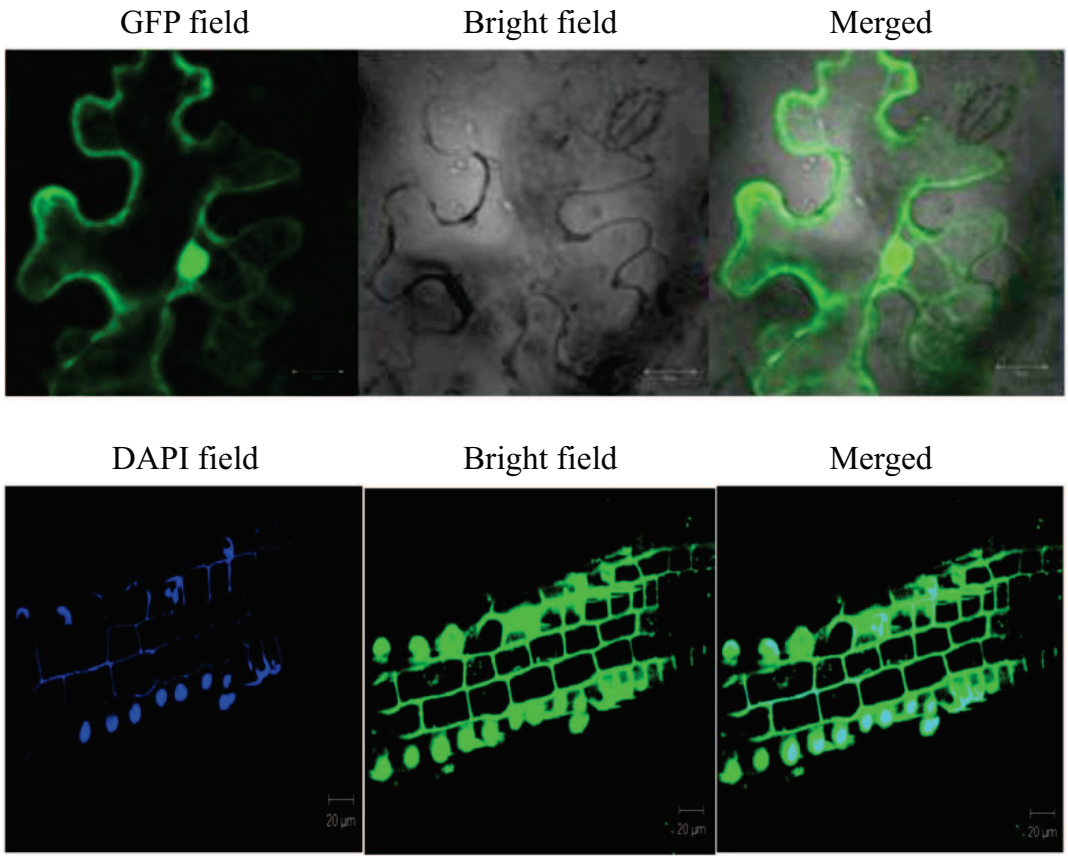

Figure III.5. Cellular localization of AtZRF1b protein

Subcellular localization of AtZRF1b–GFP fusion protein. The three top panels show GFP fluorescence (left), bright field image (middle) and merge image (right) of *N. benthamiana* epidermal cells expressing the fusion protein. The bottom panels show confocal scanning microscopy images of GFP-AtZRF1b fusion protein in root cells of a transgenic *Arabidopsis* line.

III.2. Identification and characterization of loss-of-function mutants of *AtZRF1a* and *AtZRF1b*

III.2.1 Identification of single and generation of double mutants of *AtZRF1a* and *AtZRF1b*

To study the biological roles of *AtZRF1a* and *AtZRF1b*, we first obtained from the *Arabidopsis* Biological Resource Center (ABRC; http://www.arabidopsis.org/) two T-DNA insertion mutant lines for each of *AtZRF1a* and *AtZRF1b*. They are named *Atzrf1a-1, Atzrf1a-2, Atzrf1b-1* and *Atzrf1b-2*. The mutant *Atzrf1a-1* (SAIL_786_F09) harbors a T-DNA insertion 486 bp downstream of the translational start codon of *AtZRF1a* and the T-DNA carries the selection marker for BASTA (PPT,

phosphinothricin) resistance. The mutant *Atzrf1a-2* (SALK_070956. 55.25. x) harbors a T-DNA insertion 426 bp upstream of the translational stop codon of *AtZRF1a* and the T-DNA carries the selection marker for kanamycin (Kan) resistance. The mutant *Atzrf1b-1* (FLAG_110A05) has a T-DNA insertion 849 bp downstream of the translational start codon of *AtZRF1b* and the T-DNA carries the selection marker for BASTA resistance. The mutant *Atzrf1b-2* (SAIL_716_D04) harbors a T-DNA insertion in the *AtZRF1b* 3'-UTR, 159 bp downstream of the translational stop codon of *AtZRF1b* and the T-DNA carries the selection marker for BASTA resistance (Figure III.7A). For all these single mutants we confirmed the location of the T-DNA byPCR (polymerase chain reaction) amplification using the T-DNA-specific oligonucleotide primer LB1 and two gene-specific primers located at each side of T-DNA insertion site (Figure III.7A). Homozygous mutant plants were obtained for *Atzrf1a-1*, *Atzrf1a-2, Atzrf1b-1* and *Atzrf1b-2* by self-pollination; each line was identified by genotyping 30 antibiotic-resistant plants in PCR reactions.

To further confirm these mutants, we examined the *AtZRF1a* and *AtZRF1b* mRNA transcript levels in wild type and mutants by reverse transcription PCR (RT-PCR). The analysis revealed that full-length transcripts of *AtZRF1a* and *AtZRF1b* are undetectable in homozygous mutants *Atzrf1a-1*, *Atzrf1a-2* and *Atzrf1b-1*, indicating that T-DNA insertion caused a knockout of the respective gene in these mutants. Under standard laboratory growth conditions, none of the four mutants showed any obvious growth or developmental defect (Figure III.6A), probably due to the functional redundancy of the two *AtZRF1* genes. Considering the high homology of *AtZRF1a* and *AtZRF1b* and their similar expression profiles, we generated double mutants through crosses of different single mutants (Figure III.6B) to investigate the possible redundant function of these genes.

A

B

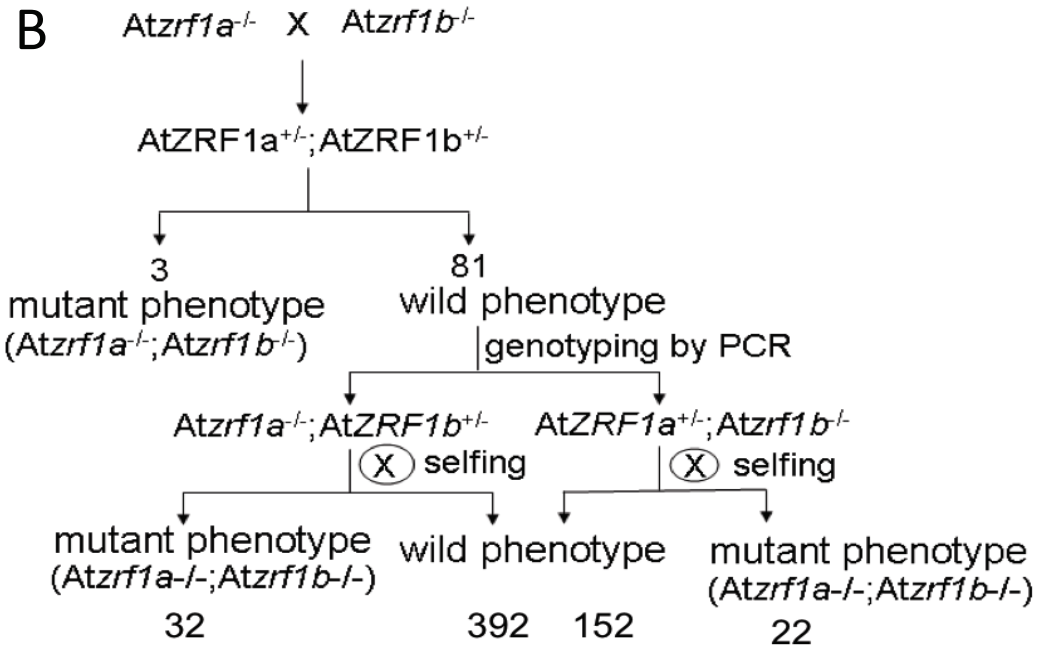

Figure III.6. Phenotype of single mutants and generation of *Atzrf1a*$^{-/-}$ *Atzrf1b*$^{-/-}$ mutant

(A) Phenotype of single mutants *Atzrf1a*$^{-/-}$ and *Atzrf1b*$^{-/-}$ in the Columbia background.

(B) A schematic representation of the procedure used to generate the double mutant *Atzrf1a*$^{-/-}$ *Atzrf1b*$^{-/-}$. The two homozygous mutant alleles *Atzrf1a*$^{-/-}$ and *Atzrf1b*$^{-/-}$ were combined together by crossing. Then, genotyping by PCR was performed on F2 progenies. For the WT allele, PCR was carried out by gene-specific forward and reverse primers on the genomic sequence. For the T-DNA insertion, PCR was carried out using one primer on the left border of the T-DNA insertion and another gene-specific primer on the flanking genomic sequence.

III.2.2 Phenotype observation of double mutants of *AtZRF1a* and *AtZRF1b*

In contrast to single mutants, the double mutants *Atzrf1a-1 Atzrf1b-1* and *Atzrf1a-2 Atzrf1b-1* are highly similar: they show not only defects in the vegetative phase of development (Figure III.7C), but also developmental aberrations in the inflorescence and siliques. For example, we found that the length of wild-type siliques is 1.5±0.2 cm (n=10), while the length of the siliques of *Atzrf1a-1 Atzrf1b-1* double mutant plants is 0.49±0.14 cm (n=10) and the length of the siliques of *Atzrf1a-2 Atzrf1b-1* double mutant plants is 0.52±0.1 cm (n=10). Thus, the silique length of the mutants is significantly shorter than that of wild-type plants. Moreover, wild-type plants have 55.0±3.5 (n=10) seeds per silique, whereas *Atzrf1a-1 Atzrf1b-1* double mutant plants have only 6.3±1.6 (n=10) seeds per silique and *Atzrf1a-2 Atzrf1b-1* double mutant plants have only 7.0±2.2 (n=10) seeds per silique (Figure III.8). In contrast, we found that the double mutants *Atzrf1a-1 Atzrf1b-2* and *Atzrf1a-2 Atzrf1b-2* have a normal phenotype. This is consistent with data showing that *AtZRF1b* is normally expressed in *Atzrf1b-2*. Consequently, *Atzrf1b-2* was no more used in our studies hereinafter.

Because of low fertility, we have maintained the double mutants in genetic backgrounds with one gene in the heterozygous state. e.i. *Atzrf1a*$^{+/-}$ *Atzrf1b*$^{-/-}$ and *Atzrf1a*$^{-/-}$ *Atzrf1b*$^{+/-}$. Upon selfing, both lines produced mutant-phenotype progeny at a frequency of segregation lower than expected for recessive mutations (Figure III.6B), indicating that simultaneous loss-of-function of both *AtZRF1a* and *AtZRF1b* is responsible of the mutant phenotype.

III.2.3 Complementation and allelism test of mutants

We further investigated the association of mutant phenotype with loss-of-function of the genes using the complementation test. A full-length cDNA of *AtZRF1b* was ligated by Gateway cloning into the binary plant-transformation vector *pGWB11* which contains 35S promoter upstream of the cloning site and the hygromycin (Hyg) selection marker gene in the T-DNA. *Agrobacterium tumefaciens*-mediated plant transformation was used to introduce the 35-promoter-*AtZRF1b* transgene into *Atzrf1a Atzrf1b* double mutant plants. Because of low fertility of homozygous double mutants, we used double mutant *Atzrf1a-1*$^{-/-}$ *Atzrf1b-1*$^{+/-}$ heterozygote transformation, whose

genotype was verified by PCR-based genotyping before transformation. The F_1 seeds post transformation were collected and plated on MS medium containing the antibiotics PPT and Hyg. The growing plants were transferred into soil and analyzed to identify the background of double mutant homozygotes by PCR-based genotyping using gene-specific primers. We found that introduction of the *35S:AtZRF1b* completely rescued the *Atzrf1a*$^{-/-}$ *Atzrf1b*$^{-/-}$ mutant to the wild-type phenotype (Figure III.9), demonstrating that *AtZRF1* gene knockout is indeed responsible for the phenotypic defects observed in the *Atzrf1a Atzrf1b* mutant.

In parallel, we identified novel T-DNA insertion mutant lines and performed an allelism test. First, we crossed *Atzrf1a-1*$^{+/-}$ *Atzrf1b-1*$^{-/-}$ with *Atzrf1a-3*$^{-/-}$ (SALK_ 070965.50.20.x), which contains a T-DNA insertion in the 3'-coding region of *AtZRF1a* (Figure III.10A) and the T-DNA carries the kanamycin resistance selection marker. The F_2 seeds resulting from the cross were plated on MS medium containing PPT and Kan, and the growing plants were transferred onto soil for further genotyping and phenotype analysis. We found that plants with the *Atzrf1a-1*$^{+/-}$ *Atzrf1a-3*$^{+/-}$ *Atzrf1b-1*$^{-/-}$ genotype or with the *Atzrf1a-3*$^{-/-}$ *Atzrf1b-1*$^{-/-}$ genotype display a growth phenotype similar to that of *Atzrf1a-1*$^{-/-}$ *Atzrf1b-1*$^{-/-}$ (Figure III.10B). This indicates that *Atzrf1a-3* is also a loss-of-function mutant allele of *AtZRF1a*. In a similar way, we found that *Atzrf1b-3* (SAIL_625_B03.v2), *Atzrf1b-4* (SAIL_629_F09.v1) and *Atzrf1b-5* (FLAG-099c10) are allelic to *Atzrf1b-1* and represent novel loss-of-function mutant alleles of *AtZRF1b* (Figure III.10).

Taken together, our molecular data, transgenetic complementation, and identification of multiple loss-of-function allelic mutants firmly establish that *AtZRF1a* and *AtZRF1b* have redundant functions and that simultaneous loss of function of both genes caused the *Atzrf1a*$^{-/-}$ *Atzrf1b*$^{-/-}$ mutant phenotype.

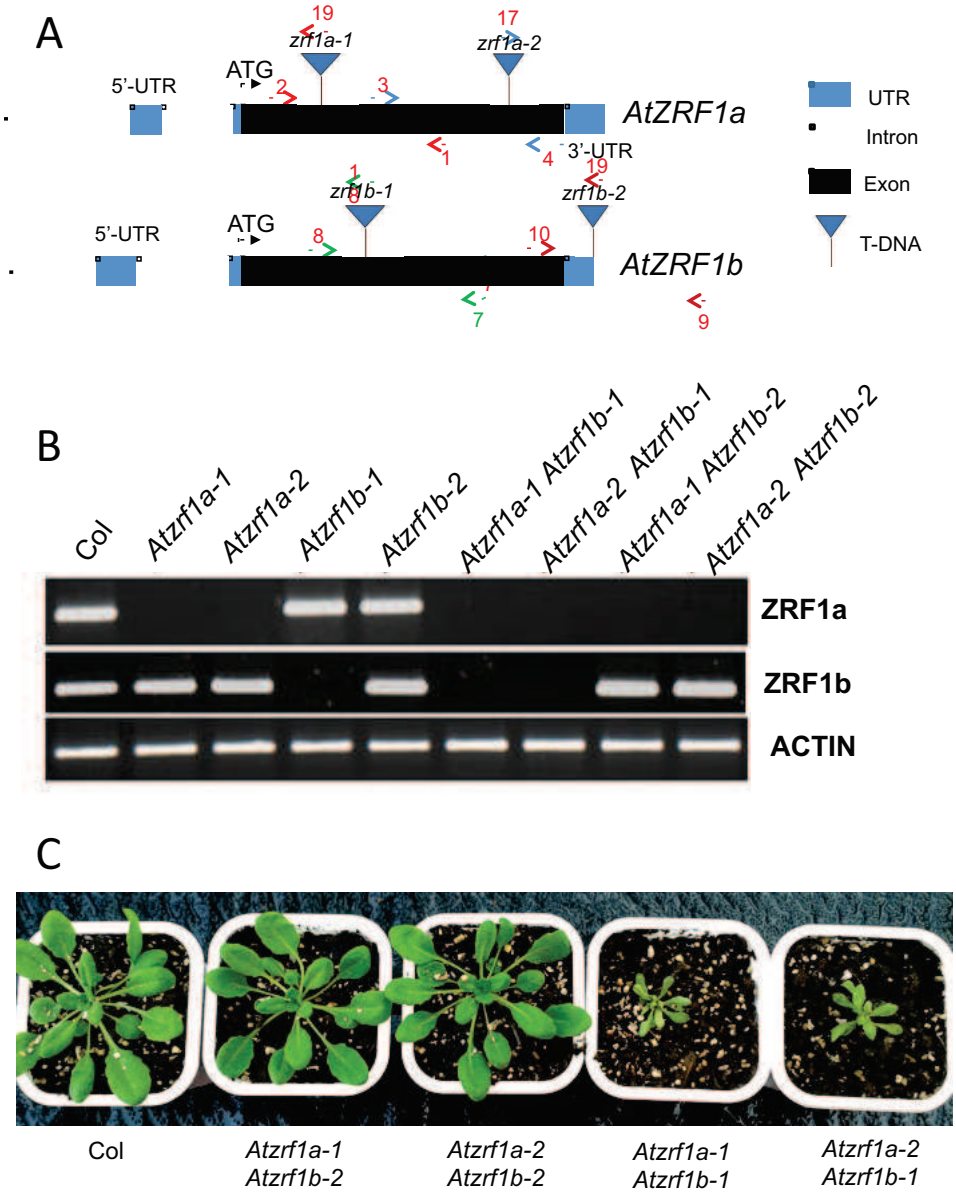

Figure III.7. Structures and expression patterns of *Atzrf1a*$^{-/-}$ and *Atzrf1b*$^{-/-}$ mutant

(A) (A) Diagram of the gene structures of *Atzrf1a*$^{-/-}$ and *Atzrf1b*$^{-/-}$ mutant alleles. Black boxes represent exons; Blue boxes represent UTR; White boxes represent introns; and triangles indicate T-DNA insertions. Primers of same colors represent primer pairs used together. The primer number (1 to 19) corresponds to the position in the primer list in Materials and Mehtods (Genotyping).

(B) RT-PCR analysis of *AtZRF1a* and *AtZRF1b* expression in rosette leaves of the single mutants *Atzrf1a*$^{-/-}$ and *Atzrf1b*$^{-/-}$, and in the double mutant *Atzrf1a*$^{-/-}$ *Atzrf1b*$^{-/-}$ (*Atzrf1a-1 Atzrf1b-1; Atzrf1a-1 Atzrf1b-2; Atzrf1a-2 Atzrf1b-1; Atzrf1a-2 Atzrf1b-2)*. Full-length AtZRF1a, and AtZRF1b sequences were amplified from wild-type (Col), single and double mutant cDNAs, ACTIN serves as an internal control.

(C) 35-day-old Col and double mutants grown under 12h light/ 12h dark at 21°C

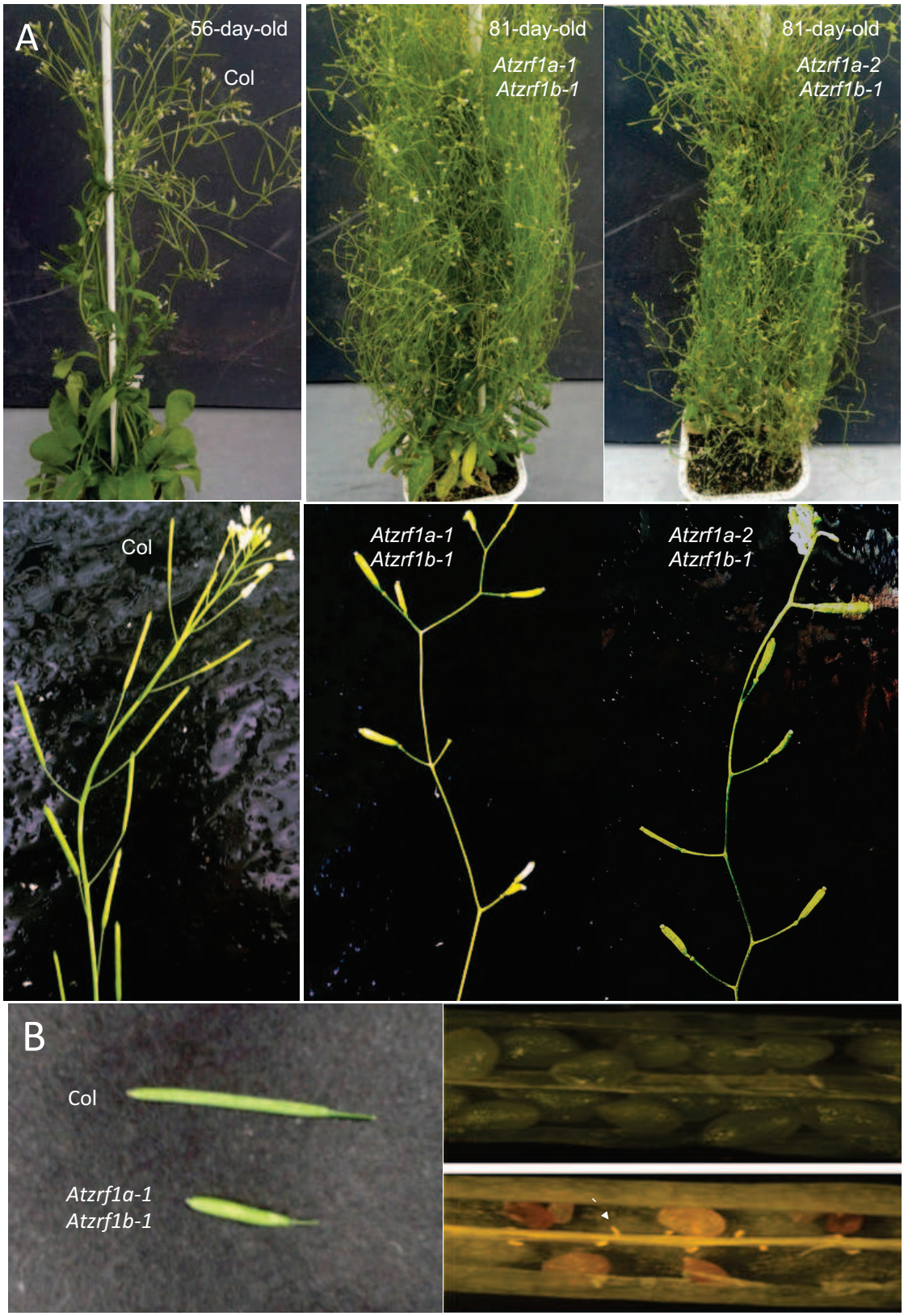
A
56-day-old
Col
81-day-old
Atzrf1a-1
Atzrf1b-1
81-day-old
Atzrf1a-2
Atzrf1b-1
Col
Atzrf1a-1
Atzrf1b-1
Atzrf1a-2
Atzrf1b-1
B
Col
Atzrf1a-1
Atzrf1b-1

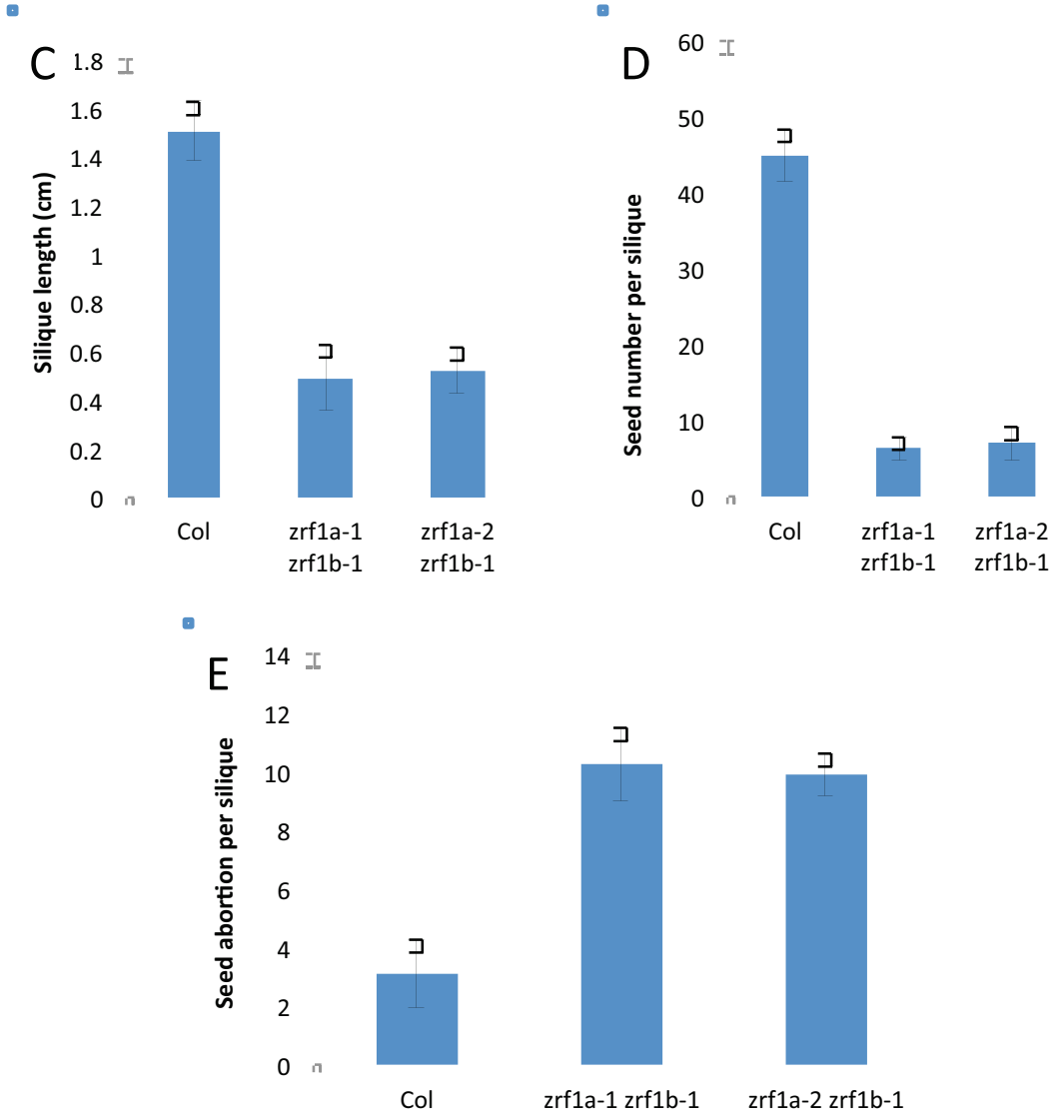

Figure III.8. Production and mature plant phenotype of *Atzrf1a*$^{-/-}$ *Atzrf1b*$^{-/-}$ mutant

A. Comparison of a 45-day-old wild-type Col plant and 81-day-old mutant *Atzrf1a*$^{-/-}$ *Atzrf1b*$^{-/-}$ plants (*Atzrf1a-1 Atzrf1b-1* and *Atzrf1a-2 Atzrf1b-1*) (top of Figure A)). At the bottom of the figure, Siliques of wild-type and double mutants (bottom of Figure A).

B. Representative photograph of wild-type (Col) and *Atzrf1a Atzrf1b* double mutant siliques. An abortion event, apparently frequent on *Atzrf1a Atzrf1b* double mutant siliques, is highlighted (arrow). Comparison between wild-type (Col) and *Atzrf1a-1 Atzrf1b-1* and *Atzrf1a-2 Atzrf1b-1* homozygous lines:

C. length of siliques

D. number of seeds per silique

E. seeds aborted per silique.

The error bars represent SE from 10 siliques along the stem of 5 independent plants (n= 50 for each).

Figure III.9. Rescue of the *Atzrf1a-1*$^{-/-}$ *Atzrf1b-1*$^{-/-}$ mutant phenotype

35S:AtZRF1b was used to rescue of the *Atzrf1a-1*$^{-/-}$ *Atzrf1b-1*$^{-/-}$ mutant. Phenotypes of 5-week-old Col, *Atzrf1a-1*$^{-/-}$ *Atzrf1b-1*$^{-/-}$ mutants and rescued plants. 12h light/12h dark, 21℃.

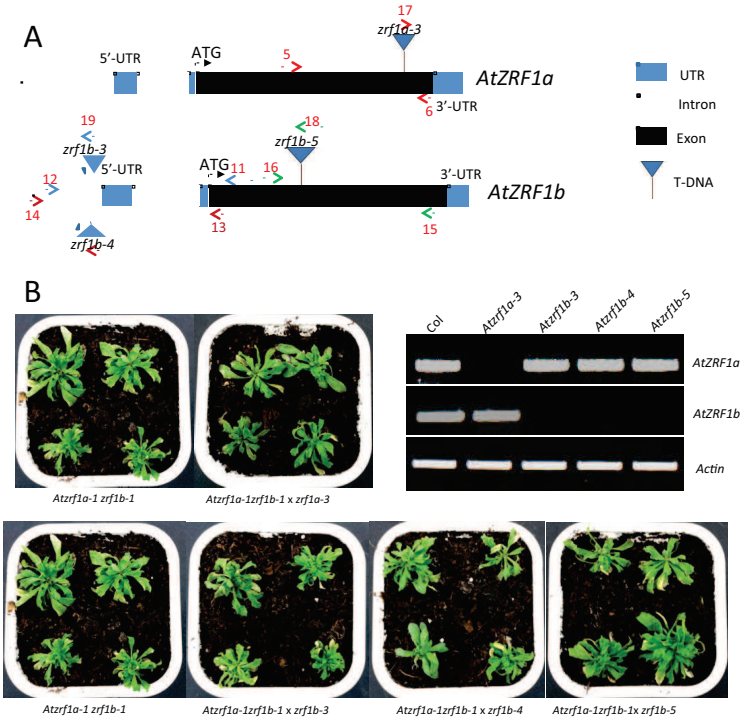

Figure III.10. Allelism test of *Atzrf1a*$^{-/-}$ and *Atzrf1b*$^{-/-}$ mutant

(B) Schematic representation of the *AtZRF1a* gene and *AtZRF1b* gene. Black boxes represent exons; Blue boxes represent UTRs; White boxes represent introns; triangles indicate T-DNA insertions. Primers of same colors represent primer pairs used together. The primer number (1 to 19) corresponds to the position in the primer list in Materials and Mehtods (Genotyping).

(C) Top left: allelism test between *Atzrf1a-3* and *Atzrf1a* as scored by *Atzrf1a-1*$^{-/-}$*Atzrf1b-1*$^{-/-}$ mutant phenotype. Bottom: allelism test between *Atzrf1b-3*, *Arzrf1b-4*, *Atzrf1b-5* and *Atzrf1b* as scored by *Atzrf1a-1*$^{-/-}$*Atzrf1b-1*$^{-/-}$ mutant phenotype. All plants (5-week-old) grown under long day conditions (16h light and 8h dark). Top right: RT-PCR analysis of *AtZRF1a* and *AtZRF1b* expression in the single mutants *Atzrf1a-3*, *Atzrf1b-3*, *Arzrf1b-4*, *Atzrf1b-5* and wild-type (Col). Full-length of *AtZRF1a*, and *AtZRF1b* sequences were amplified from single mutants and Col using gene specific primers, *ACTIN* served as an internal control

III.3. Loss of function of *AtZRF1a* and *AtZRF1b* drastically affects many aspects of plant growth and development

III.3.1 Plant organ and cell sizes are reduced in *Atzrf1a Atzrf1b* mutants

Compared to the wild-type plants, the *Atzrf1a-1 Atzrf1b-1* and *Atzrf1a-2 Atzrf1b-1* double mutant seedlings showed varied degrees of phenotype severity on cotyledons, such as single cotyledon (~12.65%), asymmetrical cotyledon (~21.61%) and fleshy cotyledon (~3.27%) seen in the *Atzrf1a*$^{-/-}$ *Atzrf1b*$^{-/-}$ mutant seedlings (Figure III.11). Moreover, development and growth of the *Atzrf1a Atzrf1b* double mutant were significantly delayed and prolonged, compared to those of the wild type (Col) and the two single mutants. After 10 d, wild-type seedlings developed two rosette leaves in addition to two cotyledons, while most of the double mutant plants only had two cotyledon leaves or were just starting to produce the first true leaves. At the vegetative stage, fresh weight measurements of whole rosettes of 4-week-old plants confirmed the smaller size of *Atzrf1a-1 Atzrf1b-1* (18.33 ± 6.87 mg, n = 10) and *Atzrf1a-2 Atzrf1b-1* (18.59 ± 6.90 mg, n = 10), compared to Col-0 (75.0 ± 11.18 mg, n = 10) (Figure III.12A-B). Scanning electron microscopy analysis of mature leaf adaxial epidermal cells from the seventh true leaf of 6-week-old wild-type and double mutants *Atzrf1a-1 Atzrf1b-1* and *Atzrf1a-2 Atzrf1b-1* plants revealed smaller cell size in double mutants compared to Col-0 leaves (Figure III.12C). The epidermal pavement cell surface is reduced to ~40% in *Atzrf1a-1 Atzrf1b-1* and *Atzrf1a-2 Atzrf1b-1* as compared to that in Col-0 (Figure III.12D). Taken together, these data indicate that cell expansion is drastically constrained, which largely accounts for the reduced leaf size in *Atzrf1a-1 Atzrf1b-1* and *Atzrf1a-2 Atzrf1b-1*.

III.3.2 Cell cycle and regulatory gene's expression are affected in *Atzrf1a Atzrf1b* mutants

To investigate cell cycle progression, we compared the ploidy levels of *Atzrf1a-1 Atzrf1b-1, Atzrf1a-2 Atzrf1b-1* and Col-0 leaves by measurement of the relative nuclear DNA content via flow cytometry analysis. DNA was isolated from the first true leaf on three different 2-week-old plantlets. The cell cycle consists of four phases: the postmitotic interphase (G1), with 2C nuclear DNA content; the S phase, meaning DNA synthetic phase, with an intermediate 2C and 4C nuclear DNA content;

the postsynthetic interphase (G2), with a 4C nuclear DNA content; and finally the M phase, meaning mitosis. I observed a slightly lower proportion of 2C cells in *Atzrf1a-1 Atzrf1b-1* and *Atzrf1a-2 Atzrf1b-1* double mutants as compared to Col (Figure III.12E), suggesting a relatively shorter duration of G1 in the mutant. Higher ploidy levels (⩾ 8C) are the result of endoreduplication cycles in which nuclear DNA is replicated without subsequent mitotic division. The relative proportion of cells with higher ploidy levels is slightly increased in *Atzrf1a-1 Atzrf1b-1* and *Atzrf1a-2 Atzrf1b-1* double mutants as compared with Col (Figure III.12E). In addition, the leaf shape, leaf margin and leaf vein of *Atzrf1a-1 Atzrf1b-1* and *Atzrf1a-2 Atzrf1b-1* double mutants displayed an abnormal phenotype. Compared to wild-type, the double mutant displayed twisted blades. The leaf was folded from the midrib of the blade (Figure III.13). While the leaf margin of the wild-type is serrated, the leaf margin of double mutants is smooth. Moreover, the leaf vein of wild-type plants is netted while in the the double mutant it is very special in that there is a primary vein in the middle of leaf and the two sides of the leaf have a net-like venation(Figure III.13).

Observation of the first true leaves of two-week-old *Atzrf1a-1 Atzrf1b-1, Atzrf1a-2 Atzrf1b-1* double mutants and wild-type seedlings showed that the number of trichomes on the leaf epidermis of double mutants decreased compared to wild-type. Also the trichomes of double mutants mainly have only one or two branches, while the trichomes of wild-type rosette leaves typically have three branches (Figure III.14). Trichomes are specialized epidermal cells. Their distribution is spatially and temporally regulated and can serve as a trait to distinguish between juvenile and adult leaves. Trichome density and age of leaf are associated (Telfer *et al*., 1997).

The cell cycle is defined by a series of complex events, and is normally divided into phases with a defined temporal order. Each transition phase is controlled by cyclins and co-factors. To investigate the regulation of cell cycle progression in *Atzrf1a-1 Atzrf1b-1* and *Atzrf1a-2 Atzrf1b-1* double mutants, we performed a qRT-PCR analysis on transcripts from cell cycle-related genes in 2-week-old wild-type and *Atzrf1a-1 Atzrf1b-1* and *Atzrf1a-2 Atzrf1b-1* double mutants seedlings. These genes include *CDKA*, *CYCB*, *CYCD*, *RBR*, *E2F*, and *KRP2* which are key components of the pathway regulating entry into the cell cycle (Dewitte and Murray, 2003; Francis, 2007).

qRT-PCR analysis indicates that, in the *Atzrf1a Arzrf1b* double mutant, *KRP2* and *CyclinB1;1* showed a significant reduction in their expression level as compared to

wild-type plants (Figure III.15). *CyclinB1;1* controls cell cycle progression at the G2-to-M transition, while KRP2 specifically inhibits CDKA;1 (Verkest *et al*., 2005). CDKA;1 acts in both the mitotic cell cycle and the endoreduplication cycle. Distinct CDKA;1/cyclin complexes have been shown to regulate the mitotic cell cycle and the endoreduplication cycle (Verkest *et al*., 2005). The expression of *CDKA;1* in the double mutants shows no obvious difference with the wild-type. These results suggest that deletion of *AtZRF1a* and *AtZRF1b* may affect G2-M transition. The expression levels of E2Fa and E2Fc were increased in the double mutant, compared to wild-type. In *Arabidopsis*, the CYCD3-RBR-E2F pathway acts as a key regulator that controls G1-S transition (de Jager *et al.*, 2009; Dewitte *et al*. 2003; Menges *et al*. 2006). There are three typical E2Fs: E2Fa, E2Fb and E2Fc. Both *E2Fa* and *E2Fb* are transcriptional activators of the cell cycle, and they positively regulate the S phase (De Veylder *et al*., 2002; Sozzani *et al*., 2006); in contrast, E2Fc serves as a repressor (del Pozo *et al*., 2006). The qRT-PCR results showed a reduction of *CYCD3;1* expression level, suggesting that the absence of *AtZRF1a* and *AtZRF1b* delays progression of the cell cycle into S-phase. The expression level of *E2Fa* is not consistent with our conclusion. However, some experimental data suggest that CYCD3;1 and E2Fa have divergent effects on the cell cycle (de Jager *et al.*, 2009).

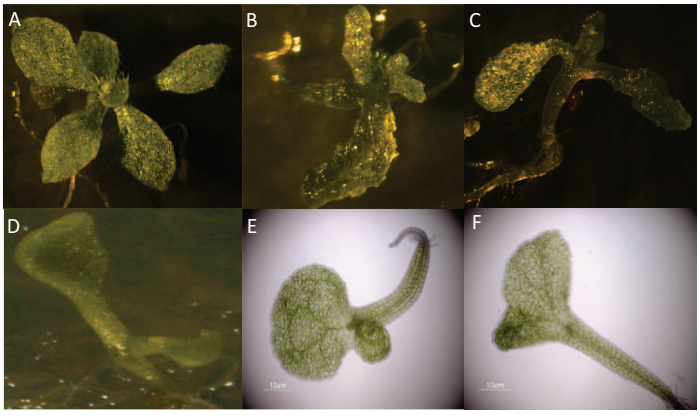

Figure III.11. Abnormal cotyledons in *Atzrf1a-1 Atzrf1b-1* and *Atzrf1a-2 Atzrf1b-1* double mutants

A. Weak mutant of 4-week old plants grown under 12h light and 12h dark conditions.
B-C. Fleshy cotyledons (4-week-old, under medium day conditions).
D-F. Asymmetrical cotyledons (2-week-old, under medium day conditions).

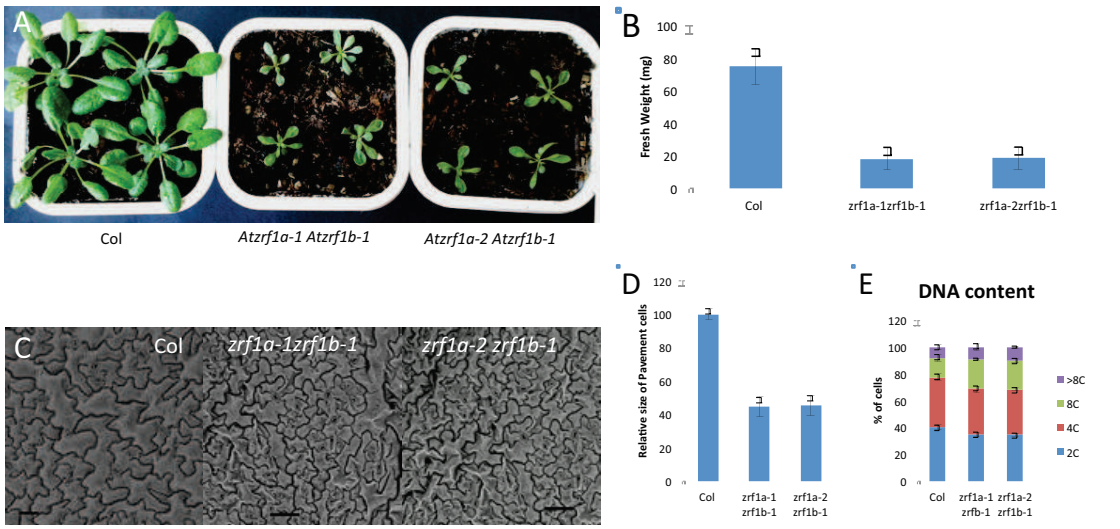

Figure III.12. Phenotype between *Atzrf1a-1 Atzrf1b-1 and Atzrf1a-2 Atzrf1b-1* mutants and wild-type

(A) Phenotype of wildtype and double mutants *Atzrf1a-1 Atzrf1b-1* and *Atzrf1a-2 Atzrf1b-1*. 4-week-old plants,12h light/12h dark, 21℃.

(B) Fresh weight of wildtype and double mutants *Atzrf1a-1 Atzrf1b-1* and *Atzrf1a-2 Atzrf1b-1* grown in soil and harvested without root. Error bars represent the mean±SE from data obtained from three independent experiments, each performed with 30 plants.

(C) Scanning electron microscope (SEM) images of mature leaf adaxial epidermal cells from the seventh true leaf of 6-week-old wild-type and double mutants *Atzrf1a-1 Atzrf1b-1* and *Atzrf1a-2 Atzrf1b-1* plants. Bar=500μm.

(D) Relative size of leaf adaxial epidermal pavement cells evaluated by measurement of the cell area from SEM images. The y axis indicates the relative cell size (wild type is set to 100%) calculated from the mean value of 30 cells, and error bars indicate SD.

(E) Ploidy levels of cells from the first true leaf of 2-week-old plants. Mean values from three independent experiments are shown. Error bars indicate SD.

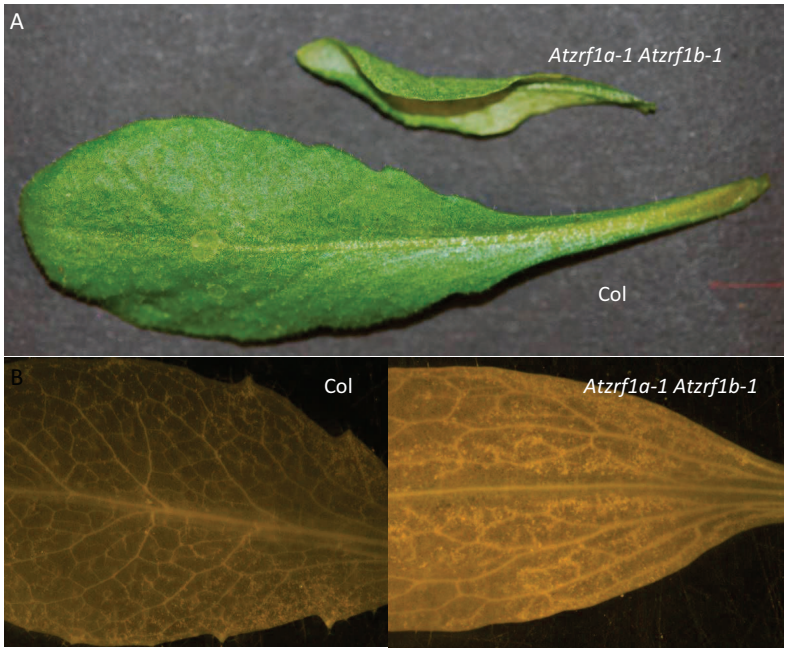

Figure III.13. Leaf shape, leaf margin and the distribution of leaf vein

A. Comparison of leaf shape between wild-type and *Atzrf1a-1 Atzrf1b-1* double mutant (4-week-old, under medium day conditions).

B-C. Comparison of leaf margin and the distribution of leaf vein between wild-type (B) and *Atzrf1a-1 Atzrf1b-1* double mutant (C).

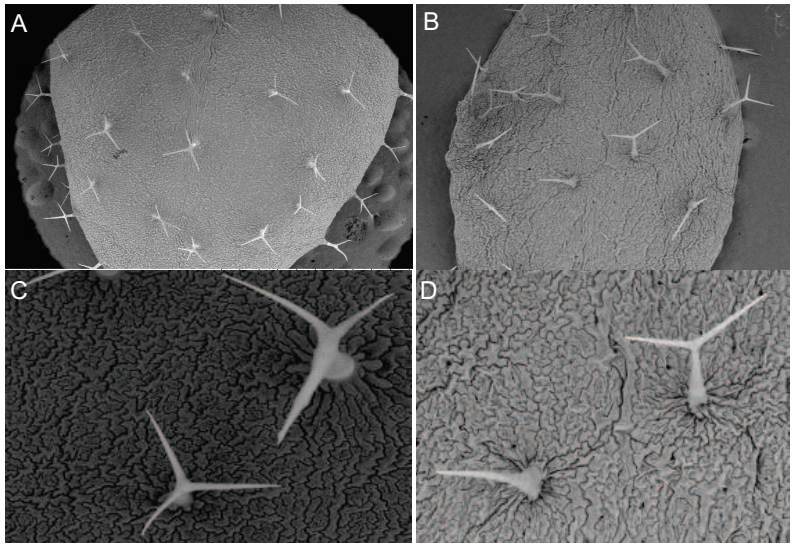

Figure III.14. Trichome phenotype of wild-type and *Atzrf1a Atzrf1b* double mutants

(A-B) Scanning electron micrographs of trichomes from the first true leaves of two-week-old *Atzrf1a-1 Atzrf1b-1, Atzrf1a-2 Atzrf1b-1* double mutants and wild-type seedlings. (A) Wild-type. (B) Double mutant.

(C-D) Scanning electron micrographs of wild-type and mutant trichomes branch. (C) Wild-type. (D) Double mutant.

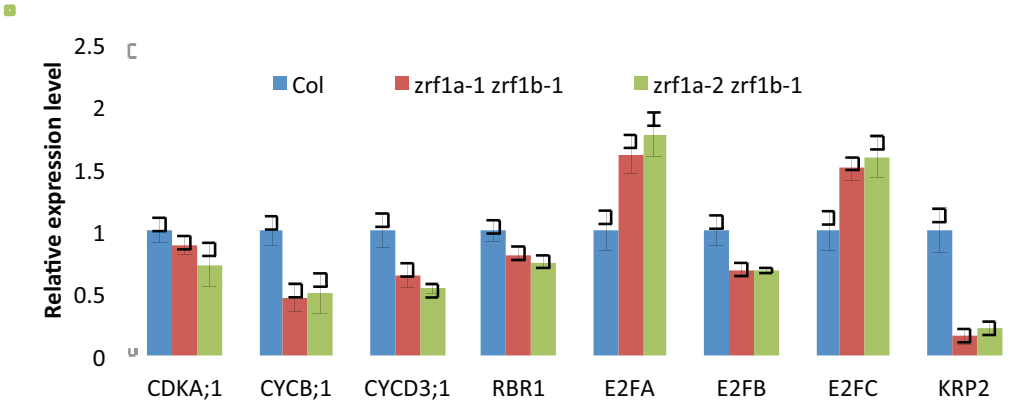

Figure III.15. qRT-PCR analysis of expression of cell cycle genes in wild- type and *Atzrf1a-1 Atzrf1b-1 and Atzrf1a-2 Atzrf1b-1* double mutants plants

Relative expression levels of cell cycle related genes determined by quantitative RT-PCR analysis. RNA was prepared from seedlings of 14-day-old Col-0 (blue bars) and *Atzrf1a-1 Atzrf1b-1* (red bars) and *Atzrf1a-2 Atzrf1b-1* (green bars). RT-PCR was performed using gene-specific primers and normalized using *Tip4.1*, *EXP* and *PP2A* as references. Relative expression levels of the indicated genes are shown as mean values from three biological repeats and with Col value setting as 1. Bars indicate SD.

III.3.3. Shoot stem cell activity and expression of Class I *KNOX* genes are affected in *Atzrf1a Atzrf1b* mutants

Compared to the wild-type plant, the *Atzrf1a-1 Atzrf1b-1* and *Atzrf1a-2 Atzrf1b-1* strong double mutants showed fasciated inflorescence meristems (Figure III.16 A-C). Those disrupt the normal spiral phyllotaxis of emerging flowers, pointing a defect in floral primordium initiation on the flanks of SAM. Homeotic transformations (i.e., the replacement of one type of organ with another) were also observed on the strong mutant flowers. Secondary flowers (～25%) and terminal flowers (～18.2%) were observed in *Atzrf1a-1 Atzrf1b-1* and *Atzrf1a-2 Atzrf1b-1* strong double mutants (Figure III.16 E-J). Taken together, the data indicate that loss of function of both *AtZRF1a* and *AtZRF1b* result in a superactivation of SAM and a perturbation of cell-fate determination, which affects initiation, maintenance, and differentiation of inflorescence and floral organs.

Previous research showed that AtRING1a/b and AtBMI1a/b are required for stem activity (Bratzel *et al*., 2010; Chen *et al*., 2010). To investigate the molecular mechanisms underlying the *Atzrf1a Atzrf1b* mutant phenotype, we first analyzed the expression of genes involved in SAM (Class I *KNOX* genes, *WUS*, and *CLV3*), floral homeotic genes (*AG* and *ULT1*) and PRC1 complex core components genes by qRT-

PCR using 2-week-old seedlings. As shown in Figure III.17A, *AtRING1a* and *AtRING1b* genes were slightly up-regulated in the mutants while the expression of *AtBMI1c* was strongly up-regulated in mutants and expression of *AtBMI1a*, *AtBMI1b* and *LHP1* was dramatically down-regulated in mutants (Figure III.17A). Moreover, we analyzed the expression of *AtZRF1a* and *AtZRF1b* in double mutants *Atring1a Atring1b* and *Atbmi1a Atbmi1b* by qRT-PCR. The results indicated that both *AtZRF1a* and *AtZRF1b* were up-regulated in the double mutants *Atring1a Atring1b* and *Atbmi1a Atbmi1b* (Figure III.17B). Ectopic expression of Class I *KNOX* genes (*STM*, *KNAT1*/ *BP*, *KNAT2* and *KNAT6*) and *CLV3* was detected in *Atzrf1a-1 Atzrf1b-1* and *Atzrf1a-2 Atzrf1b-1* double mutants seedlings. *STM* and *BP* are important for meristem maintenance and inflorescence architecture (Long *et al*., 1996; Venglat *et al*., 2002). Both *STM* and *BP* expression levels were higher (6-fold for *STM* and 4-fold for *BP*) in the *Atzrf1a-1 Atzrf1b-1* and *Atzrf1a-2 Atzrf1b-1* double mutants than in the wild-type. In contrast, expression of *WUS*, *AG*, and *ULT1* was detected down- regulated in *Atzrf1a-1 Atzrf1b-1* and *Atzrf1a-2 Atzrf1b-1* double mutants. It thus appears that loss of function of both *AtZRF1a* and *AtZRF1b* specifically induces ectopic expression of Class I *KNOX* genes.

To further confirm that loss of both *AtZRF1a* and *AtZRF1b* caused ectopic expression of *KNOX* genes, we used the *pSTM* promoter to drive β-glucuronidase (*GUS*) expression in the *Atzrf1a-1 Atzrf1b-1* double mutant and wild-type backgrounds. In the seedling stage, GUS activity was detected in an enlarged zone containing the SAM in the mutant (Figure III.18), indicating that suppression of *KNOX* gene expression has been released.

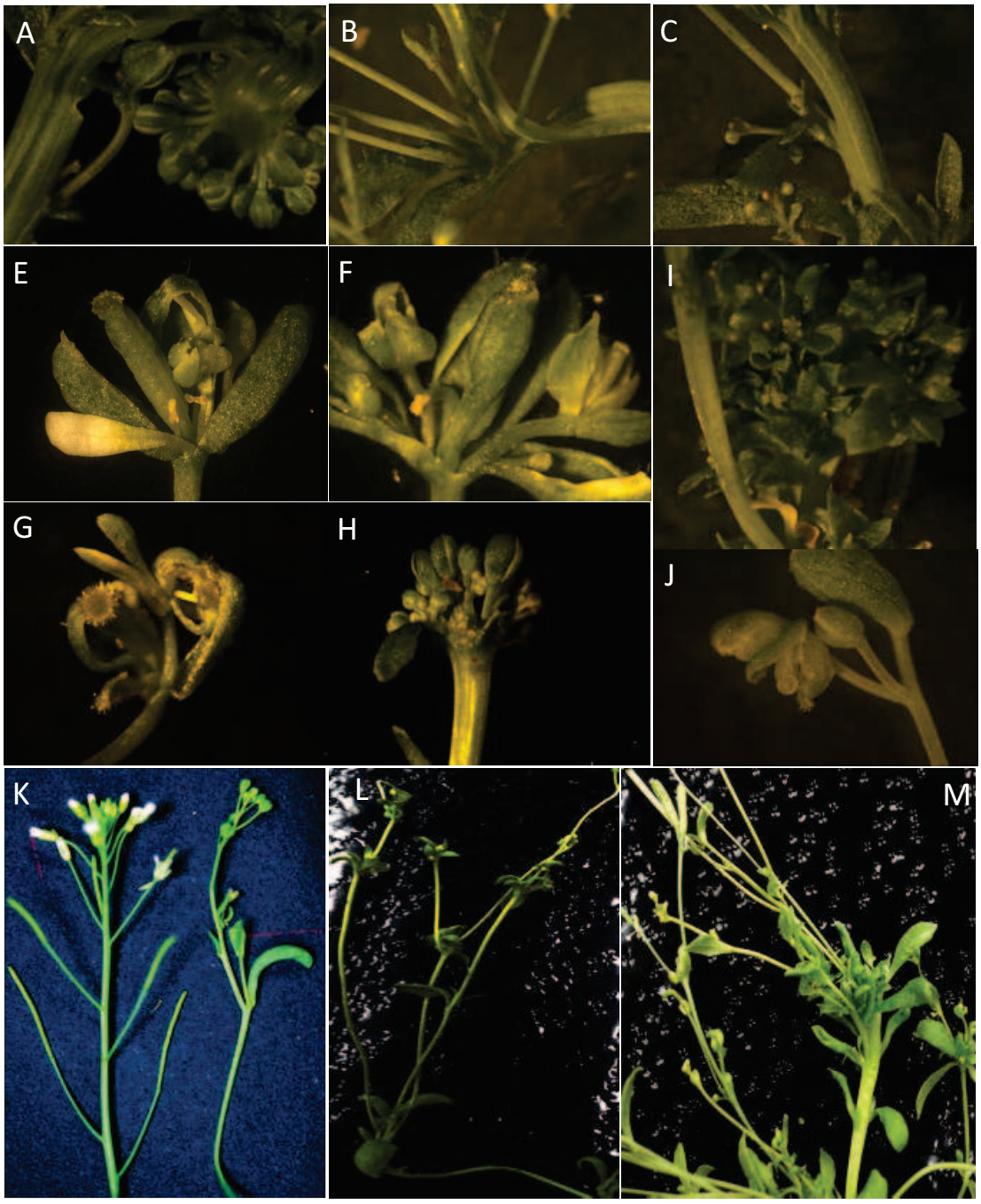

Figure III.16. Simultaneous knockout of *AtZRF1a* and *AtZRF1b* causes ectopic-meristem formation

A-C: Fasciated stem and hook-like apex on primary *Atzrf1a-1 Atzrf1b-1* inflorescence.

E-G: Flower reversions, *Atzrf1a-1 Atzrf1b*-1 flowers producing one or more secondary flowers (E, F). *Atzrf1a-1 Atzrf1b-1* floral organ reversion, with pistil (G).

H-J: Terminal flowers of the double mutant.

K-M: Abnormal inflorescence of the double mutant. (K) Florescence branch. The left is wild-type and the right is double mutant; (L-M) Cauline leaf. Inflorescences of double mutants.

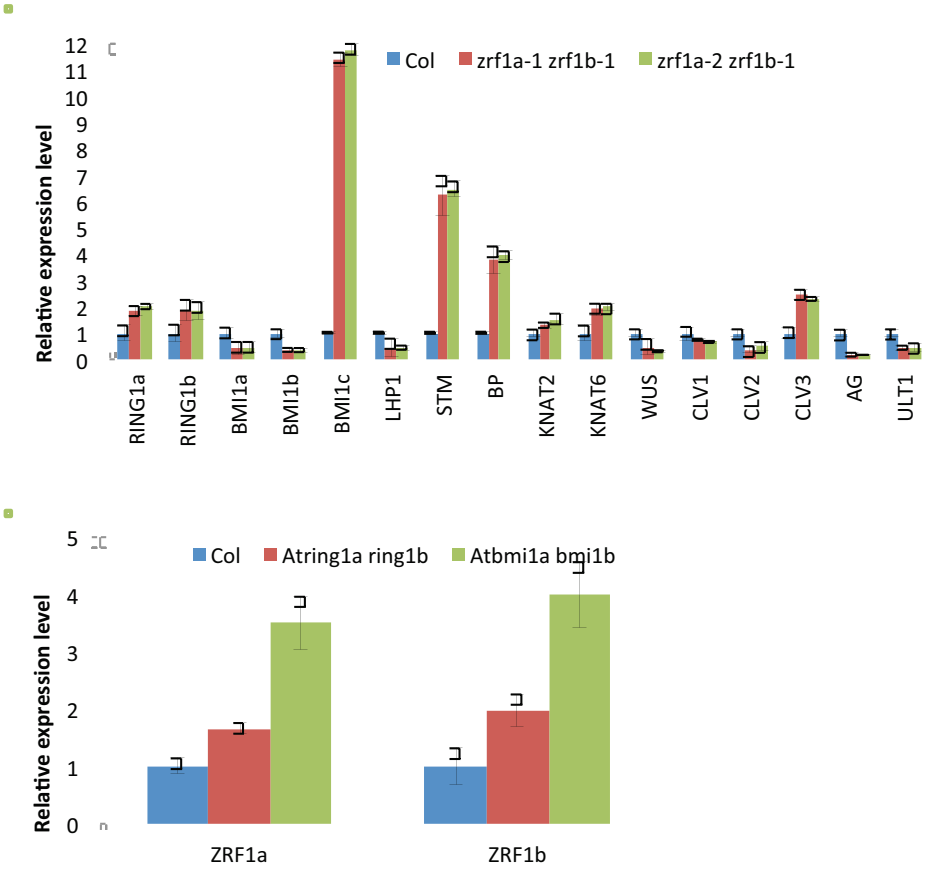

Figure III.17. Quantitative RT-PCR analysis of genes expression in 2-week-old wild-type and double mutants seedlings

A: Relative expression levels are shown as induction fold in 2-week-old *Atzrf1a-1 Atzrf1b-1* and *Atzrf1a-2 Atzrf1b-1* seedlings compared with 2-week-old wild-type (set as 1) seedlings.

B: Relative expression levels are shown as induction fold in *Atring1a Atring1b* and *Atbmi1a Atbmi1b* compared with wild-type (set as 1). Error bars represent standard deviation from triplicate repeats.

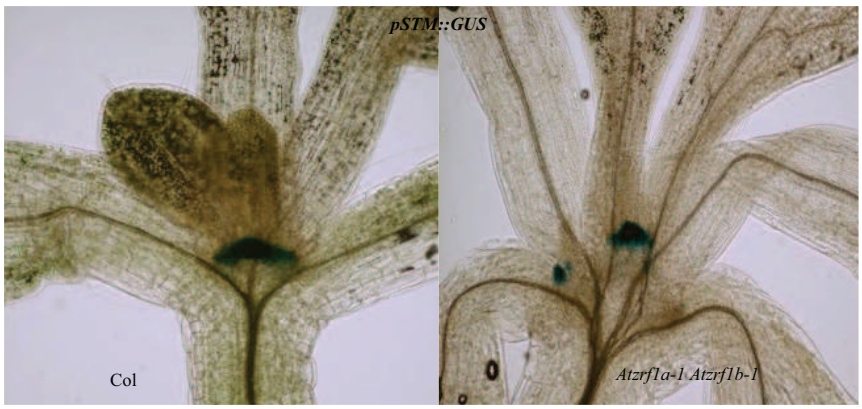

Figure III.18. *STM-GUS* expression in wild-type and *Atzrf1a-1 Atzrf1b-1* double mutant

Histochemical GUS staining of *pSTM:GUS* in double mutant *Atzrf1a-1 Atzrf1b-1* and wild-type Col. Seedlings at 10 DAS were stained for overnight. Blue staining indicates the reporter GUS activity.

III.3.4. Proper suppression of key embryogenesis regulatory genes is released during vegetative growth in *Atzrf1a Atzrf1b* mutants

Four weeks after germination, compared to the wild-type, the *Atzrf1a-1 Atzrf1b-1* and *Atzrf1a-2 Atzrf1b-1* mutants present abnormal embryonic traits in their somatic cells. The intermediate mutants started to form fleshy and callus-like structures. These structures arose from cotyledons or leaves (Figure III.18). The strong mutants formed callus-like structures, which have no clear structures (Figure III.19C). Together account for ~11% of *Atzrf1a Atzrf1b* mutant plants show derepression of embryonic traits. To investigate the molecular events underlying derepression of embryonic traits in *Atzrf1a-1 Atzrf1b-1* and *Atzrf1a-2 Atzrf1b-1* mutants plants, we analyzed expression levels of selected key regulatory genes involved in stem cell activity and embryogenesis (Figure III.20). The key SAM-regulatory genes (*STM*, *BP/KNAT1*, *KNAT2* and *KNAT6*) encoding *KNOX* transcription factors are upregulated by 2- to 6-fold in the mutant. The NAC-domain transcription factor genes *CUP-SHAPED COTYLEDON* 1 (*CUC1*), *CUC2* and *CUC3*, are required for organ boundary establishment and SAM initiation (Vroemen *et al*., 2003). They are upregulated by 5- to 7-fold in the double mutant (Figure III.20). While the homeodomain transcription factor gene *WUSCHEL* (*WUS*) and its homologue *WUSCHELRELATED HOMEOBOX 2 (WOX2)*, which are essential for SAM organizing center activity and apical embryo-axis cell fate (Breuninger *et al*., 2008; Laux *et al*., 1996), are drastic down-regulated and up-regulated, respectively. *WOX5* and *WOX8* are crucial for RAM function and basal embryo-axis cell fate termination (Breuninger *et al.*, 2008), are upregulated by more than 5- to 10-fold in the mutants (Figure III.20). The embryonic competence-enhanced factor gene *AGAMOUS-LIKE15* (*AGL15*) (Harding *et al.*, 2003) is upregulated by 2-fold, whereas expression of the somatic embryogenesis receptor-like kinase genes *SERK1* and *SERK2* (Schmidt *et al.*, 1997) is almost unaffected in the mutant (Figure III.20). Drastic upregulation of expression was observed for several key embryonic regulatory genes (Figure III.20), including the root stem cell regulator *BABY BOOM* (*BBM*) encoding an *AP2/ERF* transcription factor (Boutilier *et al.*, 2002), *LEAFY COTYLEDON 1* (*LEC1*) encoding a CCAAT-binding transcription factor (Lotan *et al.*, 1998), as well as *LEC2*. It was reported that overexpression of *LEC1* triggers spontaneous somatic embryo formation in plants (Stone et al., 2001). *ABI3* encoding B3 domain factors (Giraudat *et al.*, 1992; Stone *et al.*, 2001). It is

known that the phytohormone auxin plays an important role in embryogenesis and somatic embryo formation (Verdeil *et al.*, 2007). We detected a 2- to 3-fold upregulation of *PIN1* in *Atzrf1a-1 Atzrf1b-1* and *Atzrf1a-2 Atzrf1b-1* mutants, but neither *PIN4* nor *PIN7* expression was down- regulated, all from a gene family encoding polar auxin transporters (Blilou et al., 2005) (Figure III.20). Taken together, our results show that some but not all stem cell and embryonic regulatory genes are ectopically derepressed in *Atzrf1a-1 Atzrf1b-1* and *Atzrf1a-2 Atzrf1b-1* mutants.

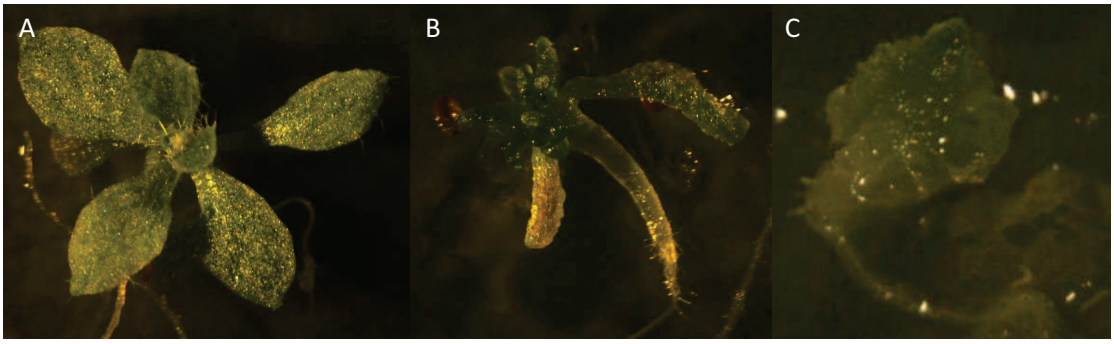

Figure III.19. Phenotypic variability of *Atzrf1a-1 Atzrf1b-1* double mutant seedlings

A. Weak mutant B-C: Dedifferentiation mutants

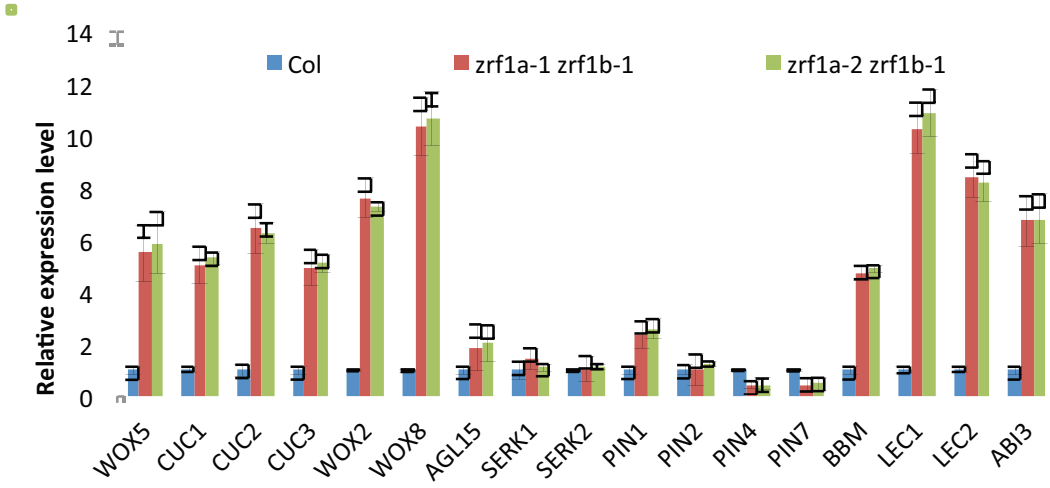

Figure III.20. Expression analysis of embryonic and stem cell regulatory genes in *Atzrf1a-1 Atzrf1b-1* and *Atzrf1a-2 Atzrf1b-1*.

Quantitative RT-PCR analysis of gene expression in 2-week-old seedlings. Relative expression levels are shown as induction fold in *Atzrf1a-1 Atzrf1b-1* and *Atzrf1a-2 Atzrf1b-1* compared with wild-type. Error bars represent standard deviation from triplicate repeats.

III.3.5. Floral organogenesis and regulatory genes expression are affected in *Atzrf1a Atzrf1b* mutants

Flowers are typically composed of four organ types, which are disposed in four floral whorls. From the outside of the flower to the center, they are the sepals, the petals, the stamens, and the carpels (the subunits of the gynoecium). In wild-type Arabidopsis plants, the floral meristem terminates in forming a flower with four sepals, four petals, six stamens and two fused carpels (Figure III.21A, B). In *Atzrf1a-1 Atzrf1b-1* and *Atzrf1a-2 Atzrf1b-1* double mutants plants, flowers show a dramatic variation in morphology. Statistic analysis of simple flowers from 10 plants and 10 single flowers of each plant revealed that the weak mutant flowers contain fewer sepals (3.8±0.7 for *Atzrf1a-1 Atzrf1b-1* and 3.9±0.4 for *Atzrf1a-2 Atzrf1b-1*), fewer petals (2.4±0.9 for *Atzrf1a-1 Atzrf1b-1* and 3.3±0.8 for *Atzrf1a-2 Atzrf1b-1*), and fewer stamens (4.25±0.6 for *Atzrf1a-1 Atzrf1b-1* and 4.9±0.7 for *Atzrf1a-2 Atzrf1b-1*), whereas the number of carpels is close to that of wild-type flowers (Figure III.21). In flowering plants, these different types of floral organs are specified by the activities of a small set of master regulators, termed floral organ identity genes. According to ABC model, sepals are specified by A function genes, petals by a combination of A and B function activities, stamens by B and C function genes, and carpels by C function gene activity alone (Coen and Meyerowitz, 1991). To investigate the molecular mechanisms underlying the *Atzrf1a Atzrf1b* double mutant phenotype, we extracted RNA from floral buds at stage 6 to perform quantitative PCR. We analyzed the expression of *APETALA1* (*AP1)*, *PISTILLATA* (*PI*) and *AGAMOUS (AG)* which belong to A, B and C function genes, respectively. *AG* is a key regulator of *Arabidopsis thaliana* flower development, where it is involved in the formation of the reproductive floral organs as well as in the control of meristem determinacy. *SEP3* is a direct target of *AP1*, specifying flower organ identity. qRT-PCR results showed that the expression levels of *AP1*, *PI* and *AG* were reduced and *SEP3* was slightly increased in *Atzrf1a-1 Atzrf1b-1* and *Atzrf1a-2 Atzrf1b-1* double mutant floral buds (Figure III.22). Moreover, we analyzed the master regulators of gynoecium establishment and development *AG* and the *AG*-like gene *SEEDSTICK* (*STK*). Their expression levels were decreased in the tested floral buds. What is more, the expression level of downstream effectors such as *CRABS CLAW* (*CRC*), *SPATULA* (*SPT)* and *GIANT KILLER* (*GIK*) was decreased in *Atzrf1a-1 Atzrf1b-1* and *Atzrf1a-2 Atzrf1b-1* floral buds (Figure III.22).

In addition, we analyzed the relative expression levels of some key regulators of the inflorescence meristem (IM) to flower meristem (FM) transition (*AGL24*, *SVP*, *LFY*, *CAL, UFO*) by qRT-PCR. These tested loci are known to balance IM and TM fate, the *LEAFY* (LFY) protein being a master regulator of the organ identity genes and its function is essential for both conferring floral meristem identity and the subsequent identity of the individual floral organs. Our results showed that *AGL24*, *SVP* and *LFY* were overexpressed, while *CAULIFLOWER* (*CAL*) and *UNUSUAL FLORAL ORGANS* (*UFO*) were repressed in *Atzrf1a-1 Atzrf1b-1* and *Atzrf1a.2 Atzrf1b.1* floral buds (Figure III.22). We selected regulators balancing termination and maintenance of flower meristematic cells for analysis. Expression levels of stem cell maintenance genes (*i.e. KNOX*, *WUS*) and repressors (*i.e. AG* and *ULT1*) in *Atzrf1a-1 Atzrf1b-1* and *Atzrf1a-2 Atzrf1b-1* young flower buds around stage 8 of flower development (Smyth *et al*., 1990) were examined. Strikingly, the main players in floral meristem determinacy *AG* and *WUS* were not repressed by AtZRF1a and AtZRF1b. Compared to wild-type, the expression levels of *AG* and *WUS* were reduced in *Atzrf1a-1 Atzrf1b-1* and *Atzrf1a-2 Atzrf1b-1* floral buds (Figure III.22). The trancriptional activity of *STM*, *BP*, *KNAT6* and *ULT1* were increased in *Atzrf1a-1 Atzrf1b-1* and *Atzrf1a-2 Atzrf1b-1* floral buds.

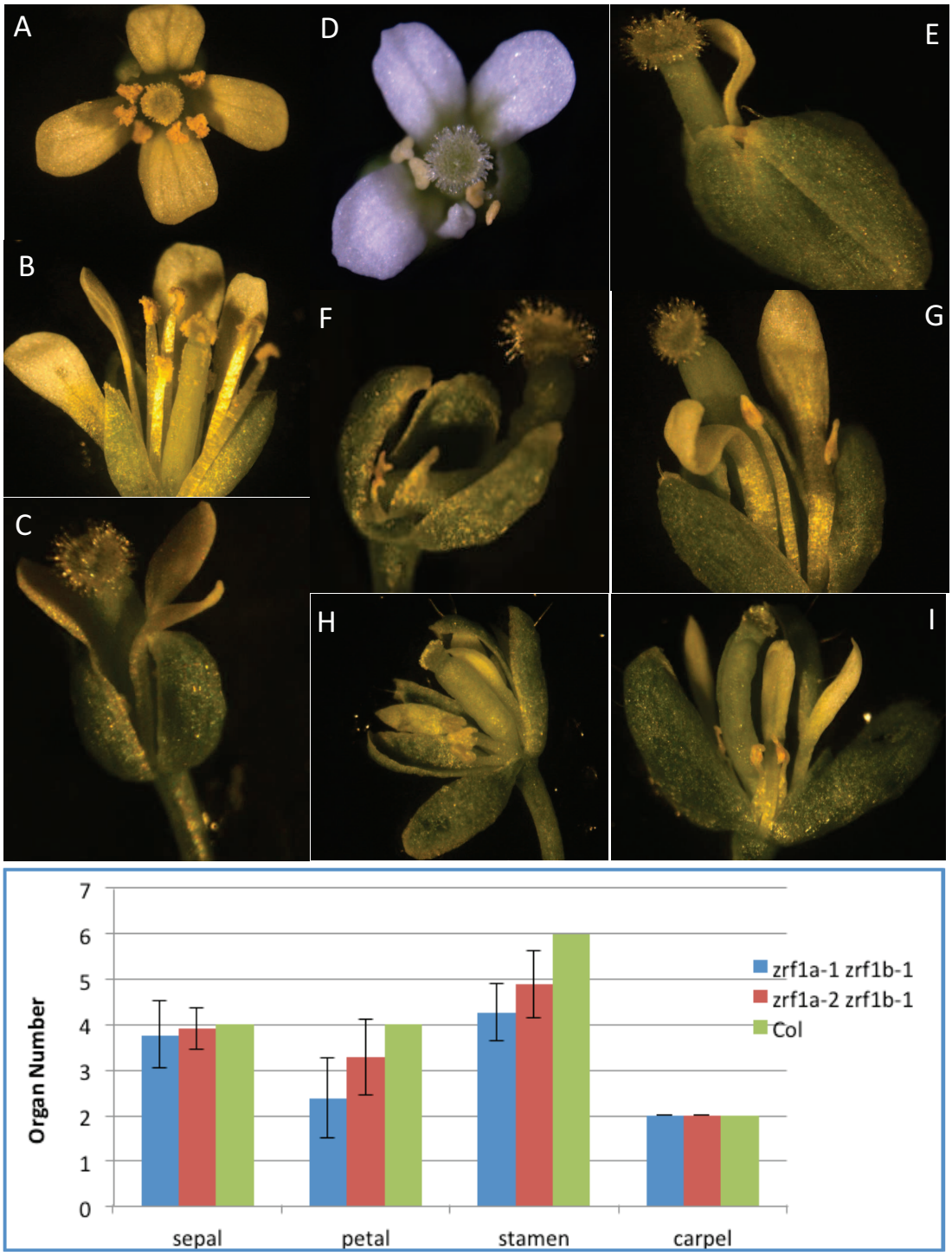

Figure III.21. Abnormal flower organs in *Atzrf1a Atzrf1b* mutant

(A-B) Wild-type. Arabidopsis WT flowers usually have 4 sepals, 4 petals, 6 stamens, and two fused carpels.

(C-I) Defective flower organs of *Atzrf1a Atzrf1b* weak double mutant. (D) has 3 normal petals and 1 smaller petal. (E) Flower no opened, but pistil and petal have appeared. Disruption of *AtZRF1a* and *AtZRF1b* leads to very short stamens (I). And produce sterile flowers with dramatically reduced number of floral organs (F). Statistic analysis of simple flowers from 10 wild-type plants or 10 weak double mutant plants and 10 single flowers of each plant.

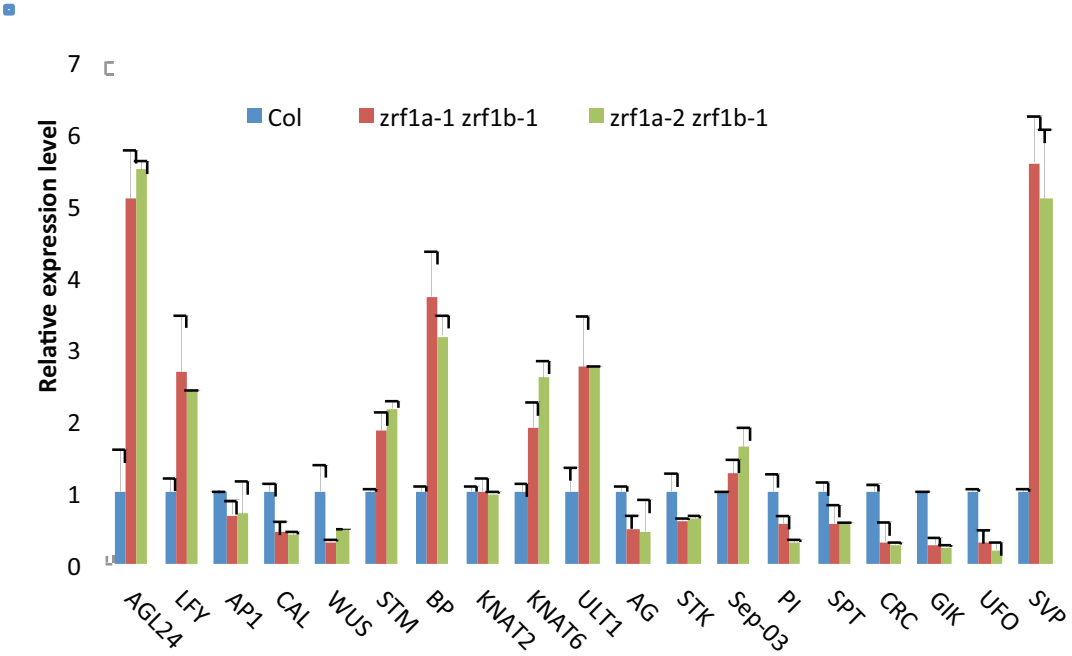

Figure III.22. Relative expression levels of flower developmental genes in *Atzrf1a Atzrf1b* mutants flower buds.

In young flower buds around stage 6 of flower development, expression levels of flower developmental genes were determined by qRT-PCR in wild-type (Col), *Atzrf1a-1 Atzrf1b-1* and *Atzrf1a-2 Atzrf1b-1* double mutants. Expression levels are relative to Col and normalized to internal reference genes (*Tip4.1*, *PP2A* and *Exp*). Data shown are means ± SD of technical replicates. Similar results were obtained in three independent experiments.

III.3.6. Both male and female transmission efficiencies are reduced in *Atzrf1a Atzrf1b* mutants

To examine gametophyte function under normal sporophytic growth, we investigated the inheritance of *Atzrf1a Atzrf1b* mutant alleles in heterozygous mutant plants. Growth tests on seeds produced by self-pollination of heterozygous plants revealed that the ratio of wildtype phenotype plants to double mutant plants is significantly higher than the expected ratio of 3:1 (Table III.1). The *Atzrf1a-1*$^{-/+}$ *Atzrf1b-1*$^{-/-}$, *Atzrf1a-2*$^{-/+}$ *Atzrf1b-1*$^{-/-}$, *Atzrf1a-1*$^{-/-}$ *Atzrf1b-1*$^{-/+}$ and *Atzrf1a-2*$^{-/-}$ *Atzrf1b-1*$^{-/+}$ lines behaved very similarly, but we found a reduced transmission of the *Atzrf1b-1*$^{-/-}$ gamete in the *Atzrf1a*$^{-/-}$ background; this reduced transmission is more obvious in the *Atzrf1a-1*$^{-/-}$ background than in the *Atzrf1a-2*$^{-/-}$ background (Table III.1). As no seed abortion could be observed, this suggested that male and/or female transmission of the *Atzrf1a Atzrf1b* mutant alleles was decreased. In order to further

determine the inheritance of the *Atzrf1a Atzrf1b* mutant alleles in the male and female gametes, reciprocal backcrosses of heterozygous mutant plants with the wild-type Col-0 plants (pollination of mutant pistils with Col pollen grains or pollination of Col pistils with mutant pollen grains) were performed. Genotyping by PCR analysis revealed that the inheritance of each of the *Atzrf1a-1*$^{-/+}$ *Atzrf1b-1*$^{-/-}$, *Atzrf1a-2*$^{-/+}$ *Atzrf1b-1*$^{-/-}$, *Atzrf1a-1*$^{-/-}$ *Atzrf1b-1*$^{-/+}$ and *Atzrf1a-2*$^{-/-}$ *Atzrf1b-1*$^{-/+}$ double mutants was reduced drastically through male and female gametes; when they are used as the pollen donor, the transmission rate is lower than when they are used as the egg donor (Table III.1). Taken together, these genetic data establish a gametophytic function of *AtZRF1a/b*, which is largely independent from its sporophytic function. It affects both male and female gametophytes, with a stronger effect on the male than on the female.

Parent	progeny	observed ratio	expected ratio
Self-pollination	WT m		
zrf1a-1$^{-/+}$ *zrf1b-1*$^{-/-}$	152 22	6.9:1***	3:1
zrf1a-1$^{-/-}$ *zrf1b-1*$^{-/+}$	392 32	13.25:1***	3:1
zrf1a-2$^{-/+}$ *zrf1b-1*$^{-/-}$	401 45	8.91:1***	3:1
zrf1a-2$^{-/-}$ *zrf1b-1*$^{-/+}$	379 37	10.24:1***	3:1
Reciprocal Cross (♀ × ♂)			
zrf1a-1$^{-/+}$ *zrf1b-1*$^{-/-}$ × Col	101 77	1:0.76*	1:1
Col × *zrf1a-1*$^{-/+}$ *zrf1b-1*$^{-/-}$	149 71	1:0.48**	1:1
zrf1a-1$^{-/-}$ *zrf1b-1*$^{-/+}$ × Col	185 101	1: 0.55**	1:1
Col ×*zrf1a-1*$^{-/-}$ *zrf1b-1*$^{-/+}$	241 103	1: 0.43**	1:1
zrf1a-2$^{-/+}$ *zrf1b-1*$^{-/-}$ × Col	176 125	1: 0.71*	1:1
Col × *zrf1a-2*$^{-/+}$ *zrf1b-1*$^{-/-}$	225 135	1: 0.60*	1:1
zrf1a-2$^{-/-}$ *zrf1b-1*$^{-/+}$ × Col	153 93	1:0.61*	1:1
Col × *zrf1a-2*$^{-/-}$ *zrf1b-1*$^{-/+}$	324 169	1:0.52**	1:1

Table III.1. Segregation analysis of *Atzrf1a Atzrf1b* double mutant in progeny derived from self-pollination or reciprocal crosses

Wild-type phenotype of heterozygous *Atzrf1a*$^{+/-}$ *Atzrf1b*$^{-/-}$ or *Atzrf1a*$^{-/-}$ *Atzrf1b*$^{+/-}$ mutant (WT) and mutant phenotype of *Atzrf1a*$^{-/-}$ *Atzrf1b*$^{-/-}$ (s) alleles were determined by PCR analysis. The ratios (WT: m) obtained from experimental data are higher than those expected from normal segregation, indicating reduced transmission efficiency of mutant alleles. Statistical significance: ***P < 0.001; **P < 0.01; *P < 0.05.

III.4. Characterization of *AtZRF1a* and *AtZRF1b* roles in root growth and development

The root is a very important organ of plant development. During embryogenesis, the *Arabidopsis* primary root formation is initiated by hypophysis specification. The hypophysis is a single extraembryonic suspensor cell. The suspensor cell generates the quiescent centre (QC) after several rounds of asymmetrical cell divisions and expansions, leading to the generation of the root meristem of the primary root. A larger basal cell generates the lower tier of stem cells for the columella. During this process, it is very important that the hypophysis is specified properly, otherwise, a root meristem is not formed, which eventually results in rootless seedlings (De Smet *et al*. 2010; Tian *et al*., 2014). Compared to wild-type, we found that the primary root growth of the double mutants *Atzrf1a-1 Atzrf1b-1* and *Atzrf1a-2 Atzrf1b-1* was strongly impaired. The mutants exhibit almost a rootless or short-root phenotype (Figure III.23A). Primary root growth was measured between 1 and 12 d after stratification (DAS). Compared to wild-type, the *Atzrf1a-1 Atzrf1b-1* and *Atzrf1a-2 Atzrf1b-1*double mutant showed clear primary root growth retardation, and the difference became increasingly evident along with plant age, e.g. the primary root length at 12 DAS of the *Atzrf1a-1 Atzrf1b-1* (4.88±0.83 mm, n=30) and *Atzrf1a-2 Atzrf1b-1* (5.27±1.02 mm, n=30) double mutants only reached about 10% of that of wild-type plants (55.4± 5.27 mm, n=30) (Figure III.23B). Subsequently we focused on the *Atzrf1a-1 Atzrf1b-1* double mutant for a more detailed analysis.

III.4.1 Auxin regulation is partly disrupted by loss of *AtZRF1a* and *AtZRF1b* function

Auxin is important for many aspects of root development, including initiation and emergence, patterning of apical meristem, gravitropism, and root elongation. In order to investigate whether ZRF impaired auxin regulation of the primary root, we introgressed *DR5∷GFP* into *Atzrf1a-1 Atzrf1b-1* double mutant by genetic crossing. The auxin-sensitive reporter *DR5∷GFP* reveals auxin signaling in single cells (Friml *et al*., 2003; Grieneisen *et al*., 2007). Observation of root tips by confocal microscopy revealed that *DR5::GFP* displays high expression in the tip of the RAM, specifically in the columella and QC in wild-type. However, compared to wild-type, in 22 out of 23

(95.7%) of the *Atzrf1a-1 Atzrf1b-1* double mutant roots examined, we found the expression level of *DR5::GFP* drastically reduced in *Atzrf1a-1 Atzrf1b-1* double mutant and most importantly the auxin gradient and maximum in QC were lost; almost no GFP signal could be detected at QC position (Figure III.24A). Next, we performed quantitative real-time RT-PCR analysis for auxin-related genes to compare their expression in wild-type and *Atzrf1a-1 Atzrf1b-1* double mutant roots. As shown in Figure 33B, expression of *IAA2, IAA16, IAA28, IAA29* and *IAA30* was drastically decreased whereas expression of *IAA14*, *IAA19* and *IAA34* was increased in the *Atzrf1a-1 Atzrf1b-1* double mutant. *IAA14* and *IAA19* genes are known to negatively regulate root growth (Fukaki *et al*., 2002; Tatematsu *et al*., 2004); their up-regulation is consistent with the root growth suppression phenotype of the *Atzrf1a-1 Atzrf1b-1* double mutant. In addition to auxin, other phytohormones such as brassinosteroids (BRs) are also involved in the regulation of root meristem activity (Perilli *et al*., 2012). A downregulation of *BES1*, which encodes a key transcription factor of the BR signaling pathway (Li *et al*., 2010), was observed in *Atzrf1a-1 Atzrf1b-1* double mutant (Figure III.24B).

We wanted to address whether auxin supply would rescue the *Atzrf1a-1 Atzrf1b-1* double mutant phenotype. Root growth was investigated in the presence of various concentrations of exogenous 1-naphthalene acetic acid (NAA). We measured root length of 8-day-old wild-type and double mutants supplemented with 0, 1, 10, 100 nM NAA, respectively. We found that root growth is less responsive to NAA inhibition in *Atzrf1a-1 Atzrf1b-1* and *Atzrf1a-2 Atzrf1b-1* double mutants compared to wild-type (Figure III.24C). *Atzrf1a-1 Atzrf1b-1* and *Atzrf1a-2 Atzrf1b-1* double mutants root growth weren't obviously affected by different concentration of auxin. Nevertheless, in no case *Atzrf1a-1 Atzrf1b-1* and *Atzrf1a-2 Atzrf1b-1* double mutants roots growth could reach that of WT. Taken together, our data indicate that loss of *AtZRF1a* and *AtZRF1b* function affects auxin regulation and exogenous auxin supply could not rescue the mutant root defects.

III.4.2 Loss of *AtZRF1a* and *AtZRF1b* disturbed root cell organization

To determine to what extent the cell proliferation activity of the RAM was affected in the *Atzrf1a-1 Atzrf1b-1* mutant, various parameters related to RAM activity were analyzed. Previous studies in the *Atzrf1a-1 Atzrf1b-1* double mutant showed that the *DR5::GFP* expression level obviously decreased in QC. The QC is crucial for

maintaining the identities of the surrounding stem cells which have the highest rate of cell division. To assess whether the QC was correctly specified in the primary root of the *Atzrf1a-1 Atzrf1b-1* double mutant, we introgressed the *WOX5*∶∶*GFP* marker into the *Atzrf1a-1 Atzrf1b-1* double mutant by genetic crossing. *WOX5* is specifically expressed and functions in root QC cells to regulate the balance between cell division and differentiation of the adjacent stem cells. Microscopy analysis revealed GFP fluorescence in the QC cells of *Atzrf1a-1 Atzrf1b-1 pWOX5::GFP*, however, compared with wild-type, in 23 out of 25 (92%) of the *Atzrf1a-1 Atzrf1b-1* double mutant roots examined, we found that the *Atzrf1a-1 Atzrf1b-1* double mutant contains a disorganized stem cell niche (SCN) with a reduced number of QC cells (Figure III.25). Moreover, in order to investigate whether surrounding stem cells were destroyed in *Atzrf1a-1 Atzrf1b-1* double mutant, we introgressed the enhancer-trap line *J1092* and the columella stem cell-specific enhancer trap line *J2341* into the *Atzrf1a-1 Atzrf1b-1* double mutant by genetic crosses. The *J1092* enhancer trap line showed weak GFP expression in the columella, including the columella stem cells, and a strong GFP signal in the lateral root cap of the wild-type seedlings (Figure III.26A). However, in 19 out of 21 (90.5%) of the *Atzrf1a-1 Atzrf1b-1* double mutant roots examined, the GFP expression level was reduced in the root cap (Figure III.26). The *J2341* enhancer trap line showed that GFP was specifically expressed in columella stem cells (CSCs) in the wild type root (Figure III.26), whereas in 25 out of 26 (96%) of the *Atzrf1a-1 Atzrf1b-1* double mutant roots examined, GFP was detected in the cells at the position of CSCs, and the number of CSCs was reduced (Figure III.26B). Columella cells function in gravity sensing; we found a few *Atzrf1a Atzrf1b* double mutants that had lost geotropism when germinating. Taken together, this indicates that deletion of both AtZRF1a and AtZRF1b leads to a defective cellular organization in the root stem cell niche.

The *Atzrf1a-1 Atzrf1b-1* double mutant showed a similar phenotype as the *shr* mutant. They both have severely reduced primary root growth; nevertheless, their mutants' seedlings are able to grow and complete their life cycle. The *Arabidopsis* root is composed of single layers of epidermis, cortex, endodermis and pericycle (Dolan *et al*., 1993). However, in the *shr-1* mutant, the root lacks the endodermal cell layer (Benfey *et al*., 1993). We therefore wanted to check whether there was a loss of cell layers in *Atzrf1a-1 Atzrf1b-1* double mutant. To study this, we introgressed *SCR*∶∶

SCR-GFP and *CO2::GFP* into the *Atzrf1a-1 Atzrf1b-1* double mutant by genetic crosses. *SCARECROW (SCR)*, a GRAS family transcription factor, is involved in RAM maintenance and radial patterning. While *SCR∶∶SCR-GFP* is specifically expressed in the endodermis and QC, *CO2::GFP* is specifically expressed in the cortex. The results showed that in the *Atzrf1a-1 Atzrf1b-1* double mutant, the cortex layer and endodermis layer were abnormal. In 23 out of 27 (85.2%) of the *Atzrf1a-1 Atzrf1b-1* double mutant roots examined, the cortex layer was partially lost. And in 19 out of 23 (82.6%) of the *Atzrf1a-1 Atzrf1b-1* double mutant roots examined, the endodermis layer was disorganized (Figure III.27).

Collectively, the results indicated that AtZRF1a and AtZRF1b are required for the maintenance of QC identity, for RAM organization, and for cell patterning.

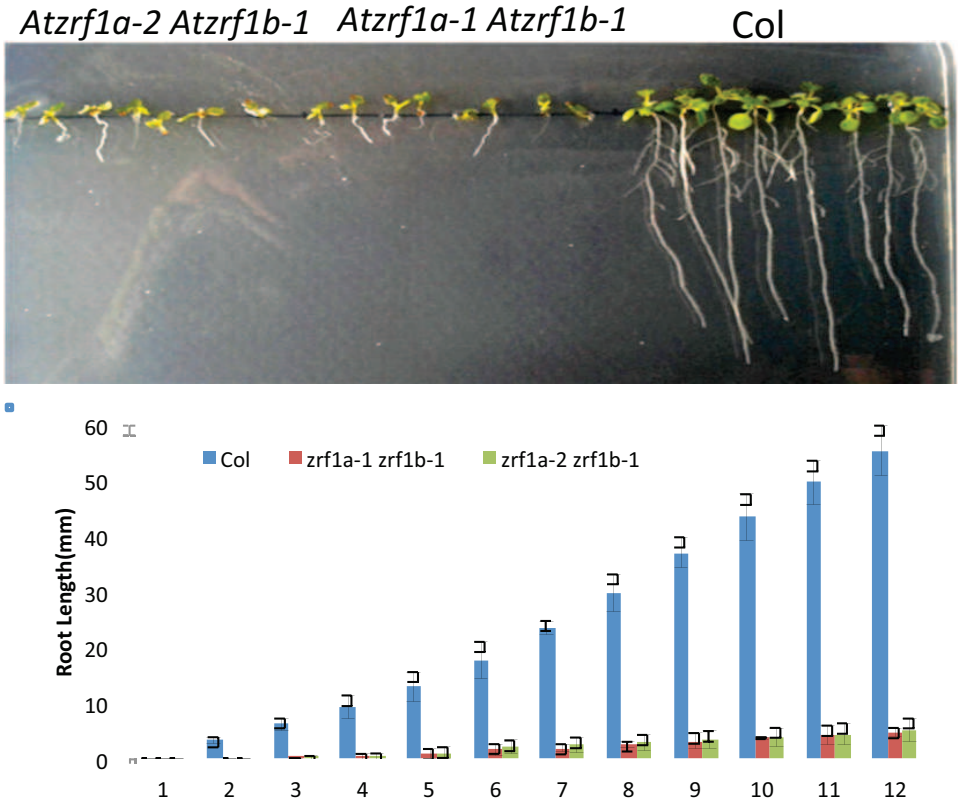

Figure III.23. *Atzrf1a Atzrf1b* double mutants exhibit altered primary root development

(A) Representative photograph of wild-type and double mutants *Atzrf1a-1 Atzrf1b-1* and *Atzrf1a-2 Atzrf1b-1* 12 DAG seedlings.

(B) Primary root length changes with time. Starting from 1 DAG, observed between wild-type (Col) and double mutants *Atzrf1a-1 Atzrf1b-1* and *Atzrf1a-2 Atzrf1b-1*. Error bars represent the mean±SE from30 seedlings analyzed at each indicated DAG. The experiment was repeated three times with similar results.

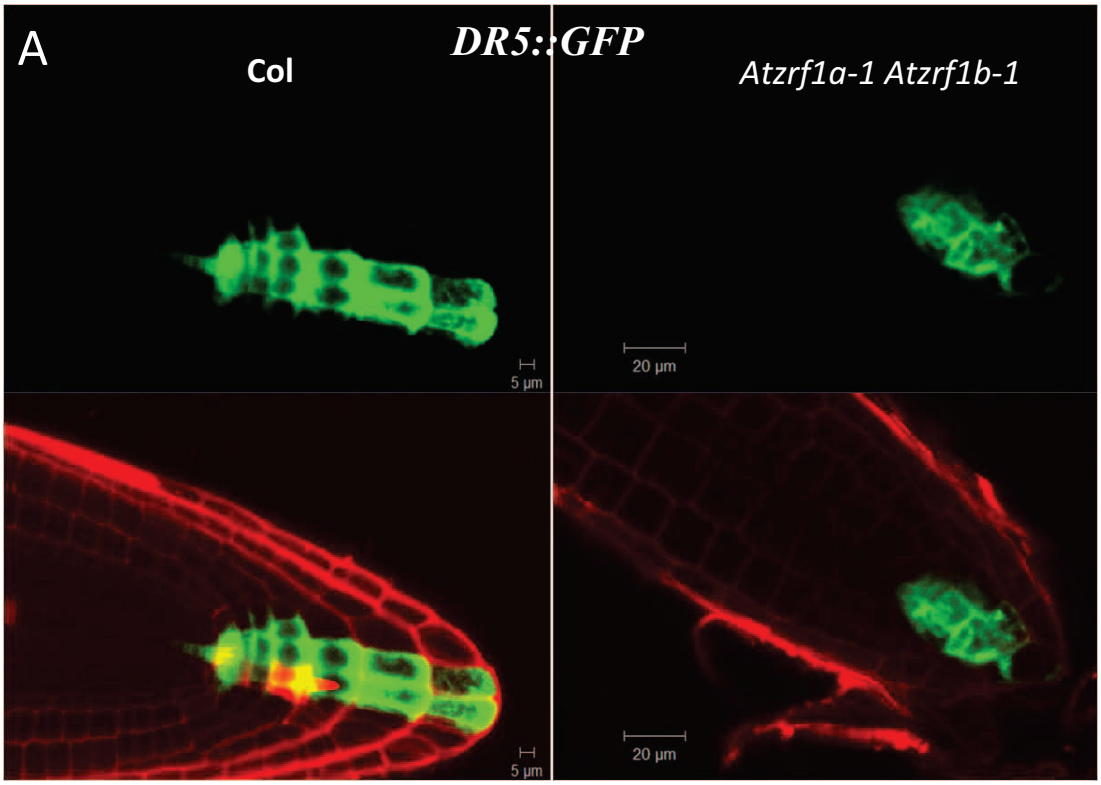
A
Col
DR5::GFP
Atzrf1a-1 Atzrf1b-1
5 μm
20 μm
5 μm
20 μm

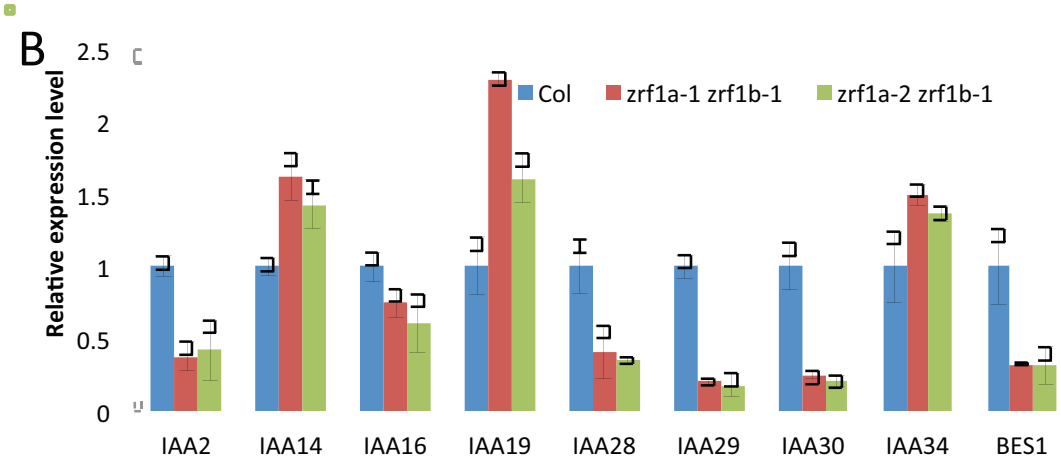
B
Relative expression level
2.5
2
1.5
1
0.5
0
Col
zrf1a-1 zrf1b-1
zrf1a-2 zrf1b-1
IAA2
IAA14
IAA16
IAA19
IAA28
IAA29
IAA30
IAA34
BES1

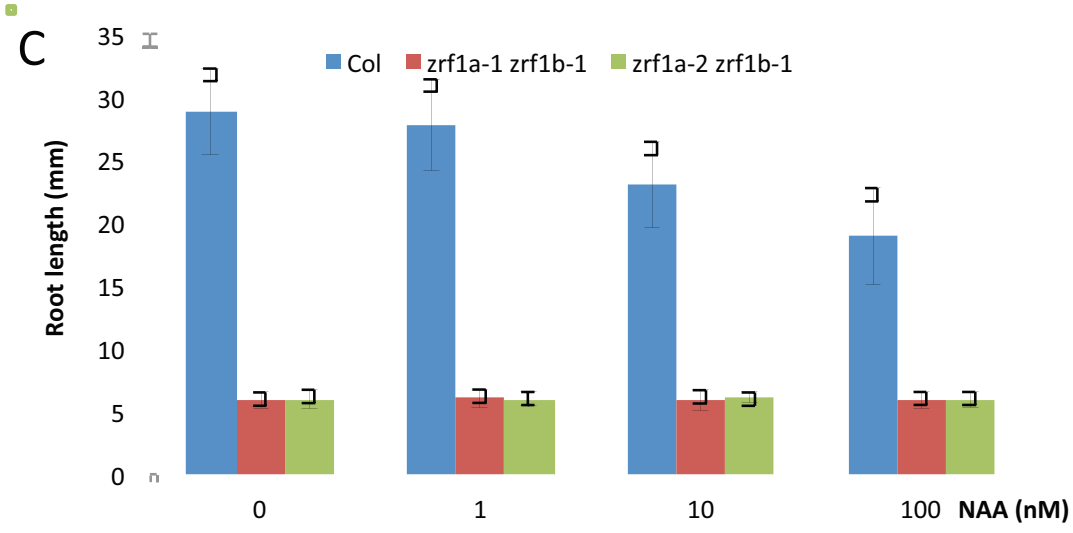
C
Root length (mm)
35
30
25
20
15
10
5
0
Col
zrf1a-1 zrf1b-1
zrf1a-2 zrf1b-1
0
1
10
100
NAA (nM)

Figure III.24. Loss of *AtZRF1a* and *AtZRF1b* partially affects auxin regulation in roots

(A) Comparison of the expression pattern of the *DR5:GFP* reporter in 5-day-old wild-type Col and in the mutant *Atzrf1a-1 Atzrf1b-1*, respectively. Note that the auxin gradient maximum in QC visualized by *DR5:GFP* expression in Col is lost in *Atzrf1a-1 Atzrf1b-1*. Images are representative of 12–22 plants in four replicate experiments. GFP signal is shown in green, propidium iodide signal in red.

(B) Relative expression level of auxin-related genes determined by quantitative RT-PCR analysis. RNA was prepared from roots of 20-day-old Col (blue bars) or *Atzrf1a-1 Atzrf1b-1* (red bars) and *Atzrf1a-2 Atzrf1b-1* (green bars) roots. RT-PCR was performed using gene-specific primers and normalized using *Tip4.1*, *EXP* and *PP2A* as references. Relative expression levels of the indicated genes are shown as mean values from three biological repeats and with Col value setting as 1. Bars indicate SD.

(C) Effects of exogenous NAA on root elongation of 8-day-old Col and *Atzrf1a-1 Atzrf1b-1* and *Atzrf1a-2 Atzrf1b-1* seedlings. Seeds were germinated and grown on medium containing the indicated concentration of NAA. Root length is shown as a mean value obtained from three independent experiments with each experiment comprising 30 plants. Bar indicates SD.

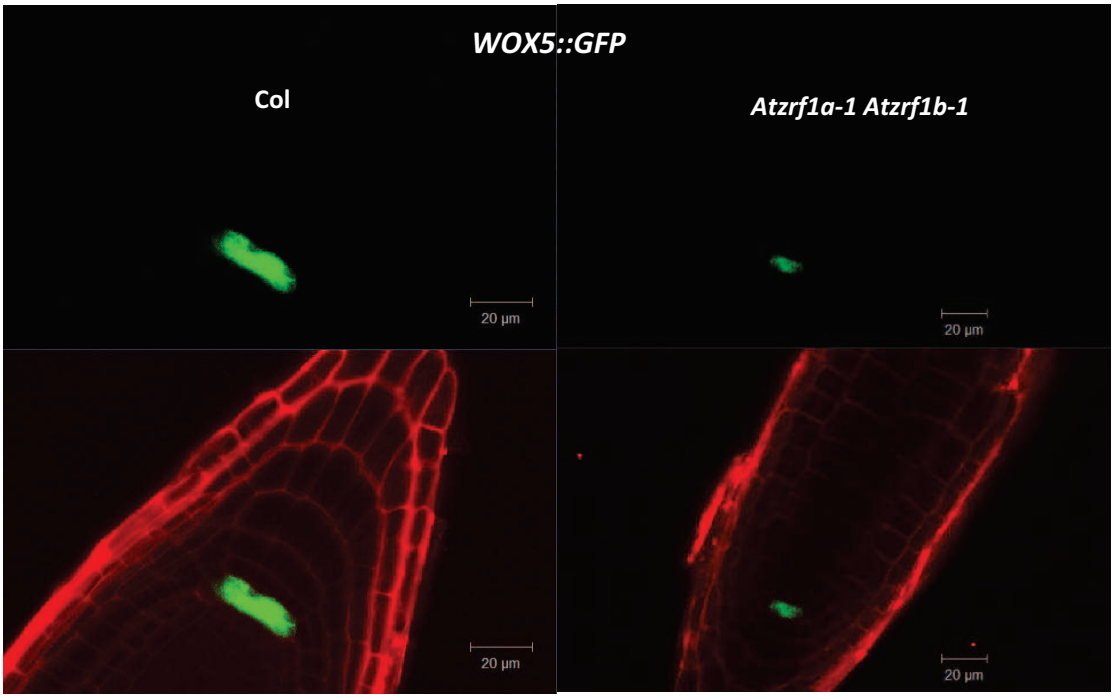

Figure III.25. Loss of AtZRF1a and AtZRF1b impairs the primary root stem cell niche maintenance

Confocal fluorescence micrographs of PI-stained root tips taken from five days seedlings from wild-type Col (left) and the double mutant *Atzrf1a-1 Atzrf1b-1* (right), respectively. Comparison of the expression pattern of *WOX5:GFP* reporter, which is the quiescent center specific marker. Images are representative of 12–23 plants in four replicate experiments. GFP signal is shown in green, propidium iodide signal in red.

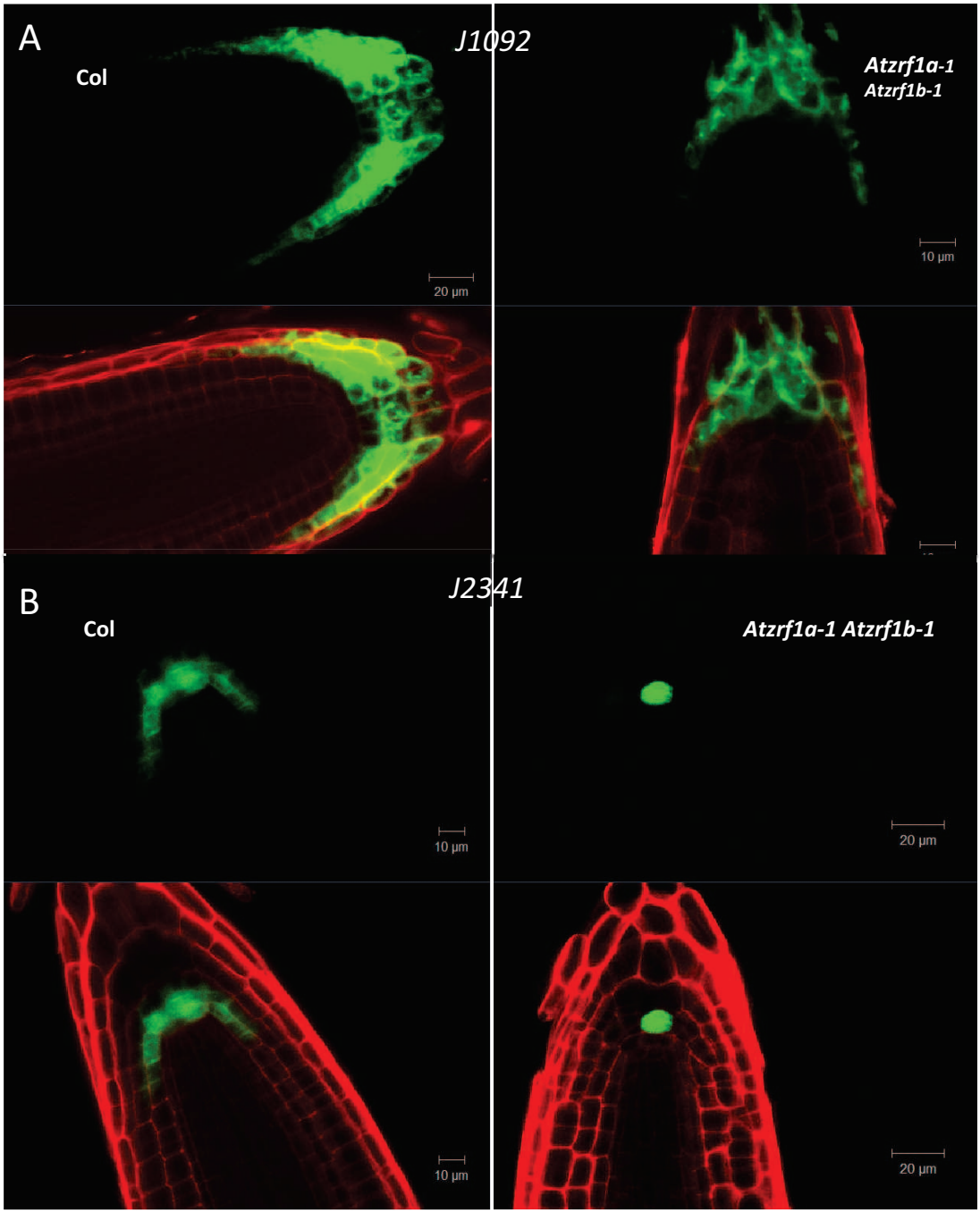

Figure III.26. Cell-marker gene expression in wild-type and *Atzrf1a-1 Atzrf1b-1* double mutant root tips

Confocal fluorescence micrographs of PI-stained root tips taken at five days. Expression of root cap marker *J1092* in wild-type roots (A left) and in *Atzrf1a-1 Atzrf1b-1* double mutant (A right). Expression of the columella initials marker *J2341* in wild-type roots (B left) and in *Atzrf1a-1 Atzrf1b-1* double mutant (B right). Images are representative of 12–16 plants in four replicate experiments. GFP signal is shown in green, propidium iodide signal in red.

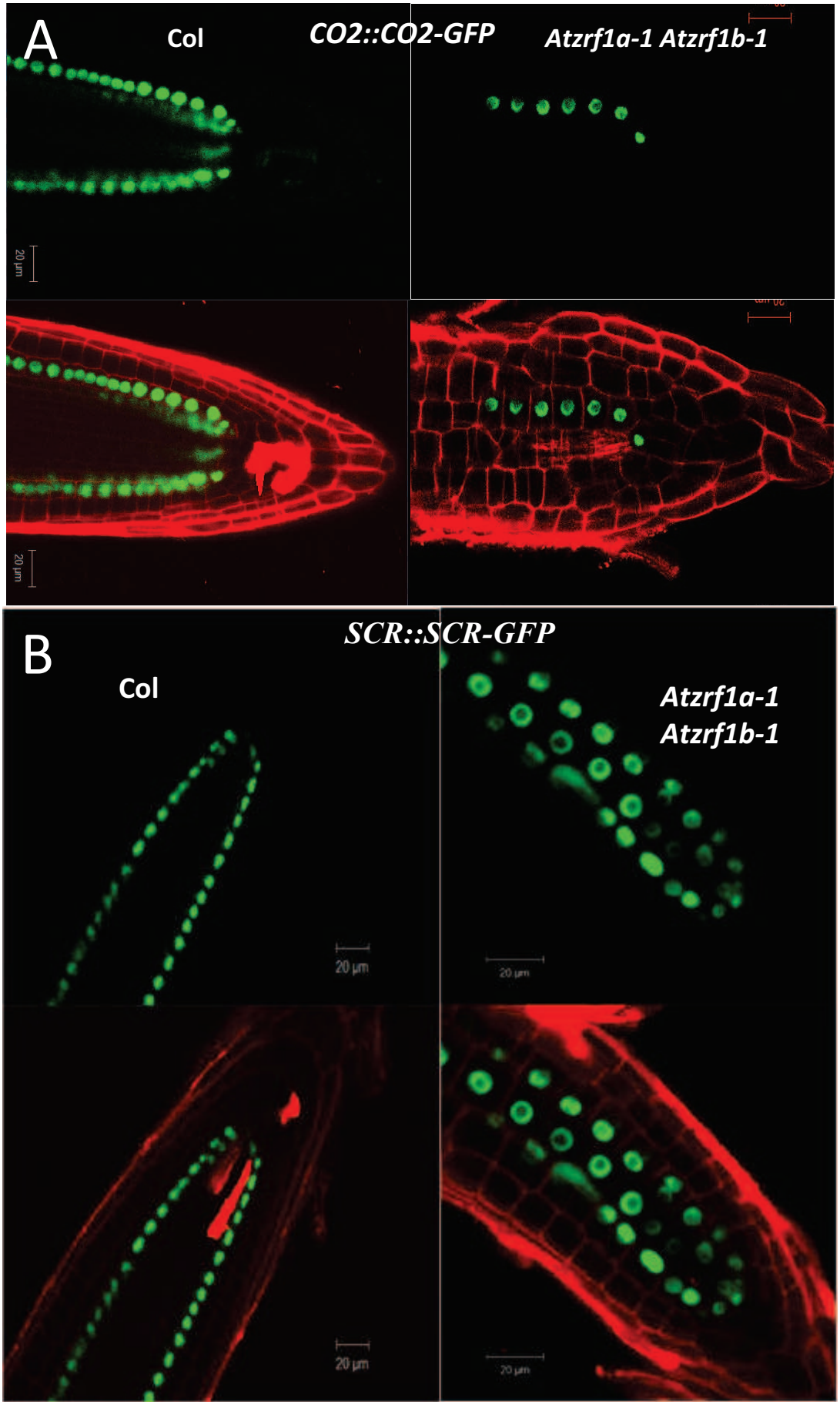
A
Col
CO2::CO2-GFP
Atzrf1a-1 Atzrf1b-1
20 µm
20 µm
B
SCR::SCR-GFP
Col
Atzrf1a-1
Atzrf1b-1
20 µm
20 µm
20 µm
20 µm

Figure III.27. Loss of AtZRF1a and AtZRF1b impairs the primary root internal cell layers

Confocal fluorescence micrographs of PI-stained root tips taken from 5-days-seedlings from wild-type Col (left) and from the double mutant *Atzrf1a-1 Atzrf1b-1* (right), respectively. Comparison of the expression pattern of the *CO2:GFP* reporter (A), which is the cortex-specific marker, and of the expression pattern of *pSCR:SCR-GFP* (B). Images are representative of 12–16 plants in four replicate experiments. GFP signal is shown in green, propidium iodide signal in red.

III.5. Characterization of AtZRF1a AtZRF1b roles in flowering time control

III.5.1 Flowering phenotype of single and double mutants under SD or LD

Deletion of both *AtZRF1a* and *AtZRF1b* generated plants with flowering defects (Figure III.28A). Moreover, double mutants showed more branches than wild-type plants (Figure III.28B). To examine whether loss of functions of *AtZRF1a* and *AtZRF1b* affect flowering time, we have grown *Atzrf1a-1*, *Atzrf1a-2* and *Atzrf1b-1* single mutants in long day (LD; 16 h light/8 h dark) and short day (SD; 8 h light/16 h dark) conditions, respectively., We counted the days the plants have grown until first flower emerged. As a result, in LD, the wild-type plants grew approximately 28 days before bolting (27.7 ± 2.2, n =10), the *Atzrf1a-1* plants grew approximately 26 days before bolting (26.2 ± 0.6, n =10), the *Atzrf1a-2* plants grew also approximately 26 days before bolting (26.0 ± 0.3, n =10) and the *Atzrf1b-1* plants grew approximately 24 days before bolting (24.2 ± 0.6, n=10). This indicates that single mutants show slightly earlier flowering time than wild-type in LD condition. However, in SD, the wild-type plants grew approximately 78 days before bolting (78.8 ± 4.4, n =10), the *Atzrf1a-1* plants grew approximately 66 days before bolting (66.6 ± 2.9, n =10), the *Atzrf1a-2* plants grew approximately 69 days before bolting (69.7 ± 4.1, n =10) and the *Atzrf1b-1* plants grew approximately 59 days before bolting (58.9 ± 1.0, n=10). Hence, single mutants show a more obvious earlier flowering time than wild-type in SD (Figure III.28C-D). Furthermore, we used double mutants *Atzrf1a-1 Atzrf1b-1* and *Atzrf1a-2 Atzrf1b-1* to study the flowering time in LD and SD conditions. We found that the heterozygous double mutant shows early flowering in LD (Figure III.29), however, the *Atzrf1a-1Atzrf1b-1* double mutant plants grew approximately 47 days before bolting

(47.3 ± 3.6, *n* =10) and the *Atzrf1a-2 Atzrf1b-1* double mutant plants grew approximately 46 days before bolting (46.1 ± 5.2, *n* =10) in LD. Moreover, in SD, the *Atzrf1a-1Atzrf1b-1* double mutant plants grew approximately 115 days before bolting (115.1 ± 11.2, *n* =10) and the *Atzrf1a-2 Atzrf1b-1* double mutant plants grew approximately 114 days before bolting (114.1 ± 10.5, *n* =10). These data indicate that the flowering time in the double mutants *Atzrf1a-1 Atzrf1b-1* and *Atzrf1a-2 Atzrf1b-1* was strongly delayed both in LD and SD (Figure III.28C-D).

III.5.2 *AtZRF1a* and *AtZRF1b* affect flowering time by promoting *FLC* and *MAF* gene expression

Flowering is a central event in the life cycle of plants; proper flowering time ensures reproductive success. Thus, flowering is a highly regulated biological process in *Arabidopsis*. In order to explore the molecular mechanisms responsible for the change in flowering time, we performed quantitative PCR to analyse the expression levels of some endogenous flowering–related genes in seedlings. These include *FLC*, and *FLC* close homologs, *MADS AFFECTING FLOWERING1 (MAF1/FLM)*, *MAF2*, *MAF4*, *MAF5*, and *SHORT VEGETATIVE PHASE (SVP)*. We also studied promoters of flowering such as *SOC1*, *FT*, and *AGAMOUS-like 24 (AGL24)*. *FLC* is a central floral repressor working in a dose-dependent manner, which is delicately controlled by various activators and repressors. *FLC* blocks the expression of floral activators such as *FT* and *SOC1* to prevent the initiation of flowering during vegetative development. The down-regulation of *FLC* activates *FT* and *SOC1* and promotes flowering (Helliwell *et al*., 2006; Li *et al*., 2008). The floral integrator *FT* is a major target of multiple flowering pathways and of the photoperiod pathway in particular (Samach *et al*., 2000). *AGL24* is a dosage-dependent promoter of flowering (Yu *et al*., 2002).

qRT-PCR results showed that the expression of *FLC*, *FLM*, *MAF2* and *MAF4* was strongly decreased compared to wild-type, while *MAF5* expression remained unchanged both in *Atzrf1a-1 Atzrf1b-1* and *Atzrf1a-2 Atzrf1b-1* double mutants (Figure III.30). These results indicate that deletion of *AtZRF1a* and *AtZRF1b* should exhibit early flowering. Instead, the phenotype of double mutants showed late flowering. Therefore, to further explore the flowering time regulatory pathway in the double mutants, I compared the expression level of several floral integrators between mutant and wild-type. Consistent with the decrease in *FLC* expression, an increase in the expression of *FT* compared to wild-type level was observed both in *Atzrf1a-1 Atzrf1b-*

1 and *Atzrf1a-2 Atzrf1b-1* double mutants. And a strong decrease in *SVP* expression was observed in *Atzrf1a-1 Atzrf1b-1* and *Atzrf1a-2 Atzrf1b-1* double mutants (Figure III.30). In both *Atzrf1a-1 Atzrf1b-1* and *Atzrf1a-2 Atzrf1b-1* double mutants, the *SOC1* expression level did not change significantly.

These results indicate that the alteration in flowering time was caused by loss of functions of both *Atzrf1a* and *Atzrf1b*. However, AtZRF1a and AtZRF1b may participate in repression of flowering time. The double mutants show late flowering, which may be caused by a delay in growth development.

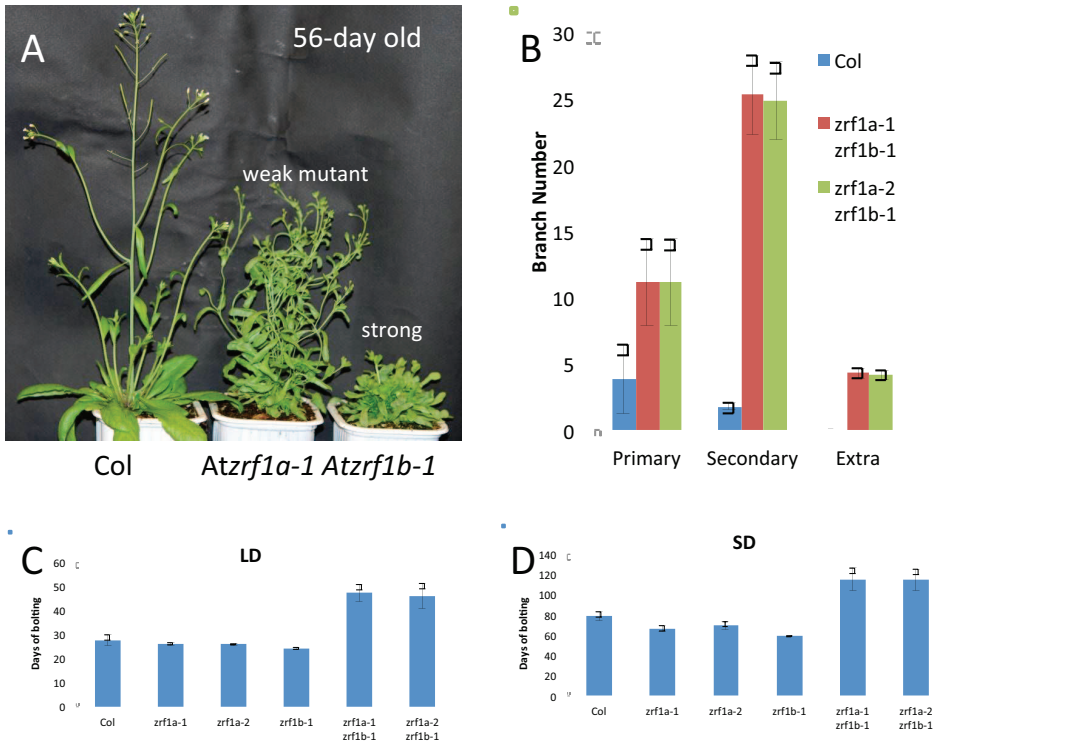

Figure III.28. Flowering time of single mutants and double mutants

(A) Phenotypes of 56-day-old double mutants *Atzrf1a-1 Atzrf1b-1* and wild-type Col plants, under long-day (16 h light and 8 h dark) conditions.

(B) Comparison of branch number of 56-day-old double mutant with wild-type Col plants. Values shown represent the means and standard deviations for at least 10 plants of each genotype.

(C) Flowering time of wild-type, single mutants and double mutants grown under LDs. Values were scored from at least 15 plants of each genotype. Error bars indicate s.d. Flowering time was measured by counting days when the first flower emerged under long-day conditions.

(D) Flowering time of wild-type, single mutants and double mutants grown under SDs. Values were scored from at least 15 plants of each genotype. Error bars indicate s.d. Flowering time was measured by counting days when the first flower emerged under short-day conditions.

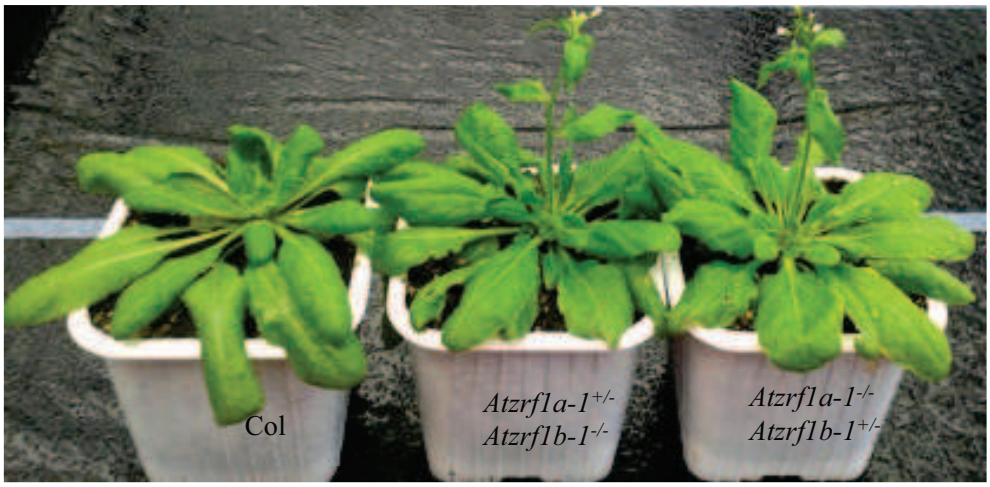

Figure III.29. Phenotypes of heterozygous mutants *Atzrf1a-1*$^{+/-}$ *Atzrf1b-1*$^{-/-}$, *Atzrf1a-1*$^{-/-}$ *Atzrf1b-1*$^{+/-}$ and Col

4-week-old heterozygous mutants *Atzrf1a-1*$^{+/-}$ *Atzrf1b-1*$^{-/-}$, *Atzrf1a-1*$^{-/-}$ *Atzrf1b-1*$^{+/-}$ and Col plants grown in long day condition. 16h light and 8h dark.

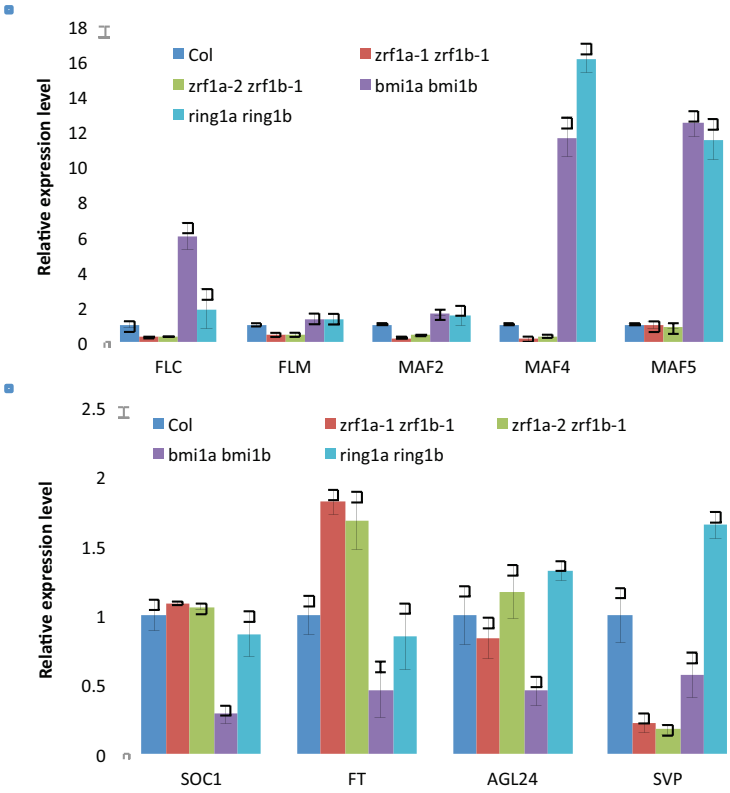

Figure III.30. Quantitative RT-PCR analysis of gene expression in double mutants

(A) Relative expression level of *FLC* and *FLC*-related genes (*MAF* genes)

(B) Relative expression level of floral integrators *SOC1*, *FT*, *AGL24* and *SVP* are shown. A pool of 2-week old seedlings was used for RNA extraction and the averages of three biological replicates are shown. Each experiment was normalized to *Tip4.1*, *Exp* and *PP2A* expression. Error bar indicates standard error (SE).

III.5.3. *AtZRF1a* and *AtZRF1b* affect H3K27me3 levels at *FLC* and *MAFs*

To test whether *AtZRF1a* and *AtZRF1b* regulate floral transition through affecting histone modifications, we first compared global the methylation levels of H3K27me3, H3K4me3, H3K36me3 and H2AK119ub1 in 2-week-old *Atring1a Atring1b*, *Atbmi1a Atbmi1b*, *Atzrf1a Atzrf1b* versus wild-type seedlings. There were no obvious differences in trimethylation levels at H3K4, H3K36 and H3K27 in *Atring1a Atring1b*, *Atbmi1a Atbmi1b*, *Atzrf1a Atzrf1b* and wild-type seedlings (Figure III.31), indicating that *AtRING1a*, *AtRING1b*, *AtBMI1a*, *AtBMI1b*, *AtZRF1a* and *AtZRF1b* do not affect the global methylation levels of H3K4me3, H3K36me3 and H3K27me3 during floral transition. However, as a component of the PRC1 complex that catalyzes the ubiquitylation of histone H2AK119 (Wang *et al*., 2004), AtRING1a/b and AtBMI1a/b were shown to mediate H2A monoubiquitylation (H2Aub1) *in vitro* (Bratzel *et al*., 2010). We found that the level of H2AK119ub1 in the *Atring1a Atring1b* double mutant was obviously increased compared with wild-type plants (Figure III.31). This could be due to increased H2AK119ub1 catalyzing activity of the other PRC1 RING-finger proteins, namely AtRING1b, AtBMI1a, AtBMI1b and AtBMI1c. Compared to wild-type plants, the level of H2AK119ub1 was significantly decreased in the *Atbmi1a Atbmi1b* double mutant (Figure III.31). while in the *AtZRF1a* and *AtZRF1b* double mutant, the level of H2AK119ub1 was slightly down-regulated.

To further understand the mechanism by which *AtZRF1a* and *AtZRF1b* regulate floral transition, we measured the H3K27me3, H3K4me3 and H2AK119ub1 levels at the *FLC*, *MAF4* and *FT* loci by ChIP assays of 2-week-old wild-type and *Atring1a Atring1b*, *Atbmi1a Atbmi1b*, *Atzrf1a Atzrf1b* as well as *clf* seedlings. H3K4me3 levels at *FLC, MAF4* and *FT* were increased in *clf* seedlings. In the *Atbmi1a Atbmi1b* double mutant, H3K4me3 levels were increased at *FLC* and *MAF4*, but not affected at the *FT* locus. In *Atring1a Atring1b* and *Atzrf1a Atzrf1b* double mutants, H3K4me3 levels at *FLC, MAF4* and *FT* were not obviously affected (Figure III.32). Furthermore, as expected, we found that H3K27me3 levels at *FLC, MAF4* and *FT* were strongly reduced in *clf* seedlings. In the *Atbmi1a Atbmi1b* double mutant, H3K27me3 levels at both *FLC* and *MAF4* were also reduced, but at *FT* locus, the level of H3K27me3 was increased. Interestingly, although AtRING1a/b and AtBMI1a/b are RING finger proteins, and both *atring1a atring1b* and *atbmi1a atbmi1b* mutants are late flowering, we found that they have different methylation levels at *FLC*, *MAF4* and

FT. In *Atring1a Atring1b* double mutant, H3K27me3 levels at *FLC* and *FT* were not obviously affected, but reduced at *MAF4*. In *Atzrf1a-1 Atzrf1b-1* and *Atzrf1a-2 Atzrf1b-1* double mutants, the level of H3K27me3 was increased at both *FLC* and *MAF4*, but not obviously affected at *FT* (Figure III.32). ChIP analysis revealed that H2AK119ub1 levels at *FLC*, *MAF4* and *FT* were not significantly changed in *Atring1a Atring1b*, *Atbmi1a Atbmi1b*, *Atzrf1a Atzrf1b* and *clf* (Figure III.32), indicating that H2AK119ub1 might not directly contribute to the modulation of *FLC*, *MAF4* and *FT* expression by AtRING1a/b, AtBMI1a/b or AtZRF1a/b.

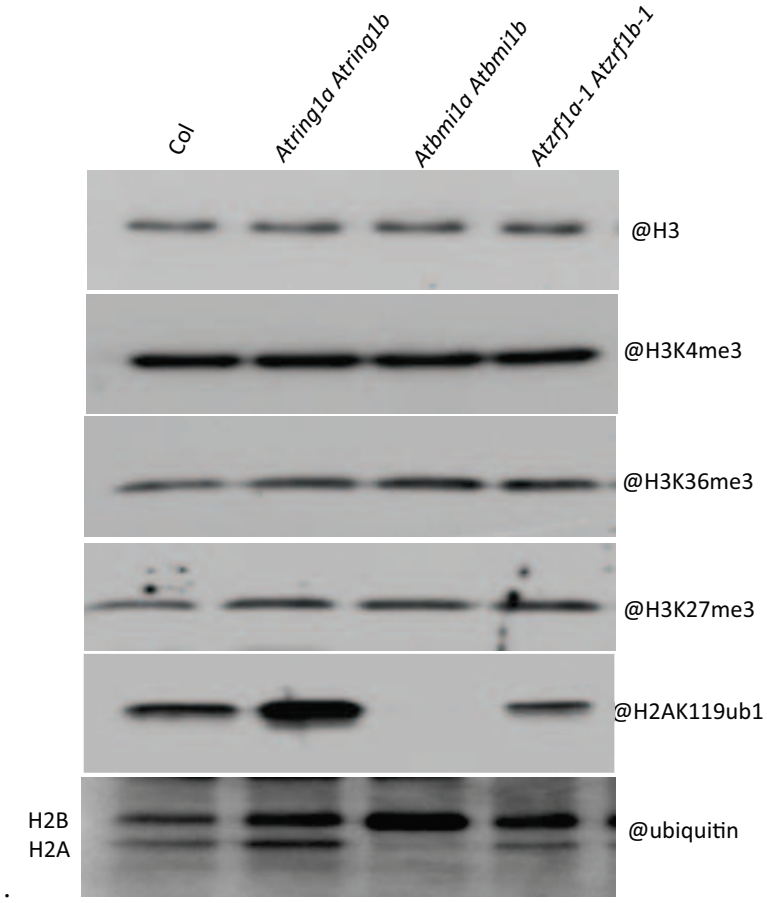

Figure III.31. Western blot analysis of global H3K4me3, H3K27me3, H3K36me3 and ubiquitination levels in the *Atzrf1a-1 Atzrf1b-1*, *Atring1a Atring1b*, *Atbmi1a Atbmi1b* mutants and wild-type plants.

Histone-enriched protein extracts from plants 14 days after germination grown under medium-day (12 h light and 12 h dark) conditions were analyzed by Western blotting using antibodies that specifically recognize the indicated forms of histones.

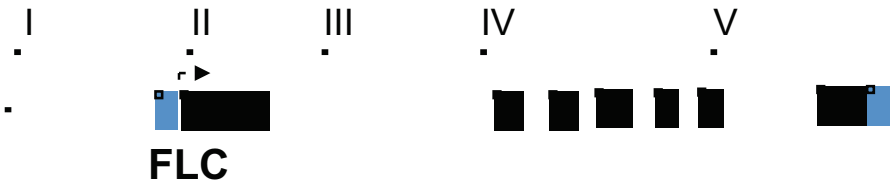
I
II
III
IV
V
FLC

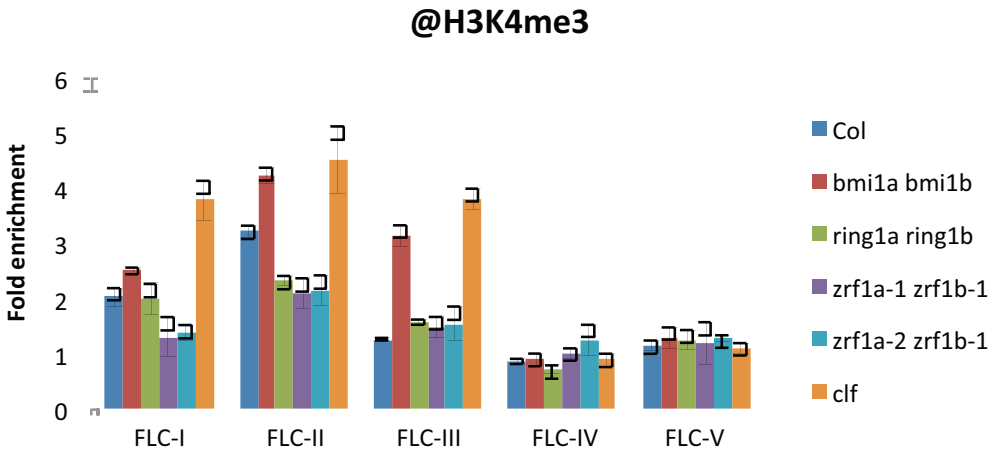
@H3K4me3
Fold enrichment
6
5
4
3
2
1
0
FLC-I
FLC-II
FLC-III
FLC-IV
FLC-V
Col
bmi1a bmi1b
ring1a ring1b
zrf1a-1 zrf1b-1
zrf1a-2 zrf1b-1
clf

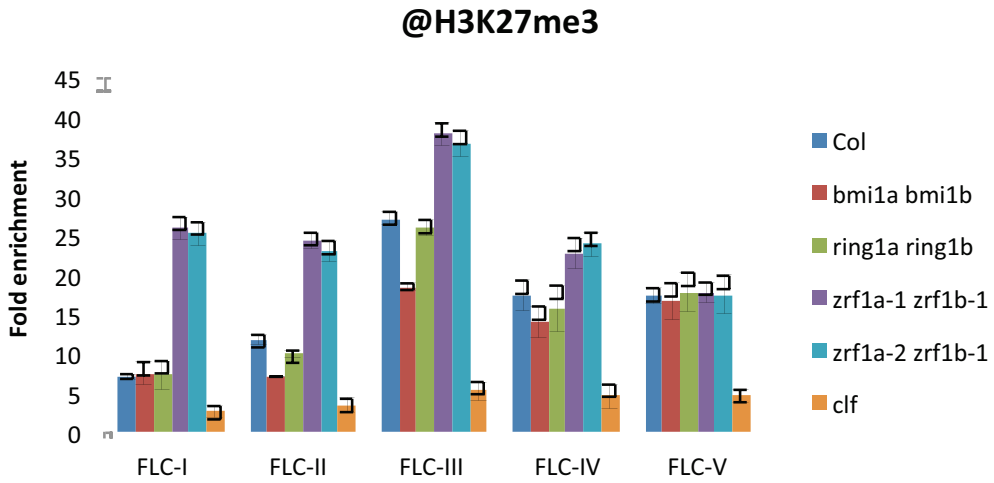
@H3K27me3
Fold enrichment
45
40
35
30
25
20
15
10
5
0
FLC-I
FLC-II
FLC-III
FLC-IV
FLC-V
Col
bmi1a bmi1b
ring1a ring1b
zrf1a-1 zrf1b-1
zrf1a-2 zrf1b-1
clf

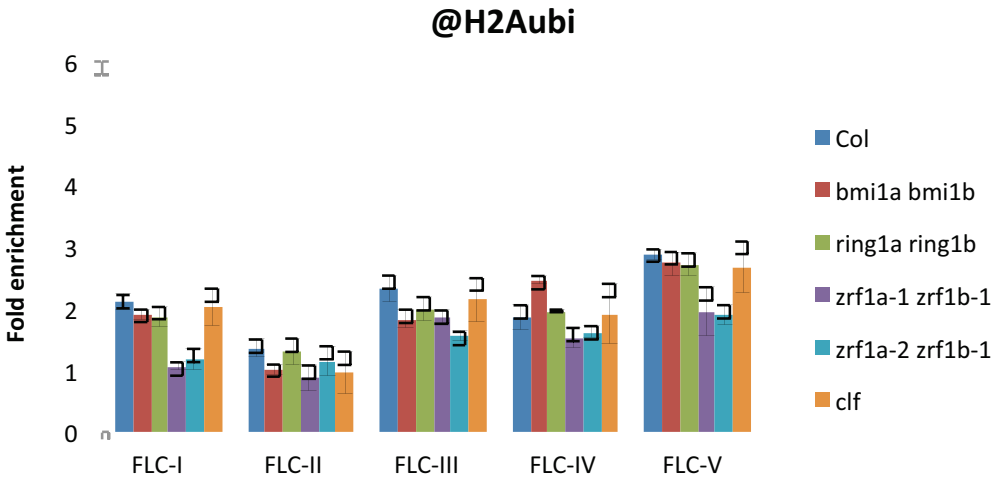
@H2Aubi
Fold enrichment
6
5
4
3
2
1
0
FLC-I
FLC-II
FLC-III
FLC-IV
FLC-V
Col
bmi1a bmi1b
ring1a ring1b
zrf1a-1 zrf1b-1
zrf1a-2 zrf1b-1
clf

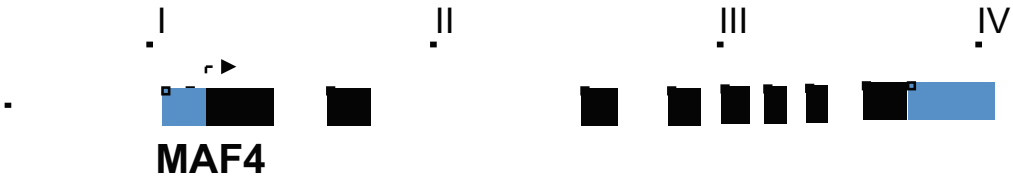
I
II
III
IV
MAF4

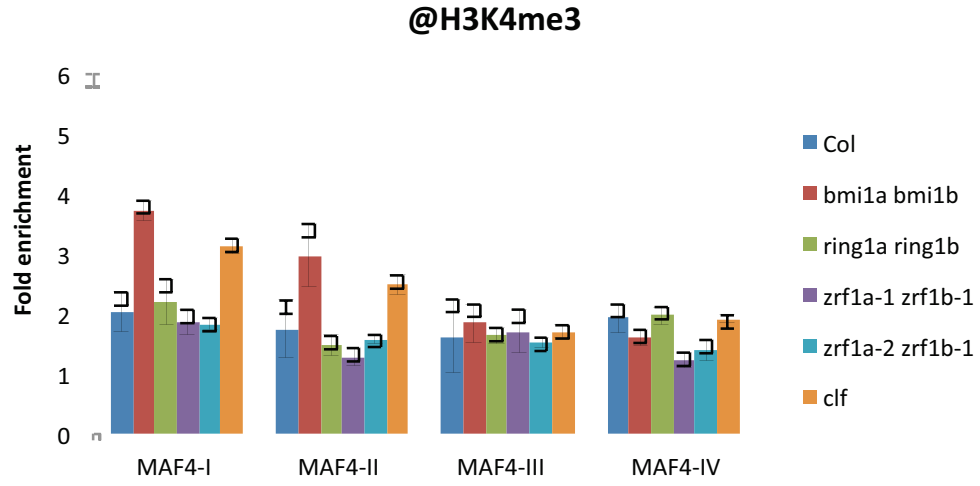
@H3K4me3
Fold enrichment
0
1
2
3
4
5
6
MAF4-I
MAF4-II
MAF4-III
MAF4-IV
Col
bmi1a bmi1b
ring1a ring1b
zrf1a-1 zrf1b-1
zrf1a-2 zrf1b-1
clf

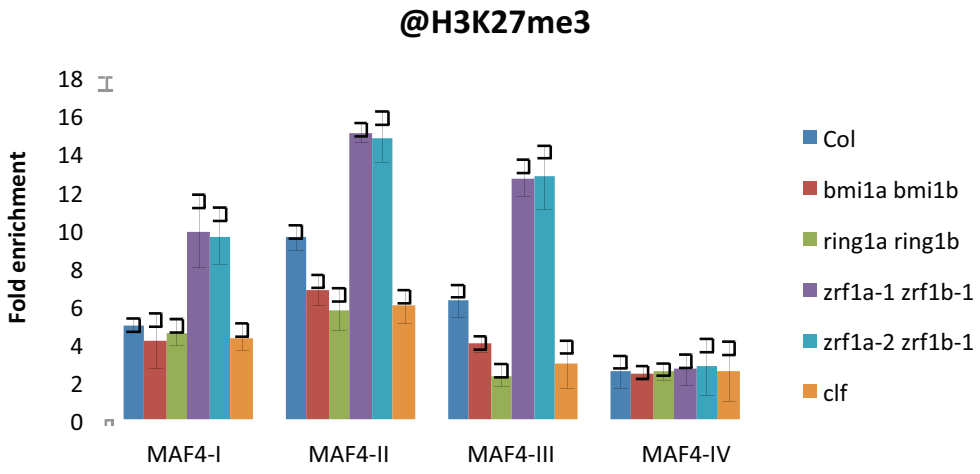
@H3K27me3
Fold enrichment
0
2
4
6
8
10
12
14
16
18
MAF4-I
MAF4-II
MAF4-III
MAF4-IV
Col
bmi1a bmi1b
ring1a ring1b
zrf1a-1 zrf1b-1
zrf1a-2 zrf1b-1
clf

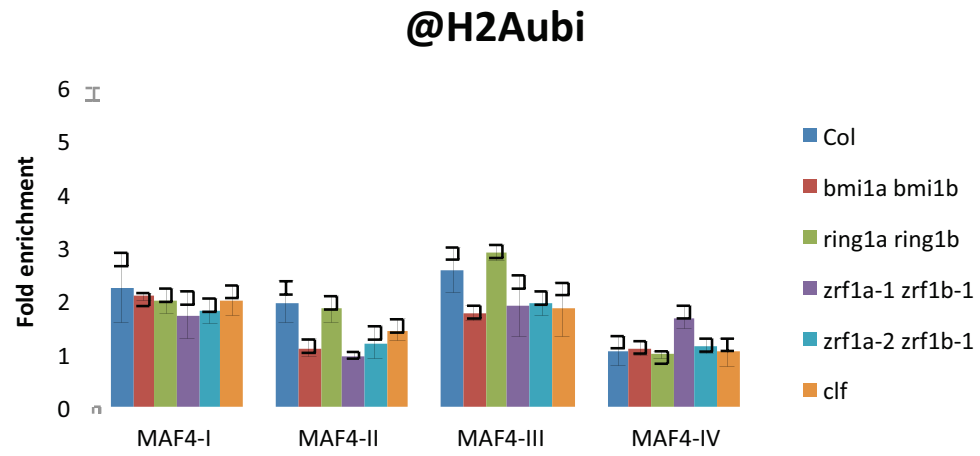
@H2Aubi
Fold enrichment
0
1
2
3
4
5
6
MAF4-I
MAF4-II
MAF4-III
MAF4-IV
Col
bmi1a bmi1b
ring1a ring1b
zrf1a-1 zrf1b-1
zrf1a-2 zrf1b-1
clf

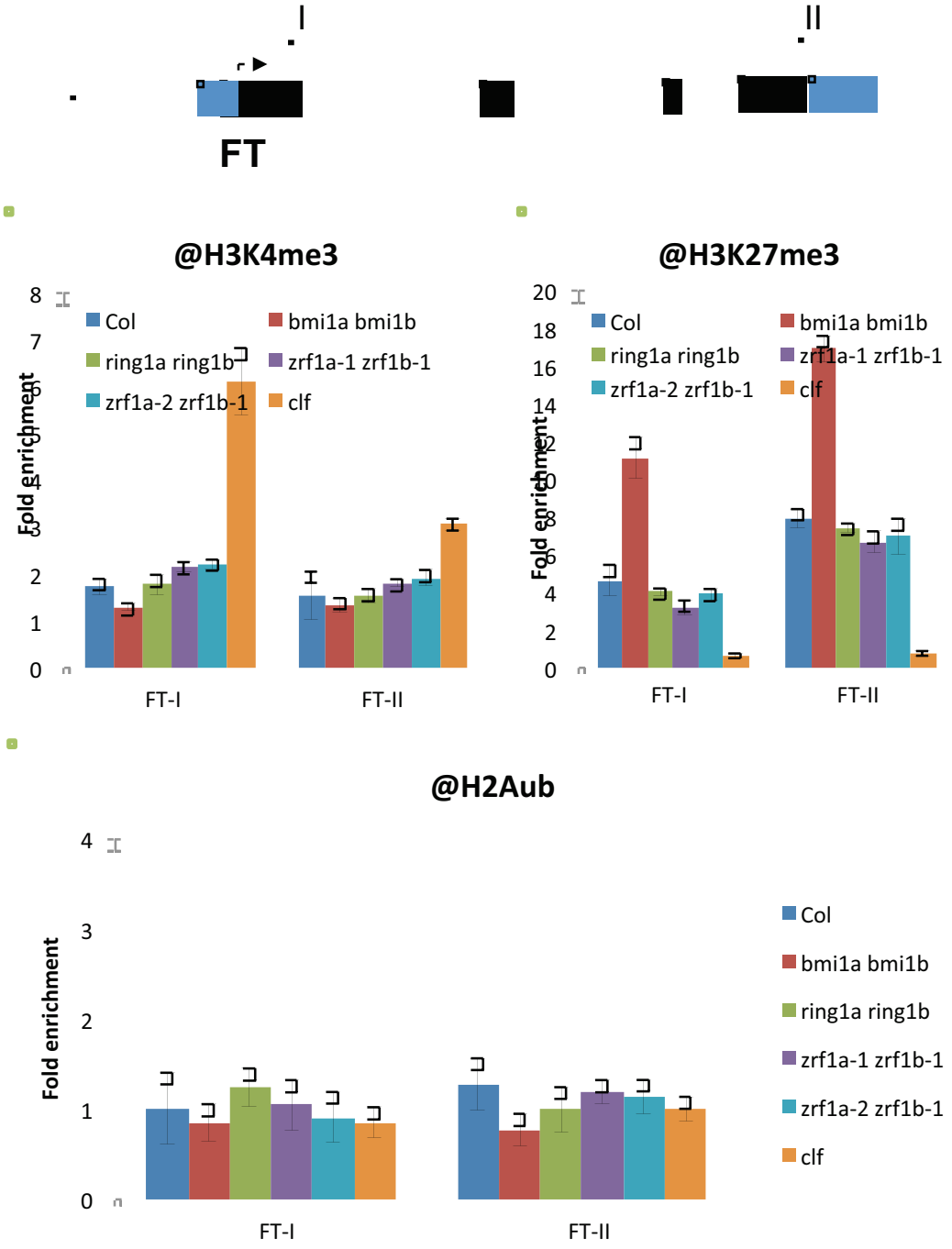

Figure III.32. Relative enrichments of H3K4me3, H3K27me3 and H2Aub1 at flowering time genes in Col-0 and mutants

Relative levels of histone modifications on *FLC*, *MAF4* and *FT* chromatin were analyzed by ChIP using antibodies against H3K4me3, H3K27me3 and anti-hH2Aub. Chromatin from Col, *Atbmi1a Atbmi1b*, *Atring1a Atring1b*, *Atzrf1a-1 Atzrf1b-1, Atzrf1a-2 Atzrf1b-1* and *clf* was prepared from 2-week-old seedlings. The immunoprecipitated DNA fragments were quantified by qRT-PCR and normalized to internal controls (relative to Input and normalized to *TUB2*). Data shown are means±SD of three technical replicates. Similar results were obtained in three independent experiments. Amplified regions are numbered and indicated on the schematic representation of the *FLC*, *MAF4* and *FT* genomic structure. Exons are represented by black boxes, untranslated regions by dashed boxes and introns by black lines.

III.6. Characterization of *AtZRF1a* and *AtZRF1b* roles in seed germination

III.6.1 Simultaneous loss of *AtZRF1a* and *AtZRF1b* affects seed germination

Seeds of wild-type (Col), single mutants *Atzrf1a-1*, *Atzrf1a-2* and *Atzrf1b-1* and double mutants *Atzrf1a-1 Atzrf1b-1* and *Atzrf1a-2 Atzrf1b-1* were put on plates, stratified and the germination rates were scored by counting the radical emergence for 12 days after stratification (DAS). Under standard growth conditions (MS medium), germination kinetics were not significantly affected in *Atzrf1a-1*, *Atzrf1a-2* and *Atzrf1b-1* single mutants (Figure III.28A and B), whereas under the same conditions, the *Atzrf1a-1 Atzrf1b-1* and *Atzrf1a-2 Atzrf1b-1* double mutants displayed a significantly decreased germination efficiency (Figure III.33D-E).

The *Atbmi1a Atbmi1b* mutant also displayed a delay in seed germination in our assays (Figure III.33E). Interestingly, compared to that of *Atzrf1a-1 Atzrf1b-1* and *Atzrf1a-2 Atzrf1b-1*, the exponential phase of the *Atbmi1a Atbmi1b* germination rate curve started earlier after stratification, but reached a comparatively maximum percentage value. AtBMI1a/b may be involved primarily in the maintenance of the germination process (Molitor *et al*., 2014). These results indicate that AtZRF1a/b may be involved primarily in initiation of the germination process. We also obtained the quadruple mutant *Atzrf1a-1 Atzrf1b-1 Atbmi1a Atbmi1b* and showed that it is drastically impaired in both germination initiation time and maximum percentage of germination rate (Figure III.33E). Gibberellic acid 3 (GA3) is generally known to effectively stimulate the breaking of seed dormancy and promote germination. However, at different tested concentrations (0.5, 1.0 and 2.0 µmol/L) GA3 could not rescue the germination defects of the *Atzrf1a-1 Atzrf1b-1*and *Atzrf1a-2 Atzrf1b-1* double mutants (Figure III.33H).

Next, the mutants were challenged under osmotic treatments with salt or mannitol, two stresses known to have a negative impact on seed germination. At 100 mM NaCl or 200 mM mannitol, the *Atzrf1a-1 Atzrf1b-1* and *Atzrf1a-2 Atzrf1b-1* double mutants but not the single mutants showed a delay in seed germination compared to the wild-type Col-0 (Figure III.33F and G). Interestingly, like on MS medium, in comparison to wild-type, the *Atbmi1a Atbmi1b*, *Atzrf1a-1 Atzrf1b-1* and *Atzrf1a-2 Atzrf1b-1* double mutants as well as the *Atzrf1a-1 Atzrf1b-1 Atbmi1a*

Atbmi1b quadruple mutant also displayed a significantly decreased germination efficiency. Among these mutants, the decrease level of the *Atzrf1a-1 Atzrf1b-1 Atbmi1a Atbmi1b* quadruple mutant was highest while the decrease level of *Atbmi1a Atbmi1b* was lower than in *Atzrf1a-1 Atzrf1b-1* and *Atzrf1a-2 Atzrf1b-1* double mutants (Figure III.33F and G). Indeed, under the tested stress conditions, all wild-type seeds had germinated after 5 days, while germination rates were reduced to ~40% and ~50% for *Atzrf1a-1 Atzrf1b-1* and *Atzrf1a-2 Atzrf1b-1* double mutants on 100 mM NaCl and 200 mM mannitol, respectively. Moreover for the *Atbmi1a Atbmi1b* double mutant the germination rates were reduced to ~70% and ~85% on 100 mM NaCl and 200 mM mannitol, respectively (Figure III.33F and G). While germination rates were reduced by ~40% for the *Atzrf1a-1 Atzrf1b-1 Atbmi1a Atbmi1b* quadruple mutant on 100 mM NaCl or 200 mM mannitol (Figure III.33F and G).

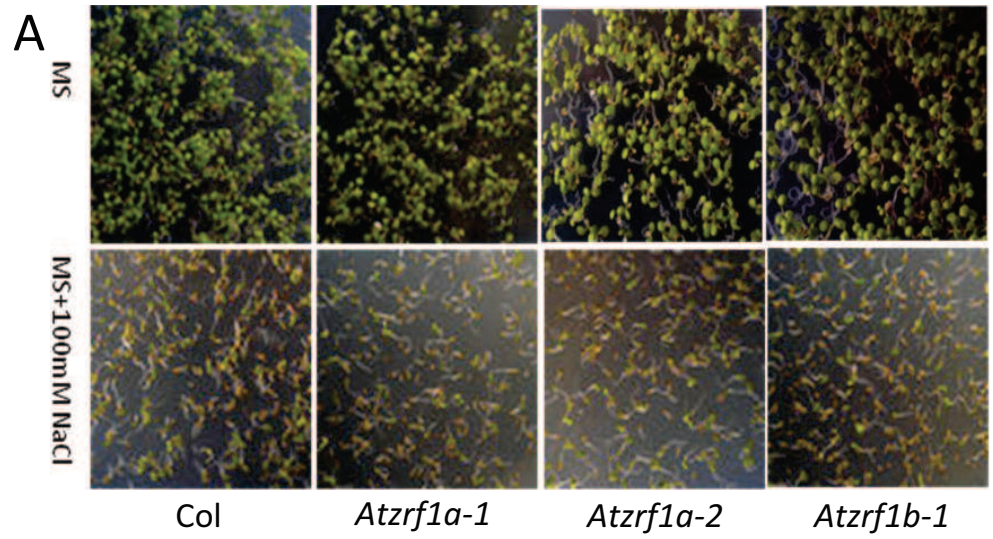

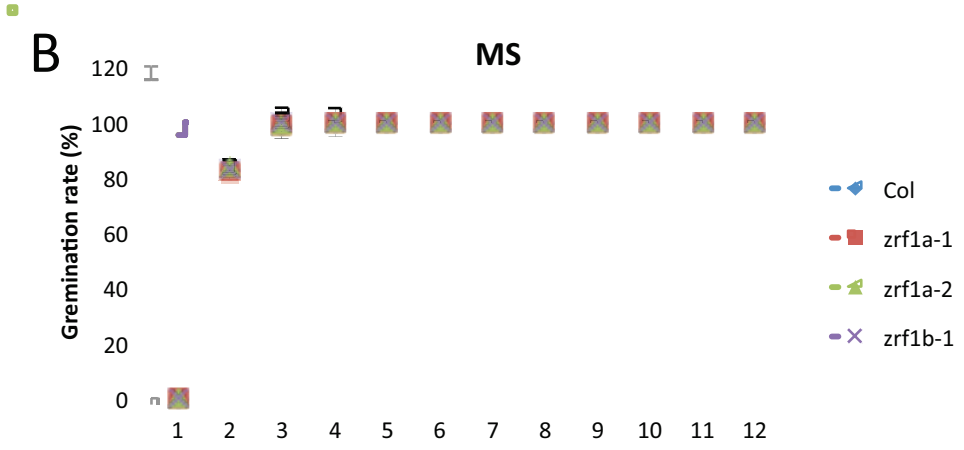

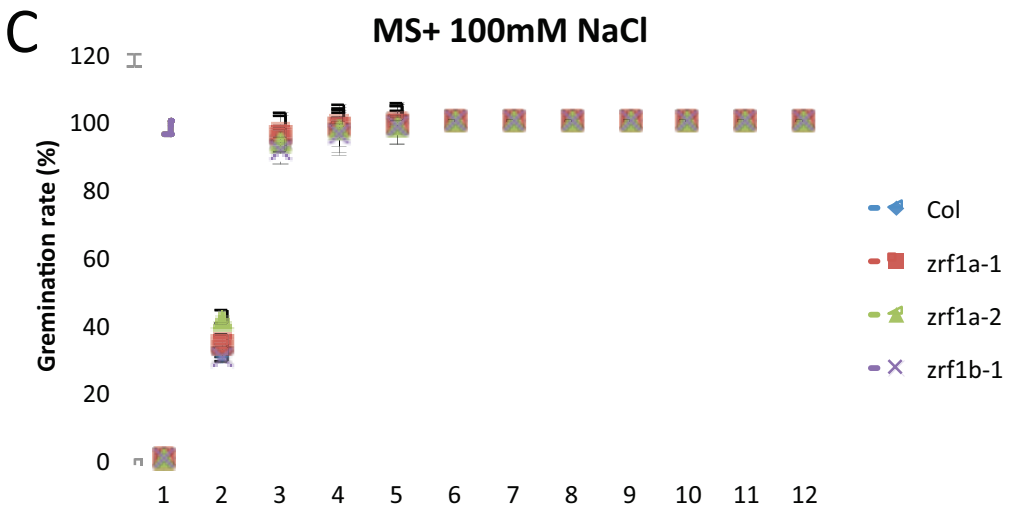
C
MS+ 100mM NaCl
Gremination rate (%)
120
100
80
60
40
20
0
1
2
3
4
5
6
7
8
9
10
11
12
Col
zrf1a-1
zrf1a-2
zrf1b-1

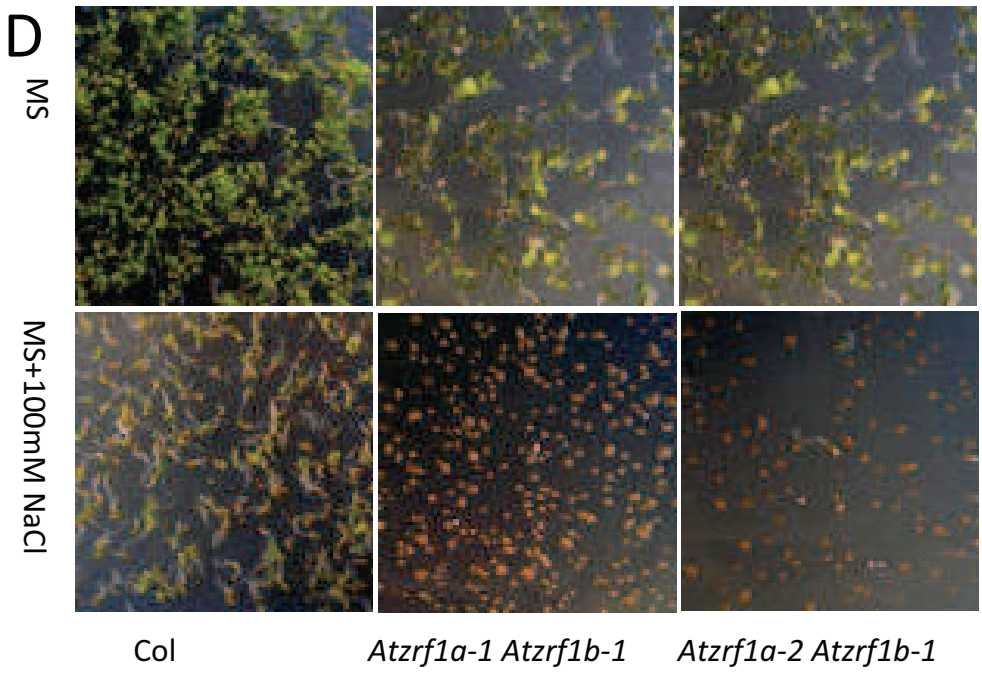
D
MS
MS+100mM NaCl
Col
Atzrf1a-1 Atzrf1b-1
Atzrf1a-2 Atzrf1b-1

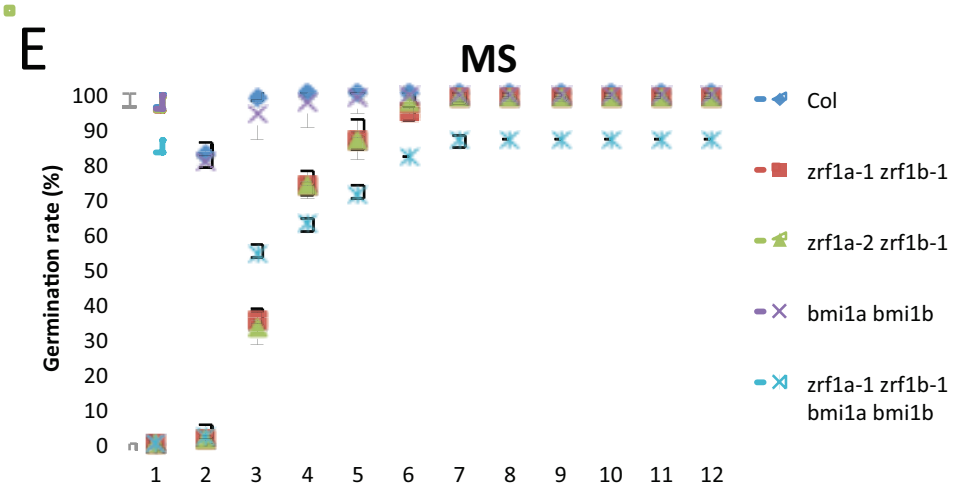
E
MS
Germination rate (%)
100
90
80
70
60
50
40
30
20
10
0
1
2
3
4
5
6
7
8
9
10
11
12
Col
zrf1a-1 zrf1b-1
zrf1a-2 zrf1b-1
bmi1a bmi1b
zrf1a-1 zrf1b-1
bmi1a bmi1b

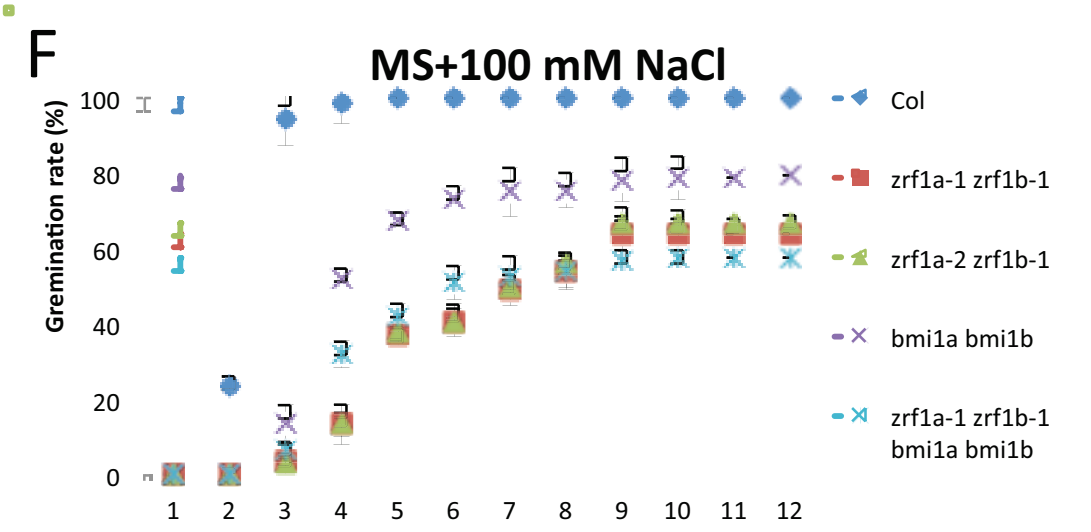
F
MS+100 mM NaCl
Gremination rate (%)
100
80
60
40
20
0
1
2
3
4
5
6
7
8
9
10
11
12
Col
zrf1a-1 zrf1b-1
zrf1a-2 zrf1b-1
bmi1a bmi1b
zrf1a-1 zrf1b-1
bmi1a bmi1b

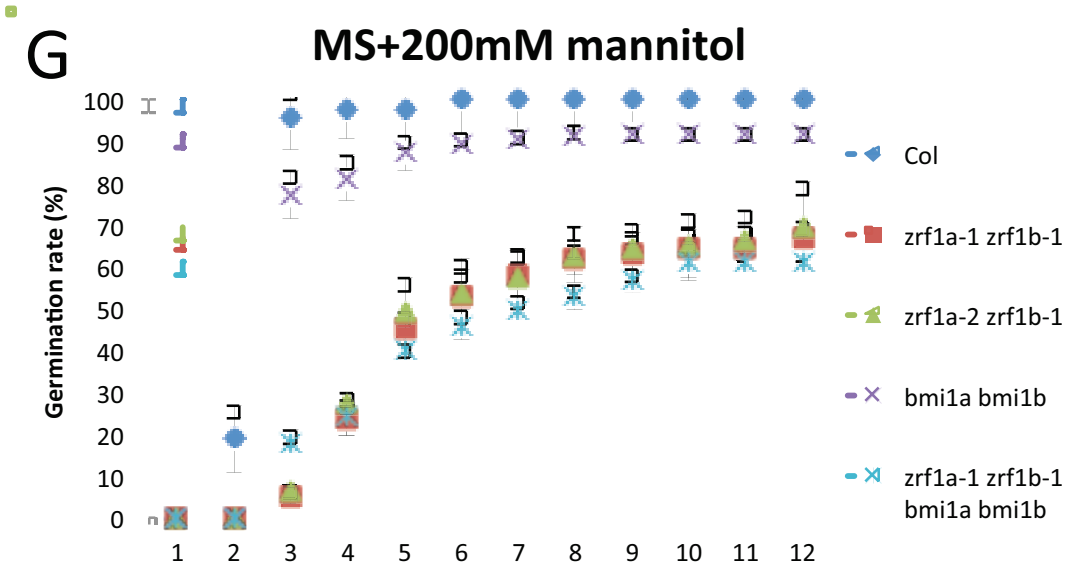
G
MS+200mM mannitol
Germination rate (%)
100
90
80
70
60
50
40
30
20
10
0
1
2
3
4
5
6
7
8
9
10
11
12
Col
zrf1a-1 zrf1b-1
zrf1a-2 zrf1b-1
bmi1a bmi1b
zrf1a-1 zrf1b-1
bmi1a bmi1b

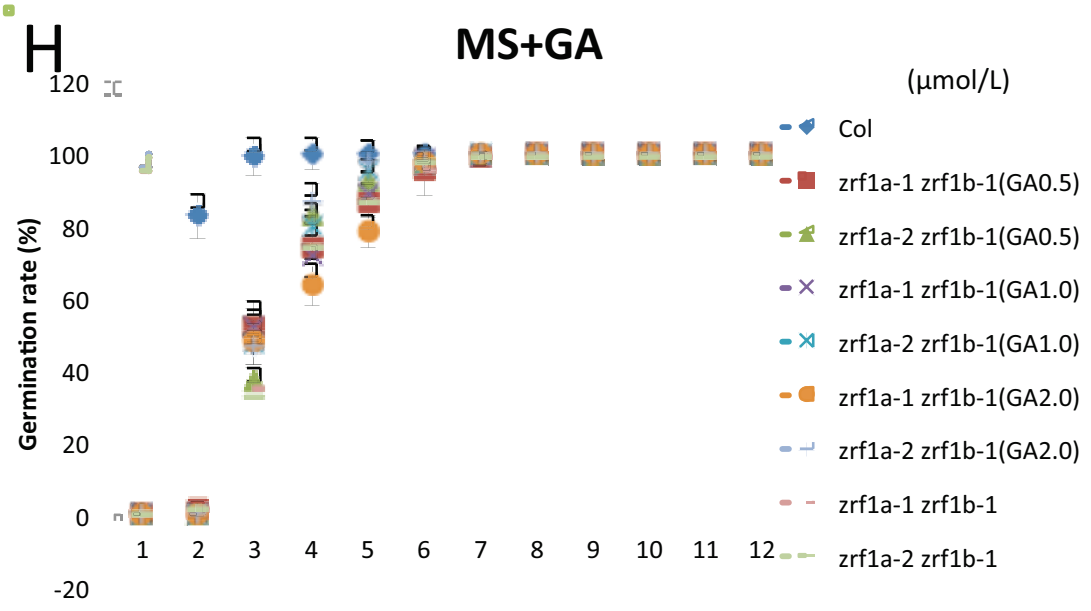
H
MS+GA
(μmol/L)
Germination rate (%)
120
100
80
60
40
20
0
-20
1
2
3
4
5
6
7
8
9
10
11
12
Col
zrf1a-1 zrf1b-1(GA0.5)
zrf1a-2 zrf1b-1(GA0.5)
zrf1a-1 zrf1b-1(GA1.0)
zrf1a-2 zrf1b-1(GA1.0)
zrf1a-1 zrf1b-1(GA2.0)
zrf1a-2 zrf1b-1(GA2.0)
zrf1a-1 zrf1b-1
zrf1a-2 zrf1b-1

Figure III.33. Germination rate of single mutants and double mutants

(A) Representative seed germination images of Col-0, single mutants *Atzrf1a-1*, *Atzrf1a-2* and *Atzrf1b-1*. Images were taken five days after stratification from plates containing MS media or MS supplemented with 100 mM NaCl.

(B) Germination rate of Col-0 and single mutants *Atzrf1a-1*, *Atzrf1a-2* and *Atzrf1b-1* plated on MS.

(C) Germination rate of Col-0 and single mutants *Atzrf1a-1*, *Atzrf1a-2* and *Atzrf1b-1* plated on MS supplemented with 100 mM NaCl.

(D) Representative seed germination images of Col-0 and double mutants *Atzrf1a-1 Atzrf1b-1* and *Atzrf1a-2 Atzrf1b-1*. Images were taken five days after stratification from plates containing MS media or MS supplemented with 100 mM NaCl.

(E) Germination rate of Col-0 and double mutants *Atbmi1a Atbmi1b, Atzrf1a-1 Atzrf1b-1*and *Atzrf1a-2 Atzrf1b-1* and *Atzrf1a-1 Atzrf1b-1 Atbmi1a Atbmi1b* quadruple mutant plated on MS.

(F) Germination rate of Col-0 and double mutants *Atbmi1a Atbmi1b, Atzrf1a-1 Atzrf1b-1* and *Atzrf1a-2 Atzrf1b-1* and *Atzrf1a-1 Atzrf1b-1 Atbmi1a Atbmi1b* quadruple mutant plated on MS supplemented with 100 mM NaCl.

(G) Germination rate of Col-0 and double mutants *Atbmi1a Atbmi1b, Atzrf1a-1 Atzrf1b-1*and *Atzrf1a-2 Atzrf1b-1* and *Atzrf1a-1 Atzrf1b-1 Atbmi1a Atbmi1b* quadruple mutant plated on MS supplemented with 200 mM mannitol.

(H) Germination rate of Col-0 plated on MS and double mutants *Atzrf1a-1 Atzrf1b-1*and *Atzrf1a-2 Atzrf1b-1* plated on supplemented with different concentrations of GA (0.5, 1.0 and 2.0μmol/L, respectively).

All data represent average germination percentages ±SD of three biological replicates, each 80 seeds, observed daily for 12 days after stratification.

III.6.2 Seed genes are ectopically expressed in seedlings of *Atzrf1a Atzrf1b*

To investigate which seed germination genes are responsible for the germination defective phenotypes in the double mutants *Atzrf1a-1 Atzrf1b-1* and *Atzrf1a-2 Atzrf1b-1*, we harvested the seedlings at 5 DAS, and then compared the expression levels of several seed development related genes including *ABI3*, *DOG1*, *CRA1*, *CRC*, *PER* and *AIL5* between WT and double mutants *Atzrf1a-1 Atzrf1b-1, Atzrf1a-2 Atzrf1b-1, Atring1a Atring1b* and *Atbmi1a Atbmi1b*. As expected, all the examined genes except *DOG1* displayed derepression in the double mutants *Atzrf1a-1 Atzrf1b-1* and *Atzrf1a-2 Atzrf1b-1* seedlings (Figure III.34). Moreover, we investigated the expression levels of the six seed developmental genes in the *Atring1a Atring1b* and *Atbmi1a Atbmi1b* mutants. As shown in Figure III.29, all six seed developmental genes showed higher expression levels in the *Atring1a Atring1b* and *Atbmi1a Atbmi1b* mutants as compared to Col-0. More important, the expression levels of these seed developmental genes were highest in double mutants *Atzrf1a-1 Atzrf1b-1* and *Atzrf1a-2*

Atzrf1b-1. These data demonstrate that AtZRF1a/b, AtRING1a/b and AtBMI1a/b are involved in the repression of seed developmental genes during germination and early seedling growth.

To investigate the mechanism of seed gene repression, we performed a ChIP analysis on H3K27me3, H3K4me3 or H2Aub levels during seed germination. ChIP fractions were analyzed using PCR primers covering the promoter, UTR and gene body regions of *ABI3* (Figure III.35) and *DOG1* (Figure III.35). In addition, we analyzed the deposition of H3K27me3, H3K4me3 or H2Aub1 marks at the gene body regions of *CRC* (Figure III.35) and *AIL5* (Figure III.35). We found that H3K4me3 levels were slightly upregulated at all genes in *Atbmi1a Atbmi1b* mutants. *Atring1a Atring1b*, *Atzrf1a-1 Atzrf1b-1* and *Atzrf1a-2 Atzrf1b-1* mutants showed a slight increase of H3K4me3 levels at CRC and AIL5. But *Atzrf1a-1 Atzrf1b-1* and *Atzrf1a-2 Atzrf1b-1* mutants also showed a slight decrease of H3K4me3 levels at DOG1. *Atbmi1a Atbmi1b* mutants showed a drastic decrease of H3K27me3 levels at ABI3, DOG1, CRC and AIL5 (Figure III.35), indicating that these genes are specific targets of AtBMI1a/b. *Atzrf1a-1 Atzrf1b-1*, *Atzrf1a-2 Atzrf1b-1* and *Atring1a Atring1b* mutants also showed a drastic decrease of H3K27me3 levels at ABI3, CRC and AIL5 (Figure III.35). While there is an increase of H3K27me3 levels at DOG1 in *Atzrf1a-1 Atzrf1b-1* and *Atzrf1a-2 Atzrf1b-1* mutants, these levels are not significantly affected at DOG1 in *Atring1a Atring1b* mutants

PRC1 RING-finger proteins as E3 ligase enzymes specifically catalyze H2A.1 monoubiquitination in *Arabidopsis* (Bratzel *et al*., 2010). We used a commercial ChIP-grade anti-human H2Aub antibody to recognize H2Aub1. The levels of H2Aub1 were strongly down-regulated at the examined seed development genes in *Atring1a Atring1b*, *Atbmi1a Atbmi1b and A*tzrf1a-1 Atzrf1b-1 and Atzrf1a-2 Atzrf1b-1 mutants. For ABI3, the level of H2Aub1 is lower in *Atring1a Atring1b* than in *Atbmi1a Atbmi1b*. For DOG1 and CRC, the level of H2Aub1 is drasticly lower in *Atbmi1a Atbmi1b* than in *Atring1a Atring1b*. Interestingly, in *Atzrf1a-1 Atzrf1b-1* and *Atzrf1a-2 Atzrf1b-1* mutants, the levels of H2Aub1 were also strongly reduced at the examined seed development genes. Taken together, it indicates that AtZRF1a and AtZRF1b are required for maintaining H3K27me2 and H2Aub to repress the seed development genes *ABI3*, *CRA1*, *CRC*, *PER* and *AIL5*, to promote seed germination (Figure III.35).

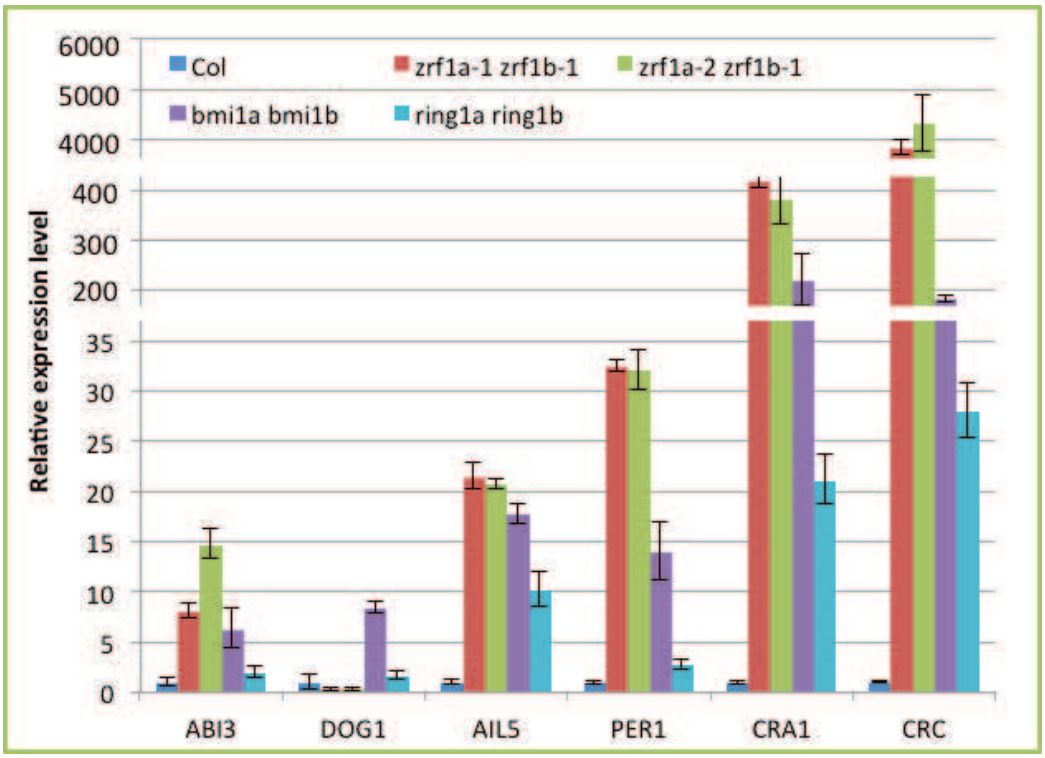

Figure III.34. Expression of seed related genes during double mutants *Atzrf1a-1 Atzrf1b-1*, *Atzrf1a-2 Atzrf1b-1* and Col germination

Relative expression levels of *ABI3*, *DOG1*, *CRA1*, *CYC*, *PER* and *AIL5* were compared by qRT-PCR between Col (blue bars) and double mutants *Atzrf1a-1 Atzrf1b-1* (red bars), *Atzrf1a-2 Atzrf1b-1* (green bars) at 5 DAS. Indicated values are means±SD from 3 technical replicates; three biological replicates gave similar results.

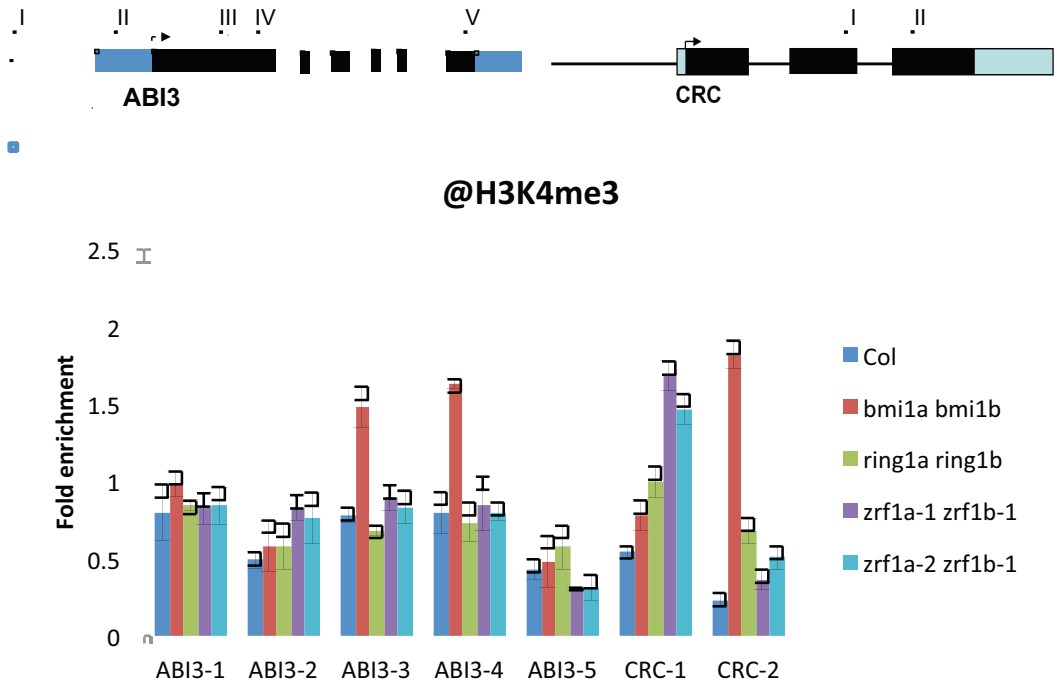

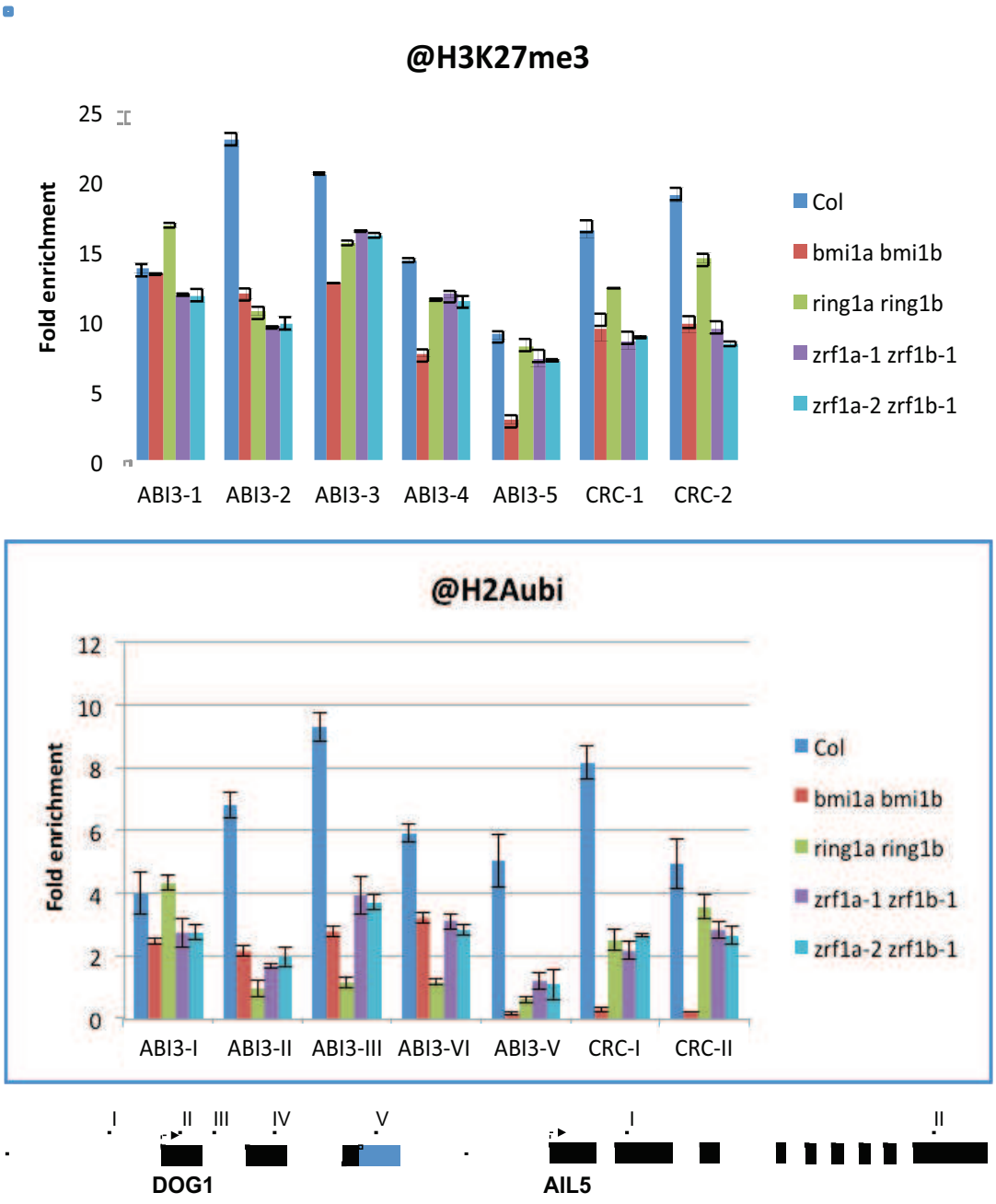
@H3K27me3
Fold enrichment
25
20
15
10
5
0
ABI3-1
ABI3-2
ABI3-3
ABI3-4
ABI3-5
CRC-1
CRC-2
Col
bmi1a bmi1b
ring1a ring1b
zrf1a-1 zrf1b-1
zrf1a-2 zrf1b-1
@H2Aubi
Fold enrichment
12
10
8
6
4
2
0
ABI3-I
ABI3-II
ABI3-III
ABI3-VI
ABI3-V
CRC-I
CRC-II
Col
bmi1a bmi1b
ring1a ring1b
zrf1a-1 zrf1b-1
zrf1a-2 zrf1b-1
I
II
III
IV
V
I
II
DOG1
AIL5

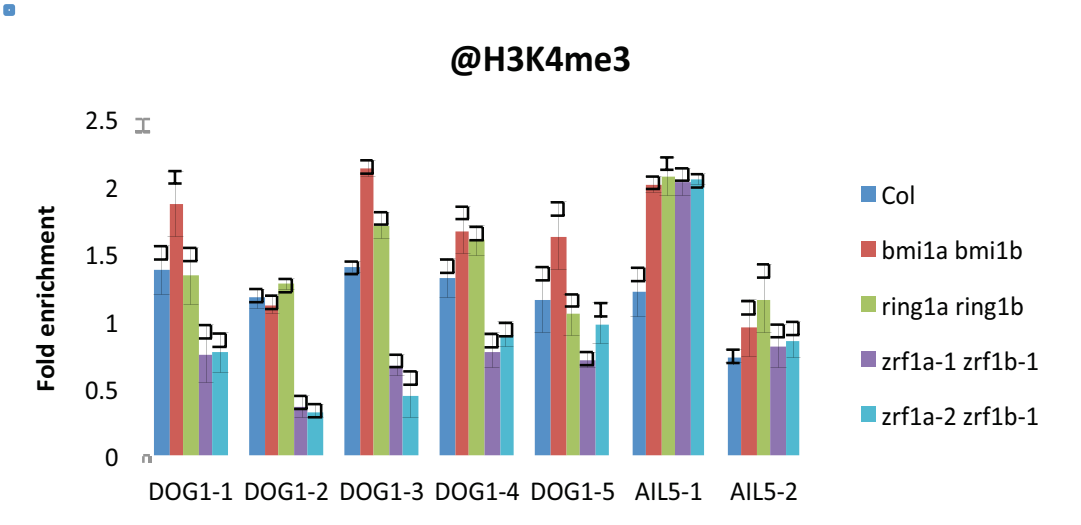
@H3K4me3
Fold enrichment
2.5
2
1.5
1
0.5
0
DOG1-1
DOG1-2
DOG1-3
DOG1-4
DOG1-5
AIL5-1
AIL5-2
Col
bmi1a bmi1b
ring1a ring1b
zrf1a-1 zrf1b-1
zrf1a-2 zrf1b-1

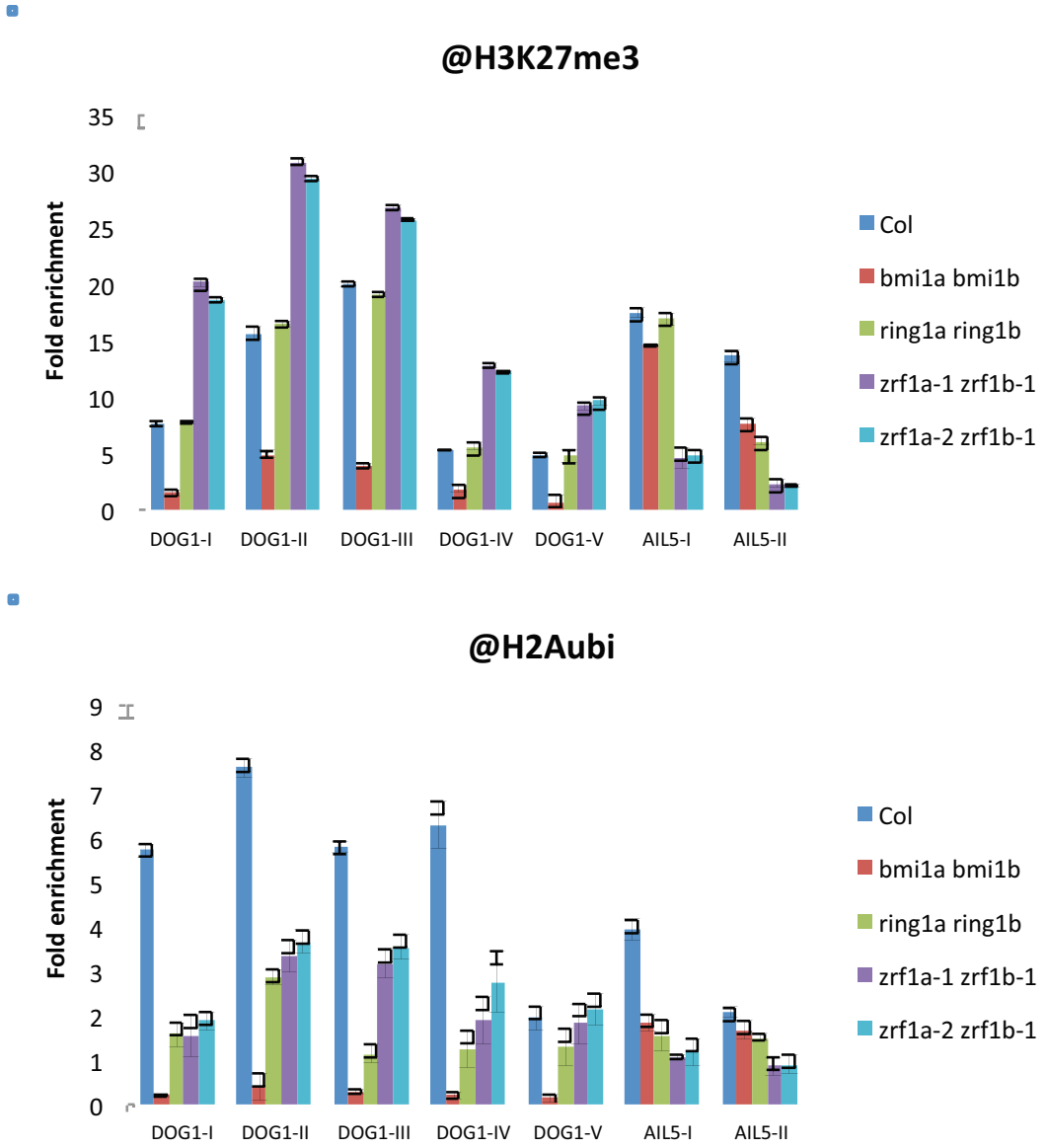

Figure III.35. *AtZRF1a AtZRF1b* double mutant affects H3K27me3 and H2Aubi markers on *ABI3*, *DOG1*, *CRC* and *AIL5* loci

Relative levels of histone modifications on *ABI3*, *DOG1*, *CRC* and *AIL5* chromatin were analyzed by ChIP using antibodies against H3K4me3, H3K27me3 and anti-hH2Aub. Chromatin from Col, *Atbmi1a Atbmi1b*, *Atring1a Atring1b*, *Atzrf1a-1 Atzrf1b-1* and *Atzrf1a-2 Atzrf1b-1* was prepared from 5 DAG. The immunoprecipitated DNA fragments were quantified by qRT-PCR and normalized to internal controls (relative to Input and normalized to Actin). Data shown are means±SD of three technical replicates. Similar results were obtained in three independent experiments. Amplified regions are numbered and indicated on the schematic representation of the *ABI3*, *DOG1*, *CRC* and *AIL5* genomic structure. Exons are represented by black boxes, untranslated regions by dashed boxes and introns by black lines.

III.7. Characterization of the interactionships between AtZRF1 and PRC1-like ring-finger components

III.7.1. Transcriptome analysis of *Atzrf1a Atzrf1b* mutants

Atzrf1a-1 Atzrf1b-1 and *Atzrf1a-2 Atzrf1b-1* genome-wide expression levels were profiled by microarray in comparison to wild-type. Total RNA were isolated from 15-days-old *in vitro* seedlings, three independent biological replicates for each sample, and analyzed by Agilent single channel arrays. Loci were considered significantly deregulated compared to Col-0 when the expression fold-change exceeded 2 with a p-value inferior to 0.05.

Transcriptome analysis showed a total of 11116 and 11291 mis-regulated genes in *Atzrf1a-1 Atzrf1b-1* and *Atzrf1a-2 Atzrf1b-1* mutants, respectively. Among the 11116 mis-regulated genes, the analysis identified 5235 genes (47.09%) that were up-regulated and 5881 genes (52.91%) that were down-regulated in *Atzrf1a-1 Atzrf1b-1* double mutant. In the *Atzrf1a-2 Atzrf1b-1* double mutant, among the 11291 mis-regulated genes we identified 5240 genes (46.41%) that were up-regulated and 6051 genes (53.59%) that were down-regulated. A comparison showed that the *Atzrf1a-1 Atzrf1b-1* and *Atzrf1a-2 Atzrf1b-1* mutants exhibited a very high degree of overlap.

The statistical significance of the overlap between two gene sets was qualified by a representation factor (RF) and P-value. The RF characterizes the fold increase of overlapping genes compared to the expected overlap of two random gene populations. It takes into account the size of the two analyzed data sets and the global gene sets (i.e. number of protein-encoding loci according to The Arabidopsis Information Resource 10 database (TAIR10)). Thus, the overlap between two random gene populations is qualified by a RF of one, while the RF of an overlap between two populations enriched in common members is superior to one.

The significance of the overlaps between the commonly mis-regulated genes in *Atzrf1a-1 Atzrf1b-1* and *Atzrf1a-2 Atzrf1b-1* mutants was calculated considering the entire populations of commonly mis-regulated genes or solely up- or down-regulated gene sets. The total number of commonly mis-regulated genes is 8956 (RF=1.95, P<3.54e-10). Among them, our analysis identified that 4103 genes (RF=4.10, P<1.2e-11) were up-regulated, which is 45.88% of commonly mis-regulated genes. And 4840

genes (RF=3.73, P<1.32e-10) were down-regulated, which is 54.12% of commonly mis-regulated genes (Figure III.36). These results indicate that *AtZRF1a* and *AtZRF1b* are involved in establishing both an active transcriptional state and a repressive transcriptional state. The predominant function is involved in transcriptional activity.

In seedlings, global gene expression was more strongly affected in the *Atzrf1a Atzrf1b* than in the *Atring1a Atring1b* and *Atbmi1a Atbmi1b* mutants. Indeed, a total of 8956 loci were affected in the *Atzrf1a Atzrf1b* mutant, while 678 were mis-regulated in the *Atring1a Atring1b* mutant (Molitor, unpublished results) and 432 in the *Atbmi1a Atbmi1b* mutant (Qin *et al*., 2008). Interestingly, in the *Atzrf1a Atzrf1b* mutant the number of mis-regulated genes that were down-regulated (54.12%) was higher than those that were up-regulated (45.88%). In *Atring1a Atring1b* and *Atbmi1a Atbmi1b* mutants the up-regulated loci, were predominant, with 69.57% and 73.38%, respectively. Only 30.43% and 26.62% respectively of the genes were down-regulated in the two mutants. Furthermore, I analyzed the transcriptional overlaps of up-regulated loci between *Atzrf1a Atzrf1b* and *Atring1a Atring1b* or *Atzrf1a Atzrf1b* and *Atbmi1a Atbmi1b*.

The number of transcripts overlapping between *Atzrf1a Atzrf1b*-up and *Atring1a Atring1b*-up is 171 (25.22% of *Atring1a Atring1b* total; RF=2.42, P<1.47e-5) and between *Atzrf1a Atzrf1b*-up and *Atbmi1a Atbmi1b*-up it is 104 (24.07% of *Atbmi1a Atbmi1b* total). Even though these percentages may not appear to be very high, however, the insertions for both microarray data sets were more than two-fold increased compared to a random distribution (Figure III.37).

	Atzrf1a-1 Atzrf1b-1	*Atzrf1a-2 Atzrf1b-1*
Total	11116	11291
UP%	47.09	46.41
DOWN%	52.91	53.59

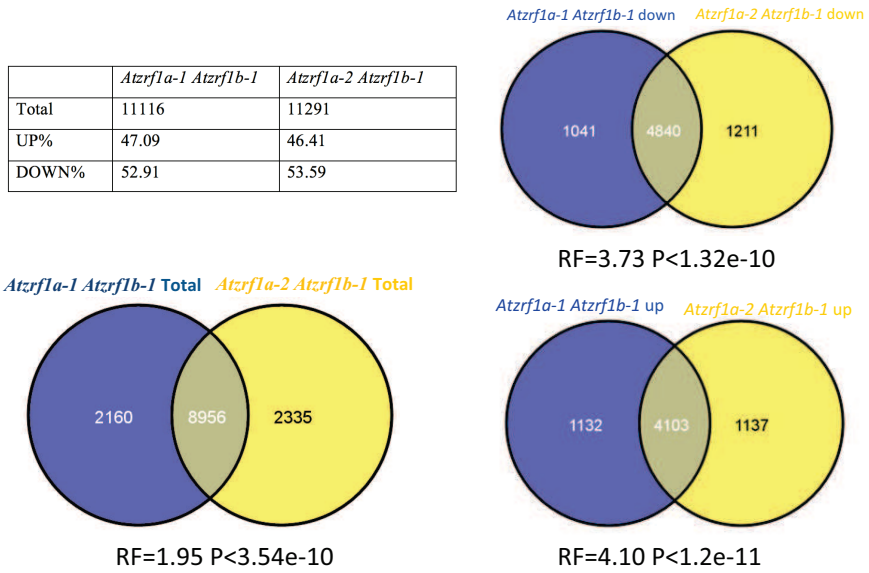

Figure III.36. *Atzrf1a-1 Atzrf1b-1* and *Atzrf1a-2 Atzrf1b-1* mutants mis-regulated genes.

Venn diagrams showing the number and overlap of differentially expressed genes found in *Atzrf1a-1 Atzrf1b-1* and *Atzrf1a-2 Atzrf1b-1* mutants. Microarray analyses were performed on Agilent Chip using total RNA extracted from 15 days old seedlings. The differentially expressed genes in the mutant compared to wild-type are validated by a change of at least 2-fold and Bonferroni P value inferior to 0.05 from three replicates of hybridization. The corresponding overlaps are indicated by the percentage of common loci and the statistical significance is qualified by a representation factor (RF) and an associated p-value.

	Atzrf1a Atzrf1b	*Atring1a Atring1b*	*Atbmi1a Atbmi1b*
Total	8956	678	432
UP%	45.88	69.57	73.38
Down%	54.12	30.43	26.62

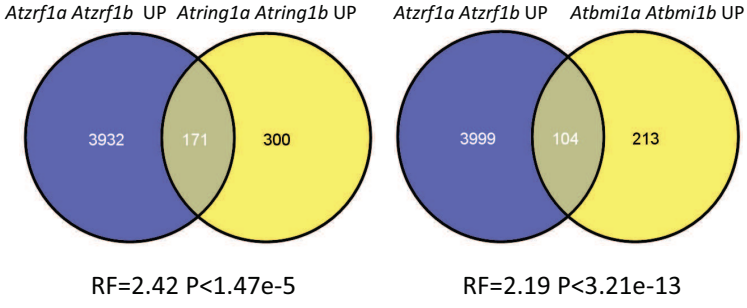

Figure III.37. Comparison of mis-regulated loci identified by microarray analysis of gene expression in *Atzrf1a Atzrf1b*, *Atring1a Atring1b* and *Atbmi1a Atbmi1b* mutants seedlings.

III.7.2 AtZRF1b physically interacts with AtBMI1

Some of the *Atzrf1a Atzrf1b* double mutant defects are similar to those previously reported for the PRC1 mutants *Atring1a Atring1b* and *Atbmi1a Atbmi1b.* Our microarray analysis (behind section) showed that there are significant overlaps of the perturbed genes between *Atzrf1a Atzrf1b* and *Atring1a Atring1b* or *Atbmi1a Atbmi1b.* We tested the physical interaction of AtZRF1b with AtRING1 and AtBMI1 proteins. For this, we carried out pull-down experiments. Recombinant plasmids of GST-RING1A, GST-BMI1A, GST-BMI1B and GST-BMI1C have been produced in our lab. Following plasmid transformation, protein expression, isolation and purification, we obtained the recombinant proteins GST-RING1A, GST-BMI1A, GST-BMI1B and GST-BMI1C. AtZRF1b protein comes from *p35S::FLAG-ZRF1b* transgenic plants in the wild-type background. Agarose beads coated with GST, GST-RING1A, GST-BMI1A, GST-BMI1B or GST-BMI1C were incubated with an equal aliquot of total nuclear protein extracts of *Arabidopsis* plants expressing FLAG-AtZRF1b. Then the pulldown fractions were analyzed by Western blot using antibodies against FLAG. We found that AtZRF1b can interact with AtBMI1A, AtBMI1B and AtBMI1C but not with AtRING1A (Figure III.38A). In order to confirm the observed interaction, we performed FLIM analysis to examine GFP-AtZRF1b interaction with RFP-AtRING1A, RFP-AtBMI1A, RFP-AtBMI1B or RFP-AtBMI1C, which are coexpressed in *Nicotiana benthamiana* leaves. We confirmed the interaction between AtZRF1b and AtBMI1A or AtBMI1B (Figure III.38B).

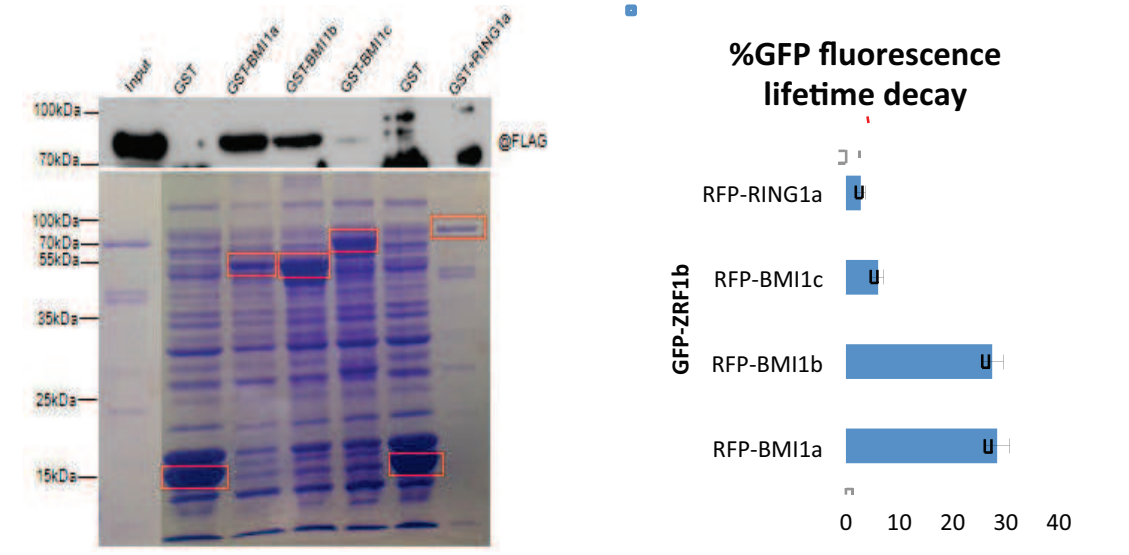

Figure III.38. AtZRF1b physically interacts with AtBMI1 proteins

Pulldown assay. Agarose beads coated with GST, GST-RING1a, GST-BMI1a, GST-BMI1b or GST-BMI1c were incubated with an equal aliquot of total protein extracts of *Arabidopsis* plants expressing FLAGAtZRF1b. The pulldown fractions and inputs were analyzed by Western blot using antibodies against FLAG (@FLAG, top panel). Coomassie staining is shown as loading control (bottom panel). The positions of GST, GST-RING1a, GST-BMI1a, GST-BMI1b and GST-BMI1c are indicated by red squares, respectively.

FLIM detection of the GFP-AtZRF1b interaction with RFP-AtRING1a, RFP-AtBMI1a, RFP-AtBMI1b and RFP-AtBMI1c *in planta*. GFP- and RFP-tagged proteins as indicated were transiently coexpressed in *Nicotiana benthamiana* leaves. The fluorescence lifetime of GFP fusion proteins was recorded two days post infiltration. Data represent the average GFP fluorescence lifetime decay 6 SD of three biological replicates, with over 30 nuclei for each recording. Values above 5% indicate positive protein-protein interactions.

III.7.3. Genetic interaction between *Atzrf1a Atzrf1b* and *Atbmi1a Atbmi1b* or *Atring1a Atring1b*

On the basis of the microarray results, we found there are many common functions in AtZRF1a/b and AtRING1a/b or AtBMI1a/b. To further understand the mechanism of AtZRF1a and AtZRF1b chromatin regulation, we used the double mutants *Atzrf1a-1 Atzrf1b-1* and *Atring1a Atring1b* or *Atbmi1a Atbmi1b* to obtain quadruple mutants by genetic crossing. By screening offspring phenotype, we obtained homozygous quadruple mutants *Atzrf1a-1 Atzrf1b-1 Atring1a Atring1b* and *Atzrf1a-1 Atzrf1b-1 Atbmi1a Atbmi1b*. To further confirm the two quadruple mutants, we performed RT-PCR to check the expression of *AtZRF1a*, *AtZRF1b*, *AtRING1a* or *AtRING1b* in the quadruple mutant *Atzrf1a-1 Atzrf1b-1 Atring1a Atring1b*. And we also tested the expression of *AtZRF1a*, *AtZRF1b*, *AtBMI1a* or *AtBMI1b* in the quadruple mutant *Atzrf1a-1 Atzrf1b-1 Atbmi1a Atbmi1b*. As expected, a loss of these genes caused loss-of-function of *AtZRF1a*, *AtZRF1b*, *AtRING1a*, *AtRING1b*, *AtBMI1a* or *AtBMI1b* (Figure III.39). Interestingly, we found the two quadruple mutants have a phenotype similar to that of the *Atzrf1a-1 Atzrf1b-1* double mutant (Figure III.39).

Figure III.39. Phenotype of quadruple mutants

Left: Analysis of the expression of *AtZRF1a*, *AtZRF1b*, *AtRING1a* or *AtRING1b* in the quadruple mutant *Atzrf1a-1 Atzrf1b-1 Atring1a Atring1b*, and of the expression of *AtZRF1a*, *AtZRF1b*, *AtBMI1a* or *AtBMI1b* in the quadruple mutant *Atzrf1a-1 Atzrf1b-1 Atbmi1a Atbmi1b*. Full-length *AtZRF1a*, *AtZRF1b*, *AtRING1a*, *AtRING1b*, *AtBMI1a* and *AtBMI1b* sequences were amplified from wild-type (Col) and quadruple mutant cDNAs. *ACTIN* served as an internal control.

Right: Phenotype of quadruple mutants.

IV. Conclusion and Discussion

IV.1 *AtZRF1a* and *AtZRF1b* are functionally redundant, and they serve as a novel factor binding H2A.1ubi

In *Arabidopsis*, AtZRF1a and AtZRF1b are the homologs of human ZRF1. They contain a tandem repeat of the SANT domain and a Zuotin domain. The Zuotin homology region includes a DnaJ motif, considered to interact with Hsp70s. Our results indicate that ZRF1, which contains a ubiquitin-binding domain, can interact with H2A-ubiquitin. These properties are comparable with those described for mammalian ZRF1 (Richly *et al*., 2010). The human chromatin-binding factor ZRF1 has a strong link with PRC1. In differentiation conditions, ZRF1 can displace the PRC1 complex from chromatin by competing for the binding to mono-ubiquitinated H2A; it can directly antagonize gene silencing (Richly *et al*., 2010).

Arabidopsis contains AtZRF1a and AtZRF1b exhibiting high sequence homology. The AtZRF1 function and the underlying molecular mechanisms remain largely unknown. So far, our study has revealed a redundant function of *AtZRF1a* and *AtZRF1b* in the regulation of plant development. The AtZRF1b protein is localized in both the cytoplasm and the nucleus. Moreover, both *AtZRF1a* and *AtZRF1b* genes are widely expressed in various plant organs including roots, stems, leaves, and inflorescences.

IV.2 AtZRF1 carries out roles in diverse processes of plant development

The *Atzrf1a Atzrf1b* mutant plants are small in size. Plant size is intrinsically determined by cell division and cell expansion activities. In the *Atzrf1a Atzrf1b* mutant, the pavement cell size is smaller than wild-type, and the final leaf size is drastically reduced in *Atzrf1a Atzrf1b* compared with Col. The reduced leaf size is largely associated with a major reduction of cell expansion. Moreover, cell division and differentiation in *Atzrf1a Atzrf1b* double mutants are also affected; the G1 phase is relatively shorter, and polyploidy levels are slightly increased in the *Atzrf1a Atzrf1b* mutant leaves. And qPCR data showed a strong enrichment in M-phase-specific genes down-regulated in the *Atzrf1a Atzrf1b* mutant, namely, the A-type and B-type cyclins that are key regulators in the G2-to-M transition (Inzé and De Veylder, 2006).

During development, a block of the G2-to-M transition may also result in an increased endoreduplication. Endoreduplication occurs after cells have ceased the

mitotic cycles, and endoreduplicated cells do not reenter the mitotic cell cycle. Thus, endoreduplication is characteristic of a switch between cell proliferation and differentiation. It is also believed to be essential for enhancing metabolic capacity and supporting cell growth and for maintaining an optimal balance between cell volume and nuclear DNA content (reviewed in Kondorosi *et al*., 2000; Inzé and De Veylder, 2006). Interestingly, the double mutant *Atzrf1a Atzrf1b* shows slightly elevated polyploidy levels but reduced cell size. Ploidy-dependent epigenetic regulation has been reported to be involved in differential reprogramming of orthologous gene expression and in stable silencing of epialleles (Lee and Chen, 2001; Baubec *et al*., 2010). Based on its global effect on H2Aub1 deposition, it is reasonable to speculate that *AtZRF1a* and *AtZRF1b* are involved in the regulation of chromatin structure and gene expression in diploid and polyploid cells, playing important roles in the coordination of cell division, differentiation, and expansion to determinate organ size.

The *Atring1a Atring1b* and *Atbmi1a Atbmi1b* (*drip1-1 drip2-1*) mutants show pleiotropic phenotypes (Qin *et al*., 2008; Xu and Shen, 2008). During seedling growth these mutants reveal a crucial function of PRC1-like complexes in the repression of embryogenesis and stem cell activities for proper vegetative growth. Some defects of the *Atzrf1a Atzrf1b* mutant are similar to the previously reported phenotype of the *Atring1a Atring1b* or *Atbmi1a Atbmi1b* mutant. In the *Atzrf1a Atzrf1b* mutant, we observed callus-like plants. By qRT-PCR, we found many regulatory genes involved in embryogenesis and stem cell maintenance were upregulated in the *Atzrf1a Atzrf1b* mutant. These include the key embryonic regulatory genes *LEC1*, *LEC2*, *ABI3* and *BBM* (Boutilier *et al*., 2002; Giraudat *et al*., 1992; Lotan *et al*., 1998; Stone *et al*., 2001), the embryonic competence-enhanced gene *AGL15* (Harding *et al*., 2003), the key RAM-regulatory and basal embryo-axis cell fate genes *WOX5* and *WOX8* (Breuninger *et al*., 2008), the key SAM-regulatory genes *STM*, *BP*, *KNAT2* and *KNAT6* (Xu and Shen, 2008), the organ boundary regulatory genes *CUC1*, *CUC2* and *CUC3* (Vroemen *et al*., 2003) and the auxin transporter gene *PIN1* (Blilou *et al*., 2005). The *LEC1*, *LEC2*, *ABI3*, *BBM*, *AGL15*, *WOX5*, *WOX8* and *CUC1* genes were also found to be upregulated to varying extents in the *Atring1a Atring1b* and *Atbmi1a Atbmi1b* mutants. Interestingly, like in *Atring1a Atring1b,* the Class I KNOX genes (*STM*, *BP*, *KNAT2* and *KNAT6*) were upregulated in the *Atzrf1a Atzrf1b* double mutant, but barely changed in *Atbmi1a Atbmi1b*. This is consistent with the highly fasciated stem phenotype observed in *Atzrf1a Atzrf1b* and *Atring1a Atring1b* but not in *Atbmi1a*

Atbmi1b (*drip1-1 drip2-1*).

AtZRF1a and *AtZRF1b* transcripts were detected in the inflorescence meristem and in floral organs. We found that *Atzrf1a Atzrf1b* mutant flowers showed abnormal numbers of floral organs. Flower organ identity is determined by the interplay between homeotic transcription factor genes, including *AG*, *PI*, *AP3*, *AP2*, and *AP1*, which are subjected to chromatin-remodelling regulation (reviewed in Shen and Xu, 2009). Consistent with its phenotype, downregulation of *AG, PI* and *AP1* was observed in *Atzrf1a Atzrf1b.*

The *Atzrf1a Atzrf1b* mutant plants are almost completely sterile. Several defects may contribute to *Atzrf1a Atzrf1b* sterility: first, abnormal floral organs, such as fewer stamens than wild-type or stamen filaments too short to allow effective pollination of the stigma; second, short siliques and seed abortion; and third, reduction of transmission efficiency of mutant alleles in heterozygous mutant plants (Table III.1).

IV.3 *AtZRF1a* and *AtZRF1b* are required for maintaining root development

The root system is the main organ of the plant responsible for nutrient and water uptake. In this study, we have demonstrated that loss-of-function mutant *Atzrf1a Atzrf1b* exhibits SCN disorganization and stem cell termination, causing primary root growth arrest. The auxin gradient maximum which appeared in the QC cells in WT is almost lost in *Atzrf1a Atzrf1b* roots. Previous genetic analysis showed that auxin acts upstream of the major regulators of stem cell activity (Ding and Friml, 2010; Sabatini *et al*., 1999), and QC ablation experiments demonstrated that reestablishment of auxin maximum is earlier than the re-specification of a new QC in root (Grieneisen *et al*., 2007). We therefore believe that the loss of auxin accumulation and gradient is a potent cause of the irregular cell shape and position of QC in *Atzrf1a Atzrf1b*. High levels of auxin promote proteasome-mediated degradation of IAA proteins, which act as repressors of auxin response by binding Auxin Response Factors (ARFs) to regulate downstream gene transcription. Several IAA genes, including the previously characterized ones IAA14 and IAA19 (Fukaki *et al*., 2002; Tatematsu *et al*., 2004), are upregulated in *Atzrf1a Atzrf1b*, further supporting a perturbed auxin pathway by loss of AtZRF1a and AtZRF1b function.

In addition to QC, we have demonstrated that the surrounding stem cells of

QC also exhibited varied degrees of impairment in the *Atzrf1a Atzrf1b* double mutant. Development of the *Arabidopsis* root is a dynamic process that involves a complex interplay between transcriptional regulators and plant hormones. Understanding how AtZRF1 regulates root growth and development will require the integration of many different types of data.

IV.4 *AtZRF1a* and *AtZRF1b* repressed flowering by promoting *FLC* and *MAF* gene expression

In this study, we found that loss-of-function mutants of *AtZRF1a* or *AtZRF1b* displayed a weak early-flowering phenotype. However, the simultaneous loss of *AtZRF1a* and *AtZRF1b* drastically delayed flowering time. To explore the molecular mechanisms responsible for the change in flowering time in *Atzrf1a Atzrf1b* double mutants, we tested flowering-related genes by quantitive PCR. In the *Atzrf1a Atzrf1b* double mutant, the expression of *FLC* was about 5 times lower than in wild type (Figure III.16A). And the expression of *MAF1* (*FLM*), *MAF2* and *MAF4* was 2.5-5 times lower than that in wild type (Figure III.16A). As a result of the down-regulation of *FLC* and *MAFs*, the expression of *FT* in *Atzrf1a Atzrf1b* double mutant was about two times higher than in wild type (Figure III.16B). These results suggest that *AtZRF1a* and *AtZRF1b* are involved in flowering regulation.

Enrichment of the H3K27me3 repressive mark at the *FLC* and *MAF4* loci is up-regulated by *AtZRF1*. However, in the *Atring1a Atring1b* mutant, enrichment of H3K27me3 at the *FLC* locus is not affected and is down-regulated at the *MAF4* locus. In the *Atbmi1a Atbmi1b* (*drip1-1 drip2-1*) mutant, enrichment of H3K27me3 at the *FLC* and *MAF4* loci is down-regulated. These findings suggest that the function of *AtZRF1a* and *AtZRF1b* in flowering time regulation is opposite to that of the PRC1 complex, *AtZRF1a* and *AtZRF1b* promoting the expression of *FLC* and *MAF4* through affecting their H3K27me3 levels to regulate the floral transition in *Arabidopsis* (Figure III.18).

The function of *AtZRF1a* and *AtZRF1b* in mediating H3K27me3 levels could be restricted to a limited number of target genes in a specific developmental context. As shown in this study, although elevated levels of H3K27me3 were found to be associated with down-regulation of *FLC* and *MAF4* in *Atzrf1a Atzrf1b*, ,global H3K27 methylation levels are not altered in *Atzrf1a Atzrf1b* as compared to wild-type plants

during the floral transition, indicating that *AtZRF1a* and *AtZRF1b* might only affect H3K27me3 levels at a few specific flowering regulators.

We failed to detect an elevated level of H2Aub1, which would support the animal model where *ZRF1* is involved in H2Aub1 removal for transcriptional activation. In this study, H2Aub1 levels at *FLC* and *MAF4* are not altered and global H2Aub1 levels are slightly down-regulated in *Atzrf1a Atzrf1b* as compared to wild-type plants during the floral transition. This may be because the loss of *AtZRF1a* and *AtZRF1b* affects the expression levels of AtRING1a, AtRING 1b, AtBMI1a, AtBMI1b and AtBMI1c .However, the *Atbmi1a Atbmi1b* and *Atring1a Atring1b* mutants also did not show detectable changes of H2Aub1 at *FLC* and *MAF4*.

IV.5 *AtZRF1a* and *AtZRF1b* play crucial roles in seed germination

Seed germination is crucial for next-generation plant growth and it is regulated by a very complicated signaling network and gene expression regulation. Different plants may share similar molecular mechanisms. *Atzrf1a* and *Atzrf1b* single mutants showed a normal germination ratio, while the *Atzrf1a Atzrf1b* double mutant exhibited a delayed germination under osmotic stress growth conditions (treatment with salt or mannitol). Similarly, the *Atbmi1a Atbmi1b* and *Atring1a Atring1b* double mutants also displayed a germination delay. The enhanced germination defects observed in the *Atzrf1a Atzrf1b Atbmi1a Atbmi1b* quadruple mutant indicate that AtZRF1a/b and AtBMI1a/b may also work in parallel pathways.

AtZRF1a/b and AtBMI1a/b promote seed germination likely through repression of seed developmental genes. Consistently, the *Atzrf1a Atzrf1b* mutant and the *Atbmi1a Atbmi1b* mutant showed derepression of *ABI3*, *CRU1/CRA1*, *CRU3/CRC*, *CHO1/AIL5* and *PER1*. The expression of these seed developmental genes was previously shown to negatively regulate seed germination (Bentsink *et al*., 2006; Haslekas *et al*., 2003; Parcy *et al*., 1994; Yamagishi *et al*., 2009). Quantitative differences in gene expression and the stress-inducible nature of these genes in seed germination regulation might explain the *Atzrf1a Atzrf1b* mutant phenotype observable under osmotic stress conditions. The detected gene derepression was more severe and persisting in *Atzrf1a Atzrf1b* than in *Atbmi1a Atbmi1b*.

Some defects of the *Atzrf1a Atzrf1b* mutant are similar to the previously reported phenotypes of the *Atbmi1a Atbmi1b* or *Atring1a Atring1b* mutants; and there are significant overlaps of genome-wide perturbed genes between these mutants.

Genetic interaction tests revealed that *Atzrf1a Atzrf1b* is epistatic to *Atbmi1a Atbmi1b* and *Atring1a Atring1b*, suggesting that AtZRF1 acts downstream of AtRING1 and AtBMI1.

Chromatin analysis at seed developmental genes revealed that their up-regulation is associated with reduced levels of H2Aub1 and H3K27me3 in *Atzrf1a Atzrf1b* as in *Atbmi1a Atbmi1b* and *Atring1a Atring1b* to varied degrees.

IV.6 *AtZRF1a* and *AtZRF1b* functions are partially related to PRC1

Some phenotypic defects observed in the double mutant *Atzrf1a Atzrf1b* are similar to those previously observed in PRC1 mutants *Atring1a Atring1b* and *Atbmi1a Atbmi1b*. Our microarray date are consistent with a genetic interaction, since they reveal a significant overlap of deregulated genes between *Atzrf1a Atzrf1b* and *Atring1a Atring1b* or *Atbmi1a Atbmi1b*. I further analyzed the physical interaction of AtZRF1b with AtRING1 or AtBMI1. Beads of agarose coupled to GST, or to GST-fusion proteins RING1A, GST-BMI1a, GST-BMI1B or GST-BMI1C were incubated with total extracts of nuclear proteins from *Arabidopsis* expressing the fusion protein FLAG-AtZRF1b. GST pull-down followed by Western blot analysis using anti-FLAG antibodies allowed me to demonstrate the interaction between AtZRF1B and AtBMI1A, AtBMI1B or AtBMI1C but not AtRING1A.

My results allowed the first functional characterization of the genes *AtZRF1a* and *AtZRF1b*. My data have shown that AtZRF1a and AtZRF1b play roles in part related with PRC1 but also with specific aspects. Their role in the kidnapping of H2Aub1, as proposed for ZRF1 in animals (Richly *et al*., 2010) has not been observed in plants. Recent data suggest that ZRF1 also exerts a Polycomb-independent role (Aloia *et al.*,.2014). The physical interaction between AtZRF1b and AtBMI1a/AtBMI1b is novel and has crucial importance for understanding AtZRF1 function. This needs to be confirmed by additional methods.

AtZRF1 has very important roles in plant development. Our microarray results show that, of the total of misexpressed genes in AtZRF1a and AtZRF1b knock out mutants, half were down-regulated of and half were up-regulated. These data are consistent with tthose observed in human cells (Demajo *et al*., 2013). The microarray data indicate that AtZRF1a/b may act as a bifunctional protein in plant development. But the mechanism remains unclear, and therefore *AtZRF1*-binding at target chromatin regions requires further studies.

V. Materials and Methods

-

Ⅴ.1. Materials

Ⅴ.1.1 Plant materials and growth conditions

The *Atring1a Atring1b* mutant was previously described (Xu and Shen, 2008). The *Atbmi1a Atbmi1b* mutant was reported by Calonje (Calonje *et al*., 2008). The Columbia (Col-0) ecotype was used as genetic background for both wild-type and mutant plants, but enhancer trap lines J2341 and J1092 are in C24 ecotype. The reporter lines *WOX5::GFP*, *DR5::GFP*, *SCR::GFP*, *CO2::GFP* and *STM::GUS* were provided by Dr. Donghong CHEN. *Arabidopsis thaliana* mutants were obtained from the *Arabidopsis* Biological Resource Center (ABRC, http://www.arabidopsis.org) and the European *Arabidopsis* Stock Center (NASC, http://arabidopsis.info). They were either grown on soil (16 h light and 8 h dark) in the greenhouse or *in vitro* on 0.8% MS medium. Seeds grown on plates were stratified in the dark at 4°C for 48 h to synchronize the germination time. Then the plants were transferred to a growth chamber (16 h light and 8 h dark, 22°C). To generate flowering plants, seedlings were transferred to soil 10 days after germination and cultivated under long day conditions (LD; 16 h light and 8 h dark).

Table Ⅴ.1

Mutant	T-DNA line or Stock number
Atzrf1a-1	Sail_786_F09 (N876841)
Atzrf1a-2	Salk_070956.55.25.X (N570956)
Atzrf1a-3	Salk_070965.50.20.X (N570965)
Atzrf1b-1	FLAG_110A05
Atzrf1b-2	Sail_716_D04 (N876215)
Atzrf1b-3	Sail_625_B03 (N826768)
Atzrf1b-4	Sail_629_F09 (N827014)
Atzrf1b-5	FLAG_099C10

-

V.1.2 Vectors

Vectors used during my thesis are listed below (Table V.2)

Vector	**Experiment**	**Resistance**
pDONR207	Gateway cloning	Gentamycin
pENTR3C	Gateway cloning	Kanamycin
pGWB5	Gateway cloning	Spectinomycin
pGWB11	Gateway cloning	Spectinomycin
pB7WGF2	Gateway cloning	Spectinomycin
pB7FWG2	Gateway cloning	Spectinomycin
pH7WGR2	Gateway cloning	Spectinomycin
pH7RWG2	Gateway cloning	Spectinomycin
pGEX-4T-1	Protein expression	Ampicillin
pET30a	Protein expression	Kanamycin
pCAMBIA1300	Binary vector	Kanamycin

V.1.3 Antibodies

Antibodies used are listed below (Table V.3)

	Host	Company
Anti-trimethyl-Histone –H3-(K4) antibody (Cat. 07-473)	Rabbit	Millipore
Anti-trimethyl-Histone –H3-(K36) antibody (Cat. Ab9050)	Rabbit	Abcam
Anti-trimethyl-Histone –H3-(K27) antibody (Cat. 07-449)	Rabbit	Millipore
Anti- Histone –H3 antibody	Rabbit	Millipore
anti-hH2Aub antibody (Cell Signaling Technology 8240)	Rabbit	
Anti-FLAG (F1804)		Sigma-Aldrich

V.1.4 Primers

Name	Sequences 5'-3' (Genotying)
zrf1a.1-LP	TTGTTGTTGTGCAGATTCTGC
zrf1a.1-RP	CGTACTCTGAGGAGCTTGTGG
zrf1a.2-LP	AGGCTAGAAAGGAGGAGCATG
zrf1a.2-RP	TCATCGTTTTACCAGGGACAG
zrf1a.3-LP	AGA AGA AGC AGG AAG AGG ACG
zrf1a.3-RP	CTT GCT TCT CGC AAA GTA ACG

-

zrf1b.1-LP	AAAAGCTTTAGCTGAGTCGGG
zrf1b.1-RP	GAAAAAGTTATCGCGATGCTG
zrf1b.2-LP	TGGATATAACAAGGCCTGACG
zrf1b.2-RP	CTGGAGAATAGGAAACCTGCC
zrf1b.3-LP	CGA AGC AAT CAA AAC CAA GAG
zrf1b.3-RP	ACC ATT CGA TAC TGT GCA AGG
zrf1b.4-LP	CGA AGC AAT CAA AAC CAA GAG
zrf1b.4-RP	ACC ATT CGA TAC TGT GCA AGG
zrf1b.5-LP	AAA AGC TTT AGC TGA GTC GGG
zrf1b.5-RP	GAA AAA GTT ATC GCG ATG CTG
LBb1.3	ATTTTGCCGATTTCGGAAC
FLAG_LB1	CGGCTATTGGTAATAGGACACTGG
SAIL LB	GCC TTT TCA GAA ATG GAT AAA TAG CCT TGC TTC C
Name	Sequences 5'-3' (Clone)
H2A.1-F	GGC GGTACC ATGGCTGGTCGTGGAAAAAC
H2A.1-R	GGC GAGCTC CTAATCTTCCTGAGGCTTTGAAG
Z1aF-BamHI	ggatcc ATG CCG AGC CGG AGA AGT GAG TC
Z1aR-EcoRI	gaattc TCA TAC TCC GGT TTT CTT GTT TCT AAT GAT TTC
ZRF1bF-EcoR1	GGC GAATTC ATGCAGAGTTGGGGAATTAAC
ZRF1bF-BamH1	GGC GAATCC ATGCAGAGTTGGGGAATTAAC
ZRF1bR-Xho1	GGC CTCGAG TTAGGCTGTGGGTTTCTTGG
ZRF1bR-BamH1	GGC GGATCC GGC TGT GGG TTT CTT GGT TCT GAT G
ZRF1b△SANT-R	GGC CTC GAG CTT CTC ATG AGT AGC AGT ATC C
ZRF1bSANT-F	GGC GAA TTC AAA GAG AAA CCT TGG AGC AAG
ZRF1bSANT-R	GGC CTC GAG GGC TGT GGG TTT CTT GG
ZRF1bUBD-F	GGC GAA TTC AGA AGA ATA TTT GAC TCT ACA GAT
ZRF1bUBD-R	GGC CTC GAG TTT CTG TAT TCT TAT GTC TTT TTT A
ZRF1b△UBD-R	GGC GAA TTC TTT TGT TGA GTC CAT CAA AAC C
Name	Sequences 5'-3' (Q-PCR)
actin-F	AAGTCATAACCATCGGAGCTG
actin-R	ACCAGATAAGACAAGACACAC
EXP-Q1	GAGCTGAAGTGGCTTCCATGA
EXP-Q2	GGATCATGGGTATGTCGGACC
PP2AA3-Q1	TAACGTGGCCAAAATGATGC
PP2AA3-Q2	GTTCTCCACAACCGCTTGGT
Tip4.1-Q1	GTGAAAACTGTTGGAGAGAAGCAA
Tip4.1-Q2	TCAACTGGATACCCTTTCGCA
ZRF1a-Q1	CCTCTCGTGGCTCAGCGTCT
ZRF1a-Q2	GTCCTTCTTTGTTTCCCATTTT
ZRF1b-Q1	AAAGGCGAAAAGAAGAAGAAGC
ZRF1b-Q2	GAACAGGGGCGGAGAGAACT
RING1a1283Q1	ATCTCTGTTGCCGACCCACT
RING1a1406Q2	GCCGCATCTTCTCCTACTCT
RING1b789Q1	TGAGAGGCAACGAAAAAAGC
RING1b928Q2	AGTTCCACACAAGCACAGGT
DRIP1-Q1	GGTCCCGTTTGGTTCTCACT
DRIP1-Q2	TGTATTTCCATCCCTTATTCTC

-

DRIP2-Q1	AGTTGTGTCCTCCATCTCATT
DRIP2-Q2	GCTTTTGTTCTTTTTCCTGTT
BMI1c-Q1	AACTTCACTGCGGGTCTCTTCA
BMI1c-Q2	ACGGTCTCCCTATGTTTCTCCT
CDKA;1-Q1	ACTGGCCAGAGCATTCGGTATC
CDKA;1-Q2	TCGGTACCAGAGAGTAACAACCTC
CYCD3;1-Q1	CCAAACTAATCTCCTCGGTGTCC
CYCD3;1-Q2	TGATGATGAATCGTGACTCTTGCG
CYCB1;1-Q1	TCAGCAATGGAAGCAACAAG
CYCB1;1-Q2	AGCAGATTCAGTTCCGGTCA
RBR1-Q1	CGCTTCCATTTTGGTTTTGA
RBR1-Q2	TGAACAACAGCAGCAGCAAC
E2Fa-Q1	CGAAGCCTTAACTGTTGACAACC
E2Fa-Q2	GCATTTGAGAGAAGCCAGTAGTCC
E2Fb-Q1	CCGATGAAAGAGGAAAGCACCG
E2Fb-Q2	CGCCTACCTCTGATCGAAACC
E2FC-Q1	TGCCGTTATGACAGTTCTTTAGGG
E2FC-Q2	AGTGTTCCATCCTCAGCTTCCT
KRP2-Q1	TCGTCGGTTTCGTGTTGTTC
KRP2-Q2	CCTGCGGCGAGACTCTAC
IAA2-F	CGT TGG TTG GCC ACC AGT GA
IAA2-R	ACG CTT TGA GAA GCT CGG GGT
IAA14-F	CAG CTC CTT TAC CAT GGG GAG
IAA14-R	ACC AAC GAG CAT CCA GTC AC
IAA16-F	TGG GAT GGC CAC CGG TAC GA
IAA16-R	CAC GGT GGC ACA TGC GGA GG
IAA19-F	CGT GGC ATC GGT GTG GCC TT
IAA19-R	GCT GCA GCC CAA ACC CGG TA
IAA28-F	GCT CCT CCT TGT CAC CAA TTC ACT
IAA28-R	ACT GGA GCT ACC TCA ACC CTG TTA
IAA29-F	TGT GCG ATC GAG GGT GCT GC
IAA29-R	CGT CTT CCT CGT TGG GCT GGC
IAA30-F	GAG ACT CGG GCT CAG CTT CGG A
IAA30-R	CTC TGC CGC ACC GAC TCC AT
IAA34-F	GCA GCG ATC CTC CCC ATC CCT
IAA34-R	ACG CCA CCA AAC TCC GTG GTC
BES1-F	CGC CAG TTC CAT GCT CCG GC
BES1-R	GGT AGG CGA GGT TGG CAC CAT
LEC1-Q1	AAATCCATCTCTGAATTGAACTT
LEC1-Q2	CACGATACCATTGTTCTTGT
LEC2-Q1	TACGAGGACGAAAGCAAGAA
LEC2-Q2	CGTTAGGGATGGGATAGTGA
ABI3-Q1	ATGTATCTCCTCGAGAACAC
ABI3-Q2	CCCTCGTATCAAATATTTGCC
AG-Q1	ACGGAATTATTTCCAAGTCGC
AG-Q2	GCCTATATTACACTAACTGGAGAG
BBM-Q1	GGTGGTTATCAAGGATTCGC
BBM-Q2	TCTCAGCAGCAGTAAAGGGA
AGL15-Q1	CGAAAGGAACGATTGCTGAC

-

AGL15-Q2	GGATGGAACATAGTGGGTGAA
PIN1-Q1	GCAACAAAACGACGCAGGCT
PIN1-Q2	TGAAGGAAATGAGGGACCAG
PIN2-Q1	TAGGAGGACAAAACAAGGAG
PIN2-Q2	CGTGAGGAGGAATAGAAACT
PIN4-Q1	TGATAATGGTGTGGAGAAAGC
PIN4-Q2	TCTGAGAGTATGGAGATGGAT
PIN7-Q1	GGAAACTCATAAGAAACCCA
PIN7-Q2	CATCCCACCTGAAAGCAACA
LHP1-Q1	GAGGAAGTCTGGTTCTGTGA
LHP1-Q2	TCTGTAGGTGCTGTGTGGTT
WOX2-Q1	CGCCAAAAGCAGAAACAGGA
WOX2-Q2	TTGAGCAAGGAGGGGGGTAG
WOX5-Q1	CCAAGGTGGACAAAATGAGAG
WOX5-Q2	ATGATGAGTATGGAGAAAACG
WOX8-Q1	GGTGGTAACGGAAGAAGGGA
WOX8-Q2	TAATGGAACAGTCAAAGGAG
CUC1-Q1	ACATTCCTTCCCGCTCCACC
CUC1-Q2	AACTGACCAAACGCCACGCC
CUC2-Q1	GAGCAACTGTGAGCGTAAGC
CUC2-Q2	GGAGTGAGACGGAGGAAGGA
CUC3-Q1	GGAACAACAACAACGACGAAG
CUC3-Q2	AGACGAAAAACCCAACAGACC
SERK1-Q1	GGAAGAGCGAACTCCAGGTG
SERK1-Q2	GGTCGGTGTCATACAGAAAC
SERK2-Q1	TTTAGCGGAGAAATGGGACG
SERK2-Q2	CAGAGGTGGGGTGAGAAGAG
WUS-Q1	CAGTTCGGAAAGATTGAGGG
WUS-Q2	GGTGATGAAGATGGTGTGGT
CRC-Q1	TGGCGTTCTCCAGGGTAAT
CRC-Q2	TGACCACTTGGATCCTTCCT
DOG1-Q1	TAGGCTCGTTTATGCTTTGTGTGG
DOG1-Q2	CGCACTTAAGTCGCTAAGTGATGC
AIL5-Q1	CTCCATGTACAGAGGCGTCA
AIL5-Q2	GCAGCTTCCTCTTGAGTGCTA
CRA1-Q1	CCGTGGATCTATCCGTCAAA
CRA1-Q2	CAAACACTCTGTTACCATTGTCG
PER1-Q1	CATATTGTTGGTCCTGACAGTAAGA
PER1-Q2	GGCGATCTTGTTATTGTGCTT
FLC-Q1	TGTGGATAGCAAGCTTGTGG
FLC-Q2	TAGTCACGGAGAGGGCAGTC
FLM-F	GGAAAGAATACGTTGCTGGCAACA
FLM-R	CCGTTGATGATGGTGGCTAATTGA
MAF2-F	GGCTCCGGAAAACTCTACAA
MAF2-R	TTCTGCAAGATCTAAGGCTTCA
MAF4-Q1	ATGGGAAGAAGAAAAGTAGAG
MAF4-Q2	AGAGATGATGATAAGAGCGAC
MAF5-Q1	ATTTTGGAAACAGGGGATGA
MAF5-Q2	TTACTTGAGAAGCGGGAGAG

-

SOC1-F	CGAGAAGCTCTCTGAAAAGTGG
SOC1-R	TCAGAACTTGGGCTACTCTCTTC
FT-F	GGTGGAGAAGACCTCAGGAA
FT-R	GGTTGCTAGGACTTGGAACATC
AGL24-F	AGCCGTGTGTCTGAAAAGAAG
AGL24-R	AATTCCGATCCCCGTTTCT
SVP-F	GGACAAGAGCCACCGACTAA
SVP-R	TGCTGAAGCTCTTCAATGTCA
STM-Q1	GCAACACATCCTCACCATTACTTCA
STM-Q2	ATCAAAGCATGGTGGAGGAGA
BP-Q1	TCCCATTCACATCCTCAACA
BP-Q2	CCCCTCCGCTGTTATTCTCT
KNAT2-Q1	AAACGCCATTGGAAGCCT
KNAT2-Q2	ACAATGCACAATTTCATGTCTCTCT
KNAT6-Q1	CCAAGAGAAGCAAGACAAGCTC
KNAT6-Q2	CAGCTAATGCTATCTTATCTCCTTCAG
LFY-F	TTGATGCTCTCTCCCAAGAAG
LFY-R	TTGACCTGCGTCCCAGTAA
AP1-F	CCATCTCCTTTTCTCAACATGG
AP1-R	CGGGTTCAAGAGTCAGTTCG
PI-F	AACATGGCCTCGACAAAGTC
PI-R	CGCCATCATCTTCTCATTTCT
SEP3-F	CAACAACAACACTCCCAAGC
SEP3-R	TTGTTGCCCCTGATACCC
CAL-F	TCAGACTTCTCCTTTCCTAAATATGG
CAL-R	TCCAGATTGTTCCTCCTCATC
GIK-F	CGGAGGTAACGTAGTTGGTGA
GIK-R	TGTAAAAGACGCTGCCATGA
ULT1-F	TCAGATTTCCCATACGACAAGAT
ULT1-R	TGTGCACCCTCTGTACACCT
STK-F	GGGTGAAGCAAATTCTCAGG
STK-R	CGATTTGTTGAGTTCTCTATCCTCT
UFO-F	TCAGCCGCTCTACACACAGT
UFO-R	CCGACACACTCGAATCCTTT
Name	Sequences 5'-3' (Gateway Clone)
ZRF1a-1658F	GGGGACAAGTTTGTACAAAAAAGCAGGCTCCCAAGAT GGGCACAAGAAG ACA GAA CAC
ZRF1a-F	GGGGACAAGTTTGTACAAAAAAGCAGGCTCCATGCCG AGC CGG AGA AGTGAGTC
ZRF1a-R	GGGGACCACTTTGTACAAGAAAGCTGGGTTTACTCCGG TTTTCTTGTTTCT AAT GAT TTC
ZRF1b-1403F	GGGGACAAGTTTGTACAAAAAAGCAGGCTCCTGAGCA CAGAAAACGGAA ACA GTA AGGAG
ZRF1b-F	GGGGACAAGTTTGTACAAAAAAGCAGGCTCCATGCAG

-

	AGTTGGGGAATTAAC TCT GCT AT
Name	Sequences 5'-3' (ChIP-QPCR)
qChABI3-1F	GTTTAAGAACCACCGCTTGG
qChABI3-1R	CTC CTC GTG CCG CTA GTA TC
qChABI3-2F	TCGGATCTTTTCATATGCTTTG
qChABI3-2R	GAGATTCAAAAAGAACTCTTGATAAGG
qChABI3-3F	CAAAGAAGACGCACCACCA
qChABI3-3R	TGGATCTTGTTGGAATGATTGT
qChABI3-4F	GCTGGCTCAGCTTCTGCTAT
qChABI3-4R	AAAGATGATTGTGCATGTCTACCT
qChABI3-5F	CAACCGAGCGGACAAAAG
qChABI3-5R	TGTTCCTTTGCGACTTGTTTT
qChDOG1-1F	TGGAACAACAACTCGCACTC
qChDOG1-1R	GTG CTT TCC GAG CAA ATA AAA
qChDOG1-2F	TCTCGAGTGGATGAGTTTGC
qChDOG1-2R	TCTTCATCACCGTGAGAT CG
ChDOG1-3F	AACATCGACGGCTACGAATC
qChDOG1-3R	GCACCGTACTGACTACCGAAC
ChDOG1-4F	TCAAGCTCTCGACAAGCAAG
qChDOG1-4R	AGAAATCCGCTCCTTGTACC
ChDOG1-5F	TCACGTCGTGGCATTTTG
qChDOG1-5R	TCG AGA CGA GAT CAT GTT GC
qChCRC-F1	GCTCTGCCCACTGGATCTAC
qChCRC-R1	CGAGAAGAGCGATGATGACA
qChCRC-F2	TCAGCAGCTTCAGAACCAAC
qChCRC-R2	TGGAAAGGTCCCTTAACACG
qChAIL5-F1	CTACAGCCACCGCTTCATC
qChAIL5-R1	GCTAGCGGCTATTGACTTGAG
qChAIL5-F2	CTAACCACACCGTCCCTCAC
qChAIL5-R2	GTAAAAAGTTCCTCCATGGTCATT
qChFT-F1	CCA AGA GTT GAG ATT GGT GGA
qChFT-R1	CAT TTT TAA CCA AGG TCT
qChFT-F2	GAT CTA CAA TCT CGG CCT TCC
qChFT-R2	ATC ATC ACC GTT CGT TAC TCG
qChFLC-F1	ATT TAG CAA CGA AAG TGA AAA CTA AG
qChFLC-R1	GCC ACG TGT ACC GCA TGA C
qChFLC-F2	AGA AAT CAA GCG AAT TGA GAA CAA
qChFLC-R2	CGT TGC GAC GTT TGG AGA A
qChFLC-F3	AAT TGC ATG TCA TTC ACG ATT TG
qChFLC-R3	TGA AAC TTC ACT CAA CAA CAT CGA
qChFLC-F4	CAT CTC TCC AGC CTG GTC AAG
qChFLC-R4	GGC TTT AAG ATC ATC AGC ATG CT
qChFLC-F5	AGC CAG GTA ACG AAA GCT ACA TTT
qChFLC-R5	ACA TGG ACA TTG GAC ACA CAA CA
qChMAF4-F1	GAC CAA CGC GCC ACA AG
qChMAF4-R1	CGG TGC GTT TTT AAT AGG AGT TTA G
qChMAF4-F2	CCG AAT TGA GAC CTT GTA GAA GTA GA

-

qChMAF4-R2	ATC AAG CAT TTG TGG TGT TAA GTA TGA
qChMAF4-F3	GTT GTT TTC CTT TTC TGT TGT TTA TCT A
qChMAF4-R3	ATA CTT ACA TTA TCG CTT TTC GCT TCT
qChMAF4-F4	GCG GAA AGC CGG TAA AAG AC
qChMAF4-R4	CGA ATC TGG GCT TAA CAG TAA CAG T
qChSOC1-F1	CTT TCT TTC TTC TTC TCC CTC CAG T
qChSOC1-R1	CCT AAC CAG GAG GAA GCT TTC G
qChSOC1-F2	GCA TCC TTC AAT TAA ACC GAT AAC
qChSOC1-R2	AAG TCA ACG AAA GAT TAA GTA CCC
qChFT-F1	CCA AGA GTT GAG ATT GGT GGA
qChFT-R1	CAT TTT TAA CCA AGG TCT
qChFT-F2	GAT CTA CAA TCT CGG CCT TCC
qChFT-R2	ATC ATC ACC GTT CGT TAC TCG

V.2. Methods

V.2.1 Plant methods

V.2.1.1 Crossing *Arabidopsis* plants

Mother plants are chosen at a stage when they have developed 5-6 inflorescences (they have the largest buds). A bud, at the correct stage, should contain short immature stamens with anthers that are greenish-yellow in color and should not have opened and potentially exposed its pistil to parental pollen. Father plants should have have started to form siliques (this indicates that the pollen is o.k.).

The steps are as follows:

1. From the inflorescence of the mother plant, remove mature siliques as well as open flowers and buds that have already a white tip, with fine scissors or forceps.
2. Remove the meristem with those buds that are too small: usually 3-5 flower buds have the right size and should remain.
3. Open one flower bud by inserting the tip of one pair of forceps between petals and sepals. And remove all immature anthers with the other pair of forceps.
4. Repeat this for all remaining buds of the inflorescence.
5. Mark the emasculated inflorescence with a piece of thread around its stem.
6. Let the plant grow for 2-3 days.
7. The stigmas have by now developed a rough, sticky surface. Take an open, mature flower (but not yet yellow) from the father plant with one pair of forceps and bring it under the binocular. With the other forceps, take hold of the filament of an anther with visible pollen shedding. Tap the anther on the stigma and cover it with pollen

grains as much as possible. Repeat for all stigmas. Take a second male flower if necessary.

8. Mark the pollinated inflorescence with a colored thread and document the cross (mother, father, date, color code, number of pollinated flowers).

9. Depending on the growth conditions, siliques with the hybrid seeds will be mature after 15-25 days. They are harvested by cutting them into a paper bag when the siliques are a little yellow, but prior to opening. They should be kept for a couple of days at room temperature for further maturation.

V.2.1.2 Seed germination tests

Dispose around 100 seeds in a 2 ml tube (eppendorf), add 1.5 ml 70% ethanol and shake or vortex for 5-8 min (be sure not to wipe off the label with the ethanol). Pipet off ethanol, add 1.5 ml 96% ethanol and shake or vortex for 5-8 min. Use 1 ml tip to transfer seeds to sterilized filter paper, and then wait for seeds to dry completely. Sow the seeds carefully on petri dishes containing the growth media: Murashige and Skoog (MS) salts, 0.8% agar with or without addition of 100 mM NaCl or 200 mM mannitol. To synchronize germination, stratify the seeds after sowing for 3 days at 4^{o}C and subsequently transfer to a growth chamber (22^{o}C, photoperiod 16 h light, 8 h dark). Score germination rates daily for 12 days following stratification. Seeds are considered to have germinated when radicle emergence is visible under a dissecting microscope.

V.2.1.3 *Arabidopsis* transformation using the floral dip method

Grow healthy *Arabidopsis* plants until they are flowering. Clip first bolts to encourage proliferation of many secondary bolts. Plants will be ready roughly 4-6 days after clipping. Optimal plants have many immature flower clusters and not many fertilized siliques, although a range of plant stages can be successfully transformed. Prepare an *Agrobacterium tumefaciens* strain carrying gene of interest on a binary vector. A single colony is inoculated in 3 ml LB with antibiotics and incubated at 28°C overnight. This 3 ml overnight culture is then diluted in 300 ml LB supplemented with the same antibiotics and incubated at 28^{o}C for 16-24 hours. The bacterial cells are harvested by centrifugation at 5000 rpm for 10 min. Spin down *Agrobacterium*, resuspend to OD_{600} = 0.8 (can be higher or lower) in 5% Sucrose solution (if made fresh, no need to autoclave). You will need 100-200 ml for each two

-

or three small pots to be dipped. Before dipping, add Silwet L-77 to a concentration of 0.05% (500 ul/L) and mix well. Dip above-ground parts of plant in *Agrobacterium* solution for 1 min, with gentle agitation. You should then see a film of liquid coating the plant. Some investigators dip the inflorescence only, while others also dip the rosette to hit the shorter axillary inflorescences. Place dipped plants under a dome or cover for 16 to 24 hours to maintain high humidity (plants can be laid on their side if necessary). Do not expose to excessive sunlight (air under dome can get hot). Water and grow plants normally, tying up loose bolts with wax paper, tape, stakes, twist-ties, or other means. Stop watering as seeds become mature.

V.2.1.4 Transient expression using tobacco leaf infiltration

Inoculate one single colony of *Agrobacterium* (GV3103) in 5 ml LB with appropriate antibiotics. Grow overnight at 28-30°C. Using 1 ml of the overnight culture to inoculate 25 ml LB (with same antibiotics, plus 20 μM acetosyringone added after autoclaving and immediately before use) and grow overnight. Measure the OD_{600} of overnight culture. Pellet the bacteria (5000 x g, 15 min) and resuspend the pellet in Resuspension Solution. The final OD_{600} should be adjusted to 0.4. Leave on the bench (room temperature) for 2-3 hours (or overnight) before infiltration. Perform the infiltration with 5 ml syringe. Simply press the syringe (no needle) on the underside of the leaf (avoid cotyledons!), and exert a counter-pressure with finger on the other side. Successful infiltration is often observed as a spreading “wetting” area in the leaf. 2-5 days after infiltration, observe the fluorescence labeled protein under a fluorescence microscope or confocal laser scanning microscope. Or harvest leaves for protein purification.

Resuspension solution: 10 mM $MgCl_2$; 10 mM MES-KpH 5.6 (First make 0.5 M MES, adjust pH with KOH to 5.6); Autoclave 15 min. 100 μM acetosyringone, added after autoclaving and immediately before using.

V.2.2 Nucleic acid techniques

V.2.2.1 Genotyping

Seeds (F1) from crosses were collected from individual siliques on the parent plants and these seeds were then grown and self-pollinated to obtain the F2 generation. These F2 or later generation plants were genotyped by PCR. For the PCR reaction, at

-

first, collect leaves for PCR sample and place them in 96-well plastic plate. Then add 200 μL Extraction Buffer to the tube. Crush leaf with plastic rod against the tube wall. The solution turns transparent green, and visible tissue residue is left in the solution. If you want to remove tissue residue, centrifuge tube at 14,000 rpm for 5 min and recover supernatant. This solution is stable at -20°C for several months with or without tissue residue. Add 1 μL of this solution to a total volume of 20 μL of the PCR reaction.

Extraction Buffer: 200 mM Tris-HCl (pH 7.5), 250 mM NaCl, 25 mM EDTA, and 0.5% SDS; dilute 10-fold with TE Buffer to obtain Extraction Buffer
TE Buffer: 10 mM Tris-HCl (pH 8) and 1 mM EDTA

V.2.2.2 Gateway cloning

The Gateway cloning technology is a universal system for cloning and subcloning DNA sequences, facilitating gene functional analysis, and protein expression. In this operating system, DNA segments are transferred between vectors using site-specific recombination.

This technology contains two reactions: the BP reaction and the LR reaction. The BP reaction is a recombination reaction between an expression clone (and an attB-flanked PCR product) and a donor (pDONR™) vector to create an entry clone. The LR reaction is a recombination reaction between an entry clone and a destination vector, mediated by a cocktail of recombination proteins, to create an expression clone. It is used to move the sequence of interest to one or more destination vectors in parallel reactions.

BP reaction: Amplify PCR products containing the *attB* site and purify them. Then in 1.5 ml tubes at room temperature add 40-100 fmol PCR product (a 1-kb PCR product is ~0.65 ng/fmol), ~150 ng donor vector (pDONR207) and TE or water to a final volume of 8 μl. Remove BP clonase TM II Enzyme Mix and thaw on ice (~2 min). Vortex briefly (2 s) twice and add 2 μl of BP clonase enzyme mix to BP reaction. Mix well by vortexing briefly twice. After that, reactions are incubated at 25°C for 60 min or overnight. Finally, add 1 μl of proteinase K solution and incubate for 10 min at 37°C to stop the reaction.

LR reaction: In 1.5-ml tubes at room temperature add ~150 ng entry clone, ~150 ng destination vector and TE or water to a final volume of 8 μl. Remove LR

clonase TM II Enzyme Mix and thaw on ice (~2 min). Vortex briefly (2 s) twice and add 2 µl of LR clonase enzyme mix to the LR reaction. Mix well by vortexing briefly twice. After that reactions are incubated at 25°C for 60 min or overnight. Finally, add 1 µl of proteinase K solution and incubate for 10 min at 37°C to stop the reaction.

V.2.2.3 RNA isolation

15-days-old *in vitro*-grown seedlings or soil-grown other young tissues (100-200 mg) were inserted into an eppendorf tube containing glass beads (diameter 1 mm) and frozen in liquid nitrogen. Samples were ground using the Silama S5 apparatus (Ivoclar, Vivadent). Total RNA was extracted by using the Nucleospin RNA kit (Macherey-Nagel) according to the manufacturer's instructions. RNA concentration was evaluated by measuring the absorbance at 260 nm (1 unit of OD_{260}= 40 µg/ml of RNA) using Nanodrop 2000.

V.2.2.4 Reverse transcription

In a 200 µl PCR tube, 11 µl of RNA (≦5 µg total RNA) with 5 µl of Rxn buffer (Promega) and 5 µl $MgCl_2$ (25 mM) were treated with 1 µl of RQ1 Dnase (Promega) at 37°C for 10 min and 65°C for 10 min to inactivate Dnase. 1 µl of oligo dT (100 mM) was added to the reaction. The reaction was incubated at 70°C for 5 min, after that it was put on ice immediately for 5 min. 2.5 µl of dNTPs (10 mM) and 1µl of ImProm-II Reverse Transcriptase (Promega) were added into the mixture. The reaction mixture was incubated at 42°C for 70 min, followed by heat inactivation at 70°C for 15 min. The synthesized cDNA was used as template for quantitative PCR.

V.2.2.5 Quantitative PCR

Quantitative PCR is a method used to detect relative or absolute gene expression levels. It was performed in 384-wells optical plates on a light cycler 480 Ⅱ (Roche) apparatus, according to the manufacturer's instructions. Each PCR reaction total volume was scaled to 10 µl. At first, pipette 2µl of primer mix (containing 2.5 mM forward and reverse gene specific primers) into each well. Then add 8 µl of PCR master mix (Roche) containing 5 µl of 480 SYBER Green Ⅰ fluorescent reporter, 2 µl water and 1 µl template into each well. For each sample, PCR was performed in triplicate using fixed amounts of cDNA template and *PP2A*, *EXP* and *Tip4.1* which were used as internal reference genes. The PCR was carried out using the following

conditions: pre-heating at 95°C for 10 min, followed by 40 cycles of 15 sec at 95°C, 30 sec at 60°C and 15 sec at 72°C. Melting curves of PCR reactions were checked to ensure the quality of the PCR reaction and to avoid any DNA contamination. The threshold cycle value (CT) was set so that the fluorescent signal was above the baseline noise but as low as possible in the exponential amplification phase.

V.2.3 Microarrays

6-days-old wild type and *Atzrf1a-1 Atzrf1b-1*, *Atzrf1a-2 Atzrf1b-1* homozygous mutants seedlings were harvested. Three independently derived sets of 6-days-old seedlings (30 to 40 plants per set) were pooled for each genotype. Total RNA was isolated from each sample and used for hybridization on Agilent microarray slides. The microarray analysis was performed using Affymetrix Gene-Chips by Biochip Company (Shanghai, China). Data analysis was performed using GeneSpring 5 software (Silicon Genetics, Redwood City, CA). Genes were considered significantly mis-expressed in a mutant when the change in expression was at least 2-fold compared to the wild type control and the P-values inferior to 0.05 in the three independent biological replicates.

V.2.4 Histochemical staining

For histochemical GUS activity assays, *Arabidopsis* seedlings were fixed for 30 min in ice-cold 90% acetone, then washed in 50 mM sodium phosphate buffer (pH7.2) for 15 min at room temperature and subsequently incubated for various periods (30 min to overnight) at 37°C in GUS staining solution (0.1 M sodium phosphate buffer pH7.2, 0.5 mM $Fe(CN)_2$, 0.5 mM $Fe(CN)_3$, 0.1% Tween-20 and 2 mM 5-bromo-4-choro-3-indolyl-3β-d-glucuronide). The length of the incubation period depends on the activity of each reporter gene construct. Seedlings were cleared in 70% ethanol overnight at 4°C.

V.2.5 Protein techniques

V.2.5.1 Nuclear protein extraction

Grow *Arabidopsis* seeds on MS for 2 weeks or on soil for 4 weeks. Collect approximately 5 g of *Arabidopsis* tissues, freeze in liquid nitrogen, and then follow the steps listed below. Note: always keep the sample on ice.

-

1. Grind the tissues to a fine powder in liquid nitrogen (3-5 ml materials) using a cold mortar and pestle. Collect the powder into a 50 mL Falcon tube.
2. Add 20 mL cold Lysis buffer into the powder, vortex and place on a rotation wheel for 30 min at 4°C.
3. Filter the solution through a 100 µm nylon mesh.
4. Centrifuge the filtered homogenate at 4000 x g at 4°C for 20 min to pellet the nuclei.
5. Discard the supernatant and add 2 mL Lysis buffer to the pellet. Re-suspend the nuclei by pipetting and transfer to a 2 ml tube.
6. Centrifuge the sample at 4000 x g at 4°C for 20 min.
7. Discard the supernatant and add 150 to 400 µl (depending on the starting powder quantity) 1xSDS loading buffer to the pellet and vortex.
8. Incubate at 95°C, 10 min.
9. Centrifuge 5 min at 12000 rpm at room temperature.
10. Remove the supernatant to a new tube. Use 10 µl to load for western blot.
Material can be stored at -20°C for no more than 2-3 weeks.
11. Test with corresponding antibody and/or @ H3 to adjust quantities between samples.

Low salt wash buffer (200 ml): 20 ml 0.5 M HEPES pH 7.5 + 6 ml 5 M NaCl + 400 µl 500 mM EDTA (keep at 4°C)
Lysis Buffer (50 ml): 45 ml Low salt wash buffer + 500 µl Triton X-100 + 5 ml glycerol + 50 µl 100 mM PMSF + 20 µl β-mercaptoethanol (on ice) (freshly prepared)
PMSF should be kept at RT for 5-10 min and added last!

V.2.5.2 Protein quantification

Three times 10 µL of each sample are pipetted in three tubes. 90 µL of water and 500 µL Amidoblack staining solution are added and well mixed before 10 min centrifugation at full speed. The supernatant is removed, and the pellet is washed with 750 µL washing buffer by inverting and following centrifugation 10 min at full speed. Washed amidoblack pellets are let dry under the hood for 30 min.
Dried pellets are resuspended in 250 µL NaOH 0.2 M and 200 µL of this solution are transferred to an ELISA plate for measurement of extinction at 595 nm (Microplate-reader Model 680, BioRad).

-

Staining solution: 10% acetic acid (v/v); 90% methanol (v/v); 0.05% Amidoblack (w/v)
Washing solution: 10% acetic acid (v/v); 90% ethanol (v/v)

V.2.5.3 SDS (Sodium dodecylsulfate) gel electrophoresis

Protein samples are loaded directly after heating in 1x SDS loading buffer at 95℃ for 5-10 min or after storage at -20 °C (in this latter case, samples are warmed up 5 min at 65 °C before loading because of SDS buffer). Gel is run in 1xSDS electrophoresis buffer at 100 V to allow the samples to separate. To visualize the proteins, the gel is incubated under shaking in a Coomassie solution for 20 minutes at RT. Remove Coomassie solution and incubate under shaking in destaining solution for 30 minutes (adapt to intensity of the staining). Finally, incubate the gel overnight in distilled water with glycerol (~500 µL for 150 mL H_2O). Dry the gel if necessary. Scan.

Resolving gel: 10-15% Acrylamide/Bis-acrylamide (29:1); 375 mM Tris-HCl pH8.8; 0.1% SDS; 0.1% AP; 0.4 µl/ml TEMED
Stacking gel: 5% Acrylamide/Bis-acrylamide (29:1); 125 mM Tris-HCl pH6.8; 0.1% SDS; 0.1% AP; 1 µl/ml TEMED
1X SDS running buffer: 25 mM Tris; 250 mM glycine; 0.1% SDS
1X SDS loading buffer: 50 mM Tris-HCl pH6.8; 100 mM DTT; 2% SDS; 0.1% bromophenol blue; 10% glycerol
Coomassie blue solution: 40% methanol; 10% acetic acid 50% water; 0.1% (w/v) Coomassie brilliant blue R250
Coomassie destaining solution (1L): 400 mL Ethanol 100%; 100 mL Acetic Acid; 500 mL H2O

V.2.5.4 Western blot

After protein samples are separated by 10%-15% SDS-PAGE, the gel is equilibrated in transfer buffer for at least 10 min before transfer. Immobilon-P PVDF transfer membrane (Millipore) is pre-wetted by 100% methanol, rinsed in water for 5 min and equilibrated in transfer buffer for at least 10 min before use. Then proteins

-

are transferred onto the immobilon-P PVDF membrane in the transfer buffer at 300 mA for 2 hours at 4°C. The membrane is subsequently washed in 1xTTBS for 5 min, blocked in 5% non-fat milk in TTBS for 1 hour, and incubated in diluted primary antibody (1:500-1:5000) at 4°C overnight. After washing 3 times with the milk-TTBS, the membrane is incubated in the diluted secondary antibody (1:5000-1:10000) for 1 hour at room temperature. Then the membrane is washed once with milk-TTBS, 3 times with TTBS, and each time for 10 min. Finally the membrane is detected using the ECL western blot detection kit (Amersham Biosciences).

Transfer buffer: 25 mM Tris; 192 mM glycine; 15% methanol
TBS buffer: 20 mM Tris-HCl pH7.4; 150 mM NaCl
TTBS buffer: TBS buffer plus 0.1% Triton X-100

V.2.5.5 Recombinant protein expression in *E. coli*

Complete ORFs of target genes were subcloned into an appropriate expression vector. All constructs were introduced into *E. coli* Rosetta (DE3) strain. The next day, the bacteria on the plate are transferred to liquid LB medium for an overnight culture. The overnight culture is transferred into auto-induction medium at a dilution 1: 300, incubated for 3 hours at 37°C, then the temperature is changed to 25°C and the culture is incubated overnight. Cells are harvested and resuspended in 1xSDS loading buffer. Protein expression is detected by SDS-PAGE.

Auto-induction medium (1 L): Tryptone 10 g; yeast extract 5 g; 50 X M 40 ml; 50 X 5052 40 ml; 1 M $MgSO_4$ 2 ml; adjust pH to 7.2
50 X M: 1.25M Na_2HPO_4; 1.25M KH_2PO_4; 2.5M NH_4Cl; 0.25M Na_2SO_4
50 X 5052: 25% glycerol; 2.5% glucose; 10% alpha-lactose monohydrate

V.2.5.6 GST fusion protein purification

GST-fusion protein purification was carried out by harvesting and resuspending the cell in 20 ml of ice-cold GST lysis buffer plus 100 μg/ml lysozyme and protease inhibitor cocktail (Roche). After disrupting the cells by sonification, the cell lysate was centrifuged at 13200 rpm for 20 min at 4°C. Then the supernatant was mixed with settled glutathione-Sepharose-4B beads (Amersham Bioscences), which was pre-washed 3 times with water and 3 times with 1x PBS. The suspension was

-

then incubated on a rotation wheel for 2 hours or overnight at 4°C. Beads are spinned down, washed once in 1x PBS plus 0.1% Triton X-100 and 3 times in 1x PBS plus 10% glycerol. Finally, 1x PBS plus 10% glycerol was added to make 10% slurry. Proteins fixed to the beads were determined by SDS-PAGE.

PBS: 140 mM NaCl; 2.7 mM KCl; 10 mM Na_2HPO_4; 1.8 mM KH_2PO_4; pH7.4
GST lysis buffer: 1X PBS; 0.1% Triton X-100; 1 mM DTT; 10% glycerol

V.2.5.7 GST pull-down assay

15-day-old stably transformed *Arabidopsis* seedlings were harvested. After grinding in liquid nitrogen, 5 g fine powder was homogenized in 30 ml pull-down buffer plus protease inhibitor cocktail (Roche). Dnase Ⅰ (Roche) was added to 10 μg/ml as a final concentration to release the chromatin proteins. The whole cell lysate was centrifuged at 20000 g for 20 min at 4°C. The supernatant was collected and mixed with GST or GST fusion proteins. After rotating for 2 hours or overnight at 4°C on a wheel, the beads were washed four times with pull-down buffer. After washing, specifically bound proteins were eluted from the beads by pull-down buffer containing 1 M NaCl and then precipitated by 10% TCA. A quarter of each pull-down fraction was analyzed by SDS-PAGE and western blot using relative polyclone antibody.

Pull-down buffer: 20 mM Tris-Cl (pH 8.0); 200 mM NaCl; 1 mM EDTA (pH 8.0); 0.5% Nonidet P-40; 25 μg/mL PMSF

V.2.5.8 Fluorescence lifetime imaging (FLIM) assay

The *AtZRF1b*, *AtRING1a*, *AtBMI1a*, *AtBMI1b* and *AtBMI1c* cDNAs were PCR-amplified and introduced into the Gateway system and cloned as 39 or 59 in-frame fusions to RFP or GFP sequences in plant expression vectors downstream of the 35S promoter (pB7WGF2; pB7FWG2; pH7WGR2; pH7RWG2; http:// gateway. psb.ugent.be/). Plasmids were introduced into *A. tumefaciens* (GV3101). Bacterial cultures grown overnight were centrifuged and pellets resuspended in 10 mM $MgCl_2$ to an optical density of 0.5 at 600 nm and incubated 2-3 h at RT. Leaves of 2–3 week old *Nicotiana benthamiana* plants were co-infiltrated with an equimolar bacterial suspension of the two constructs to be tested. Confocal laser scanning images of

protein co-localization and FLIM data were recorded 2 days post-infiltration (LSM-700, Carl Zeiss; LIFA frequency domain fluorescence lifetime imaging system, Lambert Instruments). The percentage of GFP fluorescence lifetime decay was calculated relative to the absence of RFP fusion protein as an average of 3 biological replicates, each recording over 30 nuclei. Proteins were considered to interact if the presence of RFP-tagged proteins decreased GFP fluorescence lifetime by more than 5%, a reference value established according to the negative control: RFP with GFP.

V.2.6 Chromatin immunoprepitation (ChIP)

Day 1: *Arabidopsis* two weeks old seedlings were harvested in 100 ml fixation buffer. Following vacuum infiltration for 10 min for cross-linking, the fix buffer should boil (too much cross-linking may mask epitope while too little cross-linking leads to incomplete fixation). Subsequently 5 ml freshly prepared 2.5 M glycine were added per 100 ml fix buffer and infiltration in vacuum was continued for a further 5 min to stop crosslinking. Seedlings were rinsed with MilliQ water 5 times and as much as possible water was removed (seedlings after fixation should be transparent and dark-green. They should sink to the bottom of beaker after merged into water). The dried seedlings were subsequently ground in liquid nitrogen to a fine powder and kept at -80°C (remember DO NOT over-grind! Grinding should be done only twice per material, which means the powder may not be very fine).

Day 2: To 5 ml power of each sample 30 ml of ChIP lysis buffer was added and the mixture was incubated on a rotation wheel for 40 min at 4°C. Then it was filtered through 100 µm nylon mesh and centrifuged for 20 min at 4000 rpm at 4°C. After removing the supernatant, the pellet may appear grey; otherwise the pellet was resuspended again in ChIP lysis buffer and centrifuged again. The pellet was then resuspended in 700 µl of ChIP lysis buffer and the solution was transferred to a new 1.5 ml tube. The solution was centrifuged 20 min at 4000 rpm at 4°C. As much as possible of the supernatant was removed and the pellet was resuspended in 180 µl lysis buffer plus 0.8% SDS (the final SDS concentration should be between 0.5% and 1%. The more SDS added, the smaller the DNA fragment would be after sonication). Chromatin in ice water was sonicated four times with a Bioruptor (Diagenode), for every cycle work 30 sec and pulse 30 sec for 5 min. The chromatin sample was then centrifuged for 10 min at 13000 rpm at 4°C and the supernatant was transferred to a new tube (chromatin can be frozen at -80°C at this point). To check the sonication

-

efficiency, 40 µl of solution was taken and 360 µl ChIP elution buffer and 16 µl of 5 M NaCl were added and incubated at 65°C least 6 hour or overnight. DNA was recovered by adding equal volume of phenol:chloroform and precipitated following addition of 1/10 volume of 3 M sodium acetate pH5.2, 2 volumes of 100% ethanol and 1 µl of glycogen. After washing with 70% ethanol, the pellet was resuspended in 30 µl of water. Then 5 µl DNA was treated with 1 µl RNase and used for gel electrophoresis to control the quality of the sonication (DNA fragments should be 100-500 bp). Later, this DNA was used as an input for qPCR analysis.

If the sonication was correct, the chromatin solution was diluted with adequate ChIP lysis buffer to make the final volume enough for the following experiments (generally speaking, 100 µl chromatin should be taken for input and 200 µl for every sample). For every sample, combine 1.2 ml antibody binding buffer with 200 µl chromatin in one 1.5 ml tube. Add antibodies to each tube (from 1 to 3 µl depending on the antibody, but usually using 2 µl is fine) and incubate these tubes on a rotating mixer wheel overnight at 4°C. In parallel, chromatin without any antibody was used as a mock control.

Day 3: The chromatin antibody complex was collected by adding 20 µl slurry of magnetic Protein A beads (Millipore) for one reaction and incubated at 4°C for 1-3 hours under rotation. The beads were pelleted using a Magana GrIP racks (Millipore) and washed successively with 1 ml low salt wash buffer, and rotated at 4°C for 10 min. Then the supernatant was removed, the pellet was washed with 1 ml high salt wash buffer, and rotated at 4°C for 10 min. Then it was washed with 1 ml LiCl wash buffer, and rotated again at 4°C for 10 min. Finally it was washed with 1 ml TE buffer, and rotated at room temperature for 10 min. After the last wash, as much as poossible TE buffer was removed and immune complexes were eluted by adding 400 µl freshly prepared Elution buffer and incubation at 65°C for 30 min with agitation. The supernatant was transferred to another 1.5 ml EP tube. 300 µl Elution buffer were added to the prepared input. Then add 16 µl elution and input. Reverse protein-DNA cross-links at 65°C overnight.

Day 4: 6.4 µl 0.5 M EDTA pH8.0, 12.8 µl Tris-HCl pH8.0 and 2 µl 20mg/ml proteinaes K were added and incubated at 45°C for 1 hour. Recover DNA was recovered by NucleoSpin Gel and PCR Clean-up kit (Macherey-nagel). At first, mix 1 volume of sample with 5 volumes of Buffer NTB to adjust DNA binding condition.

-

Then place a NucleoSpin Gel and PCR Clean-up Column into a collection tube and load up to 700 µl sample, centrifuge for 30 s at 11000g. Discard flow-through and add 700 µl Buffer NT3 to the column. Centrifuge for 30 s at 11000 g, discard flow-through and centrifuge for 1 min at 11000 g to remove Buffer NT3 completely. At last, place the column into 1.5 ml tube and add 150 µl Buffer NE, incubating at room temperature for 1 min. Centrifuge for 1 min at 11000g. Fold-enrichment of each fragment was determined by quantitative real-time PCR. Genomic fragments of *ACTIN2* were amplified as internal controls for measurement of H3K27me3, H3K4me3 and H2AK119ub1 enrichment, respectively. Fold enrichment of each fragment was calculated first by normalizing the amount of a target DNA fragment against a genomic fragment of an internal control, and then by normalizing the value for immunoprecipitated samples against that for input.

Fix buffer: 0.4 M sucrose; 10 mM Tris-HCl pH8.0; 1 mM EDTA pH8.0; 1.0% Formaldehyde add PMSF before use
ChIP lysis buffer: 50 mM HEPES pH7.5; 1 mM EDTA pH8.0; 150 mM NaCl; 1% Triton X-100; 5 mM β-mercaptoethanol; 10% glycerol add cocktail before use
Antibody binding buffer: 50 mM Tris-HCl pH8.0; 1 mM EDTA pH8.0; 150 mM NaCl; 0.1% Triton X-100; 5 mM β-mercaptoethanol add cocktail before use
Low salt wash buffer: 50 mM HEPES pH7.5; 150 mM NaCl; 1 mM EDTA pH8.0
High salt wash buffer: 50 mM HEPES pH7.5; 500 mM NaCl; 1 mM EDTA pH8.0
LiCl wash buffer: 10 mM Tris-HCl pH8.0; 1 mM EDTA pH8.0; 0.5% NP-40; 0.25 M LiCl
TE buffer: 10 mM Tris-HCl pH8.0; 1 mM EDTA pH8.0
Elution buffer: 1% SDS; 0.1 M $NaHCO_3$

V.2.7 Microscopy

The Nikon E800 microscope was used for GUS staining observations. The LSM 700 Laser Scanning Microscopy (Carl Zeiss) was used for root cell observations. The images were processed with ZEN software (Carl Zeiss).

V.2.8 Propidium iodide staining

Seedlings were grown in 1/2MS agar plates vertically for 5 days. Roots were incubated in the dark for 10 min in 15 µM (10 µg/mL) propidium iodide (PI)

(Invitrogen). Then rinsed twice in water. Following transfer of the roots onto a microscopic slide, they were covered with a cover slip and observed under the LSM 700 microscope.

V.2.9 Flow cytometry

A small quantity of rosette leaves were roughly chopped (1-2 mm side pieces or strips) with a razor blade in nuclear extraction buffer (CyStain UV precise P kit, Partec). All preparations were subsequently filtered through 50 μm (pore diameter) nylon mesh and stained with nuclear staining solution (CyStain UV-precise P) containing 4, 6-diamidino-2-phenylindole (DAPI). Flow cytometry was performed on a Ploid Analysis PA-1 (Partec). Ploidy levels of three individual plants were averaged and doublets were excluded from the analysis by gating on single nuclei in a DAPI-width versus DAPI-area. A total of 5000 nuclei per sample were analyzed. Data were analyzed using Flowjo (TreeStar).

V.2.10 Bacterial techniques

V.2.10.1 Preparation of competent cells

Single colonies were picked from a plate freshly grown for 16-20 hours at 37°C and transferred into 5 ml of LB broth medium and incubated by shaking at 37°C overnight. Overnight culture was used to inoculate new LB (1: 100) and incubated at 37°C with vigorous shaking (300 cycles per minute). Monitor growth until OD_{600} reaches 0.4-0.6. Aseptically transfer the cells to sterile, disposable, ice-cold 50 mL Falcon tubes. Cool the cultures to 0°C by storing the tubes on ice for 10 minutes. Spin cells at 4000 rpm for 10 minutes at 4°C. Pour off supernatant and stand tubes upside down for 1 minute to drain remaining media. Resuspend each pellet in 10 ml of ice-cold 0.1 M $CaCl_2$ and store on ice. Spin cells at 4000 rpm for 10 minutes at 4°C. Pour off supernatant and stand tubes upside down for 1 minute to drain remaining media. Resuspend each pellet in 2 ml of ice-cold 0.1 M $CaCl_2$ and store on ice. Dispense in 100 ul aliquots, freeze in liquid nitrogen, and store in at 80°C.

In addition, we can prepare competent cells by electroporation. When the OD_{600} equals 0.4-0.6 (log phase growth), remove the cells from the shaker and place on ice. Split the culture into four equal parts by pouring ~250 ml of culture into each chilled 250 ml Corning pointed bottle. Centrifuge at 4000 rpm, 25 min at 4°C. Place bottles on ice. Remove supernatant immediately as cell pellet begins to lift off quickly.

-

Gently resuspend each pellet in 200 ml ice-cold dH_20. Centrifuge at 4000 rpm, 25 min at 4°C. Place bottles on ice. Remove supernatant. Gently resuspend each pellet in 100 ml of ice-cold dH_20. Centrifuge at 4000 rpm, 25 min at 4°C. Place bottles on ice. Remove supernatant. Gently resuspend each pellet in 20 ml ice-cold 10% glycerol. For each pair of 250 ml Corning bottles, transfer both 20 ml cell suspension into one chilled 50 ml conical tube. Therefore one should end up with two 50 ml conical tubes on ice where each tube contains ~40 ml of cells in 10% glycerol. Centrifuge at 4000 rpm, 10 min at 4°C. Place tubes on ice. Remove supernatant. Gently resuspend each cell pellet in 1 ml of ice-cold 10% glycerol. Finally prepare 70 µl aliquots of cells in pre-chilled 1.5 ml eppendorf tubes. Snap freeze tubes containing cells in liquid N2. Store frozen cells at -80°C.

V.2.10.2 Heat shock transformation

Add 1 µl of DNA or 5-20 µl DNA ligation products to 100 µl of competent cells. Mix contents by swirling gently. Store the tubes on ice for 30 minutes. Transfer tubes to a rack placed in a circulating water bath that has been preheated to 42°C. Leave the tubes in the rack for exactly 45 seconds. Do not shake the tubes. Rapidly transfer the tubes to an ice bath. Allow the cells to chill for 1-2 minutes. Add 400 ul LB to each tube. Incubate cultures for 45 minutes in a water bath set at 37°C or rotate cell at 37°C to allow the bacteria to recover and to express the antibiotic resistance marker encoded in the plasmid. Transfer the appropriate volume of transformed competent cells onto agar LB plate with appropriate antibiotic. Using a sterile bent glass rod gently spread the transformed cells over the surface of the agar plate. Leave the plate at room temperature until the liquid has been absorbed. Invert the plates and incubate at 37°C. Colonies should appear in 12-16 hours.

V.2.10.3 Electroporation transformation

Locate Electroporator power source and cuvette holder (Bio-Rad). Set the conditions for transformation according to strain. For DH5α cells, use 25 µFD, 200 Ω, and 2.5 kV. The time constant (tau value) should be 3-4 msec. Thaw required number of frozen cell aliquots (each tube 70 µl = two transformations) on ice. Thaw plasmid DNA in TE/H_20 on ice. Place 15 ml conical tube containing 10 ml of LB media without antibiotics on ice. Place 3 µl of DNA along wall of 0.2 cm cuvette. Pipet 35 µl of thawed electrocompetent cells onto DNA drop. Flick cuvette to settle DNA +

-

cells mixture into bottom of cuvette. Have 1 ml pipette containing 1 ml of LB media ready. Dry off any moisture from cuvette outside and immediately place cuvette in white plastic holder. Slide holder into position and zap cells. If you hear a high constant tone, immediately add the 1ml of LB to cells! Transfer cells from cuvette into 1.5 ml eppendorf tube and store on ice. The tone indicates that you have successfully electroporated your cells. Record the time constant value. Repeat procedure for remaining samples. If you see or hear sparking coming from your cuvette of cells, then the cells are dead! Repeat that sample again. Things that can cause sparking: excess water on cuvette outside, human skin oil on cuvette outside, too high salt conc. in DNA sample (try diluting DNA 10-fold), and poorly made electrocompetent cells. Outgrow transformed cells in eppendorf tubes by incubating the tubes in 37°C water bath for 1-1.5 hrs. Place transformant plates in 37°C bacterial incubator for 16-24 hrs until colonies appear.

V.2.10.4 Extraction of plasmid DNA

Plasmid DNA was extracted by the alkaline lysis method from 1.5 ml bacterial culture. Overnight-grown bacterial cells were harvested and resuspended in ice-cold 100 µl of solution I by vortexing vigorously. Then freshly prepared 200 µl of solution II were added and gently mixed by inverting the tube 6-8 times. After chilling 5 min on ice, 150 µl of solution III were added and mixed by inverting the tube. The bacterial lysate was centrifuged at 13000 rpm for 5 min and the supernatant was transferred to a new tube. The solution was cleared with one volume of phenol: chloroform and plasmid DNA was precipitated with 2 volumes of ethanol and washed with 70% ethanol. Finally, the DNA pellet was dissolved in 50 µl of distilled water containing 10 ug/ml DNase-free RNase A (Fermentas).

Solution I: 50 mM Glucose; 10 mM EDTA; 25 mM Tris-HCl pH8.0
Solution II: 0.2 M NaOH; 1% SDS
Solution III: 3 M KAc; 11.5% acetic acid

-

VI. REFERENCES

-

Aasland, R., Stewart, A.F. and Gibson, T. (1996) The SANT domain: a putative DNA-binding domain in the SWI-SNF and ADA complexes, the transcriptional co-repressor N-CoR and TFIIIB. *Trends Biochem Sci*, **21**, 87-88.

Aida, M., Beis, D., Heidstra, R., Willemsen, V., Blilou, I., Galinha, C., Nussaume, L., Noh, Y.S., Amasino, R. and Scheres, B. (2004) The PLETHORA genes mediate patterning of the *Arabidopsis* root stem cell niche. *Cell*, **119**, 109-120.

Alabadi, D., Blazquez, M.A., Carbonell, J., Ferrandiz, C. and Perez-Amador, M.A. (2009) Instructive roles for hormones in plant development. *Int J Dev Biol*, **53**, 1597-1608.

Alatzas, A. and Foundouli, A. (2006) Distribution of ubiquitinated histone H2A during plant cell differentiation in maize root and dedifferentiation in callus culture. *Plant Sci*, **171**, 481-487.

Aloia, L., Di Stefano, B., Sessa, A., Morey, L., Santanach, A., Gutierrez, A., Cozzuto, L., Benitah, S.A., Graf, T., Broccoli, V. and Di Croce, L. (2014) Zrf1 is required to establish and maintain neural progenitor identity. *Genes & Development* **28**, 182-197.

Arrowsmith, C.H., Bountra, C., Fish, P.V., Lee, K. and Schapira, M. (2012) Epigenetic protein families: a new frontier for drug discovery. *Nat Rev Drug Discov*, **11**, 384-400.

Ballerini, E.S. and Kramer, E.M. (2011) Environmental and molecular analysis of the floral transition in the lower eudicot *Aquilegia formosa*. *EvoDevo*, **2**, 4.

Barow, M. and Meister, A. (2003) Endopolyploidy in seed plants is differently correlated to systematics, organ, life strategy and genome size. *Plant Cell Environ*, **26**, 571-584.

Baubec, T., Dinh, H.Q., Pecinka, A., Rakic, B., Rozhon, W., Wohlrab, B., von Haeseler, A. and Mittelsten Scheid, O. (2010) Cooperation of multiple chromatin modifications can generate unanticipated stability of epigenetic states in *Arabidopsis*. *Plant Cell*, **22**, 34-47.

Belles-Boix, E., Hamant, O., Witiak, S.M., Morin, H., Traas, J. and Pautot, V. (2006) KNAT6: an *Arabidopsis* homeobox gene involved in meristem activity and organ separation. *Plant Cell*, **18**, 1900-1907.

Bemer, M. and Grossniklaus, U. (2012) Dynamic regulation of Polycomb group activity during plant development. *Curr Opin Plant Biol*, **15**, 523-529.

-

Benfey, P.N., Linstead, P.J., Roberts, K., Schiefelbein, J.W., Hauser, M.T. and Aeschbacher, R.A. (1993) Root development in *Arabidopsis*: four mutants with dramatically altered root morphogenesis. *Development*, **119**, 57-70.

Bentsink, L., Jowett, J., Hanhart, C.J. and Koornneef, M. (2006) Cloning of DOG1, a quantitative trait locus controlling seed dormancy in *Arabidopsis*. *Proc Natl Acad Sci U S A*, **103**, 17042-17047.

Bentsink, L. and Koornneef, M. (2008) Seed dormancy and germination. *Arabidopsis Book:* **e0119. doi: 10.1199/tab.0119**.

Bergink, S., Salomons, F.A., Hoogstraten, D., Groothuis, T.A., de Waard, H., Wu, J., Yuan, L., Citterio, E., Houtsmuller, A.B., Neefjes, J., Hoeijmakers, J.H., Vermeulen, W. and Dantuma, N.P. (2006) DNA damage triggers nucleotide excision repair-dependent monoubiquitylation of histone H2A. *Genes Dev*, **20**, 1343-1352.

Berr, A., McCallum, E.J., Alioua, A., Heintz, D., Heitz, T. and Shen, W.-H. (2010) *Arabidopsis* histone methyltransferase SET DOMAIN GROUP 8 mediates induction of the jasmonate/ethylene pathway genes in plant defense response to necrotrophic fungi. *Plant Physiol*, **154**, 1403-1414.

Berr, A., Ménard, R., Heitz, T. and Shen, W.-H. (2012) Chromatin modification and remodelling: a regulatory landscape for the control of *Arabidopsis* defence responses upon pathogen attack. *Cell Microbiol*, **14**, 829-839.

Berr, A., Shafiq, S. and Shen, W.H. (2011) Histone modifications in transcriptional activation during plant development. *Biochim Biophys Acta*, **1809**, 567-576.

Blilou, I., Xu, J., Wildwater, M., Willemsen, V., Paponov, I., Friml, J., Heidstra, R., Aida, M., Palme, K. and Scheres, B. (2005) The PIN auxin efflux facilitator network controls growth and patterning in *Arabidopsis* roots. *Nature*, **433**, 39-44.

Bourbousse, C., Ahmed, I., Roudier, F., Zabulon, G., Blondet, E., Balzergue, S., Colot, V., Bowler, C. and Barneche, F. (2012) Histone H2B monoubiquitination facilitates the rapid modulation of gene expression during *Arabidopsis* photomorphogenesis. *PLoS Genet*, **8**, e1002825.

Boutilier, K., Offringa, R., Sharma, V.K., Kieft, H., Ouellet, T., Zhang, L., Hattori, J., Liu, C.M., van Lammeren, A.A., Miki, B.L., Custers, J.B. and van Lookeren Campagne, M.M. (2002) Ectopic expression of BABY BOOM

triggers a conversion from vegetative to embryonic growth. *Plant Cell*, **14**, 1737-1749.

Bouyer, D., Roudier, F., Heese, M., Andersen, E.D., Gey, D., Nowack, M.K., Goodrich, J., Renou, J.P., Grini, P.E., Colot, V. and Schnittger, A. (2011) Polycomb repressive complex 2 controls the embryo-to-seedling phase transition. *PLoS Genet*, **7**, e1002014.

Bowman, J.L., Smyth, D.R. and Meyerowitz, E.M. (1989) Genes directing flower development in *Arabidopsis*. *Plant Cell*, **1**, 37-52.

Boyer, L.A., Latek, R.R. and Peterson, C.L. (2004) The SANT domain: a unique histone-tail-binding module? *Nat Rev Mol Cell Biol*, **5**, 158-163.

Brand, U., Fletcher, J.C., Hobe, M., Meyerowitz, E.M. and Simon, R. (2000) Dependence of stem cell fate in *Arabidopsis* on a feedback loop regulated by CLV3 activity. *Science*, **289**, 617-619.

Bratzel, F., Lopez-Torrejon, G., Koch, M., Del Pozo, J.C. and Calonje, M. (2010) Keeping cell identity in *Arabidopsis* requires PRC1 RING-finger homologs that catalyze H2A monoubiquitination. *Curr Biol* **20**, 1853-1859.

Braun, S. and Madhani, H.D. (2012) Shaping the landscape: mechanistic consequences of ubiquitin modification of chromatin. *EMBO Rep*, **13**, 619-630.

Bres, V., Yoshida, T., Pickle, L. and Jones, K.A. (2009) SKIP interacts with c-Myc and Menin to promote HIV-1 Tat transactivation. *Mol Cell*, **36**, 75-87.

Breuninger, H., Rikirsch, E., Hermann, M., Ueda, M. and Laux, T. (2008) Differential expression of WOX genes mediates apical-basal axis formation in the *Arabidopsis* embryo. *Dev Cell*, **14**, 867-876.

Bu, Z., Yu, Y., Li, Z., Liu, Y., Jiang, W., Huang, Y. and Dong, A.W. (2014) Regulation of *Arabidopsis* flowering by the histone mark readers MRG1/2 via interaction with CONSTANS to modulate FT expression. *PLoS Genet*, **10**, e1004617.

Byrne, M.E. (2005) Networks in leaf development. *Curr Opin Plant Biol*, **8**, 59-66.

Byrne, M.E., Simorowski, J. and Martienssen, R.A. (2002) ASYMMETRIC LEAVES1 reveals knox gene redundancy in *Arabidopsis*. *Development*, **129**, 1957-1965.

Calonje, M., Sanchez, R., Chen, L. and Sung, Z.R. (2008) EMBRYONIC FLOWER1 participates in polycomb group-mediated AG gene silencing in

Arabidopsis. *Plant Cell*, **20**, 277-291.

Cao, Y., Dai, Y., Cui, S. and Ma, L. (2008) Histone H2B monoubiquitination in the chromatin of FLOWERING LOCUS C regulates flowering time in *Arabidopsis*. *Plant Cell*, **20**, 2586-2602.

Carles, C.C., Choffnes-Inada, D., Reville, K., Lertpiriyapong, K. and Fletcher, J.C. (2005) ULTRAPETALA1 encodes a SAND domain putative transcriptional regulator that controls shoot and floral meristem activity in *Arabidopsis*. *Development*, **132**, 897-911.

Carlsten, J.O., Zhu, X. and Gustafsson, C.M. (2013) The multitalented Mediator complex. *Trends Biochem Sci*, **38**, 531-537.

Carrozza, M.J., Utley, R.T., Workman, J.L. and Cote, J. (2003) The diverse functions of histone acetyltransferase complexes. *Trends Genet*, **19**, 321-329.

Chen, D., Molitor, A., Liu, C. and Shen, W.H. (2010) The *Arabidopsis* PRC1-like ring-finger proteins are necessary for repression of embryonic traits during vegetative growth. *Cell Res*, **20**, 1332-1344.

Chen, D.H., Huang, Y., Liu, C., Ruan, Y. and Shen, W.H. (2014) Functional conservation and divergence of J-domain-containing ZUO1/ZRF orthologs throughout evolution. *Planta*, **239**, 1159-1173.

Chen, H., Banerjee, A.K. and Hannapel, D.J. (2004) The tandem complex of BEL and KNOX partners is required for transcriptional repression of ga20ox1. *Plant J*, **38**, 276-284.

Cheng, Y., Dai, X. and Zhao, Y. (2006) Auxin biosynthesis by the YUCCA flavin monooxygenases controls the formation of floral organs and vascular tissues in *Arabidopsis*. *Genes Dev*, **20**, 1790-1799.

Cheng, Z.J., Wang, L., Sun, W., Zhang, Y., Zhou, C., Su, Y.H., Li, W., Sun, T.T., Zhao, X.Y., Li, X.G., Cheng, Y., Zhao, Y., Xie, Q. and Zhang, X.S. (2013) Pattern of auxin and cytokinin responses for shoot meristem induction results from the regulation of cytokinin biosynthesis by AUXIN RESPONSE FACTOR3. *Plant Physiol*, **161**, 240-251.

Chernikova, S.B., Dorth, J.A., Razorenova, O.V., Game, J.C. and Brown, J.M. (2010) Deficiency in Bre1 impairs homologous recombination repair and cell cycle checkpoint response to radiation damage in mammalian cells. *Radiat Res*, **174**, 558-565.

-

Clark, S.E., Williams, R.W. and Meyerowitz, E.M. (1997) The CLAVATA1 gene encodes a putative receptor kinase that controls shoot and floral meristem size in *Arabidopsis*. *Cell* **89**, 575–585.

Coen, E.S. and Meyerowitz, E.M. (1991) The war of the whorls: genetic interactions controlling flower development. *Nature*, **353**, 31-37.

Corbesier, L., Vincent, C., Jang, S., Fornara, F., Fan, Q., Searle, I., Giakountis, A., Farrona, S., Gissot, L., Turnbull, C. and Coupland, G. (2007) FT protein movement contributes to long-distance signaling in floral induction of *Arabidopsis*. *Science*, **316**, 1030-1033.

de Jager, S.M., Scofield, S., Huntley, R.P., Robinson, A.S., den Boer, B.G. and Murray, J.A. (2009) Dissecting regulatory pathways of G1/S control in *Arabidopsis*: common and distinct targets of CYCD3;1, E2Fa and E2Fc. *Plant Mol Biol*, **71**, 345-365.

De Smet, I., Lau, S., Mayer, U. and Jurgens, G. (2010) Embryogenesis - the humble beginnings of plant life. *Plant J*, **61**, 959-970.

De Veylder, L., Beeckman, T., Beemster, G.T., de Almeida Engler, J., Ormenese, S., Maes, S., Naudts, M., Van Der Schueren, E., Jacqmard, A., Engler, G. and Inze, D. (2002) Control of proliferation, endoreduplication and differentiation by the *Arabidopsis* E2Fa-DPa transcription factor. *EMBO J*, **21**, 1360-1368.

Dean, G., Casson, S. and Lindsey, K. (2004) KNAT6 gene of *Arabidopsis* is expressed in roots and is required for correct lateral root formation. *Plant Mol Biol*, **54**, 71-84.

del Pozo, J.C., Diaz-Trivino, S., Cisneros, N. and Gutierrez, C. (2006) The balance between cell division and endoreplication depends on E2FC-DPB, transcription factors regulated by the ubiquitin-SCFSKP2A pathway in Arabidopsis. *Plant Cell*, **18**, 2224-2235.

Dello Ioio, R., Nakamura, K., Moubayidin, L., Perilli, S., Taniguchi, M., Morita, M.T., Aoyama, T., Costantino, P. and Sabatini, S. (2008) A genetic framework for the control of cell division and differentiation in the root meristem. *Science*, **322**, 1380-1384.

Demajo, S., Uribesalgo, I., Gutierrez, A., Ballare, C., Capdevila, S., Roth, M., Zuber, J., Martin-Caballero, J. and Di Croce, L. (2014) ZRF1 controls the

retinoic acid pathway and regulates leukemogenic potential in acute myeloid leukemia. *Oncogene*, **33**, 5501-5510.

Denu, J.M. (2003) Linking chromatin function with metabolic network: Sir2 family of NAD+-dependent deacetylases. *Trends Biochem Sci*, 41-48.

Derkacheva, M., Steinbach, Y., Wildhaber, T., Mozgova, I., Mahrez, W., Nanni, P., Bischof, S., Gruissem, W. and Hennig, L. (2013) *Arabidopsis* MSI1 connects LHP1 to PRC2 complexes. *EMBO J*, **32**, 2073-2085.

Dewitte, W. and Murray, J.A. (2003) The plant cell cycle. *Annu Rev Plant Biol*, **54**, 235-264.

Dewitte, W., Riou-Khamlichi, C., Scofield, S., Healy, J.M., Jacqmard, A., Kilby, N.J. and Murray, J.A. (2003) Altered cell cycle distribution, hyperplasia, and inhibited differentiation in *Arabidopsis* caused by the D-type cyclin CYCD3. *Plant Cell*, **15**, 79-92.

Dhawan, R., Luo, H., Foerster, A.M., Abuqamar, S., Du, H.N., Briggs, S.D., Mittelsten Scheid, O. and Mengiste, T. (2009) HISTONE MONOUBIQUITINATION1 interacts with a subunit of the mediator complex and regulates defense against necrotrophic fungal pathogens in *Arabidopsis*. *Plant Cell*, **21**, 1000-1019.

Ding, Z. and Friml, J. (2010) Auxin regulates distal stem cell differentiation in *Arabidopsis* roots. *Proc Natl Acad Sci U S A*, **107**, 12046-12051.

Dinneny, J.R. and Benfey, P.N. (2008) Plant stem cell niches: standing the test of time. *Cell*, **132**, 553-557.

Dolan, L., Janmaat, K., Willemsen, V., Linstead, P., Poethig, S., Roberts, K. and Scheres, B. (1993) Cellular organisation of the *Arabidopsis thaliana* root. *Development*, **119**, 71-84.

Endrizzi, K., Moussian, B., Haecker, A., Levin, J.Z. and Laux, T. (1996) The SHOOT MERISTEMLESS gene is required for maintenance of undifferentiated cells in *Arabidopsis* shoot and floral meristems and acts at a different regulatory level than the meristem genes WUSCHEL and ZWILLE. *Plant J*, **10**, 967-979.

Ezhkova, E. and Tansey, W.P. (2004) Proteasomal ATPases link ubiquitylation of histone H2B to methylation of histone H3. *Mol Cell*, **13**, 435-442.

Feng, J. and Shen, W.H. (2014) Dynamic regulation and function of histone monoubiquitination in plants. *Front Plant Sci*, **5**, 83. doi: 10.3389/fpls.2014.

00083.

Fletcher, J.C., Brand, U., Running, M.P., Simon, R. and Meyerowitz, E.M. (1999) Signaling of cell fate decisions by CLAVATA3 in *Arabidopsis* shoot meristems. *Science*, **283**, 1911-1914.

Fleury, D., Himanen, K., Cnops, G., Nelissen, H., Boccardi, T.M., Maere, S., Beemster, G.T., Neyt, P., Anami, S., Robles, P., Micol, J.L., Inzé, D. and Van Lijsebettens, M. (2007) The *Arabidopsis thaliana* homolog of yeast BRE1 has a function in cell cycle regulation during early leaf and root growth. *Plant Cell*, **19**, 417-432.

Fowler, S., Lee, K., Onouchi, H., Samach, A., Richardson, K., Morris, B., Coupland, G. and Putterill, J. (1999) GIGANTEA: a circadian clock-controlled gene that regulates photoperiodic flowering in *Arabidopsis* and encodes a protein with several possible membrane-spanning domains. *EMBO J*, **18**, 4679–4688.

Francis, D. (2007) The plant cell cycle--15 years on. *New Phytol*, **174**, 261-278.

Friml, J., Vieten, A., Sauer, M., Weijers, D., Schwarz, H., Hamann, T., Offringa, R. and Jurgens, G. (2003) Efflux-dependent auxin gradients establish the apical-basal axis of *Arabidopsis*. *Nature*, **426**, 147-153.

Fuchs, G. and Oren, M. (2014) Writing and reading H2B monoubiquitylation. *Biochim Biophys Acta*, **1839**, 694-701.

Fukaki, H., Tameda, S., Masuda, H. and Tasaka, M. (2002) Lateral root formation is blocked by a gain-of-function mutation in the SOLITARY-ROOT/IAA14 gene of *Arabidopsis*. *Plant J*, **29**, 153-168.

Fukuda, H., Sano, N., Muto, S. and Horikoshi, M. (2006) Simple histone acetylation plays a complex role in the regulation of gene expression. *Brief Funct Genomic Proteomic*, **5**, 190-208.

Galinha, C., Hofhuis, H., Luijten, M., Willemsen, V., Blilou, I., Heidstra, R. and Scheres, B. (2007) PLETHORA proteins as dose-dependent master regulators of *Arabidopsis* root development. *Nature*, **449**, 1053-1057.

Gallois, J.L., Woodward, C., Reddy, G.V. and Sablowski, R. (2002) Combined SHOOT MERISTEMLESS and WUSCHEL trigger ectopic organogenesis in *Arabidopsis*. *Development*, **129**, 3207-3217.

Gendrel, A.V., Lippman, Z., Yordan, C., Colot, V. and Martienssen, R.A. (2002)

Dependence of heterochromatic histone H3 methylation patterns on the *Arabidopsis* gene DDM1. *Science*, **297**, 1871-1873.

Ginjala, V., Nacerddine, K., Kulkarni, A., Oza, J., Hill, S.J., Yao, M., Citterio, E., van Lohuizen, M. and Ganesan, S. (2011) BMI1 is recruited to DNA breaks and contributes to DNA damage-induced H2A ubiquitination and repair. *Mol Cell Biol.*, **31**, 1972-1982.

Giraudat, J., Hauge, B.M., Valon, C., Smalle, J., Parcy, F. and Goodman, H.M. (1992) Isolation of the *Arabidopsis* ABI3 gene by positional cloning. *Plant Cell*, **4**, 1251-1261.

Goldknopf, I.L., Taylor, C.W., Baum, R.M., Yeoman, L.C., Olson, M.O., Prestayko, A.W. and Busch, H. (1975) Isolation and characterization of protein A24, a "histone-like" non-histone chromosomal protein. *J Biol Chem*, **250**, 7182-7187.

Goodrich, J., Puangsomlee, P., Martin, M., Long, D., Meyerowitz, E.M. and Coupland, G. (1997) A Polycomb-group gene regulates homeotic gene expression in *Arabidopsis*. *Nature*, **386**, 44-51.

Gregoretti, I.V., Lee, Y.M. and Goodson, H.V. (2004) Molecular evolution of the histone deacetylase family: functional implications of phylogenetic analysis. *J Mol Biol*, **338**, 17-31.

Grieneisen, V.A., Xu, J., Marée, A.F., Hogeweg, P. and Scheres, B. (2007) Auxin transport is sufficient to generate a maximum and gradient guiding root growth. *Nature*, **449**, 1008-1013.

Gu, X., Jiang, D., Wang, Y., Bachmair, A. and He, Y. (2009) Repression of the floral transition via histone H2B monoubiquitination. *Plant J*, **57**, 522-533.

Guenther, M.G., Levine, S.S., Boyer, L.A., Jaenisch, R. and R.A., Y. (2007) A chromatin landmark and transcription initiation at most promoters in human cells. *Cell*, **130**, 77-88.

Gutierrez, L., Van Wuytswinkel, O., Castelain, M. and Bellini, C. (2007) Combined networks regulating seed maturation. *Trends Plant Sci*, **12**, 294-300.

Hake, S., Smith, H.M., Holtan, H., Magnani, E., Mele, G. and Ramirez, J. (2004) The role of knox genes in plant development. *Annu Rev Cell Dev Biol*, **20**, 125-151.

Han, J., Zhang, H., Wang, Z., Zhou, H. and Zhang, Z. (2013) A Cul4 E3 ubiquitin

ligase regulates histone hand-off during nucleosome assembly. *Cell*, **155**, 817-829.

Harada, J.J. (1997) Seed maturation and control of germination. . In *Advances in Cellular and Molecular Biology of Plants Volume 4, Cellular and Molecular Biology of Seed Development* (Larkins, B.A. and Vasi, I.K. eds). Dordrecht: Kluwer Academic Publishers, pp. 545-592.

Harding, E.W., Tang, W., Nichols, K.W., Fernandez, D.E. and Perry, S.E. (2003) Expression and maintenance of embryogenic potential is enhanced through constitutive expression of AGAMOUS-Like 15. *Plant Physiol*, **133**, 653-663.

Haslekas, C., Viken, M.K., Grini, P.E., Nygaard, V., Nordgard, S.H., Meza, T.J. and Aalen, R.B. (2003) Seed 1-cysteine peroxiredoxin antioxidants are not involved in dormancy, but contribute to inhibition of germination during stress. *Plant Physiol*, **133**, 1148-1157.

Hatzold, J. and Conradt, B. (2008) Control of apoptosis by asymmetric cell division. *PLoS Biol*, **6**, e84.

Hay, A., Kaur, H., Phillips, A., Hedden, P., Hake, S. and Tsiantis, M. (2002) The gibberellin pathway mediates KNOTTED1-type homeobox function in plants with different body plans. *Curr Biol*, **12**, 1557-1565.

He, Y., Michaels, S.D. and Amasino, R.M. (2003) Regulation of flowering time by histone acetylation in *Arabidopsis*. *Science*, **302**, 1751-1754.

Helariutta, Y., Fukaki, H., Wysocka-Diller, J., Nakajima, K., Jung, J., Sena, G., Hauser, M.T. and Benfey, P.N. (2000) The SHORT-ROOT gene controls radial patterning of the *Arabidopsis* root through radial signaling. *Cell*, **101**, 555-567.

Helliwell, C.A., Wood, C.C., Robertson, M., James Peacock, W. and Dennis, E.S. (2006) The *Arabidopsis* FLC protein interacts directly in vivo with SOC1 and FT chromatin and is part of a high-molecular-weight protein complex. *Plant J*, **46**, 183-192.

Hershko, A. and Ciechanover, A. (1998) The ubiquitin system. *Annu Rev Biochem*, **67**, 425-479.

Himanen, K., Woloszynska, M., Boccardi T, M., De Groeve, S., Nelissen, H., Bruno, L., Vuylsteke, M. and Van Lijsebettens, M. (2012) Histone H2B monoubiquitination is required to reach maximal transcript levels of circadian

clock genes in *Arabidopsis*. *Plant J*, **72**, 249-260.

Hua, Z. and Vierstra, R.D. (2011) The cullin-RING ubiquitin-protein ligases. *Annu Rev Plant Biol*, **62**, 299-334.

Hunt, L.T. and Dayhoff, M.O. (1977) Amino-terminal sequence identity of ubiquitin and the nonhistone component of nuclear protein A24. *Biochem Biophys Res Commun*, **74**, 650-655.

Hwang, I., Sheen, J. and Muller, B. (2012) Cytokinin signaling networks. *Annu Rev Plant Biol*, **63**, 353-380.

Hwang, W.W., Venkatasubrahmanyam, S., Ianculescu, A.G., Tong, A., Boone, C. and Madhani, H.D. (2003) A conserved RING finger protein required for histone H2B monoubiquitination and cell size control. *Mol Cell*, **11**, 261-266.

Ikeda, M., Umehara, M. and Kamada, H. (2006) Embryogenesis-related genes; Its expression and roles during somatic and zygotic embryogenesis in carrot and *Arabidopsis*. *Plant Biotechnology*, **23**, 153-161.

Inoue, T., Higuchi, M., Hashimoto, Y., Seki, M., Kobayashi, M., Kato, T., Tabata, S., Shinozaki, K. and Kakimoto, T. (2001) Identification of CRE1 as a cytokinin receptor from *Arabidopsis*. *Nature*, **409**, 1060-1063.

Inoue, T., Shoji, W. and Obinata, M. (1999) MIDA1, an Id-associating protein, has two distinct DNA binding activities that are converted by the association with Id1: a novel function of Id protein. *Biochem Biophys Res Commun.*, **266**, 147-151.

Inoue, T., Shoji, W. and Obinata, M. (2000) MIDA1 is a sequence specific DNA binding protein with novel DNA binding properties. *Genes Cells*, **5**, 699-709.

Inze, D. and De Veylder, L. (2006) Cell cycle regulation in plant development. *Annu Rev Genet*, **40**, 77-105.

Irish, V.F. and Sussex, I.M. (1990) Function of the APETALA1 gene during *Arabidopsis* floral development. *Plant Cell*, **2**, 741-753.

Jaiswal, H., Conz, C., Otto, H., Wolfle, T., Fitzke, E., Mayer, M.P. and Rospert, S. (2011) The chaperone network connected to human ribosome-associated complex. *Mol Cell Biol*, **31**, 1160-1173.

Jasinski, S., Piazza, P., Craft, J., Hay, A., Woolley, L., Rieu, I., Phillips, A., Hedden, P. and Tsiantis, M. (2005) KNOX action in *Arabidopsis* is mediated by coordinate regulation of cytokinin and gibberellin activities. *Curr Biol*, **15**,

1560–1565.

Jenik, P.D. and Irish, V.F. (2000) Regulation of cell proliferation patterns by homeotic genes during *Arabidopsis* floral development. *Development*, **127**, 1267-1276.

Jeong, S., Trotochaud, A.E. and Clark, S.E. (1999) The *Arabidopsis* CLAVATA2 gene encodes a receptor-like protein required for the stability of the CLAVATA1 receptor-like kinase. *Plant Cell*, **11**, 1925-1934.

Johansen, K.M. and Johansen, J. (2006) Regulation of chromatin structure by histone H3S10 phosphorylation. *Chromosome Res*, **14**, 393-404.

Kagaya, Y., Okuda, R., Ban, A., Toyoshima, R., Tsutsumida, K., Usui, H., Yamamoto, A. and Hattori, T. (2005) Indirect ABA-dependent regulation of seed storage protein genes by FUSCA3 transcription factor in *Arabidopsis*. *Plant Cell Physiol*, **46**, 300-311.

Kakimoto, T. (2001) Identification of plant cytokinin biosynthetic enzymes as dimethylallyl diphosphate: ATP/ADP isopentenyltransferases. *Plant Cell Physiol*, **42**, 677-685.

Kim, J., Hake, S.B. and Roeder, R.G. (2005) The human homolog of yeast BRE1 functions as a transcriptional coactivator through direct activator interactions. *Mol Cell*, **20**, 759-770.

Kobayashi, Y., Kaya, H., Goto, K., Iwabuchi, M. and Araki, T. (1999) A pair of related genes with antagonistic roles in mediating flowering signals. *Science*, **286**, 1960-1962.

Kobayashi, Y. and Weigel, D. (2007) Move on up, it's time for change--mobile signals controlling photoperiod-dependent flowering. *Genes Dev*, **21**, 2371-2384.

Kohler, C. and Makarevich, G. (2006) Epigenetic mechanisms governing seed development in plants. *EMBO Rep*, **7**, 1223-1227.

Kondorosi, E., Roudier, F. and Gendreau, E. (2000) Plant cell-size control: growing by ploidy? *Curr Opin Plant Biol*, **3**, 488-492.

Koornneef, M., Bentsink, L. and Hilhorst, H. (2002) Seed dormancy and germination. *Curr Opin Plant Biol*, **5**, 33-36.

Kouzarides, T. (2007) Chromatin modifications and their function. *Cell*, **128**, 693-705.

-

Krichevsky, A., Zaltsman, A., Lacroix, B. and Citovsky, V. (2011) Involvement of KDM1C histone demethylase-OTLD1 otubain-like histone deubiquitinase complexes in plant gene repression. *Proc Natl Acad Sci U S A*, **108**, 11157-11162.

Kwiatkowska, D. (2006) Flower primordium formation at the *Arabidopsis* shoot apex: quantitative analysis of surface geometry and growth. *J Exp Bot*, **57**, 571-580.

Kwong, R.W., Bui, A.Q., Lee, H., Kwong, L.W., Fischer, R.L., Goldberg, R.B. and Harada, J.J. (2003) LEAFY COTYLEDON1-LIKE defines a class of regulators essential for embryo development. *Plant Cell*, **15**, 5-18.

Laugesen, A. and Helin, K. (2014) Chromatin repressive complexes in stem cells, development, and cancer. *Cell Stem Cell*, **14**, 735-751.

Laux, T., Mayer, K.F., Berger, J. and Jurgens, G. (1996) The WUSCHEL gene is required for shoot and floral meristem integrity in *Arabidopsis*. *Development*, **122**, 87-96.

Lee, H., Suh, S.S., Park, E., Cho, E., Ahn, J.H., Kim, S.G., Lee, J.S., Kwon, Y.M. and Lee, I. (2000) The AGAMOUS-LIKE 20 MADS domain protein integrates floral inductive pathways in *Arabidopsis*. *Genes Dev*, **14**, 2366-2376.

Lee, H.S. and Chen, Z.J. (2001) Protein-coding genes are epigenetically regulated in *Arabidopsis* polyploids. *Proc Natl Acad Sci U S A*, **98**, 6753-6758.

Lee, J.S., Shukla, A., Schneider, J., Swanson, S.K., Washburn, M.P., Florens, L., Bhaumik, S.R. and Shilatifard, A. (2007) Histone crosstalk between H2B monoubiquitination and H3 methylation mediated by COMPASS. *Cell*, **131**, 1084-1096.

Leibfried, A., To, J.P., Busch, W., Stehling, S., Kehle, A., Demar, M., Kieber, J.J. and Lohmann, J.U. (2005) WUSCHEL controls meristem function by direct regulation of cytokinin-inducible response regulators. *Nature*, **438**, 1172-1175.

Lenhard, M., Bohnert, A., Jurgens, G. and Laux, T. (2001) Termination of stem cell maintenance in *Arabidopsis* floral meristems by interactions between WUSCHEL and AGAMOUS. *Cell*, **105**, 805-814.

Lenhard, M., Jurgens, G. and Laux, T. (2002) The WUSCHEL and SHOOT MERISTEMLESS genes fulfil complementary roles in *Arabidopsis* shoot meristem regulation. *Development*, **129**, 3195-3206.

-

Li, D., Liu, C., Shen, L., Wu, Y., Chen, H., Robertson, M., Helliwell, C.A., Ito, T., Meyerowitz, E. and Yu, H. (2008) A repressor complex governs the integration of flowering signals in *Arabidopsis*. *Dev Cell*, **15**, 110-120.

Li, L., Ye, H., Guo, H. and Yin, Y. (2010) *Arabidopsis* IWS1 interacts with transcription factor BES1 and is involved in plant steroid hormone brassinosteroid regulated gene expression. *Proc Natl Acad Sci U S A*, **107**, 3918–3923.

Li, W., Wang, Z., Li, J., Yang, H., Cui, S., Wang, X. and Ma, L. (2011) Overexpression of AtBMI1C, a polycomb group protein gene, accelerates flowering in *Arabidopsis*. *PLoS One*, **6**, e21364.

Liu, F., Quesada, V., Crevillen, P., Baurle, I., Swiezewski, S. and Dean, C. (2007) The *Arabidopsis* RNA-binding protein FCA requires a lysine-specific demethylase 1 homolog to downregulate FLC. *Mol Cell*, **28**, 398-407.

Liu, X., Kim, Y.J., Müller, R., Yumul, R.E., Liu, C., Pan, Y., Cao, X., Goodrich, J. and Chen, X. (2011) AGAMOUS terminates floral stem cell maintenance in *Arabidopsis* by directly repressing WUSCHEL through recruitment of Polycomb Group proteins. *Plant Cell*, **23**, 3654-3670.

Liu, Y., Geyer, R., van Zanten, M., Carles, A., Li, Y., Horold, A., van Nocker, S. and Soppe, W.J. (2011) Identification of the *Arabidopsis* REDUCED DORMANCY 2 gene uncovers a role for the polymerase associated factor 1 complex in seed dormancy. *PLoS One*, **6**, e22241.

Liu, Y., Koornneef, M. and Soppe, W.J. (2007) The absence of histone H2B monoubiquitination in the *Arabidopsis* hub1 (rdo4) mutant reveals a role for chromatin remodeling in seed dormancy. *Plant Cell*, **19**, 433-444.

Lohmann, J.U., Hong, R.L., Hobe, M., Busch, M.A., Parcy, F., Simon, R. and Weigel, D. (2001) A molecular link between stem cell regulation and floral patterning in *Arabidopsis*. *Cell* **105**, 793-803.

Lolas, I.B., Himanen, K., Gronlund, J.T., Lynggaard, C., Houben, A., Melzer, M., Van Lijsebettens, M. and Grasser, K.D. (2010) The transcript elongation factor FACT affects *Arabidopsis* vegetative and reproductive development and genetically interacts with HUB1/2. *Plant J*, **61**, 686-697.

Long, J.A., Moan, E.I., Medford, J.I. and Barton, M.K. (1996) A member of the KNOTTED class of homeodomain proteins encoded by the STM gene of

Arabidopsis. *Nature*, **379**, 66-69.

Lotan, T., Ohto, M., Yee, K.M., West, M.A.L., Lo, R., Kwong, R.W., Yamagishi, K., Fischer, R.L., Goldberg, R.B. and Harada, J.J. (1998) *Arabidopsis* LEAFY COTYLEDON1 is sufficient to induce embryo development in vegetative cells. *Cell*, **93**, 1195-1205.

Lucas, M., Swarup, R., Paponov, I.A., Swarup, K., Casimiro, I., Lake, D., Peret, B., Zappala, S., Mairhofer, S., Whitworth, M., Wang, J., Ljung, K., Marchant, A., Sandberg, G., Holdsworth, M.J., Palme, K., Pridmore, T., Mooney, S. and Bennett, M.J. (2011) Short-Root regulates primary, lateral, and adventitious root development in *Arabidopsis*. *Plant Physiol*, **155**, 384-398.

Luger, K., Mader, A.W., Richmond, R.K., Sargent, D.F. and Richmond, T.J. (1997) Crystal structure of the nucleosome core particle at 2.8 A resolution. *Nature*, **389**, 251-260.

Luo, M., Luo, M.-Z., Buzas, D., Finnegan, J., Helliwell, C., Dennis, E.S., Peacock, W.J. and Chaudhury, A. (2008) UBIQUITIN-SPECIFIC PROTEASE 26 is required for seed development and the repression of PHERES1 in *Arabidopsis*. *Genetics*, **180**, 229-236.

Malapeira, J., Khaitova, L.C. and Mas, P. (2012) Ordered changes in histone modifications at the core of the *Arabidopsis* circadian clock. *Proc Natl Acad Sci U S A* **109**, 21540-21545.

Manzano, C., Abraham, Z., Lopez-Torrejon, G. and Del Pozo, J.C. (2008) Identification of ubiquitinated proteins in *Arabidopsis*. *Plant Mol Biol*, **68**, 145-158.

Maor, R., Jones, A., Nuhse, T.S., Studholme, D.J., Peck, S.C. and Shirasu, K. (2007) Multidimensional protein identification technology (MudPIT) analysis of ubiquitinated proteins in plants. *Mol Cell Proteomics*, **6**, 601-610.

Marks, P., Rifkind, R.A., Richon, V.M., Breslow, R., Miller, T. and Kelly, W.K. (2001) Histone deacetylases and cancer: causes and therapies. *Nat Rev Cancer*, **1**, 194-202.

Marteijn, J.A., Bekker-Jensen, S., Mailand, N., Lans, H., Schwertman, P., Gourdin, A.M., Dantuma, N.P., Lukas, J. and Vermeulen, W. (2009) Nucleotide excision repair–induced H2A ubiquitination is dependent on MDC1 and RNF8 and reveals a universal DNA damage response. *J Cell Biol*, **186**, 835-

847.

Martin, C. and Zhang, Y. (2005) The diverse functions of histone lysine methylation. *Nat Rev Mol Cell Biol*, **6**, 838-849.

Matsumoto-Taniura, N., Pirollet, F., Monroe, R., Gerace, L. and Westendorf, J.M. (1996) Identification of novel M phase phosphoproteins by expression cloning. *Mol Biol Cell*, **7**, 1455-1469.

Mayer, K.F., Schoof, H., Haecker, A., Lenhard, M., Jurgens, G. and Laux, T. (1998) Role of WUSCHEL in regulating stem cell fate in the *Arabidopsis* shoot meristem. *Cell*, **95**, 805-815.

Mayer, U., Torres Ruiz, R.A., Berleth, T., Misera, S. and Jürgens, G. (1991) Mutations affecting body organization in the *Arabidopsis* embryo. *Nature*, **353**, 402-407.

Ménard, R., Verdier, G., Ors, M., Erhardt, M., Beisson, F. and Shen, W.H. (2014) Histone H2B monoubiquitination is involved in the regulation of cutin and wax composition in *Arabidopsis thaliana*. *Plant Cell Physiol*, **55**, 455-466.

Menges, M., Samland, A.K., Planchais, S. and Murray, J.A. (2006) The D-type cyclin CYCD3;1 is limiting for the G1-to-S-phase transition in *Arabidopsis*. *Plant Cell*, **18**, 893-906.

Michaels, S.D. and Amasino, R.M. (1999) FLOWERING LOCUS C encodes a novel MADS domain protein that acts as a repressor of flowering. *Plant Cell*, **11**, 949–956.

Michaels, S.D. and Amasino, R.M. (1999) FLOWERING LOCUS C encodes a novel MADS domain protein that acts as a repressor of flowering. *Plant Cell*, **11**, 949-956.

Michaels, S.D. and Amasino, R.M. (2001) Loss of FLOWERING LOCUS C activity eliminates the late-flowering phenotype of FRIGIDA and autonomous pathway mutations but not responsiveness to vernalization. *Plant Cell*, **13**, 935-941.

Molitor, A. and Shen, W.-H. (2013) The Polycomb complex PRC1: composition and function in plants. *J Genet Genomics* **40**, 231-238.

Molitor, A.M., Bu, Z., Yu, Y. and Shen, W.H. (2014) *Arabidopsis* AL PHD-PRC1 complexes promote seed germination through H3K4me3-to-H3K27me3 chromatin state switch in repression of seed developmental genes. *PLoS Genet*, **10**, e1004091.

-

Moon, J., Suh, S.S., Lee, H., Choi, K.R., Hong, C.B., Paek, N.C., Kim, S.G. and Lee, I. (2003) The SOC1 MADS-box gene integrates vernalization and gibberellin signals for flowering in *Arabidopsis*. *Plant J*, **35**, 613-623.

Moubayidin, L., Di Mambro, R. and Sabatini, S. (2009) Cytokinin–auxin crosstalk. *Trends Plant Sci*, **14**, 557-562.

Moyal, L., Lerenthal, Y., Gana-Weisz, M., Mass, G., So, S., Wang, S.Y., Eppink, B., Chung, Y.M., Shalev, G., Shema, E., Shkedy, D., Smorodinsky, N.I., van Vliet, N., Kuster, B., Mann, M., Ciechanover, A., Dahm-Daphi, J., Kanaar, R., Hu, M.C., Chen, D.J., Oren, M. and Shiloh, Y. (2011) Requirement of ATM-dependent monoubiquitylation of histone H2B for timely repair of DNA double-strand breaks. *Mol Cell*, **41**, 529-542.

Nakajima, K., Sena, G., Nawy, T. and Benfey, P.N. (2001) Intercellular movement of the putative transcription factor SHR in root patterning. *Nature*, **413**, 307-311.

Nakamura, K., Kato, A., Kobayashi, J., Yanagihara, H., Sakamoto, S., Oliveira, D.V., Shimada, M., Tauchi, H., Suzuki, H., Tashiro, S., Zou, L. and Komatsu, K. (2011) Regulation of homologous recombination by RNF20-dependent H2B ubiquitination. *Mol Cell*, **41**, 515-528.

Nardmann, J. and Werr, W. (2007) The evolution of plant regulatory networks: what *Arabidopsis* cannot say for itself. *Curr Opin Plant Biol*, **10**, 653-659.

Naylor, L.H. and Clark, E.M. (1990) d(TG)n.d(CA)n sequences upstream of the rat prolactin gene form Z-DNA and inhibit gene transcription. *Nucleic Acids Res*, **18**, 1595-1601.

Nijman, S.M., Luna-Vargas, M.P., Velds, A., Brummelkamp, T.R., Dirac, A.M., Sixma, T.K. and Bernards, R. (2005) A genomic and functional inventory of deubiquitinating enzymes. *Cell*, **123**, 773-786.

Oh, S., Jeong, K., Kim, H., Kwon, C.S. and Lee, D. (2010) A lysine-rich region in Dot1p is crucial for direct interaction with H2B ubiquitylation and high level methylation of H3K79. *Biochem Biophys Res Commun*, **399**, 512–517.

Oki, M., Aihara, H. and Ito, T. (2007) Role of histone phosphorylation in chromatin dynamics and its implications in diseases. *Subcell Biochem*, **41**, 319-336.

Otto, H., Conz, C., Maier, P., Wolfle, T., Suzuki, C.K., Jeno, P., Rucknagel, P., Stahl, J. and Rospert, S. (2005) The chaperones MPP11 and Hsp70L1 form the mammalian ribosome-associated complex. *Proc Natl Acad Sci U S A*, **102**,

10064-10069.

Palma, K., Thorgrimsen, S., Malinovsky, F.G., Fiil, B.K., Nielsen, H.B., Brodersen, P., Hofius, D., Petersen, M. and Mundy, J. (2010) Autoimmunity in *Arabidopsis* acd11 is mediated by epigenetic regulation of an immune receptor. *PLoS Pathog*, **6**.

Pappas, V. and Miller, S.M. (2009) Functional analysis of the *Volvox carteri* asymmetric division protein GlsA. *Mech Dev*, **126**, 842-851.

Parcy, F., Valon, C., Raynal, M., Gaubier-Comella, P., Delseny, M. and Giraudat, J. (1994) Regulation of gene expression programs during *Arabidopsis* seed development: roles of the ABI3 locus and of endogenous abscisic acid. *Plant Cell*, **6**, 1567-1582.

Pavri, R., Zhu, B., Li, G., Trojer, P., Mandal, S., Shilatifard, A. and Reinberg, D. (2006) Histone H2B monoubiquitination functions cooperatively with FACT to regulate elongation by RNA polymerase II. *Cell*, **125**, 703-717.

Perilli, S., Di Mambro, R. and Sabatini, S. (2012) Growth and development of the root apical meristem. *Curr Opin Plant Biol*, **15**, 17-23.

Pien, S., Fleury, D., Mylne, J.S., Crevillen, P., Inze, D., Avramova, Z., Dean, C. and Grossniklaus, U. (2008) *Arabidopsis* TRITHORAX1 dynamically regulates FLOWERING LOCUS C activation via histone 3 lysine 4 trimethylation. *Plant Cell*, **20**, 580-588.

Pinder, J.B., Attwood, K.M. and Dellaire, G. (2013) Reading, writing, and repair: the role of ubiquitin and the ubiquitin-like proteins in DNA damage signaling and repair. *Front Genet*, **4**, 45.

Plass, C., Pfister, S.M., Lindroth, A.M., Bogatyrova, O., Claus, R. and Lichter, P. (2013) Mutations in regulators of the epigenome and their connections to global chromatin patterns in cancer. *Nature Reviews, Genetics*, **14**, 765-780.

Prigent, C. and Dimitrov, S. (2003) Phosphorylation of serine 10 in histone H3, what for? *J Cell Sci*, **116**, 3677-3685.

Prunet, N., Morel, P., Negrutiu, I. and Trehin, C. (2009) Time to stop: flower meristem termination. *Plant Physiol*, **150**, 1764-1772.

Qian, Y.Q., Patel, D., Hartl, F.U. and McColl, D.J. (1996) Nuclear magnetic resonance solution structure of the human Hsp40 (HDJ-1) J-domain. *J Mol Biol*, **260**, 224-235.

-

Qin, F., Sakuma, Y., Tran, L.S., Maruyama, K., Kidokoro, S., Fujita, Y., Fujita, M., Umezawa, T., Sawano, Y., Miyazono, K., Tanokura, M., Shinozaki, K. and Yamaguchi-Shinozaki, K. (2008) *Arabidopsis* DREB2A-interacting proteins function as RING E3 ligases and negatively regulate plant drought stress-responsive gene expression. *Plant Cell*, **20**, 1693-1707.

Qiu, X.B., Shao, Y.M., Miao, S. and Wang, L. (2006) The diversity of the DnaJ/Hsp40 family, the crucial partners for Hsp70 chaperones. *Cell Mol Life Sci*, **63**, 2560-2570.

Ratcliffe, O.J., Kumimoto, R.W., Wong, B.J. and Riechmann, J.L. (2003) Analysis of the *Arabidopsis* MADS AFFECTING FLOWERING gene family: MAF2 prevents vernalization by short periods of cold. *Plant Cell*, **15**, 1159-1169.

Ratcliffe, O.J., Nadzan, G.C., Reuber, T.L. and Riechmann, J.L. (2001) Regulation of flowering in *Arabidopsis* by an FLC homologue. *Plant Physiol*, **126**, 122-132.

Richly, H. and Di Croce, L. (2011) The flip side of the coin: role of ZRF1 and histone H2A ubiquitination in transcriptional activation. *Cell Cycle*, **10**, 745-750.

Richly, H., Rocha-Viegas, L., Ribeiro, J.D., Demajo, S., Gundem, G., Lopez-Bigas, N., Nakagawa, T., Rospert, S., Ito, T. and Di Croce, L. (2010) Transcriptional activation of polycomb-repressed genes by ZRF1. *Nature*, **468**, 1124-1128.

Riefler, M., Novak, O., Strnad, M. and Schmulling, T. (2006) *Arabidopsis* cytokinin receptor mutants reveal functions in shoot growth, leaf senescence, seed size, germination, root development, and cytokinin metabolism. *Plant Cell*, **18**, 40-54.

Robzyk, K., Recht, J. and Osley, M.A. (2000) Rad6-dependent ubiquitination of histone H2B in yeast. *Science*, **287**, 501-504.

Roth, S.Y., Denu, J.M. and Allis, C.D. (2001) Histone acetyltransferases. *Annu Rev Biochem*, **70**, 81-120.

Roudier, F., Ahmed, I., Berard, C., Sarazin, A., Mary-Huard, T., Cortijo, S., Bouyer, D., Caillieux, E., Duvernois-Berthet, E., Al-Shikhley, L., Giraut, L., Despres, B., Drevensek, S., Barneche, F., Derozier, S., Brunaud, V., Aubourg, S., Schnittger, A., Bowler, C., Martin-Magniette, M.L., Robin, S., Caboche, M. and Colot, V. (2011) Integrative epigenomic mapping defines

four main chromatin states in *Arabidopsis*. *EMBO J*, **30**, 1928-1938.

Rupp, H.M., Frank, M., Werner, T., Strnad, M. and Schmulling, T. (1999) Increased steady state mRNA levels of the STM and KNAT1 homeobox genes in cytokinin overproducing *Arabidopsis thaliana* indicate a role for cytokinins in the shoot apical meristem. *Plant J*, **18**, 557-563.

Sabatini, S., Beis, D., Wolkenfelt, H., Murfett, J., Guilfoyle, T., Malamy, J., Benfey, P., Leyser, O., Bechtold, N., Weisbeek, P. and Scheres, B. (1999) An auxin-dependent distal organizer of pattern and polarity in the *Arabidopsis* root. *Cell*, **99**, 463-472.

Sabatini, S., Heidstra, R., Wildwater, M. and Scheres, B. (2003) SCARECROW is involved in positioning the stem cell niche in the *Arabidopsis* root meristem. *Genes Dev*, **17**, 354-358.

Sakamoto, T., Kamiya, N., Ueguchi-Tanaka, M., Iwahori, S. and Matsuoka, M. (2001) KNOX homeodomain protein directly suppresses the expression of a gibberellin biosynthetic gene in the tobacco shoot apical meristem. *Genes Dev*, **15**, 581-590.

Samach, A., Onouchi, H., Gold, S.E., Ditta, G.S., Schwarz-Sommer, Z., Yanofsky, M.F. and Coupland, G. (2000) Distinct roles of CONSTANS target genes in reproductive development of *Arabidopsis*. *Science*, **288**, 1613-1616.

Sanchez Mde, L., Caro, E., Desvoyes, B., Ramirez-Parra, E. and Gutierrez, C. (2008) Chromatin dynamics during the plant cell cycle. *Semin Cell Dev Biol*, **19**, 537-546.

Sanchez-Pulido, L., Devos, D., Sung, Z. and Calonje, M. (2008) RAWUL: A new ubiquitin-like domain in PRC1 Ring finger proteins that unveils putative plant and worm PRC1 orthologs. *BMC Genomics*, **9**, 308.

Sang, Y., Wu, M.F. and Wagner, D. (2009) The stem cell--chromatin connection. *Semin Cell Dev Biol*, **20**, 1143-1148.

Saracco, S.A., Hansson, M., Scalf, M., Walker, J.M., Smith, L.M. and Vierstra, R.D. (2009) Tandem affinity purification and mass spectrometric analysis of ubiquitylated proteins in *Arabidopsis*. *Plant J*, **59**, 344-358.

Sarkar, A.K., Luijten, M., Miyashima, S., Lenhard, M., Hashimoto, T., Nakajima, K., Scheres, B., Heidstra, R. and Laux, T. (2007) Conserved factors regulate signalling in *Arabidopsis thaliana* shoot and root stem cell

organizers. *Nature*, **446**, 811-814.

Schmidt, E.D., Guzzo, F., Toonen, M.A. and de Vries, S.C. (1997) A leucine-rich repeat containing receptor-like kinase marks somatic plant cells competent to form embryos. *Development*, **124**, 2049-2062.

Schmitz, R.J., Tamada, Y., Doyle, M.R., Zhang, X. and Amasino, R.M. (2009) Histone H2B deubiquitination is required for transcriptional activation of FLOWERING LOCUS C and for proper control of flowering in *Arabidopsis*. *Plant Physiol*, **149**, 1196-1204.

Schubert, D., Primavesi, L., Bishopp, A., Roberts, G., Doonan, J., Jenuwein, T. and Goodrich, J. (2006) Silencing by plant Polycomb-group genes requires dispersed trimethylation of histone H3 at lysine 27. *EMBO J*, **25**, 4638-4649.

Schultz, E.A. and Haughn, G.W. (1991) LEAFY, a homeotic gene that regulates inflorescence development in *Arabidopsis*. *Plant Cell*, **3**, 771-781.

Schwartz, Y.B. and Pirrotta, V. (2013) A new world of Polycombs: unexpected partnerships and emerging functions. *Nat Rev Genet*, **14**, 853-864.

Scofield, S., Dewitte, W. and Murray, J.A. (2014) STM sustains stem cell function in the *Arabidopsis* shoot apical meristem and controls KNOX gene expression independently of the transcriptional repressor AS1. *Plant Signal Behav*, **9**. pii: e28934.

Scofield, S., Dewitte, W., Nieuwland, J. and Murray, J.A. (2013) The *Arabidopsis* homeobox gene SHOOT MERISTEMLESS has cellular and meristem-organisational roles with differential requirements for cytokinin and CYCD3 activity. *Plant J*, **75**, 53-66.

Scofield, S. and Murray, J.A. (2006) KNOX gene function in plant stem cell niches. *Plant Mol Biol*, **60**, 929-946.

Searle, I., He, Y., Turck, F., Vincent, C., Fornara, F., Krober, S., Amasino, R.A. and Coupland, G. (2006) The transcription factor FLC confers a flowering response to vernalization by repressing meristem competence and systemic signaling in *Arabidopsis*. *Genes Dev*, **20**, 898-912.

Shafiq, S., Berr, A. and Shen, W.H. (2014) Combinatorial functions of diverse histone methylations in *Arabidopsis thaliana* flowering time regulation. *New Phytol*, **201**, 312-322.

Shema, E., Kim, J., Roeder, R.G. and Oren, M. (2011) RNF20 inhibits TFIIS-

facilitated transcriptional elongation to suppress pro-oncogenic gene expression. *Mol Cell*, **42**, 477-488.

Shema-Yaacoby, E., Nikolov, M., Haj-Yahya, M., Siman, P., Allemand, E., Yamaguchi, Y., Muchardt, C., Urlaub, H., Brik, A., Oren, M. and Fischle, W. (2013) Systematic identification of proteins binding to chromatin-embedded ubiquitylated H2B reveals recruitment of SWI/SNF to regulate transcription. *Cell Rep*, **4**, 601-608.

Shen, W.H. and Meyer, D. (2004) Ectopic expression of the NtSET1 histone methyltransferase inhibits cell expansion, and affects cell division and differentiation in tobacco plants. *Plant Cell Physiol*, **45**, 1715-1719.

Shen, W.H., Parmentier, Y., Hellmann, H., Lechner, E., Dong, A., Masson, J., Granier, F., Lepiniec, L., Estelle, M. and Genschik, P. (2002) Null mutation of AtCUL1 causes arrest in early embryogenesis in *Arabidopsis*. *Mol Biol Cell*, **13**, 1916-1928.

Shen, W.H. and Xu, L. (2009) Chromatin remodeling in stem cell maintenance in *Arabidopsis thaliana*. *Mol Plant*, **2**, 600-609.

Shilatifard, A. (2006) Chromatin modifications by methylation and ubiquitination: implications in the regulation of gene expression. *Annu Rev Biochem*, **75**, 243-269.

Shoji, W., Inoue, T., Yamamoto, T. and Obinata, M. (1995) MIDA1, a protein associated with Id, regulates cell growth. *J Biol Chem*, **270**, 24818-24825.

Simon, J.A. and Kingston, R.E. (2013) Occupying chromatin: Polycomb mechanisms for getting to genomic targets, stopping transcriptional traffic, and staying put. *Mol Cell*, **49**, 808-824.

Smalle, J. and Vierstra, R.D. (2004) The ubiquitin 26S proteasome proteolytic pathway. *Annu Rev Plant Biol*, **55**, 555-590.

Smyth, D.R., Bowman, J.L. and Meyerowitz, E.M. (1990) Early flower development in *Arabidopsis*. *Plant Cell*, **2**, 755-767.

Sozzani, R., Maggio, C., Varotto, S., Canova, S., Bergounioux, C., Albani, D. and Cella, R. (2006) Interplay between *Arabidopsis* activating factors E2Fb and E2Fa in cell cycle progression and development. *Plant Physiol*, **140**, 1355-1366.

Spannhoff, A., Hauser, A.T., Heinke, R., Sippl, W. and Jung, M. (2009) The emerging therapeutic potential of histone methyltransferase and demethylase

inhibitors. *ChemMedChem*, **4**, 1568-1582.

Sridhar, V.V., Kapoor, A., Zhang, K., Zhu, J., Zhou, T., Hasegawa, P.M., Bressan, R.A. and Zhu, J.K. (2007) Control of DNA methylation and heterochromatic silencing by histone H2B deubiquitination. *Nature*, **447**, 735-738.

Srikanth, A. and Schmid, M. (2011) Regulation of flowering time: all roads lead to Rome. *Mol Life Sci* **68**, 2013-2037.

Stone, S.L., Kwong, L.W., Yee, K.M., Pelletier, J., Lepiniec, L., Fischer, R.L., Goldberg, R.B. and Harada, J.J. (2001) LEAFY COTYLEDON2 encodes a B3 domain transcription factor that induces embryo development. *Proc Natl Acad Sci U S A*, **98**, 11806-11811.

Su, Y.H., Liu, Y.B. and Zhang, X.S. (2011) Auxin-cytokinin interaction regulates meristem development. *Mol Plant*, **4**, 616-625.

Sun, B., Xu, Y., Ng, K.H. and Ito, T. (2009) A timing mechanism for stem cell maintenance and differentiation in the *Arabidopsis* floral meristem. *Genes Dev*, **23**, 1791-1804.

Tai, H.H., Tai, G.C. and Beardmore, T. (2005) Dynamic histone acetylation of late embryonic genes during seed germination. *Plant Mol Biol*, **59**, 909-925.

Takei, K., Sakakibara, H. and Sugiyama, T. (2001) Identification of genes encoding adenylate isopentenyltransferase, a cytokinin biosynthesis enzyme, in *Arabidopsis thaliana*. *J Biol Chem*, **276**, 26405-26410.

Tamada, Y., Yun, J.-Y., Woo, S.C. and Amasino, R.M. (2009) *Arabidopsis* TRITHORAX-RELATED 7 is required for methylation of Lysine 4 of histone H3 and for transcriptional activation of FLOWERING LOCUS C. *Plant Cell*, **21**, 3257-3269.

Tanny, J.C., Erdjument-Bromage, H., Tempst, P. and Allis, C.D. (2007) Ubiquitylation of histone H2B controls RNA polymerase II transcription elongation independently of histone H3 methylation. *Genes Dev*, **21**, 835-847.

Tatematsu, K., Kumagai, S., Muto, H., Sato, A., Watahiki, M.K., Harper, R.M., Liscum, E. and Yamamoto, K.T. (2004) MASSUGU2 encodes Aux/IAA19, an auxin-regulated protein that functions together with the transcriptional activator NPH4/ARF7 to regulate differential growth responses of hypocotyl and formation of lateral roots in Arabidopsis thaliana. *Plant Cell*, **16**, 379-393.

-

Taverna, S.D., Li, H., Ruthenburg, A.J., Allis, C.D. and Patel, D.J. (2007) How chromatin-binding modules interpret histone modifications: lessons from professional pocket pickers. *Nat Struct Mol Biol*, **14**, 1025-1040.

Telfer, A., Bollman, K.M. and Poethig, R.S. (1997) Phase change and the regulation of trichome distribution in *Arabidopsis thaliana*. *Development*, **124**, 645-654.

Tian, H., Jia, Y., Niu, T., Yu, Q. and Ding, Z. (2014) The key players of the primary root growth and development also function in lateral roots in *Arabidopsis*. *Plant Cell Reports*, **33**, 745-753.

Tian, H., Wabnik, K., Niu, T., Li, H., Yu, Q., Pollmann, S., Vanneste, S., Govaerts, W., Rolcík, J., Geisler, M., Friml, J. and Ding, Z. (2014) WOX5–IAA17 feedback circuit-mediated cellular auxin response is crucial for the patterning of root stem cell niches in *Arabidopsis*. *Mol Plant*, **7**, 277-289.

Tian, Q., Nagpal, P. and Reed, J.W. (2003) Regulation of *Arabidopsis* SHY2/IAA3 protein turnover. *Plant J* **36**, 643-651.

Tiwari, S.B., Shen, Y., Chang, H.C., Hou, Y., Harris, A., Ma, S.F., McPartland, M., Hymus, G.J., Adam, L., Marion, C., Belachew, A., Repetti, P.P., Reuber, T.L. and Ratcliffe, O.J. (2010) The flowering time regulator CONSTANS is recruited to the FLOWERING LOCUS T promoter via a unique cis-element. *New Phytol*, **187**, 57-66.

To, J.P., Haberer, G., Ferreira, F.J., Deruere, J., Mason, M.G., Schaller, G.E., Alonso, J.M., Ecker, J.R. and Kieber, J.J. (2004) Type-A *Arabidopsis* response regulators are partially redundant negative regulators of cytokinin signaling. *Plant Cell*, **16**, 658-671.

To, J.P. and Kieber, J.J. (2008) Cytokinin signaling: two-components and more. *Trends Plant Sci*, **13**, 85-92.

Tsuda, K., Ito, Y., Sato, Y. and Kurata, N. (2011) Positive autoregulation of a KNOX gene is essential for shoot apical meristem maintenance in rice. *Plant Cell*, **23**, 4368-4381.

Turck, F., Roudier, F., Farrona, S., Martin-Magniette, M.L., Guillaume, E., Buisine, N., Gagnot, S., Martienssen, R.A., Coupland, G. and Colot, V. (2007) *Arabidopsis* TFL2/LHP1 specifically associates with genes marked by trimethylation of histone H3 lysine 27. *PLoS Genet*, **3**, e86.

van den Berg, C., Willemsen, V., Hage, W., Weisbeek, P. and Scheres, B. (1995)

Cell fate in the *Arabidopsis* root meristem determined by directional signalling. *Nature*, **378**, 62-65.

van den Berg, C., Willemsen, V., Hendriks, G., Weisbeek, P. and Scheres, B. (1997) Short-range control of cell differentiation in the *Arabidopsis* root meristem. *Nature*, **390**, 287-289.

Veley, K.M. and Michaels, S.D. (2008) Functional redundancy and new roles for genes of the autonomous floral-promotion pathway. *Plant Physiol*, **147**, 682-695.

Venglat, S.P., Dumonceaux, T., Rozwadowski, K., Parnell, L., Babic, V., Keller, W., Martienssen, R., Selvaraj, G. and Datla, R. (2002) The homeobox gene BREVIPEDICELLUS is a key regulator of inflorescence architecture in *Arabidopsis*. *Proc Natl Acad Sci U S A* **99**, 4730-4735.

Verdeil, J.L., Alemanno, L., Niemenak, N. and Tranbarger, T.J. (2007) Pluripotent versus totipotent plant stem cells: dependence versus autonomy? *Trends Plant Sci*, **12**, 245-252.

Verkest, A., Manes, C.L., Vercruysse, S., Maes, S., Van Der Schueren, E., Beeckman, T., Genschik, P., Kuiper, M., Inzé, D. and De Veylder, L. (2005) The cyclin-dependent kinase inhibitor KRP2 controls the onset of the endoreduplication cycle during *Arabidopsis* leaf development through inhibition of mitotic CDKA;1 kinase complexes. *Plant Cell*, **17**, 1723-1736.

Vicente-Carbajosa, J. and Carbonero, P. (2005) Seed maturation: developing an intrusive phase to accomplish a quiescent state. *Int J Dev Biol*, **49**, 645-651.

Vroemen, C.W., Mordhorst, A.P., Albrecht, C., Kwaaitaal, M.A. and de Vries, S.C. (2003) The CUP-SHAPED COTYLEDON3 gene is required for boundary and shoot meristem formation in *Arabidopsis*. *Plant Cell*, **15** 1563-1577.

Wahls, W.P., Swenson, G. and Moore, P.D. (1991) Two hypervariable minisatellite DNA binding proteins. *Nucleic Acids Res*, **19**, 3269-3274.

Wang, L., Brown, J.L., Cao, R., Zhang, Y., Kassis, J.A. and Jones, R.S. (2004) Hierarchical recruitment of polycomb group silencing complexes. *Mol Cell*, **14**, 637-646.

Weake, V.M. and Workman, J.L. (2008) Histone ubiquitination: triggering gene activity. *Mol Cell*, **29**, 653-663.

Weigel, D., Alvarez, J., Smyth, D.R., Yanofsky, M.F. and Meyerowitz, E.M.

(1992) LEAFY controls floral meristem identity in *Arabidopsis*. *Cell*, **69**, 843-859.

West, M.H.P. and Bonner, W.M. (1980) Histone 2B can be modified by the attachment of ubiquitin. *Nucleic Acids Res*, **8**, 4671-4680.

Wigge, P.A. (2011) FT, a mobile developmental signal in plants. *Curr Biol*, **21**, R374-378.

Wittig, B., Dorbic, T. and Rich, A. (1991) Transcription is associated with Z-DNA formation in metabolically active permeabilized mammalian cell nuclei. *Proc Natl Acad Sci U S A*, **88**, 2259-2263.

Wolters, H. and Jurgens, G. (2009) Survival of the flexible: hormonal growth control and adaptation in plant development. *Nat Rev Genet*, **10**, 305-317.

Wood, A., Krogan, N.J., Dover, J., Schneider, J., Heidt, J., Boateng, M.A., Dean, K., Golshani, A., Zhang, Y., Greenblatt, J.F., Johnston, M. and Shilatifard, A. (2003) Bre1, an E3 ubiquitin ligase required for recruitment and substrate selection of Rad6 at a promoter. *Mol Cell*, **11**, 267-274.

Wu, J., Chen, Y., Lu, L.Y., Wu, Y., Paulsen, M.T., Ljungman, M., Ferguson, D.O. and Yu, X. (2011) Chfr and RNF8 synergistically regulate ATM activation. *Nat Struct Mol Biol*, **18**, 761-768.

Wu, L., Lee, S.Y., Zhou, B., Nguyen, U.T., Muir, T.W., Tan, S. and Dou, Y. (2013) ASH2L regulates ubiquitylation signaling to MLL: trans-regulation of H3 K4 methylation in higher eukaryotes. *Mol Cell*, **49**, 1108-1120.

Wu, M., Wang, P.F., Lee, J.S., Martin-Brown, S., Florens, L., Washburn, M. and Shilatifard, A. (2008) Molecular regulation of H3K4 trimethylation by Wdr82, a component of human Set1/COMPASS. *Mol Cell Biol*, **28**, 7337-7344.

Wyce, A., Xiao, T., Whelan, K.A., Kosman, C., Walter, W., Eick, D., Hughes, T.R., Krogan, N.J., Strahl, B.D. and Berger, S.L. (2007) H2B ubiquitylation acts as a barrier to Ctk1 nucleosomal recruitment prior to removal by Ubp8 within a SAGA-related complex. *Mol Cell*, **27**, 275-288.

Xiao, T., Kao, C.F., Krogan, N.J., Sun, Z.W., Greenblatt, J.F., Osley, M.A. and Strahl, B.D. (2005) Histone H2B ubiquitylation is associated with elongating RNA polymerase II. *Mol Cell Biol*, **25**, 637-651

Xu, C.R., Liu, C., Wang, Y.L., Li, L.C., Chen, W.Q., Xu, Z.H. and Bai, S.N. (2005) Histone acetylation affects expression of cellular patterning genes in the

-

Arabidopsis root epidermis. *Proc Natl Acad Sci U S A*, **102**, 14469-14474.

Xu, L., Menard, R., Berr, A., Fuchs, J., Cognat, V., Meyer, D. and Shen, W.H. (2009) The E2 ubiquitin-conjugating enzymes, AtUBC1 and AtUBC2, play redundant roles and are involved in activation of FLC expression and repression of flowering in *Arabidopsis thaliana*. *Plant J*, **57**, 279-288.

Xu, L. and Shen, W.H. (2008) Polycomb silencing of KNOX genes confines shoot stem cell niches in *Arabidopsis*. *Curr Biol*, **18**, 1966-1971.

Yadav, R.K., Perales, M., Gruel, J., Girke, T., Jonsson, H. and Reddy, G.V. (2011) WUSCHEL protein movement mediates stem cell homeostasis in the *Arabidopsis* shoot apex. *Genes Dev*, **25**, 2025-2030.

Yamagishi, K., Tatematsu, K., Yano, R., Preston, J., Kitamura, S., Takahashi, H., McCourt, P., Kamiya, Y. and Nambara, E. (2009) CHOTTO1, a double AP2 domain protein of *Arabidopsis thaliana*, regulates germination and seedling growth under excess supply of glucose and nitrate. *Plant Cell Physiol*, **50**, 330-340.

Yanai, O., Shani, E., Dolezal, K., Tarkowski, P., Sablowski, R., Sandberg, G., Samach, A. and Ori, N. (2005) *Arabidopsis* KNOXI proteins activate cytokinin biosynthesis. *Curr Biol*, **15**, 1566-1571.

Yang, C., Bratzel, F., Hohmann, N., Koch, M., Turck, F. and Calonje, M. (2013) VAL- and AtBMI1-mediated H2Aub initiate the switch from embryonic to postgerminative growth in *Arabidopsis*. *Curr Biol*, **23**, 1324-1329.

Yao, X.Z. and Shen, W.-H. (2011) Crucial function of histone lysine methylation in plant reproduction. *Chinese Sci Bull* **56** 3493-3499.

Yu, C.W., Liu, X., Luo, M., Chen, C., Lin, X., Tian, G., Lu, Q., Cui, Y. and Wu, K. (2011) HISTONE DEACETYLASE6 interacts with FLOWERING LOCUS D and regulates flowering in *Arabidopsis*. *Plant Physiol*, **156**, 173-184.

Yu, H., Xu, Y., Tan, E.L. and Kumar, P.P. (2002) AGAMOUS-LIKE 24, a dosage-dependent mediator of the flowering signals. *Proc Natl Acad Sci U S A*, **99**, 16336-16341.

Zhang, K., Sridhar, V.V., Zhu, J., Kapoor, A. and Zhu, J.K. (2007) Distinctive core histone post-translational modification patterns in *Arabidopsis thaliana*. *PLoS One*, **2**, e1210.

Zhang, S., Lockshin, C., Herbert, A., Winter, E. and Rich, A. (1992) Zuotin, a

putative Z-DNA binding protein in *Saccharomyces cerevisiae*. *EMBO J*, **11**, 3787-3796.

Zhang, X., Germann, S., Blus, B.J., Khorasanizadeh, S., Gaudin, V. and Jacobsen, S.E. (2007) The *Arabidopsis* LHP1 protein colocalizes with histone H3 Lys27 trimethylation. *Nat Struct Mol Biol*, **14**, 869-871.

Zhang, Y. (2003) Transcriptional regulation by histone ubiquitination and deubiquitination. *Genes Dev*, **17**, 2733-2740.

Zhang, Z., Jones, A., Joo, H.Y., Zhou, D., Cao, Y., Chen, S., Erdjument-Bromage, H., Renfrow, M., He, H., Tempst, P., Townes, T.M., Giles, K.E., Ma, L. and Wang, H. (2013) USP49 deubiquitinates histone H2B and regulates cotranscriptional pre-mRNA splicing. *Genes Dev*, **27**, 1581-1595.

Zhao, Z., Andersen, S.U., Ljung, K., Dolezal, K., Miotk, A., Schultheiss, S.J. and Lohmann, J.U. (2010) Hormonal control of the shoot stem-cell niche. *Nature*, **465**, 1089-1092.

Zhu, B., Zheng, Y., Pham, A.-D., Mandal, S.S., Erdjument-Bromage, H., Tempst, P. and Reinberg, D. (2005) Monoubiquitination of human histone H2B: the factors involved and their roles in HOX gene regulation. *Mol Cell*, **20**, 601-611.

Zhu, Y., Weng, M., Yang, Y., Zhang, C., Li, Z., Shen, W.H. and Dong, A. (2011) *Arabidopsis* homologues of the histone chaperone ASF1 are crucial for chromatin replication and cell proliferation in plant development. *Plant J*, **66**, 443-455.

-

VII. ABBREVIATIONS

-

AEBSF	4-(2-Aminoethyl) benzenesulfonyl fluoride hydrochloride
AP	Ammonium persulfate
ATP	Adenosine Triphosphate
Amp	Ampicillin
BLAST	Basic Local Alignment Search Tool
bp	base pair
cm	centimeter
Col	Columbia
ChIP	Chromatin Immunoprecipitation
Da	Dalton
DAPI	4',6-Diamidino-2-phenylindole
DAS	Days After Stratification
DNA	DeoxyriboNucleic Acid
DTT	dithiothreitol
EDTA	Ethylene Diamine Tetraacetic Acid
EGTA	Ethylene Glycol Tetraacetic Acid
GFP	Green Fluorescent Protein
GST	Glutathione-S-Transferase
g	gram
h	hour
His	histidine
Hyg	Hygromycin
Kan	Kanamycin
kb	kilo base pairs
LD	Long Day
µ	micro
m	milli
M	Molar (mole/liter)
min	minutes
MS	Murashige and Skoog
MW	molecular weight
NCBI	National Center for Bioinformation
nm	nanometer

-

OD_{600}	Optical Density, measured at 600 nm
PAGE	PolyAcrylamide Gel Electrophoresis
PBS	Phosphate Buffer Saline
PCR	Polymerase Chain Reaction
PI	Propidium Iodide
PMSF	Phenyl Methyl Sulphonyl Fluoride
PRC1	Polycomb Repression Complex 1
PVDF	PolyVinylidene DiFluoride
qPCR	quantitative Polymerase Chain Reaction
RNA	RiboNucleic Acid
rpm	rotations per minute
RT	room temperature
RT PCR	Reverse Transcription Polymerase Chain Reaction
SANT	Swi3, Ada2, NcoR1 and TFIIIB
SD	Short Day
SDS	Sodium Dodecyl Sulphate
SEM	Scanning Electron Microscope
TBS	Tris Buffer Saline
T-DNA	Transfer-DNA
TE	Tris-EDTA Buffer
TEMED	N,N,N',N',-tetramethyl-ethylene.1,2-diamine
Tris	Tris(hydroxymethyl) aminomethane
TTBS	Triton-Tris Buffer Saline
UBD	Ubiquitin Binding Domain
Ub	ubiquitin
YC	C-terminal half of yellow fluorescent protein
YFP	Yellow Fluorescent Protein
YN	N-terminal half of yellow fluorescent protein
ZRF1	ZUO1-Related Factor 1

RESUME

Des études chez les animaux ont montré que ZRF1 a une fonction lectrice au niveau de H2AK119ub1 dans la dérépression de gènes réprimés par polycomb. Deux gènes homologues au gène humain ZRF1 ont été identifiés dans le génome d'*Arabidopsis*, et ont par la suite été appelés *AtZRF1a* et *AtZRF1b*. La caractérisation fonctionnelle de ces gènes n'a pas encore été rapportée.

Ma premier objectif était d'obtenir des connaissances générales sur *AtZRF1a* et *AtZRF1b*. Tous les deux sont exprimés dans des plantes d'*Arabidopsis* et la protéine AtZRF1b est localisée dans le noyau et dans le cytoplasme. En plus, nous avons trouvé que la protéine AtZRF1b lie H2Aub1 avec les mêmes caractéristiques que la protéine ZRF1 humaine.

J'ai utilisé les outils génétiques puissants disponibles pour *Arabidopsis* pour étudier la fonction d'*AtZRF1a* et *AtZRF1b.* Plusieurs lignées d'insertion de T-DNA indépendantes ont été identifiées. A cause d'une rédondance fonctionnelle, des mutants simples n'ont pas de défauts de développement évidents. C'est pourquoi j'ai étudié un mutant double qui montre une perte de fonction pour les deux gènes *AtZRF1a* et *AtZRF1b*. Ce double mutant révèle des rôles importants pour ces gènes dans la croissance et le développement, qui vont de la prolifération et la différenciation cellulaire jusqu'au contrôle du temps de floraison.

J'ai ensuite étudié les rôles d'*AtZRF1a* et *AtZRF1b* dans la régulation de la transcription et j'ai constaté que *AtZRF1a* et *AtZRF1b* ont une fonction similaire a PRC1.

Finalement, j'ai étudié les niveaux de H3K4me3, H3K27me3 et H2Aub1 dans la chromatine de certains gènes dont l'expression est perturbée dans les doubles mutants. Les résultats montrent que la dé-ubiquitination de H2Aubi1 n'est pas un événement majeur dans la régulation de la transcription chez *Arabidopsis*.

SUMMARY

Studies in animals showed that ZRF1 can read the histone H2AK119ub1 modification in the derepression of polycomb-repressed genes. Two homologs of human ZRF1 have been identified in the *Arabidopsis* genome, and hereinafter are named *AtZRF1a* and *AtZRF1b*. So far, their functional characterization had not been reported yet.

My first objective was to acquire basic knowledge about *AtZRF1a* and *AtZRF1b.* Both genes are broadly expressed in *Arabidopsis* plants and the AtZRF1b protein is localized in the nucleus and the cytoplasm. Moreover, we found that AtZRF1b binds H2Aub1 with characteristics similar to those previously reported for the human ZRF1 protein.

I subsequently used the powerful genetic tools available in *Arabidopsis* to investigate the functions of *AtZRF1a* and *AtZRF1b*. Several independent T-DNA insertion *Arabidopsis* mutant lines were identified. Because of functional redundancy, single mutants have no obvious developmental defects. I therefore focused on double mutants displaying loss of function of both *AtZRF1a* and *AtZRF1b*. The study of a double mutant revealed important roles for these genes in plant growth and development ranging from cell proliferation and differentiation to flowering time control.

I then investigated the roles of *AtZRF1a* and *AtZRF1b* in gene transcriptional regulation and found that *AtZRF1a* and *AtZRF1b* function in a way that is partially similar to PRC1 function. Lastly, I investigated H3K4me3, H3K27me3 and H2Aub1 levels in the chromatin regions of some expression-perturbed genes in double mutants. The results show that ZRF1-mediated deubiquitination of H2Aub1 is not a major event in transcriptional regulation in *Arabidopsis*.

frontiers in
PLANT SCIENCE

REVIEW ARTICLE
published: 13 March 2014
doi: 10.3389/fpls.2014.00083

Dynamic regulation and function of histone monoubiquitination in plants

Jing Feng and Wen-Hui Shen*

Institut de Biologie Moléculaire des Plantes, UPR2357 CNRS, Université de Strasbourg, Strasbourg, France

Edited by:
Hongyong Fu, Institute of Plant and Microbial Biology – Academia Sinica, Taiwan

Reviewed by:
Keqiang Wu, National Taiwan University, Taiwan
Hongyong Fu, Institute of Plant and Microbial Biology – Academia Sinica, Taiwan

***Correspondence:**
Wen-Hui Shen, Institut de Biologie Moléculaire des Plantes, UPR2357 CNRS, Université de Strasbourg, 12 rue du Général Zimmer, 67084 Strasbourg Cedex, France
e-mail: wen-hui.shen@ibmp-cnrs.unistra.fr

Polyubiquitin chain deposition on a target protein frequently leads to proteasome-mediated degradation whereas monoubiquitination modifies target protein property and function independent of proteolysis. Histone monoubiquitination occurs in chromatin and is in nowadays recognized as one critical type of epigenetic marks in eukaryotes. While H2A monoubiquitination (H2Aub1) is generally associated with transcription repression mediated by the Polycomb pathway, H2Bub1 is involved in transcription activation. H2Aub1 and H2Bub1 levels are dynamically regulated *via* deposition and removal by specific enzymes. We review knows and unknowns of dynamic regulation of H2Aub1 and H2Bub1 deposition and removal in plants and highlight the underlying crucial functions in gene transcription, cell proliferation/differentiation, and plant growth and development. We also discuss crosstalks existing between H2Aub1 or H2Bub1 and different histone methylations for an ample mechanistic understanding.

Keywords: chromatin, epigenetics, ubiquitin, histone monoubiquitination, transcription regulation, plant development, *Arabidopsis thaliana*

INTRODUCTION

Ubiquitin (Ub) and Ub-like (e.g., SUMO) proteins constitute a family of modifiers that are linked covalently to target proteins. Although ubiquitination (also called ubiquitylation or ubiquitinylation) first came to light in the context of protein destruction, it is now clear that ubiquitination can also carry out proteolysis-independent functions. Ubiquitination can alter biochemical, molecular and/or subcellular localization activities of a target protein. The first ubiquitinated protein to be described was histone H2A in calf thymus, a finding dated more than 36 years ago (Goldknopf et al., 1975; Hunt and Dayhoff, 1977). Yet, only more recently have the underlying mechanisms and regulatory functions of histone ubiquitination begun to emerge (reviewed in Zhang, 2003; Shilatifard, 2006; Weake and Workman, 2008; Braun and Madhani, 2012; Pinder et al., 2013). Histones are highly alkaline proteins, found in the nuclei of eukaryotic cell, which package and order the DNA into structural units named nucleosomes. A nucleosome is composed of roughly 146 bp of DNA wrapping around the histone octamer comprising two molecules each of the four core histones H2A, H2B, H3, and H4 (Luger et al., 1997). Histone monoubiquitination together with other types of posttranslational modifications, e.g., acetylation, methylation, phosphorylation, and SUMOylation, can modulate nucleosome/chromatin structure and DNA accessibility and thus regulate diverse DNA-dependent processes, such as genome replication, repair, and transcription (Zhang, 2003; Shilatifard, 2006; Weake and Workman, 2008; Braun and Madhani, 2012; Pinder et al., 2013).

Ubiquitination occurs *via* conjugation of the C-terminal residue of Ub to the side chain of a lysine (K) residue of the substrate/acceptor protein, a reaction involving three coordinated enzymatic activities (reviewed in Hershko and Ciechanover, 1998). Ub is first activated by an ATP-dependent reaction involving the Ub-activating enzyme E1, then conjugated to the active site cysteine residue of the Ub-conjugating (UBC) enzyme E2, and finally transferred to the target K residue of the substrate protein by the Ub-protein isopeptide ligase E3. Most organisms have only one E1, but dozens of different E2 and hundreds up to thousands of different E3 enzymes, providing the need in coping with effective substrate specificity (Hua and Vierstra, 2011; Braun and Madhani, 2012). Identification and characterization of E3s and some E2s involved in histone ubiquitination had been a key for understanding biological functions of histone ubiquitination in various organisms. Because of its suitability for genomics, genetics, and cellular and molecular biological approaches, *Arabidopsis thaliana* is an ideal model to investigate histone ubiquitination functions. In this review, we focus on this reference plant to expose current progress made on ubiquitination of different types of histones.

H2B MONOUBIQUITINATION IN *Arabidopsis*

GENOME-WIDE DISTRIBUTION OF H2Bub1

Monoubiquitinated H2B (H2Bub1) was first discovered in mouse cells and was estimated to represent about 1–2% of total cellular H2B (West and Bonner, 1980). Later, H2Bub1 was detected widely throughout eukaryotes spanning from yeast to humans and plants (Zhang, 2003; Shilatifard, 2006; Sridhar et al., 2007; Zhang et al., 2007a; Weake and Workman, 2008). The ubiquitination site is mapped to a highly conserved K residue, H2BK123 in budding yeast, H2BK119 in fission yeast, H2BK120 in humans, and H2BK143 in *Arabidopsis*.

Genome-wide analysis revealed that in *Arabidopsis* as in animals H2Bub1 is associated with active genes distributed throughout the genome and marks chromatin regions notably in combination with histone H3 trimethylated on K4 (H3K4me3) and/or with H3K36me3 (Roudier et al., 2011). During early photomorphogenesis, gene upregulation was found to be associated with H2Bub1 enrichment whereas gene downregulation did not show detectable correlation with any H2Bub1 level changes (Bourbousse et al., 2012). In general, H2Bub1 is considered to represent an active chromatin mark broadly involved in genome transcription regulation.

ENZYMES INVOLVED IN REGULATION OF H2Bub1 LEVELS

The budding yeast Rad6 (radiation sensitivity protein 6) was the first factor identified and shown to work as an E2 enzyme involved in catalyzing H2Bub1 formation both *in vitro* and *in vivo* (Robzyk et al., 2000). It contains a highly conserved catalytic UBC domain of approximately 150 amino acids in length with an active-site cysteine for linking Ub. The E3 enzyme working together with Rad6 in catalyzing H2Bub1 formation in budding yeast is Bre1 (Brefeldin-A sensitivity protein 1), which contains a C3HC4-type RING finger domain typical for all E3s (Hwang et al., 2003; Wood et al., 2003). The depletion of either Rad6 or Bre1 eliminates genome-wide H2Bub1 and causes yeast cell growth defects (Robzyk et al., 2000; Hwang et al., 2003; Wood et al., 2003). Human contains at least two homologs of Rad6, namely hHR6A and hHR6B, and two homologs of Bre1, namely RNF20/hBRE1A and RNF40/hBRE1B (Kim et al., 2005; Zhu et al., 2005). In *Arabidopsis*, three homologs of Rad6, namely UBC1, UBC2, and UBC3, were identified and UBC1 and UBC2 but not UBC3 were shown to be redundantly responsible for H2Bub1 formation *in planta* (Cao et al., 2008; Gu et al., 2009; Xu et al., 2009). The two Bre1 homologs HUB1 (HISTONE MONOUBIQUITINATION 1) and HUB2 work non-redundantly, possibly as a hetero-tetramer composed of two copies of HUB1 and two copies of HUB2, in catalyzing H2Bub1 formation in *Arabidopsis* (Fleury et al., 2007; Liu et al., 2007; Cao et al., 2008). H2Bub1 levels are drastically reduced or undetectable in Western blot analysis in the loss-of-function *hub1* and *hub2* single mutants as well as in the *hub1 hub2* and *ubc1 ubc2* double mutants, but are unaffected in the *ubc1*, *ubc2,* and *ubc3* single mutants or in the *ubc1 ubc3* and *ubc2 ubc3* double mutants (Cao et al., 2008; Gu et al., 2009; Xu et al., 2009).

H2Bub1 levels are also regulated by deubiquitination enzymes. Two Ub-specific proteases, Ubp8 and Ubp10, are involved in deubiquitination of H2Bub1 in budding yeast. Strikingly, while Ubp8 acts as a component of the SAGA (Spt-Ada-Gcn5-acetyltransferase) complex specifically in H2Bub1 deubiquitination in transcription activation, Ubp10 functions independently of SAGA and primarily acts in Sir-mediated silencing of telomeric and rDNA regions (reviewed in Weake and Workman, 2008). In human, USP22 acts as Ubp8 ortholog in a SAGA complex in H2Bub1 deubiquitination (Weake and Workman, 2008). In *Arabidopsis*, although a SAGA complex remains uncharacterized so far, the Ub protease UBP26/SUP32 has been shown to deubiquitinate H2Bub1 involved in both heterochromatic silencing (Sridhar et al., 2007) and transcription activation of the *FLC* (*FLOWERING* LOCUS C) gene (Schmitz et al., 2009). More recently, the otubain-like deubiquitinase OTLD1 was reported as implicated in deubiquitination of H2BUb1 and repression of *At5g39160*, a gene of unknown function (Krichevsky et al., 2011).

ROLE OF H2Bub1 IN FLOWERING TIME REGULATION

The timing of flowering is critical for the reproductive success of plants. As compared to wild type, the *hub1* and *hub2* single mutants as well as the *hub1 hub2* and *ubc1 ubc2* double mutants exhibit an early flowering phenotype whereas but the *ubc1*, *ubc2,* and *ubc3* single mutants and the *ubc1 ubc3* and *ubc2 ubc3* double mutants have a normal phenotype (Cao et al., 2008; Gu et al., 2009; Xu et al., 2009). This early flowering phenotype is detectable under both long-day and short-day photoperiod plant growth conditions. Molecular analyses of the mutants indicate that H2Bub1 controls flowering time primarily through transcriptional activation of *FLC* (**Figure 1**). *FLC* encodes a key transcription repressor involved in both the autonomous/developmental and vernalization flowering pathways, and its active transcription is associated with several histone marks, e.g., H3K4me3, H3K36me2/3 and H2Bub1 (reviewed in Berr et al., 2011). In the early flowering mutants *hub1*, *hub2*, *hub1 hub2*, and *ubc1*

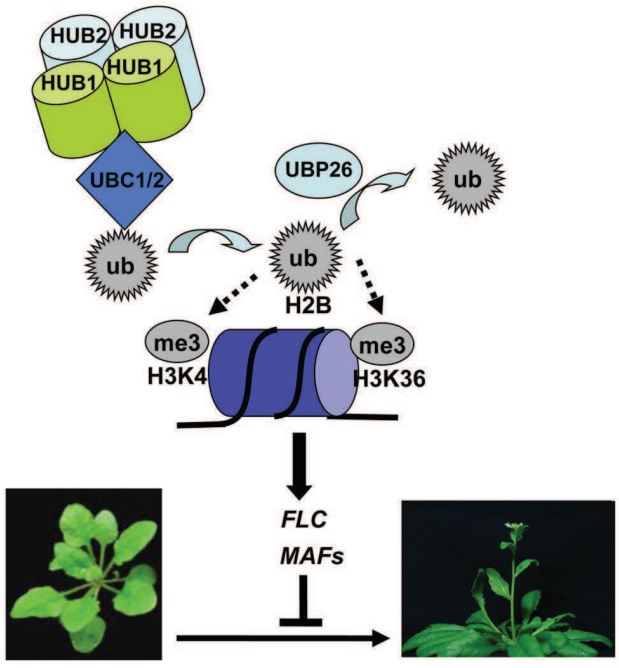

FIGURE 1 | A proposed model for deposition and removal of histone H2B monoubiquitination in transcriptional activation of *FLC* and *MAFs* in flowering time regulation. In this model, HUB1 and HUB2 form a heterotetramer and recruit UBC1 or UBC2 to *FLC*/*MAFs* chromatin, leading to transfer of a ubiquitin (ub) monomer from UBC1 or UBC2 onto H2B. H2Bub1 formation enhances H3K4me3 deposition by methyltransferases, together promoting transcription initiation. UBP26 removes ubiquitin on H2B, favoring H3K36me3 deposition in promoting transcription elongation. Active transcription of *FLC/MAFs* represses *Arabidopsis* flowering, a transition from vegetative to reproductive plant development.

ubc2, *FLC* expression levels are reduced and the *FLC* chromatin shows reduced H2Bub1 levels (Cao et al., 2008; Gu et al., 2009). The loss-of-function mutant *ubp26*/*sup32* showed also an early flowering phenotype and reduced *FLC* expression but an elevated level of H2Bub1 in the *FLC* chromatin (Schmitz et al., 2009), indicating that not only H2Bub1 formation but also H2Bub1 removal are necessary for *FLC* transcription. Accompanying H2Bub1 reduction compromised levels of H3K4me3 and to a less extent H3K36me2 were detected at *FLC* in *hub1* and *ubc1 ubc2* (Cao et al., 2008), and reduced level of H3K36me3 but elevated level of H3K27me3 was observed at *FLC* in *ubp26/sup32* (Schmitz et al., 2009). On parallels to the knowledge in yeast, it was proposed that the UBC-HUB-mediated H2Bub1 formation is necessary for H3K4me3 deposition at transcription initiation whereas UBP26/SUP32-mediated H2Bub1 removal is required for H3K36me3 deposition during transcription elongation (Cao et al., 2008; Schmitz et al., 2009). Nonetheless, this hierarchy of histone modifications needs to be cautioned because multiple factors are involved in H3K4me3 and H3K36me2/3 depositions and the SDG8 (SET DOMAIN GROUP 8)-mediated H3K36me2/3 deposition remarkably override H3K4me2/3 deposition in *FLC* transcription (Yao and Shen, 2011; Shafiq et al., 2014). Besides *FLC*, *Arabidopsis* has five *FLC* paralogs, namely *MAF1* (*MADS AFFECTING FLOWERING 1*), *MAF2, MAF3*, *MAF4* and *MAF5*. Some *MAFs* are also downregulated in the early flowering mutants *hub1*, *hub2*, *hub1 hub2*, *ubc1 ubc2,* and *ubp26/sup32* (Cao et al., 2008; Gu et al., 2009; Schmitz et al., 2009; Xu et al., 2009). Thus, H2Bub1 may also regulate flowering time through control of *MAF* gene expression under some plant growth conditions.

H2Bub1 FUNCTION IN OTHER PROCESSES

In addition to flowering, many other processes also involve H2Bub1 as evidenced by studies of the *Arabidopsis hub1* and *hub2* mutants. The *hub* mutants display reduced seed dormancy associated with reduced expression of several dormancy-related genes, including *DOG1* (*DELAY OF GERMINATION 1*), *ATS2* (*ACYLTRANSFERASE 2*), *NCED9* (*NINE-CIS-EPOXYCAROTENOID DIOXYGENASE 9*), *PER1* (*CYSTEINE PEROXIREDOXIN 1*), and *CYP707A2* (Liu et al., 2007). At vegetative growth stages, the *hub* mutants exhibit pale leaf coloration, modified leaf shape, reduced rosette biomass, and inhibited root growth (Fleury et al., 2007). Cell cycle genes, particularly some key regulators of the G2-to-M transition, are downregulated, which could largely explain the plant growth defects of the *hub* mutants (Fleury et al., 2007). A more recent study shows that several circadian clock genes, including *CCA1* (*CIRCADIAN CLOCK ASSOCIATED 1*), *ELF4* (*EARLY FLOWERING 4*) and *TOC1* (*TIMING OF CAB EXPRESSION 1*), are downregulated and their chromatin regions contain lower levels of H2Bub1 in the *hub* mutants, suggesting that H2Bub1 may contribute to the regulation of plant growth fitness to environment through expression modulation of some circadian clock genes (Himanen et al., 2012). It is worth to note that SDG2-mediated H3K4me3 deposition is also required for expression of several circadian clock genes (e.g., *CCA1, TOC1*) and the *hub* mutants exhibit reduced levels of H3K4me3 in chromatin regions of the circadian clock genes (Himanen et al., 2012; Malapeira et al., 2012).

During photomorphogenesis, hundreds of genes show upregulation associated with H2Bub1 enrichment in their chromatin in response to light exposure (Bourbousse et al., 2012). Strikingly, over 50% of these genes gain H2Bub1 enrichment upon the 1 h of illumination, illustrating the highly dynamic nature of H2Bub1 deposition during a likely cell division-independent genome regrogramming process. In contrast to the above discussed cases, in this study the H2Bub1 changes is neither accompanied by any detectable changes of H3K36me3 nor required for H3K4me3 enrichment following six hours of light exposure (Bourbousse et al., 2012). In line with the function of H2Bub1 in gene activation in response to light, the *hub1-3* mutant seedlings are overly light sensitive, exhibiting a photobleaching phenotype (Bourbousse et al., 2012).

The *hub1* mutants also show increased susceptibility to the necrotrophic fungal pathogens *Botrytis cinerea* and *Alternaria brassicicola* (Dhawan et al., 2009). Precise role of H2Bub1 in plant defense against pathogens still remains largely unclear. Structure defects, e.g., thinner cell walls and altered surface cutin and wax compositions, together with impaired induction of some defense genes might have partly contributed to the increased susceptibility to pathogen infection in the *hub* mutant plants (Dhawan et al., 2009; Ménard et al., 2014). It is worthy noting that the *sdg8* mutants impaired in H3K36me3 deposition also display reduced resistance to necrotrophic fungal pathogen infection (Berr et al., 2010, 2012; Palma et al., 2010). It will be interesting to study in future research whether a trans-histone crosstalk between H2Bub1 and H3K36me3 acts on transcription induction in plant response to pathogens.

MECHANISMS OF H2Bub1 IN TRANSCRIPTION REGULATION

So far only limited information is available concerning how H2Bub1 enzymes are recruited to the target chromatin. The evolutionarily conserved PAF1 (Polymerase Associated Factor 1) complex interacts with Pol II (RNA polymerase II) and plays a role as a "platform" for association of enzymes involved in H2bub1, H3K4me3, and H3K36me2/3 deposition, linking histone modifications with active transcription (Shilatifard, 2006; Weake and Workman, 2008; Berr et al., 2011; Braun and Madhani, 2012). A direct interaction between PAF1 complex and Rad6-Bre1 has been detected and shown as required for catalyzing H2Bub1 formation (Xiao et al., 2005). As in yeast and animals, deletion or knockdown of PAF1 components markedly reduces H2Bub1 in *Arabidopsis* (Schmitz et al., 2009). Genetic analysis shows that *HUB2* and *ELF8* encoding a PAF1 subunit act in a same floral-repression pathway in *Arabidopsis* flowering time regulation (Gu et al., 2009). Although physical interaction between UBC-HUB and PAF1 needs future investigation, interactions were observed between UBC and HUB (Cao et al., 2008) and between HUB and MED21 (mediator complex subunit 21), a subunit of the evolutionarily conserved Mediator complex (Dhawan et al., 2009). Mediator complex is associated with both general transcription factors and Pol II and is essential for activator-dependent transcription in all eukaryotes (for a recent review, see Carlsten et al., 2013). Nevertheless, the aforementioned

interactors are generally involved in Pol II transcribed genes and thus cannot fully explain why UBC-HUB targets some but not all active genes. It is reasonable to speculate that UBC-HUB recruitment might also involve some gene-specific yet uncharacterized factors.

The next question is how H2Bub1 affects transcription. In yeast and animals, H2Bub1 can promote transcription elongation by enhancing the recruitment of RNA Pol II and by facilitating nucleosome removal through interplay with FACT (facilitates chromatin transcription), an evolutionarily conserved histone chaperone complex (Pavri et al., 2006; Tanny et al., 2007). FACT acts on displacement of H2A/H2B dimer from a nucleosome core, facilitating transcription elongation on chromatin template. In *Arabidopsis*, FACT genetically interacts with HUB1 and plays critical roles in multiple plant developmental processes (Lolas et al., 2010). Yet its precise interplay with H2Bub1 in transcription regulation needs future investigations.

Alternatively or additionally, H2Bub1 may regulate transcription indirectly through crosstalk with H3K4me3 and H3K36me2/3 (Shilatifard, 2006; Weake and Workman, 2008; Berr et al., 2011; Braun and Madhani, 2012). In line with this idea, lack of H2Bub1 in *Arabidopsis* impairs H3K4me3 and H3K36me2 formation in chromatin at *FLC* and clock genes (Cao et al., 2008; Himanen et al., 2012), and elevated H2Bub1 inhibits H3K36me3 formation in the *FLC* chromatin (Schmitz et al., 2009). Nevertheless, in contrast to the requirement of H2Bub1 for genome-wide H3K4me3 formation in yeast, lack of H2Bub1 in *Arabidopsis* barely affects global H3K4me2/3 and H3K36me2/3 levels, as evidenced by Western blot analysis (Cao et al., 2008; Dhawan et al., 2009; Gu et al., 2009) as well as by ChIP (chromatin immunoprecipitation) analysis of light responsive genes during photomorphogenesis (Bourbousse et al., 2012). It is currently unclear to which extent applies the crosstalk of H2Bub1 with H3K4me2/3 and H3K36me2/3 in *Arabidopsis* gene transcription regulation and what are the molecular mechanisms underlying the crosstalk.

Finally, while H2Bub1 is generally associated with active gene transcription, it can also regulate transcription repression in a chromatin context-dependent manner. The *ubp26/sup32* mutant shows release of transgene and transposon silencing (Sridhar et al., 2007) as well as elevated expression of *PHE1* (*PHERES1*) associated with seed developmental defects (Luo et al., 2008). It has been shown that the silencing release is accompanied by reduction of H3K9me2 and of siRNA-mediated DNA methylation and the *PHE1* expression elevation is associated with a reduced level of H3K27me3. Nevertheless, whether these changes of repressive marks are directly linked with H2Bub1 still need to be investigated.

H2A MONOUBIQUITINATION IN *Arabidopsis*

PRESENCE OF H2Aub1

In contrast to H2Bub1, H2Aub1 has not been found in yeast and has been generally implicated in transcription repression in animal cells (Weake and Workman, 2008; Braun and Madhani, 2012). Albeit its early discovery and high abundance (about 5–15% of the total H2A) in animal cells (Goldknopf et al., 1975; Hunt and Dayhoff, 1977; Zhang, 2003), H2Aub1 function has only more recently begun to be elucidated, thanking to the first identification of the human PRC1 (Polycomb repressive complex 1) component Ring1B (also known as Ring2 and RNF2) as a E3 involved in catalyzing H2Aub1 formation (Wang et al., 2004). In *Arabidopsis*, H2Aub1 was undetectable in a large-scale analysis of histone post-translational modifications by mass spectrometry (Sridhar et al., 2007; Zhang et al., 2007a) and had been thought for a long time to be non-existent (Weake and Workman, 2008). However, five PRC1-like RING-finger proteins, namely AtRING1a, AtRING1b, AtBMI1a, AtBMI1b, and AtBMI1c, have been identified in *Arabidopsis* (Sanchez-Pulido et al., 2008; Xu and Shen, 2008). More recent immunodetection and *in vitro* enzyme activity assays have revealed that these RING-finger proteins are effectively involved in catalyzing H2Aub1 formation in *Arabidopsis* (Bratzel et al., 2010; Li et al., 2011; Yang et al., 2013).

PRC2 AND PRC1 IN H2Aub1 DEPOSITION

Polycomb group (PcG) proteins, first identified in *Drosophila* as repressors of homeotic (*Hox*) genes, are nowadays known to act in multiprotein complexes in transcription repression of a large number of genes in many multicellular organisms including plants (Bemer and Grossniklaus, 2012; Molitor and Shen, 2013; Schwartz and Pirrotta, 2013; Simon and Kingston, 2013). The most intensively studied complexes are PRC1 and PRC2. In *Drosophila*, PRC2 is composed of four core subunits, namely Ez (Enhancer of zeste), Suz12 (Suppressor of zeste 12), Esc (Extra sex combs) and N55 (a 55 kDa WD40 repeat protein), and PRC1 also contains four main subunits, namely Pc (Polycomb), Ph (Polyhomeotic), Psc (Posterior sex combs) and Ring1 (also known as dRing). In mammals, alternate subunit compositions create larger families of related PRC2-type and PRC1-type complexes (Schwartz and Pirrotta, 2013; Simon and Kingston, 2013). Nevertheless, defined biochemical activities of PRC2 and PRC1 are conserved from flies to humans. The classical model proposes a sequential mode of action of the two complexes: PRC2 catalyzes H3K27me3 formation, and PRC1 recognizes the H3K27me3 mark and further mediates downstream H2Aub1 deposition. The PRC1 components, acting as E3 ligases in H2Aub1 formation, are RING-finger proteins: Ring1 in *Drosophila* and Ring1A and Ring1B in human (Braun and Madhani, 2012; Schwartz and Pirrotta, 2013).

In *Arabidopsis*, the four PRC2 core components are highly conserved (**Figure 2**) and encoded by small gene families, and their function in H3K27me3 deposition and transcription repression have been intensively studied (Bemer and Grossniklaus, 2012). In contrast, PRC1 compositions are drastically diverged in plants as compared to animals (Molitor and Shen, 2013). No sequence homologue of Ph could be identified in plants so far. LHP1 (LIKE HETEROCHROMATIN PROTEIN 1), also known as TFL2 (TERMINAL FLOWER 2), binds H3K27me3 and may play a Pc-like function (Turck et al., 2007; Zhang et al., 2007b). This remarkably differs from the distinct roles of HP1 and Pc in animals, where HP1 binds H3K9me3 involved in hetereochromatin formation whereas Pc binds H3K27me3 involved in PRC1-mediated silencing in euchromatin. The best conservations found about PRC1 core components are from RING-finger proteins structured by a RING domain at N-terminus and a Ub-like RAWUL domain at C-terminus (Sanchez-Pulido et al., 2008; Xu and Shen, 2008).

These RING-finger proteins can be classified into two phylogenic groups: the first group comprises *Drosophila* Ring1, human Ring1A and Ring1B, and *Arabidopsis* AtRING1a and AtRING1b; the second group comprises *Drosophila* Psc, human Bmi1, and *Arabidopsis* AtBMI1a, AtBMI1b, and AtBMI1c. Consistent with their sequence conservation, AtRING1a, AtRING1b, AtBMI1a, and AtBMI1b each can ubiquitinate H2A *in vitro*, and loss of function of *AtBMI1a* and *AtBMI1b* causes H2Aub1 reduction *in planta* (Bratzel et al., 2010; Yang et al., 2013).

ROLE OF PRC1-LIKE RING-FINGER PROTEINS IN STEM CELL MAINTENANCE

Plant growth and development largely depend on stem cells located in SAM (shoot apical meristem) and RAM (root apical meristem), whose activities are fine-tuned by multiple families of chromatin factors (Sang et al., 2009; Shen and Xu, 2009). The first uncovered biological role of the *Arabidopsis* PRC1-like RING-finger proteins are on the regulation of SAM activity (Xu and Shen, 2008). While the single loss-of-function mutants *Atring1a* and *Atring1b* have a normal phenotype, the double mutant *Atring1a Atring1b* exhibits enlarged SAM, fasciated stem, and ectopic-meristem formation in cotyledons and leaves. This indicates that *AtRING1a* and *AtRING1b* play a redundant role in stable repression of stem cell activity to allow appropriate lateral organ differentiation. The balances between stem cell maintenance and cell differentiation for organ formation are controlled by specific transcription factors, including KNOX (Class I KNOTTED1-like homeobox) proteins. Strikingly, several *KNOX* genes, e.g., *STM* (*SHOOT-MERISTEMLESS*), *BP* (*BREVIPEDICELLUS*)/*KNAT1*, *KNAT2* and *KNAT6,* are upregulated in *Atring1a Atring1b* (Xu and Shen, 2008). Ectopic expression of *KNOX* genes colocalizes with and precedes ectopic meristem formation. It has been proposed that AtRING1a/b acts as a crucial PRC1 component in conjunction with PRC2 in repression of *KNOX* genes to promote lateral organ formation in the SAM (**Figure 2A**).

ROLE OF PRC1-LIKE RING-FINGER PROTEINS IN EMBRYONIC CELL FATE DETERMINACY

Further characterization of the ectopic meristem structures observed in *Atring1a Atring1b* unravels that these callus structures exhibit embryonic traits (Chen et al., 2010). The *Atbmi1a Atbmi1b* mutant also displays derepression of embryonic traits (Bratzel et al., 2010; Chen et al., 2010). Embryonic callus formation has been observed broadly in somatic tissues of cotyledons, leaves, shoots and roots of the mutant plants. Treatment with an auxin transport inhibitor can inhibit embryonic callus formation in *Atring1a Atring1b*, indicating that a normal auxin gradient is required for somatic embryo formation in the mutant (Chen et al., 2010). Both *Atring1a Atring1b* and *Atbmi1a Atbmi1b* mutants exhibit elevated expression of several key embryonic regulatory genes, including *ABI3* (*ABSCISIC ACID INSENSITIVE 3*), *AGL15* (*AGAMOUS LIKE 15*), *BBM* (*BABYBOOM*), *FUS3* (*FUSCA 3*), *LEC1* (*LEAFY COTYLEDON 1*), and *LEC2* (Bratzel et al., 2010; Chen et al., 2010). It is likely that derepression of these regulatory genes together with *KNOX* has contributed to the ectopic meristem and embryonic callus formation in somatic tissues of the *Atring1a Atring1b* and *Atbmi1a Atbmi1b* mutants (**Figure 2B**). The VAL (VP1/ABI3-LIKE) transcription factors can physically interact with AtBMI1 proteins and the *val1 val2* mutant exhibits comparable phenotype to *Atbmi1a Atbmi1b*, suggesting that VAL and AtBMI1 proteins may form complexes in repression of embryonic regulatory genes during vegetative development (Yang et al., 2013). Notably, loss of VAL or AtBMI1 causes H2Aub1 reduction in chromatin regions at *ABI3*, *BBM*, *FUS3* and *LEC1* but not *STM* (Yang et al., 2013). Future investigation is necessary to clarify whether AtBMI1 and AtRING1 proteins repress *KNOX* transcription *via* H2Aub1 deposition or other independent chromatin remodeling mechanisms.

ROLE OF PRC1-LIKE RING-FINGER PROTEINS IN SEED GERMINATION

Seed germination defines the entry into a new generation of the plant life cycle. It is generally accepted that the process of germination starts with water uptake followed by seed coat rupture and is completed following radicle protrusion (Bentsink and Koornneef, 2008). During the very early phase, the embryonic growth program remains latent and can be reinstated in response to unfavorable environmental cues. With the attainment of photosynthetic competence, the irreversible transition to autotrophic growth is accomplished and embryonic program is stably suppressed. A recent study (Molitor et al., 2014) has identified the *Arabidopsis* PHD-domain H3K4me3-binding AL (ALFIN1-like) proteins as interactors of AtBMI1 and AtRING1 proteins and has demonstrated a crucial function of chromatin state switch in establishment of seed developmental gene repression during seed germination (**Figure 2C**). Loss of AL6 and AL7 as well as loss of AtBMI1a and AtBMI1b retards seed germination and causes transcriptional derepression and a delayed chromatin state switch from H3K4me3 to H3K27me3 enrichment of seed developmental genes, including *ABI3* and *DOG1*. The germination delay phenotype of the *al6 al7* and *Atbmi1a Atbmi1b* mutants is more pronounced under osmotic stress (Molitor et al., 2014), suggesting that AL PHD-PRC1 complexes may participate in regulation of seed germination in response to environmental cues.

ROLE OF PRC1-LIKE RING-FINGER PROTEINS IN OTHER PROCESSES

AtBMI1a and AtBMI1b, also named DRIP1 (DREB2A-INTERACTING PROTEIN 1) and DRIP2, had been reported first as E3 ligases involved in ubiquitination of DREB2A (DEHYDRATION-RESPONSIVE ELEMENT BINDING PROTEIN 2A), a transcription factor controlling water deficit-inducible gene expression (Qin et al., 2008). The *drip1 drip2* mutant shows enhanced expression of water deficit-inducible genes and more tolerance to drought (Qin et al., 2008). Overexpression of *AtBMI1c* accelerates flowering time, which is associated with reduction of *FLC* expression (Li et al., 2011). In addition to SAM maintenance defects and derepression of embryonic traits, the *Atring1a Atring1b* mutant also displays homeotic conversions of floral tissues (Xu and Shen, 2008). Therefore, more precise functions and underlying molecular mechanisms for the PRC1-like RING-finger proteins are still waiting to be uncovered

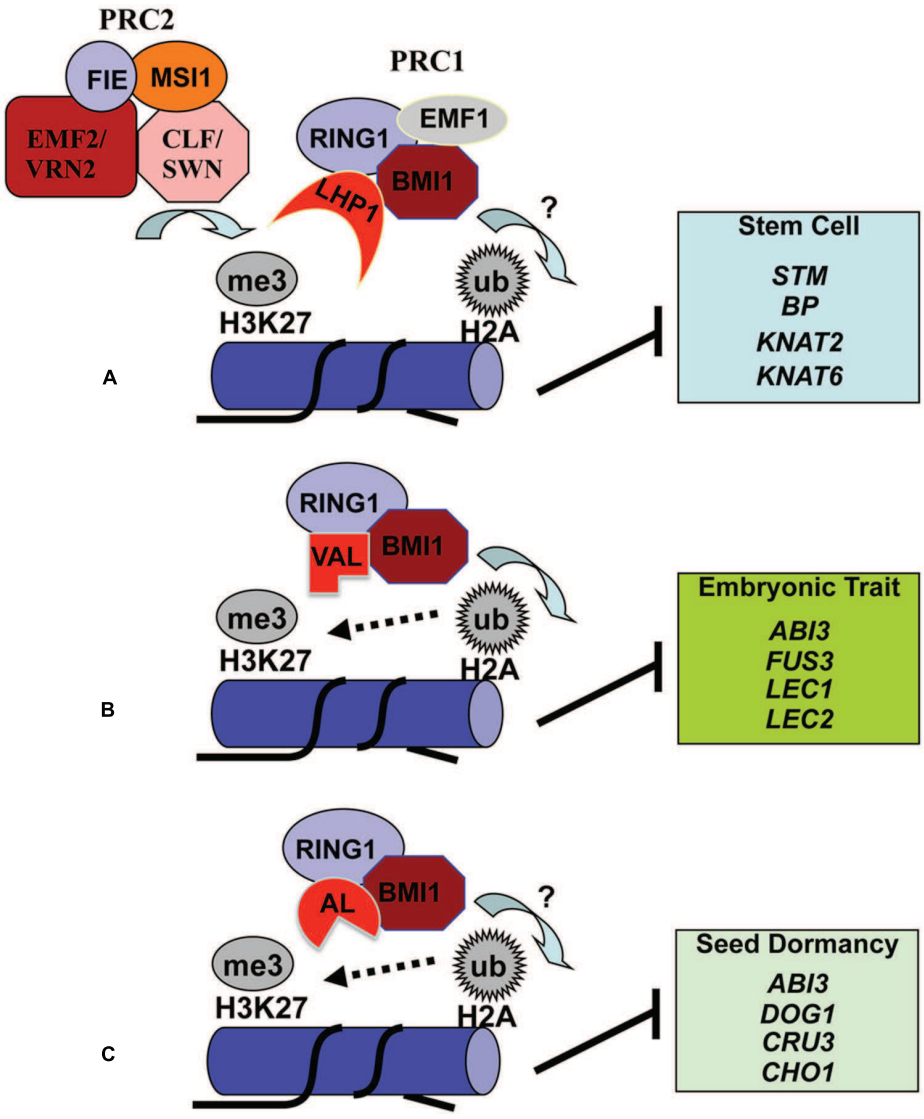

FIGURE 2 | Proposed models for histone H2A monoubiquitination deposition in transcriptional repression of varied target genes. The *Arabidopsis* PRC1-like RING-finger proteins AtRING1a/b (RING1) and AtBMI1a/b/c (BMI1) have the E3 ligase activity in catalyzing H2A monoubiquitination (H2Aub1). Comparable to the classical model of sequential PRC2 then PRC1 action in Polycomb silencing in animal cells, the *Arabidopsis* PRC1-like protein LHP1 binds H3K27me3 pre-deposited by the evolutionarily conserved PRC2 complexes and recruits RING1, BMI1 and possibly also EMF1 through protein–protein interactions **(A)**. This combinatorial action by PRC2 then PRC1 likely plays a broad role in suppression of numerous genes, including the key stem cell regulatory *KNOX* genes that need to be stably repressed during lateral organ development. The transcription factor VAL is involved in recruitment of BMI1 and RING1 in suppression of embryonic trait genes in somatic cells **(B)**. AL proteins bind BMI1 and RING1 and play important roles in suppression of several key seed dormancy regulatory genes to promote germination **(C)**. H3K27me3 deposition at embryonic/seed genes is enhanced by VAL/AL-PRC1 **(B,C)**, unraveling a non-canonical crosstalk between H3K27me3 and H2Aub1. The question marks indicate that H2Aub1 deposition in the specified target gene chromatin still requires future investigation.

during plant development and in plant response to environmental changes.

MECHANISMS OF PRC1-LIKE RING-FINGER PROTEINS IN TRANSCRIPTION REPRESSION

H2Aub1 function in plants is primarily evidenced through investigation of roles of the *Arabidopsis* PRC1-like RING-finger proteins (Xu and Shen, 2008; Bratzel et al., 2010; Chen et al., 2010; Li et al., 2011; Yang et al., 2013). Although these RING-finger proteins act nicely *in vitro* as E3 ligases, their *in vivo* functions in H2Aub1 deposition are still poorly documented. H2Aub1 level in *Arabidopsis* seems very low because large-scale analyses of either the histone-enriched or the Ub-affinity-purified protein preparations fail to detect H2Aub1 (Maor et al., 2007; Sridhar et al., 2007; Zhang et al., 2007a; Manzano et al., 2008; Saracco et al., 2009). H2Aub1 has been detected only by using specific antibodies, and in this case *AtBMI1* genes have been shown to act as positive regulators for H2Aub1 deposition in *Arabidopsis* plants (Bratzel et al.,

2010; Li et al., 2011; Yang et al., 2013). It is unknown whether any deubiquitinases might cause low levels of H2Aub1 in *Arabidopsis*. In animal cells, several deubiquitinases are characterized as specific for H2Aub1 (Weake and Workman, 2008; Simon and Kingston, 2013). Future characterization of *Arabidopsis* H2Aub1 deubiquitinases may provide useful information regarding regulatory mechanisms of H2Aub1 dynamics.

AtRING1 and AtBMI1 proteins physically interact each other and with the H3K27me3-binding protein LHP1 (Xu and Shen, 2008; Bratzel et al., 2010; Chen et al., 2010), providing a possible recruitment mechanism similar to the classical sequential PRC2 then PRC1 silencing pathway in animal cells. However, the *Atring1a Atring1b*, *Atbmi1a Atbmi1b,* or *Atbmi1a Atbmi1b Atbmi1c* mutant exhibits much more severe phenotypic defects than the *lhp1* mutant does, and *lhp1* enhances the *Atring1a Atring1b* mutant defects. It is thus apparent that AtRING1 and AtBMI1 proteins also act independently from LHP1. Recent identification of the transcriptional regulator VAL as AtBMI1-binding protein and of AL as AtRING1 and AtBMI1 interactor provides some novel insight about recruitment mechanisms (Yang et al., 2013; Molitor et al., 2014). It is particular intriguing that loss of AtBMI1 impairs H3K27me3 enrichment at seed developmental genes during seed germination and vegetative growth (Yang et al., 2013; Molitor et al., 2014). It has also been reported that loss of LHP1 impairs H3K27me3 enrichment at flower gene loci in roots (Derkacheva et al., 2013). These recent findings challenge the classic hierarchical paradigm where PRC2-mediated H3K27me3 deposition precedes PRC1 recruitment (**Figure 2**). It is obvious that future investigations are necessary to better understand the composition and function of different PRC1-like complexes in *Arabidopsis*.

CONCLUSIONS AND PERSPECTIVES

Studies over the last few years in the model plant *Arabidopsis* have greatly advanced our knowledge about the roles of H2Aub1 and H2Bub1 in transcription regulation in plant growth and development. In view of additional functions described in animal cells for both H2Aub1 and H2Bub1 in DNA damage repair (Bergink et al., 2006; Marteijn et al., 2009; Chernikova et al., 2010; Ginjala et al., 2011; Moyal et al., 2011; Nakamura et al., 2011), it is anticipated that more roles of H2Aub1 and H2Bub1 in plant response to environmental stresses are waiting to be uncovered. Mutagenesis of enzymes involved in H2Aub1 and H2Bub1 deposition or removal is required to address the question whether these enzymes effectively exert their biological functions *via* H2Aub1 and H2Bub1. Identification and characterization of factors associated with these different enzymes will be essential for understanding molecular mechanisms of their recruitment and function at specific targets within the genome. We need to know whether and how their function is spatially and temporally integrated with plant development. Genome-wide tools need to be further explored to provide a global view of links among enzyme or associated factor binding, H2Aub1/H2Bub1 enrichment, H3 methylation, and Pol II occupation. Crosstalks between H2Aub1 or H2Bub1 and different H3 methylations need to be addressed for chromatin context specificity.

In addition to H2Aub1 and H2Bub1, ubiquitinated H1, H3, and H4 are also found in *Arabidopsis* (Maor et al., 2007; Manzano et al., 2008; Saracco et al., 2009). H3 ubiquitination catalyzed by Rtt101-Mms1 in yeast and by Cul4-DDB1 in human has been recently shown to play an important role in the histone chaperone Asf1-mediated nucleosome assembly (Han et al., 2013). *Arabidopsis* contains a conserved family of CULLINs and CUL4-DDB1 complexes are reported (Shen et al., 2002; Hua and Vierstra, 2011). The Asf1 homologues in *Arabidopsis* are also identified (Zhu et al., 2011). It remains to be investigated whether CUL4-DDB and AtASF1 collaboratively act on nucleosome assembly *via* H3 ubiquitination in epigenetic regulation in *Arabidopsis*.

ACKNOWLEDGMENTS

The work in Wen-Hui Shen laboratory was supported by the French "Centre National de la Recherche Scientifique" (CNRS) and in part by the French "Agence Nationale de la Recherche" (ANR-08-BLAN-0200-CSD7; ANR-12-BSV2-0013-02). Jing Feng received a fellowship from the China Scholarship Council of the Ministry of Education of P. R. China.

REFERENCES

Bemer, M., and Grossniklaus, U. (2012). Dynamic regulation of Polycomb group activity during plant development. *Curr. Opin. Plant Biol.* 15, 523–529. doi: 10.1016/j.pbi.2012.09.006

Bentsink, L., and Koornneef, M. (2008). Seed dormancy and germination. *Arabidopsis Book* 6:e0119. doi: 10.1199/tab.0119

Bergink, S., Salomons, F. A., Hoogstraten, D., Groothuis, T. A. M., De Waard, H., Wu, J., et al. (2006). DNA damage triggers nucleotide excision repair-dependent monoubiquitylation of histone H2A. *Genes Dev.* 20, 1343–1352. doi: 10.1101/gad.373706

Berr, A., McCallum, E. J., Alioua, A., Heintz, D., Heitz, T., and Shen, W.-H. (2010). *Arabidopsis* histone methyltransferase SET DOMAIN GROUP 8 mediates induction of the jasmonate/ethylene pathway genes in plant defense response to necrotrophic fungi. *Plant Physiol.* 154, 1403–1414. doi: 10.1105/tpc.110.079962

Berr, A., Ménard, R., Heitz, T., and Shen, W.-H. (2012). Chromatin modification and remodelling: a regulatory landscape for the control of *Arabidopsis* defence responses upon pathogen attack. *Cell. Microbiol.* 14, 829–839. doi: 10.1111/j.1462-5822.2012.01785.x

Berr, A., Shafiq, S., and Shen, W.-H. (2011). Histone modifications in transcriptional activation during plant development. *Biochim. Biophys. Acta* 1809, 567–576. doi: 10.1016/j.bbagrm.2011.07.001

Bourbousse, C., Ahmed, I., Roudier, F., Zabulon, G., Blondet, E., Balzergue, S., et al. (2012). Histone H2B monoubiquitination facilitates the rapid modulation of gene expression during *Arabidopsis* photomorphogenesis. *PLoS Genet.* 8:e1002825. doi: 10.1371/journal.pgen.1002825

Bratzel, F., López-Torrejón, G., Koch, M., Del Pozo, J. C., and Calonje, M. (2010). Keeping cell identity in *Arabidopsis* requires PRC1 RING-finger homologs that catalyze H2A monoubiquitination. *Curr. Biol.* 20, 1853–1859. doi: 10.1016/j.cub.2010.09.046

Braun, S., and Madhani, H. D. (2012). Shaping the landscape: mechanistic consequences of ubiquitin modification of chromatin. *EMBO Rep.* 13, 619–630. doi: 10.1038/embor.2012.78

Cao, Y., Dai, Y., Cui, S., and Ma, L. (2008). Histone H2B monoubiquitination in the chromatin of FLOWERING LOCUS C regulates flowering time in *Arabidopsis*. *Plant Cell* 20, 2586–2602. doi: 10.1105/tpc.108.062760

Carlsten, J. O. P., Zhu, X., and Gustafsson, C. M. (2013). The multitalented mediator complex. *Trends Biochem. Sci.* 38, 531–537. doi: 10.1016/j.tibs.2013.08.007

Chen, D., Molitor, A., Liu, C., and Shen, W.-H. (2010). The *Arabidopsis* PRC1-like RING-finger proteins are necessary for repression of embryonic traits during vegetative growth. *Cell Res.* 20, 1332–1344. doi: 10.1038/cr.2010.151

Chernikova, S. B., Dorth, J. A., Razorenova, O. V., Game, J. C., and Brown, J. M. (2010). Deficiency in Bre1 impairs homologous recombination repair and cell

cycle checkpoint response to radiation damage in mammalian cells. *Radiat. Res.* 174, 558–565. doi: 10.1667/RR2184.1

Derkacheva, M., Steinbach, Y., Wildhaber, T., Mozgova, I., Mahrez, W., Nanni, P., et al. (2013). *Arabidopsis* MSI1 connects LHP1 to PRC2 complexes. *EMBO J.* 32, 2073–2085. doi: 10.1038/emboj.2013.145

Dhawan, R., Luo, H., Foerster, A. M., Abuqamar, S., Du, H.-N., Briggs, S. D., et al. (2009). HISTONE MONOUBIQUITINATION1 interacts with a subunit of the Mediator complex and regulates defense against necrotrophic fungal pathogens in *Arabidopsis*. *Plant Cell* 21, 1000–1019. doi: 10.1105/tpc.108.062364

Fleury, D., Himanen, K., Cnops, G., Nelissen, H., Boccardi, T. M., Maere, S., et al. (2007). The *Arabidopsis thaliana* homolog of yeast BRE1 has a function in cell cycle regulation during early leaf and root growth. *Plant Cell* 19, 417–432. doi: 10.1105/tpc.106.041319

Ginjala, V., Nacerddine, K., Kulkarni, A., Oza, J., Hill, S. J., Yao, M., et al. (2011). BMI1 is recruited to DNA breaks and contributes to DNA damage-induced H2A ubiquitination and repair. *Mol. Cell. Biol.* 31, 1972–1982. doi: 10.1128/MCB.00981-10

Goldknopf, I. L., Taylor, C. W., Baum, R. M., Yeoman, L. C., Olson, M. O., Prestayko, A. W., et al. (1975). Isolation and characterization of protein A24, a "histone-like" non-histone chromosomal protein. *J. Biol. Chem.* 250, 7182–7187.

Gu, X., Jiang, D., Wang, Y., Bachmair, A., and He, Y. (2009). Repression of the floral transition via histone H2B monoubiquitination. *Plant J.* 57, 522–533. doi: 10.1111/j.1365-313X.2008.03709.x

Han, J., Zhang, H., Zhang, H., Wang, Z., Zhou, H., and Zhang, Z. (2013). A Cul4 E3 ubiquitin ligase regulates histone hand-off during nucleosome assembly. *Cell* 155, 817–829. doi: 10.1016/j.cell.2013.10.014

Hershko, A., and Ciechanover, A. (1998). The ubiquitin system. *Annu. Rev. Biochem.* 67, 425–479. doi: 10.1146/annurev.biochem.67.1.425

Himanen, K., Woloszynska, M., Boccardi, T. M., De Groeve, S., Nelissen, H., Bruno, L., et al. (2012). Histone H2B monoubiquitination is required to reach maximal transcript levels of circadian clock genes in *Arabidopsis*. *Plant J.* 72, 249–260. doi: 10.1111/j.1365-313X.2012.05071.x

Hua, Z., and Vierstra, R. D. (2011). The Cullin-RING ubiquitin-protein ligases. *Annu. Rev. Plant Biol.* 62, 299–334. doi: 10.1146/annurev-arplant-042809-112256

Hunt, L. T., and Dayhoff, M. O. (1977). Amino-terminal sequence identity of ubiquitin and the nonhistone component of nuclear protein A24. *Biochem. Biophys. Res. Commun.* 74, 650–655. doi: 10.1016/0006-291X(77)90352-7

Hwang, W. W., Venkatasubrahmanyam, S., Ianculescu, A. G., Tong, A., Boone, C., and Madhani, H. D. (2003). A conserved RING finger protein required for histone H2B monoubiquitination and cell size control. *Mol. Cell* 11, 261–266. doi: 10.1016/S1097-2765(02)00826-2

Kim, J., Hake, S. B., and Roeder, R. G. (2005). The human homolog of yeast BRE1 functions as a transcriptional coactivator through direct activator interactions. *Mol. Cell* 20, 759–770. doi: 10.1016/j.molcel.2005.11.012

Krichevsky, A., Zaltsman, A., Lacroix, B., and Citovsky, V. (2011). Involvement of KDM1C histone demethylase–OTLD1 otubain-like histone deubiquitinase complexes in plant gene repression. *Proc. Natl. Acad. Sci. U.S.A.* 108, 11157–11162. doi: 10.1073/pnas.1014030108

Li, W., Wang, Z., Li, J., Yang, H., Cui, S., Wang, X., et al. (2011). Overexpression of AtBMI1C, a Polycomb group protein gene, accelerates flowering in *Arabidopsis*. *PLoS ONE* 6:e21364. doi: 10.1371/journal.pone.0021364

Liu, Y., Koornneef, M., and Soppe, W. J. J. (2007). The absence of histone H2B monoubiquitination in the *Arabidopsis* hub1 (rdo4) mutant reveals a role for chromatin remodeling in seed dormancy. *Plant Cell* 19, 433–444. doi: 10.1105/tpc.106.049221

Lolas, I. B., Himanen, K., Grønlund, J. T., Lynggaard, C., Houben, A., Melzer, M., et al. (2010). The transcript elongation factor FACT affects *Arabidopsis* vegetative and reproductive development and genetically interacts with HUB1/2. *Plant J.* 61, 686–697. doi: 10.1111/j.1365-313X.2009.04096.x

Luger, K., Mader, A. W., Richmond, R. K., Sargent, D. F., and Richmond, T. J. (1997). Crystal structure of the nucleosome core particle at 2.8 A resolution. *Nature* 389, 251–260. doi: 10.1038/38444

Luo, M., Luo, M.-Z., Buzas, D., Finnegan, J., Helliwell, C., Dennis, E. S., et al. (2008). UBIQUITIN-SPECIFIC PROTEASE 26 is required for seed development and the repression of PHERES1 in *Arabidopsis*. *Genetics* 180, 229–236. doi: 10.1534/genetics.108.091736

Malapeira, J., Khaitova, L. C., and Mas, P. (2012). Ordered changes in histone modifications at the core of the *Arabidopsis* circadian clock. *Proc. Natl. Acad. Sci. U.S.A.* 109, 21540–21545. doi: 10.1073/pnas.1217022110

Manzano, C., Abraham, Z., López-Torrejón, G., and Pozo, J. (2008). Identification of ubiquitinated proteins in *Arabidopsis*. *Plant Mol. Biol.* 68, 145–158. doi: 10.1007/s11103-008-9358-9

Maor, R., Jones, A., Nühse, T. S., Studholme, D. J., Peck, S. C., and Shirasu, K. (2007). Multidimensional protein identification technology (MudPIT) analysis of ubiquitinated proteins in plants. *Mol. Cell. Proteomics* 6, 601–610. doi: 10.1074/mcp.M600408-MCP200

Marteijn, J. A., Simon B. J., Mailand N., Lans H., Schwertman P., Gourdin A. M., et al. (2009). Nucleotide excision repair–induced H2A ubiquitination is dependent on MDC1 and RNF8 and reveals a universal DNA damage response. *J. Cell Biol.* 186, 835–847. doi: 10.1083/jcb.200902150

Ménard, R., Verdier G., Ors M., Erhardt M., Beisson F., and Shen W. H. (2014). Histone H2B monoubiquitination is involved in the regulation of cutin and wax composition in *Arabidopsis thaliana*. *Plant Cell Physiol.* 55, 455–466. doi: 10.1093/pcp/pct182

Molitor, A. M., Bu, Z., Yu, Y., and Shen, W. H. (2014). *Arabidopsis* AL PHD-PRC1 complexes promote seed germination through H3K4me3-to-H3K27me3 chromatin state switch in repression of seed developmental genes. *PloS Genet.* 10:e1004091. doi: 10.1371/journal.pgen.1004091

Molitor, A., and Shen, W.-H. (2013). The Polycomb complex PRC1: composition and function in plants. *J. Genet. Genomics* 40, 231–238. doi: 10.1016/j.jgg.2012.12.005

Moyal, L., Lerenthal, Y., Gana-Weisz, M., Mass, G., So, S., Wang, S.-Y., et al. (2011). Requirement of ATM-dependent monoubiquitylation of histone H2B for timely repair of DNA double-strand breaks. *Mol. Cell* 41, 529–542. doi: 10.1016/j.molcel.2011.02.015

Nakamura, K., Kato, A., Kobayashi, J., Yanagihara, H., Sakamoto, S., Oliveira, D. V., et al. (2011). Regulation of homologous recombination by RNF20-dependent H2B ubiquitination. *Mol. Cell* 41, 515–528. doi: 10.1016/j.molcel.2011.02.002

Palma, K., Thorgrimsen, S., Malinovsky, F. G., Fiil, B. K., Nielsen, H. B., Brodersen, P., et al. (2010). Autoimmunity in *Arabidopsis* acd11 is mediated by epigenetic regulation of an immune receptor. *PLoS Pathog.* 6:e1001137. doi: 10.1371/journal.ppat.1001137

Pavri, R., Zhu, B., Li, G., Trojer, P., Mandal, S., Shilatifard, A., et al. (2006). Histone H2B monoubiquitination functions cooperatively with FACT to regulate elongation by RNA polymerase II. *Cell* 125, 703–717. doi: 10.1016/j.cell.2006.04.029

Pinder, J. B., Attwood, K. M., and Dellaire, G. (2013). Reading, writing, and repair: the role of ubiquitin and the ubiquitin-like proteins in DNA damage signaling and repair. *Front. Genet.* 4:45. doi: 10.3389/fgene.2013.00045

Qin, F., Sakuma, Y., Tran, L.-S. P., Maruyama, K., Kidokoro, S., Fujita, Y., et al. (2008). *Arabidopsis* DREB2A-interacting proteins function as RING E3 ligases and negatively regulate plant drought stress–responsive gene expression. *Plant Cell* 20, 1693–1707. doi: 10.1105/tpc.107.057380

Robzyk, K., Recht, J., and Osley, M. A. (2000). Rad6-dependent ubiquitination of histone H2B in yeast. *Science* 287, 501–504. doi: 10.1126/science.287.5452.501

Roudier, F., Ahmed, I., Bérard, C., Sarazin, A., Mary-Huard, T., Cortijo, S., et al. (2011). Integrative epigenomic mapping defines four main chromatin states in *Arabidopsis*. *EMBO J.* 30, 1928–1938. doi: 10.1038/emboj.2011.103

Sanchez-Pulido, L., Devos, D., Sung, Z., and Calonje, M. (2008). RAWUL: a new ubiquitin-like domain in PRC1 RING finger proteins that unveils putative plant and worm PRC1 orthologs. *BMC Genomics* 9:308. doi: 10.1186/1471-2164-9-308

Sang, Y., Wu, M.-F., and Wagner, D. (2009). The stem cell–chromatin connection. *Semin. Cell Dev. Biol.* 20, 1143–1148. doi: 10.1016/j.semcdb.2009.09.006

Saracco, S. A., Hansson, M., Scalf, M., Walker, J. M., Smith, L. M., and Vierstra, R. D. (2009). Tandem affinity purification and mass spectrometric analysis of ubiquitylated proteins in *Arabidopsis*. *Plant J.* 59, 344–358. doi: 10.1111/j.1365-313X.2009.03862.x

Schmitz, R. J., Tamada, Y., Doyle, M. R., Zhang, X., and Amasino, R. M. (2009). Histone H2B deubiquitination is required for transcriptional activation

of FLOWERING LOCUS C and for proper control of flowering in *Arabidopsis*. *Plant Physiol.* 149, 1196–1204. doi: 10.1104/pp.108.131508

Schwartz, Y. B., and Pirrotta, V. (2013). A new world of Polycombs: unexpected partnerships and emerging functions. *Nat. Rev. Genet.* 14, 853–864. doi: 10.1038/nrg3603

Shafiq, S., Berr, A., and Shen, W.-H. (2014). Combinatorial functions of diverse histone methylations in *Arabidopsis thaliana* flowering time regulation. *New Phytol.* 201, 312–322. doi: 10.1111/nph.12493

Shen, W.-H., Parmentier, Y., Hellmann, H., Lechner, E., Dong, A., Masson, J., et al. (2002). Null mutation of AtCUL1 causes arrest in early embryogenesis in *Arabidopsis*. *Mol. Biol. Cell* 13, 1916–1928. doi: 10.1091/mbc.E02-02-0077

Shen, W.-H., and Xu, L. (2009). Chromatin remodeling in stem cell maintenance in *Arabidopsis thaliana*. *Mol. Plant* 2, 600–609. doi: 10.1093/mp/ssp022

Shilatifard, A. (2006). Chromatin modifications by methylation and ubiquitination: implications in the regulation of gene expression. *Annu. Rev. Biochem.* 75, 243–269. doi: 10.1146/annurev.biochem.75.103004.142422

Simon, J. A., and Kingston, R. E. (2013). Occupying chromatin: Polycomb mechanisms for getting to genomic targets, stopping transcriptional traffic, and staying put. *Mol. Cell* 49, 808–824. doi: 10.1016/j.molcel.2013.02.013

Sridhar, V. V., Kapoor, A., Zhang, K., Zhu, J., Zhou, T., Hasegawa, P. M., et al. (2007). Control of DNA methylation and heterochromatic silencing by histone H2B deubiquitination. *Nature* 447, 735–738. doi: 10.1038/nature05864

Tanny, J. C., Erdjument-Bromage, H., Tempst, P., and Allis, C. D. (2007). Ubiquitylation of histone H2B controls RNA polymerase II transcription elongation independently of histone H3 methylation. *Genes Dev.* 21, 835–847. doi: 10.1101/gad.1516207

Turck, F., Roudier, F., Farrona, S., Martin-Magniette, M., Guillaume, E., Buisine, N., et al. (2007). *Arabidopsis* TFL2/LHP1 specifically associates with genes marked by trimethylation of histone H3 lysine 27. *PLoS Genet.* 3:e86. doi: 10.1371/journal.pgen.0030086

Wang, L., Brown, J. L., Cao, R., Zhang, Y., Kassis, J. A., and Jones, R. S. (2004). Hierarchical recruitment of polycomb group silencing complexes. *Mol. Cell* 14, 637–646. doi: 10.1016/j.molcel.2004.05.009

Weake, V. M., and Workman, J. L. (2008). Histone ubiquitination: triggering gene activity. *Mol. Cell* 29, 653–663. doi: 10.1016/j.molcel.2008.02.014

West, M. H. P., and Bonner, W. M. (1980). Histone 2B can be modified by the attachment of ubiquitin. *Nucleic Acids Res.* 8, 4671–4680. doi: 10.1093/nar/8.20.4671

Wood, A., Krogan, N. J., Dover, J., Schneider, J., Heidt, J., Boateng, M. A., et al. (2003). Bre1, an E3 ubiquitin ligase required for recruitment and substrate selection of Rad6 at a promoter. *Mol. Cell* 11, 267–274. doi: 10.1016/S1097-2765(02)00802-X

Xiao, T., Kao, C.-F., Krogan, N. J., Sun, Z.-W., Greenblatt, J. F., Osley, M. A., et al. (2005). Histone H2B ubiquitylation is associated with elongating RNA polymerase II. *Mol. Cell. Biol.* 25, 637–651. doi: 10.1128/MCB.25.2.637-651.2005

Xu, L., Ménard, R., Berr, A., Fuchs, J., Cognat, V., Meyer, D., et al. (2009). The E2 ubiquitin-conjugating enzymes, AtUBC1 and AtUBC2, play redundant roles and are involved in activation of FLC expression and repression of flowering in *Arabidopsis thaliana*. *Plant J.* 57, 279–288. doi: 10.1111/j.1365-313X.2008.03684.x

Xu, L., and Shen, W.-H. (2008). Polycomb silencing of KNOX genes confines shoot stem cell niches in *Arabidopsis*. *Curr. Biol.* 18, 1966–1971. doi: 10.1016/j.cub.2008.11.019

Yang, C., Bratzel, F., Hohmann, N., Koch, M., Turck, F., and Calonje, M. (2013). VAL- and AtBMI1-mediated H2Aub initiate the switch from embryonic to postgerminative growth in *Arabidopsis*. *Curr. Biol.* 23, 1324–1329. doi: 10.1016/j.cub.2013.05.050

Yao, X. Z., and Shen, W.-H. (2011). Crucial function of histone lysine methylation in plant reproduction. *Chin. Sci. Bull.* 56, 3493–3499. doi: 10.1007/s11434-011-4814-3

Zhang, K., Sridhar, V. V., Zhu, J., Kapoor, A., and Zhu, J.-K. (2007a). Distinctive core histone post-translational modification patterns in *Arabidopsis thaliana*. *PLoS ONE* 2:e1210. doi: 10.1371/journal.pone.0001210

Zhang, X., Germann, S., Blus, B. J., Khorasanizadeh, S., Gaudin, V., and Jacobsen, S. E. (2007b). The *Arabidopsis* LHP1 protein colocalizes with histone H3 Lys27 trimethylation. *Nat. Struct. Mol. Biol.* 14, 869–871. doi: 10.1038/nsmb1283

Zhang, Y. (2003). Transcriptional regulation by histone ubiquitination and deubiquitination. *Genes Dev.* 17, 2733–2740. doi: 10.1101/gad.1156403

Zhu, B., Zheng, Y., Pham, A.-D., Mandal, S. S., Erdjument-Bromage, H., Tempst, P., et al. (2005). Monoubiquitination of human histone H2B: the factors involved and their roles in HOX gene regulation. *Mol. Cell* 20, 601–611. doi: 10.1016/j.molcel.2005.09.025

Zhu, Y., Weng, M., Yang, Y., Zhang, C., Li, Z., Shen, W.-H., et al. (2011). *Arabidopsis* homologues of the histone chaperone ASF1 are crucial for chromatin replication and cell proliferation in plant development. *Plant J.* 66, 443–455. doi: 10.1111/j.1365-313X.2011.04504.x

Conflict of Interest Statement: The authors declare that the research was conducted in the absence of any commercial or financial relationships that could be construed as a potential conflict of interest.

Received: 02 January 2014; paper pending published: 24 January 2014; accepted: 22 February 2014; published online: 13 March 2014.

*Citation: Feng J and Shen W-H (2014) Dynamic regulation and function of histone monoubiquitination in plants. Front. Plant Sci. **5**:83. doi: 10.3389/fpls.2014.00083*

This article was submitted to Plant Genetics and Genomics, a section of the journal Frontiers in Plant Science.

Caractérisation fonctionnelle des régulateurs chromatiniens ZRF1-like chez *Arabidopsis thaliana*

Le groupe des protéines Polycomb (PcG) forme deux complexes distinct appelés Polycomb Repressive Complex 2 (PRC2) et PRC1, responsables respectivement de la triméthylation de la lysine 27 sur l'histone 3 (H3K27me3) et de la monoubiquitination de la lysine 119 sur l'histone H2A (H2Aub1). Il est maintenant accepté que l'enrichissement en H3K27me3 par le PRC2 est un pré-requis essentiel à l'attachement du PRC1 à la chromatine, permettant la répression stable de la transcription chez divers organismes eucaryotes. Chez les végétaux, ces mécanismes de modification des histones par le PRC2 en lien avec la répression de la transcription sont bien connus. Cependant, ce n'est que récemment que les homologues des PRC1 animaux ont été identifiés chez Arabidopsis (AtRING1A/B et AtBMI1A/B/C) et que leur implication dans la monoubiquitination de H2A a été démontrée. En lien avec ce processus de répression, une étude intéressante a permis de démontrer le rôle joué par ZUOTIN-RELATED FACTOR 1 (ZRF1) dans la levé de la répression Polycomb-dépendante des gènes essentiels pour la différentiation des cellules humaines. Ainsi, ZRF1 se lie spécifiquement à H2Aub1 et dissocie le PRC1 de la chromatine, ce qui engendre ensuite la dissociation du PRC2 et par conséquence la levé de la répression. Deux homologues de ZRF1 ont été identifiés chez Arabidopsis et sont ci-après nommé AtZRF1a et AtZRF1b. Mon travail de doctorat s'est concentré sur la caractérisation fonctionnelle d'AtZRF1a et AtZRF1b.

AtZRF1b s'associe à H2Aub

Mes analyses de pull-down m'ont permis de démontrer que la protéine de fusion His-AtZRF1b peut se lier à la protéine de fusion GST-ub1, mais pas à la GST seule. Par la suite, des analyses de mutagenèse dirigée ont révélé que le domaine conservé UBD est responsable de la liaison à ub1. De plus, le domaine UBD seul fusionné à la GST peut se lier à H2Aub1 et

également à H2A. Ces résultats sont similaires aux observations faites avec la ZRF1 humaine.

AtZRF1a et _AtZRF1b_ ont des fonctions redondantes et jouent des rôles cruciaux pour la germination des graines

Par une approche génétique, j'ai entrepris l'analyses des rôles biologiques de *AtZRF1a* et *AtZRF1b* chez Arabidopsis. A partir de différentes banques de mutant d'insertion, j'ai isolé les simples mutants *Atzrf1a-1*, *Atzrf1a-2* et *Atzrf1b-1*, puis j'ai obtenu par croisements les doubles mutants *Atzrf1a-1 Atzrf1b-1* et *Atzrf1a-2 Atzrf1b-1*. Des graines de génotype sauvage (Col) ou provenant des simples et des doubles mutants ont été placées sur milieu MS dans des boites de pétri, puis stratifiées, afin d'analyser la cinétique de germination (l'émergence de la radicule étant ici l'indicateur de germination). Dans des conditions standard, la germination n'est pas affectée de manière significative chez les simples mutants *Atzrf1a-1*, *Atzrf1a-2* et *Atzrf1b-1*. Cependant, dans les même conditions, le taux de germination des doubles mutants *Atzrf1a-1 Atzrf1b-1* et *Atzrf1a-2 Atzrf1b-1* est lui diminué. A un niveau moindre, nous avons également observé une diminution du taux de germination du double mutant *Atbmi1a Atbmi1b*. L'acide gibbérellique 3 (GA3) est connue pour favoriser la levée de dormance et la germination, pourtant malgré les différentes concentrations testées (0.5, 1.0 and 2.0µmol/L), il n'a pas été possible de restaurer une germination normale chez les doubles mutants *Atzrf1a-1 Atzrf1b-1* et *Atzrf1a-2 Atzrf1b-1*.

Ensuite, nous avons soumis nos mutants à des stresses salin et osmotique, connus pour leurs effets négatifs sur la germination. En présence de 100 mM de NaCl ou de 200 mM de mannitol, le taux de germination des simples mutants *Atzrf1a-1*, *Atzrf1a-2* et *Atzrf1b-1* reste similaire à celui observé chez Col, alors que les doubles mutants *Atbmi1a Atbmi1b*, *Atzrf1a-1 Atzrf1b-1*et *Atzrf1a-2 Atzrf1b-1* présentent une efficacité de germination significativement réduite (le taux de germination des doubles mutants *Atzrf1a-1 Atzrf1b-1* et *Atzrf1a-2 Atzrf1b-1* étant significativement inférieure à celui du

double mutant *Atbmi1a Atbmi1b*). En effet, dans ces conditions, toutes les graines sauvages sont germées 5 jours après stratification, alors qu'au même temps, le taux de germination n'est que d'environ 40% en présence de 100 mM de NaCl et d'environ 50% en présence de 200 mM de mannitol pour les doubles mutants *Atzrf1a-1 Atzrf1b-1* et *Atzrf1a-2 Atzrf1b-1*. Le double mutant *Atbmi1a Atbmi1b* présente lui un taux de germination d'environ 70% en présence de 100 mM de NaCl et d'environ 85% en présence de 200 mM de mannitol.

J'ai entrepris l'étude des mécanismes moléculaires à la base des défauts de germination observés chez les doubles mutants *Atzrf1a-1 Atzrf1b-1* et *Atzrf1a-2 Atzrf1b-1*. En premier lieu, j'ai analysé le taux d'expression de gènes impliqués dans le développement de la graine, tels que *ABI3*, *DOG1*, *CRA1*, *CRC*, *PER* and *AIL5*. Comme attendu, les différents gènes analysés présentent tous, àl'exception de *DOG1*, une levé de répression de leur expression dans des plantules de *Atzrf1a-1 Atzrf1b-1* et *Atzrf1a-2 Atzrf1b-1*.

Afin d'aller plus en avant dans l'étude de cette dé-répression, j'ai réalisé des analyses d'immuno-précipitation de la chromatine (ChIP) des gènes listés ci-dessus, à l'aide d'anticorps dirigés spécifiquement contre H3K27me3, H3K4me3 ou H2Aub1. J'ai ainsi détecté chez *Atzrf1a-1 Atzrf1b-1* et *Atzrf1a-2 Atzrf1b-1* une légère augmentation du niveau d'H3K4me3 sur certains gènes, alors que les niveaux en H3K27me3 et H2Aub1 sont d'une manière générale diminués sur tous les gènes analysés. Ces résultats indiquent que *AtZRF1a* et *AtZRF1b* sont requis dans la maintenance du niveau de H3K27me3 et de H2Aub1 nécessaire à la répression des gènes du développement de la graine *ABI3*, *CRA1*, *CRC*, *PER* and *AIL5* afin de permettre la germination.

AtZRF1a et AtZRF1b sont impliqués dans la maintenance des cellules souches et la régulation des divers aspects développementaux des plantes

En plus de son sévère défaut de germination, le double mutant *Atzrf1a Atzrf1b* présente d'autres défauts phénotypiques. Ainsi, par rapport à des

plantules sauvages, le phénotype des cotylédons de plantules *Atzrf1a-1 Atzrf1b-1* peut présenter des degrés variables de sévérité (e.g. cotylédon unique, cotylédons asymétriques ou encore embryonnaires). Au stade végétatif, des mesures du poids frais de plantes de 4 semaines ont permis de confirmer le nanisme des doubles mutants *Atzrf1a-1 Atzrf1b-1* (18.33 ± 6.87 mg, n = 10) et *Atzrf1a-2 Atzrf1b-1* (18.59 ± 6.90 mg, n = 10) par rapport à Col (75.0 ± 11.18 mg, n = 10). En microscopie électronique à balayage, la taille des cellules chez les doubles mutants *Atzrf1a-1 Atzrf1b-1* et *Atzrf1a-2 Atzrf1b-1* apparaît réduite. La taille des cellules épidermique pavimenteuses est diminuée de 40% chez *Atzrf1a-1 Atzrf1b-1* et *Atzrf1a-2 Atzrf1b-1* par rapport à Col. Prises dans leur ensemble, ces données indiquent que l'expansion cellulaire est résolument déficiente, ce qui pourrait en grande partie expliquer la taille réduite des feuille chez *Atzrf1a-1 Atzrf1b-1* et *Atzrf1a-2 Atzrf1b-1*. Afin d'examiner la progression du cycle cellulaire, nous avons comparé les niveaux de ploïdie entre des feuilles de *Atzrf1a-1 Atzrf1b-1* et *Atzrf1a-2 Atzrf1b-1* et des feuilles de Col en mesurant le contenu relatif en ADN nucléaire par cytométrie en flux. Le cycle cellulaire se divise en quatre phases : la phase G1 ou post-mitotique, avec son niveau 2C d'ADN nucléaire ; la phase S ou phase de synthèse d'ADN, avec son niveau d'ADN intermédiaire entre 2C et 4C; la phase G2 ou post-replicative, avec son niveau 4C d'ADN; et finalement la phase M ou mitotique. Mes analyses m'ont permis d'observer que la proportion de cellules 2C était sensiblement plus faible chez *Atzrf1a-1 Atzrf1b-1* et *Atzrf1a-2 Atzrf1b-1* par rapport à Col, ce qui suggère une réduction de la durée de la phase G1 chez le double mutant. Les cellules ayant un niveau de ploïdie supérieur ou égale à 8C sont le résultat du phénomène d'endoréduplication, qui consiste en des réplications successives sans division de la cellule. La proportion de ces cellules est également légèrement augmentée chez *Atzrf1a-1 Atzrf1b-1* et *Atzrf1a-2 Atzrf1b-1* par rapport à Col.

Par rapport à des plantes sauvages, nous avons observé un très fort retard de croissance de la racine primaire chez *Atzrf1a-1 Atzrf1b-1* et *Atzrf1a-2 Atzrf1b-1*. Par l'introgression de différentes lignées rapportrices *DR5::GFP*, *WOX5::GFP*, *SCR::GFP*, *CO2::GFP*, *J1092* and *J2341* dans le double mutant *Atzrf1a-1 Atzrf1b-1*, j'ai cherché à comprendre les causes de ce phénotype. Mes observations en microscopie confocale m'ont permis de constater que les mutations perte de fonction de *AtZRF1a* et *AtZRF1b* conduisent à une importante désorganisation des différentes couches cellulaires au niveau de la racine et provoque la perte des cellules souches racinaires au niveau du centre quiescent. Des analyses de PCR quantitative m'ont de plus permis de démontrer que des gènes de régulation de la voie de l'auxine sont dérégulés chez les doubles mutants *Atzrf1a-1 Atzrf1b-1*et *Atzrf1a-2 Atzrf1b-1*. Pourtant, l'application exogène de différentes concentrations de l'auxine synthétique ANA (acide naphtalène-acétique) ne semble pas restaurer le phénotype racinaire du double mutant.

Le double mutant *Atzrf1a Atzrf1b* présente également un défaut de floraison. En comptant le nombre de feuilles formées dans la rosette avant que la hampe florale n'apparaisse j'ai pu constater que le double mutant *Atzrf1a Atzrf1b* présentait un phénotype de floraison précoce. J'ai ensuite combiné cette analyse phénotypique à l'analyse du niveau d'expression des différents gènes de floraison que sont *FLC*, les gènes *MAFs*, *FT*, *SOC1*, *AGL24* et *SVP*. Dans le double mutant, le niveau d'expression de *FLC* et des gènes *MAFs* est fortement réduit. Ainsi, ce profile d'expression est l'inverse de celui observé pour les gènes du développement racinaire décrits plus haut, d'où l'intérêt d'étudier la structure de leur chromatine. Par des analyses de ChIP, j'ai pu observer que le niveau de H3K4me3 et d'H2Aub1 reste inchangé chez *Atzrf1a-1 Atzrf1b-1* et *Atzrf1a-2 Atzrf1b-1* par rapport à Col au niveau des gènes de floraison, alors que le niveau d'H3K27me3 lui augmente. Ces résultats indiquent que *AtZRF1a* et *AtZRF1b* sont nécessaire au maintient d'un niveau faible d'H3K27me3 permettant de promouvoir l'expression des gènes *FLC* et *MAFs* et donc de réprimer la floraison.

AtZRF1a et AtZRF1b fonctionnent partiellement en relation avec PRC1

Certains défauts phénotypiques observés chez le double mutant *Atzrf1a Atzrf1b* sont similaires à ceux précédemment observés chez les mutants du PRC1 *Atring1a Atring1b* et *Atbmi1a Atbmi1b*. Mes donnés de microarray vont dans le sens d'une interaction génétique puisqu'elles révèlent une superposition significative des gènes dérégulés chez *Atzrf1a Atzrf1b* et *Atring1a Atring1b* ou *Atbmi1a Atbmi1b*. J'ai de plus analysé l'interaction physique de AtZRF1b avec AtRING1 ou AtBMI1. Des billes d'agaroses couplés à la GST, ou aux protéines de fusion GST-RING1A, GST-BMI1a, GST-BMI1B ou GST-BMI1C ont été incubées avec des extraits totaux de protéines nucléaires provenant d'Arabidopsis exprimant la protéine de fusion FLAG-AtZRF1b. Le pull-down de la GST suivie de l'analyse par Western-blot à l'aide d'anticorps anti-FLAG m'a alors permis de démontrer l'interaction entre AtZRF1B et AtBMI1A, AtBMI1B ou AtBMI1C, mais pas AtRING1A. J'ai par la suite confirmé ces résultats par des analyses de FLIM en démontrant l'interaction entre les protéines de fusion GFP-AtZRF1b et RFP-AtBMI1A ou RFP-AtBMI1B.

Ensemble de mes résultats ont permis la première caractérisation fonctionnelle des gènes *AtZRF1a* et *AtZRF1b*. Mes données ont montrés que AtZRF1a et AtZRF1b jouent des rôles en partie en relation avec PRC1, mais également avec aspects spécifiques. Leur rôle dans l'enlèvement de H2Aub1, comme cela été proposé pour ZRF1 chez l'animal, n'a pas été observé chez les plantes.

PROPOSITION DE MOTS-CLÉS :

Chromatine regulateur; Épigénétique; Ubiquitine; H2Aub1; Régulation de la transcription; Développement de la plante; ZRF1; Germination des grains

Polycomb group (PcG) proteins form two distinct complexes, polycomb repressive complex 2 (PRC2) and PRC1 that mediate trimethylation at histone 3 lysine 27 (H3K27me3) and monoubiquitination at histone H2A lysine 119 (H2AK119ub), respectively. H3k27me3 by PRC2 is believed to be a prerequisite for PRC1 binding, and such combination of PcG-mediated epigenetic modifications lead to transcriptional gene silencing in diverse eukaryotic organisms. PRC2-mediated histone modification and gene repression have also been intensively studied in plant. However, PRC1 in plants has only been more recently documented and the *Arabidopsis* PRC1-like RING-finger homologs (AtRNIG1A/B and AtBMI1A/B/C) have been characterized and shown to catalyze H2AK119ub. A recent study shows that *ZUOTIN-RELATED FACTOR 1 (ZRF1)* functions in the de-repression of polycomb-repressed genes in human cells. ZRF1 specifically binds to H2AK119ub and then displaces PRC1 from chromatin. The depletion of PRC1 subsequently causes the loss of PRC2 from the chromatin, consequently switching polycomb-repressed genes from repressive to active state. Two homologs of human ZRF1 have been identified in *Arabidopsis*, and are hereinafter named AtZRF1a and AtZRF1b. My PhD work focuses on the functional characterization of AtZRF1a and AtZRF1b.

AtZRF1b interacts with H2Aub

In pull-down experiments, the His-AtZRF1b fusion protein can bind GST-Ub but not GST alone. Mutagenesis analysis revealed that the conserved UBD-domain is responsible for Ub binding. GST-fused UBD-domain fragment of AtZRF1b also can bind H2Aub as well as H2A and H3. These observed AtZRF1b properties are similar to those previously reported for human ZRF1.

***AtZRF1a* and *AtZRF1b* have redundant functions and play crucial roles for seed germination**

Using the powerful genetic tool in Arabidopsis, I investigated the biological roles of *AtZRF1a* and *AtZRF1b*. From the Arabidopsis seed store center, we got single mutants *Atzrf1a-1*, *Atzrf1a-2* and *Atzrf1b-1*. Then by crossing, I obtained the double mutants

Atzrf1a-1 Atzrf1b-1 and *Atzrf1a-2 Atzrf1b-1*. Seeds of wild-type (Col), single mutants *Atzrf1a-1*, *Atzrf1a-2* and *Atzrf1b-1* and double mutants *Atzrf1a-1 Atzrfb-1*, *Atzrf1a-2 Atzrf1b-1* were on plates, stratified and germination rates were scored by counting the radical emergence for 12 days after stratification (DAS). Under standard growth conditions (MS medium), germination kinetics were not significantly affected in the *Atzrf1a-1*,*Atzrf1a-2* and *Atzrf1b-1* single mutants. However, under the same conditions, germination efficiency of the *Atzrf1a-1 Atzrf1b-1* and *Atzrf1a-2 Atzrf1b-1* double mutants was found reduced. In *Atbmi1a Atbmi1b* double mutant, we found the germination rate also reduced, but it is not as strong as in *Atzrf1a-1 Atzrf1b-1* and *Atzrf1a-2 Atzrf1b-1* double mutants. Gibberellin acid 3 (GA3) is generally known to effectively stimulate the breaking of seed dormancy and promote germination. However, at different tested concentrations (0.5, 1.0 and 2.0μ mol/L) GA3 could not rescue the germination defects of the *Atzrf1a-1 Atzrf1b-1* and *Atzrf1a-2 Atzrf1b-1* double mutants.

Next, mutants were challenged with salt and mannitol, which two stresses known to have a negative impact on seed germination. At 100 mM NaCl or 200 mM mannitol, the germination efficiency of the single mutants *Atzrf1a-1*, *Atzrf1a-2* and *Atzrf1b-1* was similar to that of Col, whereas the *Atbmi1a Atbmi1b*, *Atzrf1a-1 Atzrf1b-1* and *Atzrf1a-2 Atzrf1b-1* double mutants displayed a significantly decreased germination efficiency. And the decrease is stronger in *Atzrf1a-1 Atzrf1b-1* and *Atzrf1a-2 Atzrf1b-1* double mutants than in *Atbmi1a Atbmi1b*. Indeed, under the tested stress conditions, all wild-type seeds had germination after 5 days, while germination rates were reduced to ～40% and ～50% for *Atzrf1a-1 Atzrf1b-1* and *Atzrf1a-2 Atzrf1b-1* double mutants on 100 mM NaCl and 200 mM mannitol, respectively. And for *Atbmi1a Atbmi1b* double mutant the germination rates were reduced to ～70% and ～85% on 100 mM NaCl and 200 mM mannitol, respectively.

Next, I investigated molecular mechanisms underlying the seed germination defects of the double mutants *Atzrf1a-1 Atzrf1b-1* and *Atzrf1a-2 Atzrf1b-1*. I first analyzed expression levels of several seed development related genes including *ABI3*, *DOG1*,

CRA1, *CRC*, *PER* and *AIL5*. As expected, all the examined genes except *DOG1* displayed de-repression in the double mutants *Atzrf1a-1 Atzrf1b-1* and *Atzrf1a-2 Atzrf1b-1* seedlings.

To further understand the mechanism, I performed ChIP experiments using antibodies specific to H3K27me3, H3K4me3 or H2Aub. As results, we found that H3K4me3 level was slightly up-regulated at some gene regions whereas the levels of H3K27me3 and H2Aub were broadly down-regulated at the examined seed development genes in *Atzrf1a-1 Atzrf1b-1* and *Atzrf1a-2 Atzrf1b-1*. It indicates that AtZRF1a and AtZRF1b are required for maintaining H3K27me3 and H2Aub to repress the seed development genes *ABI3*, *CRA1*, *CRC*, *PER* and *AIL5*, to promote seed germination.

AtZRF1a and _AtZRF1b_ are involved in stem cell maintenance and regulation of various developmental aspects of plants

In addition to seed germination, the *Atzrf1a Atzrf1b* double mutants also exhibited other defective phenotypes. Compared to the wild-type plant, the *Atzrf1a Atzrf1b* double mutant seedlings showed varied degrees of phenotype severity on cotyledons, such as single cotyledon, asymmetrical cotyledon or embryonic cotyledon. Moreover, at the vegetative stage, fresh weight measurements of whole rosettes of 4-week-old plants confirmed the smaller size of *Atzrf1a-1 Atzrf1b-1*(18.33 ± 6.87 mg, n = 10) and *Atzrf1a-2 Atzrf1b-1* (18.59 ± 6.90 mg, n = 10) compared with Col (75.0 ± 11.18 mg, n = 10). Scanning electron microscope revealed smaller cell size in *Atzrf1a-1 Atzrf1b-1* and *Atzrf1a-2 Atzrf1b-1*. The epidermal pavement cell surface is reduced to ~40% in *Atzrf1a-1 Atzrf1b-1* and *Atzrf1a-2 Atzrf1b-1* as compared that in Col. Taken together, these data indicate that cell expansion is drastically constrained, which might largely account for the reduced leaf size in *Atzrf1a-1 Atzrf1b-1* and *Atzrf1a-2 Atzrf1b-1*. To investigate cell cycle progression, we compared the ploidy levels of *Atzrf1a-1 Atzrf1b-1, Atzrf1a-2 Atzrf1b-1* and Col leaves by measurement of the relative nuclear DNA content via flow cytometry analysis. The DNA was isolated from the first true leaf on three different plantlets. The cell cycle consists of four phases: postmitotic interphase (G1), with 2C nuclear DNA content; S phase, meaning DNA synthetic

phase, nuclear DNA content intermediate 2C and 4C; postsynthetic interphase (G2), with a 4C nuclear DNA content; and finally the M phase, meaning mitosis. I observed that the proportion of 2C cells is slightly lower in *Atzrf1a-1 Atzrf1b-1* and *Atzrf1a-2 Atzrf1b-1* compared with Col, suggesting a relatively shorter duration of G1 in the mutant. Higher ploidy levels (⩾8C) are the result of endoreduplication cycles in which nuclear DNA is replicated without a subsequent mitotic division. The relative proportion of cells with higher ploidy levels is slightly increased in *Atzrf1a-1 Atzrf1b-1* and *Atzrf1a-2 Atzrf1b-1* compared with Col.

Compared to wild-type, we found the primary root growth of the double mutants *Atzrf1a-1 Atzrf1b-1* and *Atzrf1a-2 Atzrf1b-1* was strongly impaired. To further investigate the root phenotype, by crossing we introduced reporter genes *DR5::GFP*, *WOX5::GFP*, *SCR::GFP*, *CO2::GFP*, *J1092* and *J2341* into the double mutant *Atzrf1a-1 Atzrf1b-1*. Confocal observation results showed that loss-of-function of AtZRF1a and AtZRF1b drastically affects root cell layer organization and causes loss of root stem cells. RT-PCR analysis indicated that some auxin regulatory genes are mis-regulated in the double mutants *Atzrf1a-1 Atzrf1b-1* and *Atzrf1a-2 Atzrf1b-1*. Nevertheless, when supplied with different concentrations of exogenous NAA the mutant root growth defects could not be rescued.

The *Atzrf1a Atzrf1b* double mutants also showed flowering defects. By counting the rosette leaf number, we found the flowering time of double mutant was obviously later than wild-type. Then we analyzed expression levels of the flowering genes *FLC*, *MAFs*, *FT*, *SOC1*, *AGL24* and *SVP*. In double mutant, the expression level of *FLC* and *MAFs* was reduced strongly. This expression pattern is opposite to that of the above described seed development genes in the mutants. It will be interesting to investigate H3K27me3, H3K4me3 and H2Aub at flowering genes for a comparison. I performed ChIP experiments using antibodies specific to H3K27me3, H3K4me3 or H2Aub. As results, we found that H3K4me3 and H2Aub levels were unchanged whereas the level of H3K27me3 up-regulated at the examined flowering time genes in *Atzrf1a-1 Arzrf1b-1*and *Atzrf1a-2 Atzrf1b-1*. It indicates that AtZRF1a and AtZRF1b

are required for maintaining H3K27me3 to promote the flowering time genes *FLC* and *MAFs*, to repress flowering.

AtZRF1a and _AtZRF1b_ functions are partially related to PRC1

Some of the *Atzrf1a Atzrf1b* double mutant defects are similar to those previously reported for the PRC1 mutants *Atring1a Atring1b* and *Atbmi1a Atbmi1b.* Our microarray analysis showed that there are significant overlaps of the perturbed genes between *Atzrf1a Atzrf1b* and *Atring1a Atring1b* or *Atbmi1a Atbmi1b.* I investigated physical interaction of AtZRF1b with AtRING1 and AtBMI1 proteins. Agarose beads coated with GST, GST-RING1A, GST-BMI1A, GST-BMI1B or GST-BMI1C were incubated with an equal aliquot of total nuclear protein extracts of *Arabidopsis* plants expressing FLAG-AtZRF1b. Then the pulldown fractions were analyzed by Western blot using antibodies against FLAG. We found that AtZRF1b can interact with AtBMI1A, AtBMI1B and AtBMI1C but not with AtRING1A. In order to confirm the observed interaction, we performed FLIM analysis to examine GFP-AtZRF1b interaction with RFP-AtRING1A, RFP-AtBMI1A, RFP-AtBMI1B or RFP-AtBMI1C, that are coexpressed in *Nicotiana benthamiana* leaves. We confirmed interaction between AtZRF1b and AtBMI1A or AtBMI1B.

All of my results allowed the first functional characterization of genes *AtZRF1a* and *AtZRF1b*. My data have shown that AtZRF1a and AtZRF1b play roles in part related PRC1 but also with specific aspects. Their role in the removal of H2Aub1, as was proposed for ZRF1 in animals has not been observed in plants.

Keywords :

Chromatin regulator ; Epigenetics ; Ubiquitin ; H2Aub1 ; Transcription regulation ; Plant development ; ZRF1 ; Seed germination

Jing FENG

Caractérisation fonctionnelle des régulateurs chromatiniens ZRF1-like chez *Arabidopsis thaliana*

Résumé

Des études chez les animaux ont montré que ZRF1 a une fonction lectrice au niveau de H2AK119ub1 dans la dérépression de gènes réprimés par polycomb. Deux gènes homologues au gène humain ZRF1 ont été identifiés dans le génome d'*Arabidopsis*, et ont par la suite été appelés *AtZRF1a* et *AtZRF1b*. La caractérisation fonctionnelle de ces gènes n'a pas encore été rapportée.

Mon premier objectif était d'obtenir des connaissances générales sur *AtZRF1a* et *AtZRF1b*. Tous les deux sont exprimés dans des plantes d'*Arabidopsis* et la protéine AtZRF1b est localisée dans le noyau et dans le cytoplasme. En plus, nous avons trouvé que la protéine AtZRF1b lie H2Aub1 avec les mêmes caractéristiques que la protéine ZRF1 humaine.

J'ai utilisé les outils génétiques puissants disponibles pour *Arabidopsis* pour étudier la fonction d'*AtZRF1a* et *AtZRF1b.* Plusieurs lignées d'insertion de T-DNA indépendantes ont été identifiées. A cause d'une redondance fonctionnelle, des mutants simples n'ont pas de défauts de développement évidents. C'est pourquoi j'ai étudié un mutant double qui montre une perte de fonction pour les deux gènes *AtZRF1a* et *AtZRF1b*. Ce double mutant révèle des rôles importants pour ces gènes dans la croissance et le développement, qui vont de la prolifération et la différenciation cellulaire jusqu'au contrôle du temps de floraison.

J'ai ensuite étudié les rôles d'*AtZRF1a* et *AtZRF1b* dans la régulation de la transcription et j'ai constaté que *AtZRF1a* et *AtZRF1b* ont une fonction similaire a PRC1.

Finalement, j'ai étudié les niveaux de H3K4me3, H3K27me3 et H2Aub1 dans la chromatine de certains gènes dont l'expression est perturbée dans les doubles mutants. Les résultats montrent que la dé-ubiquitination de H2Aubi1 n'est pas un événement majeur dans la régulation de la transcription chez *Arabidopsis*.

MOTS-CLÉS :

Chromatine regulateur; Épigénétique; Ubiquitine; H2Aub1; Régulation de la transcription; Développement de la plante; ZRF1; Germination des grains

Résumé en anglais

Studies in animals showed that ZRF1 can read the histone H2AK119ub1 modification in the derepression of polycomb-repressed genes. Two homologs of human ZRF1 have been identified in the *Arabidopsis* genome, and hereinafter are named *AtZRF1a* and *AtZRF1b*. So far, their functional characterization had not been reported yet.

My first objective was to acquire basic knowledge about *AtZRF1a* and *AtZRF1b.* Both genes are broadly expressed in *Arabidopsis* plants and the AtZRF1b protein is localized in the nucleus and the cytoplasm. Moreover, we found that AtZRF1b binds H2Aub1 with characteristics similar to those previously reported for the human ZRF1 protein.

I subsequently used the powerful genetic tools available in *Arabidopsis* to investigate the functions of *AtZRF1a* and *AtZRF1b*. Several independent T-DNA insertion *Arabidopsis* mutant lines were identified. Because of functional redundancy, single mutants have no obvious developmental defects. I therefore focused on double mutants displaying loss of function of both *AtZRF1a* and *AtZRF1b*. The study of a double mutant revealed important roles for these genes in plant growth and development ranging from cell proliferation and differentiation to flowering time control.

I then investigated the roles of *AtZRF1a* and *AtZRF1b* in gene transcriptional regulation and found that *AtZRF1a* and *AtZRF1b* function in a way that is partially similar to PRC1 function. Lastly, I investigated H3K4me3, H3K27me3 and H2Aub1 levels in the chromatin regions of some expression-perturbed genes in double mutants. The results show that ZRF1-mediated deubiquitination of H2Aub1 is not a major event in transcriptional regulation in *Arabidopsis*.

KEYWORDS :

Chromatin regulator ; Epigenetics ; Ubiquitin ; H2Aub1 ; Transcription regulation ; Plant development ; ZRF1 ; Seed germination